Improving mortality rate estimates for management of the Queensland saucer scallop fishery

FRDC 2017/048

March 2021

A. Courtney[1], J. Daniell[2], S. French[2], G. Leigh[1], W.-H. Yang[3], M. Campbell[1], M. McLennan[1], K. Baker[2], T. Sweetland[2], E. Woof[2], R. Robinson[2], I. Mizukami[2] and E. Mulroy[2]

[1]Department of Agriculture and Fisheries, Queensland
[2]James Cook University
[3]Centre for Applications in Natural Resource Mathematics, University of Queensland

Improving mortality rate estimates for management of the Queensland saucer scallop fishery
FRDC 2017/048
2020

Front cover image credits are as follows:

Disclaimer

The authors do not warrant that the information in this document is free from errors or omissions. The authors do not accept any form of liability, be it contractual, tortious, or otherwise, for the contents of this document or for any consequences arising from its use or any reliance placed upon it. The information, opinions and advice contained in this document may not relate, or be relevant, to a reader's particular circumstances. Opinions expressed by the authors are the individual opinions expressed by those persons and are not necessarily those of the publisher, research provider or the FRDC. The Fisheries Research and Development Corporation plans, invests in and manages fisheries research and development throughout Australia. It is a statutory authority within the portfolio of the federal Minister for Agriculture, Fisheries and Forestry, jointly funded by the Australian Government and the fishing industry.

Researcher Contact Details		FRDC Contact Details	
Name:	Dr. Tony Courtney	Address:	25 Geils Court
Address:	Level 1, Ecosciences Precinct, 41 Boggo Road, Dutton Park QLD 4102		Deakin ACT 2600
		Phone:	02 6285 0400
Phone:	07 3255 4227	Fax:	02 6285 0499
Fax:	07 3846 1207	Email:	frdc@frdc.com.au
Email:	Tony.Courtney@daf.qld.gov.au	Web:	www.frdc.com.au

In submitting this report, the researcher has agreed to FRDC publishing this material in its edited form.

Contents

List of Tables

List of Figures

1   Acknowledgements

2   Abbreviations/Acronyms

AIMS	Australian Institute of Marine Sciences
AVI	average variable importance
CARM	Centre for Applications in Natural Resource Mathematics, University of Queensland.
CFISH	Queensland commercial fishery logbook database
DAF	Department of Agriculture and Fisheries, Queensland
F	instantaneous rate of fishing mortality
GBR	Great Barrier Reef
GBRMPA	Great Barrier Reef Marine Park Authority
GBM	Generalised Boosting Method
GLM	generalised linear model
JCU	James Cook University
LTMP	Long-Term Monitoring Program
M	instantaneous rate of natural mortality
MARS	Geoscience Australia's MARine Sediment database
MBES	Multibeam echosounder
OK	Ordinary Kriging
QECOTF	Queensland East Coast Otter Trawl Fishery
SH	shell height
SRA	scallop replenishment area
SST	sea surface temperature
RF	Random Forest
VEcv	Variance Explained by cross validation
VMS	Vessel monitoring system
WTO	Wildlife Trade Operation

3   Executive Summary

3.1   WHAT THE REPORT IS ABOUT

This research was undertaken on the Queensland saucer scallop (*Ylistrum balloti*) fishery in southeast Queensland, which is an important component of the Queensland East Coast Otter Trawl Fishery (QECOTF). The research was undertaken by a collaborative team from the Queensland Department of Agriculture and Fisheries, James Cook University (JCU) and the Centre for Applications in Natural Resource Mathematics (CARM), University of Queensland and focused on 1) an annual fishery-independent trawl survey of scallop abundance, 2) relationships between scallop abundance and physical properties of the seafloor, and 3) deriving an updated estimate of the scallop's natural mortality rate. The scallop fishery used to be one of the state's most valuable commercially fished stocks with the annual catch peak at just under 2000 t (adductor muscle meat-weight) in 1993 valued at about $30 million, but in recent years the stock has declined and is currently considered to be overfished. Results from the study are used to improve monitoring, stock assessment and management advice for the fishery.

3.2   BACKGROUND

A 2016 Queensland Department of Agriculture and Fisheries (DAF) quantitative assessment demonstrated that recent standardised scallop catch rates were the lowest in the 39-year catch rate record and that the spawning stock ratio was likely to be less than 20% (Yang *et al.* 2016). Under the Australian Government (2018) Commonwealth Fisheries Harvest Strategy Policy the assessment would likely require closure of the fishery. In response to the assessment, the Queensland Government implemented temporal and spatial closures of the fishery and provided funding to reintroduce a fishery-independent trawl survey of scallop abundance in 2017, which was subsequently repeated in 2018 and 2019. Analyses and results from the survey are presented herein. The survey was first implemented in 1997 (Dichmont *et al.* 2000) and comprehensively carried out from 1997–2000, but from 2001–2006, the number of strata and sample sites were reduced and in 2006 the survey ceased.

There is growing research to indicate that seafloor properties, including bottom hardness and sediment profiles, affect the distribution of scallops (Smith *et al.* 2017; Miller *et al.* 2019). Information on scallop habitat can be used to improve stock assessments in two ways. Firstly, measures of scallop habitat (e.g., good, medium and poor habitat) can be used to explain variation in catch rate standardisation models, providing improved indices of abundance. Secondly, habitat information can be used to improve estimates of the instantaneous rate of fishing mortality (*F*). At present, *F* is assumed to be spatially uniform across the fishery, i.e., one unit of fishing effort in Hervey Bay is assumed to impose the same amount of fishing mortality as one unit of effort off Yeppoon. However, the levels of effort applied across varying scallop habitat impose different levels of *F*. This project examined the relationships between seafloor properties and saucer scallops with the intention of identifying preferred scallop habitat.

Finally, the scallop stock assessment and management advice are heavily influenced by the commercial catch and effort, survey data, and key population parameter estimates, including the scallop's instantaneous rate of natural mortality (*M*). The only previous estimate of *M* for saucer scallops was based on a tagging study over 40 years ago by Dredge (1985a). The project took advantage of the closed scallop replenishment areas (SRAs) to undertake a second tagging experiment to measure *M*. In summary, the project aimed to improve the stock assessment and management advice by a) improving the fishery-independent survey design and analyses, b) examining relationships between scallops and seafloor properties and developing predictive models of scallop habitat, and c) deriving an additional, updated estimate of *M*.

3.3   OBJECTIVES

1) Design and carry out a comprehensive fishery-independent survey of the 0+ and 1+ age classes in the Queensland saucer scallop fishery.

2) Undertake exploratory analyses on the relationship between saucer scallop abundance and bottom substrate.
3) Derive one or more tagging-based estimates of the saucer scallop's natural mortality rate (*M*).

3.4 METHODOLOGY

A brief description of the project methodology is provided below. Further details can be found in the relevant Appendices using the hyperlinked sections and page numbers (press control+click).

3.4.1 *Objective 1. Scallop fishery-independent survey*

The methodology included designing the 2017, 2018 and 2019 surveys, which were based on the first scallop survey described by Dichmont *et al.* (2000), and analysing the survey catch rates. Two additional strata were added to the original design to include a possible shift in the fishery southwards over the decades. Previous analyses reported the survey catch rates as the number of scallops per 20 min shot (Jebreen *et al.* 2008) and to improve the catch rate precision, the units were changed to number of scallops per area swept (hectares, ha) by the trawl sampling gear. This required quantifying the number, configuration and size of all nets used by vessels participating in the survey, as well as net spread factors, to calculate the swept area of each trawl sample, including previous survey years. The survey design included chartering trawlers from the Queensland fleet each year. A generalised linear model (GLM) was used to derive calibration factors to adjust the raw data for differences between vessels each year. Three modelling approaches were then used to examine the calibrated catch rates: 1) scallop density maps produced by kriging, 2) a weighted strata survey analysis (Haddon 1997), and 3) a GLM which included year, strata, lunar phase, time-of-night and the year-strata interaction explanatory terms to derive adjusted mean scallop densities for each year and stratum. The analyses were applied using all available survey data from 1997–2006 and 2017–2019. Further details of the methods can be found in section 16.3, page 44. Details for a pilot study evaluation of a towed camera system, as an additional survey method for quantifying scallop abundance, are also provided (see section 17, page 93).

3.4.2 *Objective 2. Exploring relationships between substrate and scallops*

The methods for examining relationships between substrate and scallops were as follows:
1) Sediment data were obtained by collating existing sediment datasets from Geoscience Australia's MARine Sediment (MARS) database and previous studies. In addition, 166 new samples were obtained from Gladstone in 2018 and in Hervey Bay in 2019, including co-located sediment samples, scallop trawls, multibeam echosounding (MBES) bathymetry and backscatter, and underwater camera data. Sediment samples were processed using sieve apertures of 63, 125, 250, 500, 1000, 2000, 4000, 8000, 16,000 µm and classified according to Folk (1954). The percentage of calcium carbonate in each sample was determined and used to examine the proportion of terrigenous (land derived) and biological (shelly) material in each sample. Further method details are provided in section 18.3, page 120.
2) Relationships between scallop abundance and sediment properties were examined using sediment grainsize variables. Correlations between sediment fractions and co-located measures of scallop abundance were examined. Sediment samples linked to the five most productive trawls in each location were highlighted to identify potential patterns. Univariate analysis was used to examine the relationship between backscatter intensity and scallop abundance. Predictive statistical modelling was undertaken to determine the relationship between backscatter intensity and sediment properties. A Random Forest (RF) Decision Tree was used to predict backscatter values from 15 summarised grainsize properties. See section 19.3, page 142 for more details of the methods.
3) Twelve sediment models were developed to predict the distribution of mud, sand, gravel, calcium carbonate, mean grainsize and fine sand on the southeast Queensland coast. The models included simple deterministic interpolation methods (i.e., Inverse Distance Weighted, IDW) and machine learning methods (RF and Boosted Regression Tree or Generalised Boosting Method, GBM), and their hybrids. Eleven explanatory terms were considered and the best performing models for each of the sediment parameters were identified by ranking based on the Variance Explained by cross

validation (VEcv) for each model (Li *et al.* 2017). See section 20.3, page 158 for further details of the methods.

4)   Predictions of scallop density were undertaken for each year that a comprehensive scallop fishery-independent survey was undertaken (i.e., 1997–2000, 2017–2019). The R package 'spm' was used for the spatial predictive modelling (Li 2019a). The package implements IDW, geostatistical Ordinary Kriging (OK) and machine learning (RF) methods as well as their hybrid methods for spatial predictions. IDW (default and optimised), OK (optimised) and four variants of RF were used for the prediction of scallop distributions for each survey year. The four variants of RF were designed to assess the impact of adding x and y parameters (i.e., latitude and longitude), basic sediment grainsize parameters, and high-resolution sediment grainsize parameters. Adding or removing sediment grainsize parameters provided insight into how much they can improve the predictions and which parameters are the most important. The optimum model was selected using the VEcv metric. Further details are provided in section 21.3, page 203.

3.4.3   Objective 3. Estimating the scallop's natural mortality

The methodology for measuring the scallop's natural mortality rate (*M)* was based on a tag-recapture experiment conducted inside two closed SRAs (Hervey Bay A and Yeppoon B, see Figure 22-3, page 243). Batches of scallops were tagged, released and recaptured inside the closures over a period of 15 months from May 2018 to August 2019. Because the tagged scallops were inside closures, the decline in the recapture rate over time is due to natural causes only (i.e., not fishing) and equates to *M*. Three approaches were applied to the experimental design and analyses, based on the batch tagging experiments described by Brownie *et al.* (1985) and logistic modelling of the tag-recapture data. Further details are provided in section 22.3, page 234. Findings were compared against a previous estimate by Dredge (1985a).

3.5   RESULTS/KEY FINDINGS

3.5.1   Objective 1. Fishery-independent survey

Adjusted mean scallop densities in 2019 were generally very low compared to previous surveys from 1997–2000 (see Tables on pages 15–17). The average of the adjusted total mean scallop density for the whole survey in recent years (i.e., 2017–2019) was about half that from 1997–2000, indicating a long-term decline in the stock. Adjusted means generally increased from 2017 to 2018, but densities of the 0+ and 1+ scallop age classes in 2019 were among the lowest for the time series. Scallop density maps were developed for each age class and year by applying kriging to the calibrated data (see section 16.4.3, page 61). Biomass estimates from the maps are comparable with those derived from recent quantitative assessment models of the stock (O'Neill *et al.* 2020; Wortmann *et al.* 2020). The scope of the study did not extend to investigating reasons for the decline in scallop abundance, but a discussion of environmental factors influencing *Y. balloti* and other scallops is provided in section 16.5.2, page 88.

When results from the survey time series are considered with long-term commercial catch and effort logbook data, there has been a significant decline in the scallop population throughout its main fished area (i.e., Yeppoon, Bustard Head, Hervey Bay) and an increase in the most southern extent of the fishery (east of Fraser Island). Overall, the change has been a significant decline.

The towed camera pilot study results indicate that scallop density and total abundance estimates could be improved by incorporating a towed camera system in the survey, as the imagery detects more scallops than trawls, and therefore provides more accurate abundance estimates (see section 17.3, page 97).

3.5.2   Objective 2. Scallop-substrate relationships

3.5.2.1   Correlations between sediment and scallops

Sediment samples and measures of bottom backscatter and saucer scallop abundance were obtained from 166 sites offshore from Gladstone and in Hervey Bay. Analysis of these data indicated that:

- sediments at sites with the highest abundance of scallops were mainly composed of fine sand (125–250µm) (Figure 19-8, page 152),
- at both the Gladstone and Hervey Bay sites, saucer scallops primarily occur on sediments that have a relatively narrow range of comparatively low backscatter intensity values (Figure 19-4, page 147),
- fine sand was the most important sediment grainsize variable in controlling backscatter response (Figure 19-5, page 148),
- scallop abundance was significantly correlated with the percentage of fine sand in the sediments in the offshore Gladstone area ($R^2 = 0.5409$), possibly indicating preferred habitat. However, the relationship was not significant in Hervey Bay ($R^2 = 0.1187$). Further details are provided in section 19.4, page 146.

3.5.2.2   Modelling sediment distributions

Modelling the distribution of sediments demonstrated that: 1) the accuracy of model predictions increased when latitude and longitude were included as covariates, 2) models that used only sediment data that had co-located high-resolution bathymetry measures commonly outperformed models that used the entire sediment dataset which included interpolated bathymetry data, and 3) a hybrid model between IDW and GBM that only used samples that were co-located with high-resolution bathymetry data was the most accurate model on average. Models for predicting the content of mud and calcium carbonate in sediments were the most accurate with a Variance Explained by cross validation (VEcv) of 76.1 and 82.3, respectively. The resulting sediment property maps (see pages 193–198) can be used to explain the distribution of saucer scallops and other species, and improve indices of scallop abundance used for stock assessment and management.

3.5.2.3   Modelling the distribution of saucer scallops

Modelling the distribution of scallops found that the inclusion of sediment data improved predictions in some years but was generally outperformed by OK and a simple RF model using latitude, longitude and bathymetric derivatives only. The OK model reproduced localised peaks and troughs in the sample datasets while the RF model produced a more generalised result. Averaging predictions of scallops over multiple years clearly identified broad lobes of prospective saucer scallop habitats between the coast and Capricorn-Bunker reefs, and offshore from Fraser Island. Within these lobes there are regional 'highs' in saucer scallop density overlapping with the SRAs within the fishery.

On the regional scale, Pearson's correlation coefficients showed that very coarse sand, coarse sand, mean grainsize, skewness, medium sand2 (i.e., mean sand and finer sediment), and mud variables had low to moderate correlations with scallops in most years, but commonly did not contribute greatly to improved model accuracy. The accuracy of the scallop distribution models may improve by developing hybrid models, such as RFok and RFidw , and by implementing rigorous feature selection methods which omit noisy variables that have no significant influence (Li *et al.* 2019). The models could also be improved by including oceanographic variables from the Great Barrier Reef eReefs hydrodynamic model. Additional sediment data, which could be collected during the annual scallop trawl survey, may also improve model performance. Further results, including predicted maps of scallop distributions, are provided on pages 226–230.

3.5.3   Objective 3. Estimates of M

The Brownie *et al.* (1985) Model 1 results indicated that *M* is higher over the summer months and lower over the winter months, possibly reflecting seasonal variation (see Table 22-7, page 244). All three analyses indicated *M* was higher in the Hervey Bay A SRA (HBA) than Yeppoon B SRA (YB). The logistic model detected significant effects on the recapture rate of tagged scallops due to closure,

scallop size, lunar phase at recapture, recapture trip, the number of days the scallops were at liberty and the interaction between days at liberty and closure. Predicted catch rates of tagged scallops from the logistic model show their decline over time as they die from natural causes (see Figure 22-5, page 248). Annual mean estimates of M for the whole fishery ranged from a minimum of 1.461 year^{-1} for the logistic model, to 1.501 year^{-1} for the Brownie *et al.* (1985) Model 1, to 1.548 year^{-1} (variable recapture rate) and 1.594 year^{-1} (fixed recapture rate) for the modified Brownie *et al.* method. All three estimates were higher than the previous estimate that was based on a similar tagging study over 40 years ago and possible reasons for the increase are discussed.

3.6 IMPLICATIONS FOR RELEVANT STAKEHOLDERS

For commercial fishers and processors, the long-term trend in survey catch rates, including the 2019 results, are concerning because they show a chronic decline in the stock. In addition, the most recent quantitative assessment of the stock indicates the spawning biomass is below 20% of the unfished biomass (Wortmann *et al.* 2020), which would likely require closure of the fishery under the Commonwealth Fisheries Harvest Strategy Policy. The poor status of the stock may also have implications for securing Wildlife Trade Operation (WTO) export approval of scallop meat caught in the fishery.

For monitoring and management of the stock, the survey should be continued and gaps in the time series, such as those that occurred from 2007–2016, should be avoided. Research undertaken by NOAA on Atlantic sea scallops and results from the pilot study on Queensland saucer scallops indicate that more accurate estimates of scallop density and total abundance could be achieved by incorporating a towed camera system in the survey, although this would increase monitoring costs, which are fully funded by the Queensland Government.

The sediment maps and the predictive models of scallop distribution can be used to improve the standardised commercial scallop catch rate predictions, which has implications for monitoring and assessment. At present, the spatial resolution in the catch rate standardisation models is limited to 30-minute logbook grids (i.e., coarse explanatory spatial term). Including spatial information on scallop habitat type should increase the amount of variation explained in the standardisation models, result in more reliable abundance indices, and improve the stock assessment advice.

Findings from the tagging study indicate the natural mortality rate (M) is significantly higher than previously measured by Dredge (1985a). The most recent quantitative assessment of the stock included an updated estimate based on the logistic model developed herein (i.e., M = 1.461 year^{-1}) (Wortmann *et al.* 2020). Future assessments might be improved by considering the spatial variation in M detected in the study, and possible seasonal variation. *Ylistrum balloti* has a relatively narrow temperature tolerance and results from the study indicate that M is higher over summer. Although speculative, the increase in M over the last 40 years may be related to the increase in winter sea surface temperature (SST) in the fishery over this period (O'Neill *et al.* 2020). If M increases with SST then it may affect the target reference points used for managing fishing effort and potential yields (Wortmann *et al.* 2020).

3.7 KEYWORDS

saucer scallop, *Ylistrum balloti*, trawl survey, sediment mapping, sediment properties, acoustic mapping, seabed mapping, backscatter, multibeam echosounder, natural mortality rate, Inverse Distance Weighted, Ordinary Kriging, Random Forest, Generalised Boosting Method.

4   Introduction

4.1   BACKGROUND

The Queensland saucer scallop (*Y. balloti*) trawl fishery was formerly the state's most valuable commercially fished species, with annual landings peaking at just under 2000 t (adductor muscle meat-weight) in 1993 valued at about $30 million. However, in recent years there has been growing concern over declining catches. A DAF quantitative assessment revealed that recent standardised catch rates were the lowest in the 39-year catch rate record and that the spawning stock ratio was likely to be less than 20% (Yang *et al.* 2016). The reported annual scallop catch of 201 t in 2015 was the lowest in the mandatory logbook database, which commenced in 1988. Based on the findings, the stock was concluded to be recruitment overfished. Publication of the assessment in late 2016 was coordinated with a DAF Ministerial announcement of significant management changes to the fishery and followed by discussions between Fisheries Queensland, scallop trawl fishers and processors in Tin Can Bay, Hervey Bay and Bundaberg. Under the Australian Government (2018) Fisheries Harvest Strategy Policy the assessment would likely result in closure of the fishery.

The quality of advice provided on the scallop stock status could be improved by targeted research aimed at improving the mortality rate estimates for the fishery. At present, the scallop assessment models are heavily influenced by a single published estimate of the natural mortality rate (*M*) by Dredge (1985a) from several decades ago. A second, updated estimate could benefit the assessment and provide insight into the current poor stock status. Furthermore, advances in mapping seafloor habitats (e.g., sediment profiles, seabed hardness) combined with high spatial resolution VMS data can be used to derive an improved understanding of fishing mortality rate (*F*). This assumes that *F* is not uniformly distributed, but rather a single unit of effort in the scallop's highly-preferred habitat removes a higher proportion of the population than the same level of effort in a less-preferred habitat. Studies on the relationships between seafloor properties and the Atlantic scallop (*Placopecten magellanicus*), which is the most valuable fished scallop globally, have led to improved monitoring and assessment of the stock (Smith *et al.* 2006; 2017; Miller *et al.* 2019).

This project aims to undertake innovative research to better-define key mortality rate estimates for the Queensland scallop stock. The study includes a fishery-independent survey of the abundance of 0+ and 1+ year old scallops in 2017, which is funded by the Queensland Government (i.e., project cash contribution). (Note, the Government subsequently funded the survey again in 2018 and 2019 and findings from all survey years are presented herein). The project addresses the FRDC National RD&E priority on well managed sustainable fisheries.

4.2   NEED

There is a strong need to improve the Queensland scallop stock assessment. This is achieved by undertaking a fishery-independent survey of the stock and by deriving improved mortality rate estimates used in the quantitative stock modelling. There is also a strong need to better understand the relationship between scallop abundance and benthic habitats. Information on scallop habitat can be used to explain variation in catch rate standardisation models, improving the indices of abundance. Classifying the scallop fishing grounds into habitat categories which receive varying levels of fishing effort can also improve the precision of fishing mortality (*F*) estimates. This can be achieved by measuring physical properties of the seafloor, such as bottom hardness and sediment composition, and relating them to scallop abundance.

As most of the scallop fishery is in waters of the Great Barrier Reef Marine Park (GBRMP), which is a World Heritage Area, there is an obligation to ensure that biodiversity and ecosystem services within the Park are maintained. The project addressed these needs by improving stock assessment advice. Finally, there is a need to maintain the WTO approval which is required to export saucer scallops. The project helped address the terms and conditions pertaining to sustainability of fishing

the stock required by the Commonwealth Department of Environment and Energy to secure this approval.

5 Objectives

1) Design and carry out a comprehensive fishery-independent survey of the 0+ and 1+ age classes in the Queensland saucer scallop fishery
2) Undertake exploratory analyses on the relationship between saucer scallop abundance and bottom substrate
3) Derive one or more tagging-based estimates of the saucer scallop's natural mortality rate (*M*)

6 Methods

The following brief method descriptions address each of the project objectives. More detailed descriptions of the methods can be found in the relevant Appendices using the hyperlinked sections and page numbers provided (press control+click).

6.1 OBJECTIVE 1. FISHERY-INDEPENDENT SURVEY

The scallop trawl survey was based on a stratified random design that was first implemented in 1997 (Dichmont *et al.* 2000). From 1997–2000 the survey was comprehensively implemented, but from 2001–2006 the number of strata and sample sites were reduced, and the survey ceased in 2006. In 2017 the full survey design was reintroduced and included two additional strata in the southern part of the fishery. Further details of the design can be found in section 16.3.1, page 44.

Between two and four commercial scallop vessels were chartered through a public tender process to undertake the survey each year over about 10 nights in October coinciding with the waxing lunar phase. Two DAF observers on board each vessel processed and recorded the catch details.

A generalised linear model (GLM) was used to derive calibration factors to adjust the survey catch rates for differences between participating vessels (section 16.4.2, page 59). The precision of the survey catch rates was improved by converting catch rates from number of scallops per 20 min shot (Jebreen *et al.* 2008), to number per hectare (ha) swept by the trawl nets. This required incorporating measures of net head rope length, net spread factors and distance trawled at each sample site to estimate swept area.

Three modelling approaches were used to examine the calibrated survey catch rates:
  1) density mapping via kriging (section 16.3.6, page 50),
  2) a weighted means method (Haddon 1997) (section 16.3.7, page 50), and
  3) a GLM which included year, strata, lunar phase, time-of-night and year-strata interaction explanatory terms to derive adjusted mean scallop densities (section 16.3.8, page 51) for each year and stratum.

In the early 2000s it became mandatory to include a TED and a second BRD in each trawl net in Queensland, including nets used for scientific surveys. The influence of these devices on the scallop survey catch rates was also examined.

In May 2019 the project undertook a pilot study to evaluate the use of seafloor images as a means of measuring scallop abundance, which included towing a still camera system over the 11 1-nm calibration transects inside the closed HBA SRA that were trawl sampled as part of the scallop fishery-independent survey in October 2018. The density of scallops was determined for each transect by manually processing the individual images (i.e., human annotation), which were then compared against the trawl survey densities. All the seafloor images were also processed using the AIMS autoclassification software BenthoBox (https://www.aims.gov.au/advanced-observation-

technologies/image-analysis) to determine if it could detect scallops in the images. Details of the methods for the pilot study and autoclassification software trial are provided in sections 17.3, page 97 and 17.4, page 103, respectively.

6.2 OBJECTIVE 2. EXPLORING SAUCER SCALLOP-SUBSTRATE RELATIONSHIPS

The methods for exploring relationships between scallop abundance and seabed properties were applied in the following steps:

1) collation of existing sediment datasets and field sampling to acquire additional sediment samples and seafloor backscatter data from 166 sites offshore from Gladstone and in Hervey Bay (section 18.3, page 120). The new samples were co-located with trawl samples of scallop abundance.
2) processing the newly acquired sediment samples and examining relationships between the sediment composition, grain size, backscatter and scallop abundance (section 19.3, page 142),
3) modelling and predicting sediment distributions in the southeast Queensland, including the scallop fishery spatial domain (section 20.3, page 158), and
4) modelling and predicting scallop distribution using multiple explanatory terms, including sediment properties from the existing and newly acquired sediment datasets (Table 6-1). Further details of the modelling methods can be found in section 21.3, page 203.

Table 6-1. Predictive variables used to model the distribution of saucer scallops.

Variable	Abbreviation	Source/Method
Banks	banks	Identifies the location of deep reef habitats
Bathymetry	bathy	Depth to the Seabed (Beaman 2010)
Coast_dist	coast	Distance from the coast (km)
Easting	east	Aspect of raster cell (x component)
Northing	north	Aspect of raster cell (y component)
x	x	'y' coordinate (latitude) of raster cell
y	y	'x' coordinate (longitude) of raster cell
Slope	slope	Slope gradient of the seabed (degrees from horizontal)
StdDev_1	stddev1	Standard deviation of bathymetry measured within a distance of 1 raster cell
StdDev_5	stddev5	Standard deviation of bathymetry measured within a distance of 5 raster cells
TPI	tpi	Topographic Position Index (measures of local concavity/flatness/convexity)
Gravel	gravel	Percent gravel from interpolated sediment data
Sand	sand	Percent sand from interpolated sediment data
Mud	mud	Percent mud from interpolated sediment data
MGS	mgs	Interpolated mean grainsize measured in Phi
Carbonate	carb	Interpolated Percent calcium carbonate
Very fine sand	vfs	Interpolated very fine sand (63–125 μm)
Fine sand	fs	Interpolated fine sand (125–250 μm)
Medium sand	ms	Interpolated medium sand (250–500 μm)
Coarse sand	cs	Interpolated coarse sand (500–1000 μm)
Very coarse sand	vcs	Interpolated very coarse sand and finer (1000–2000 μm)
Very fine sand2	vfs2	Interpolated very fine sand and finer (< 125 μm)
Fine sand2	fs2	Interpolated fine sand and finer (< 250 μm)
Medium sand2	ms2	Interpolated medium sand and finer (< 500 μm)
Coarse sand2	cs2	Interpolated coarse sand and finer (< 1000 μm)
Very coarse sand2	vcs2	Interpolated very coarse sand and finer (< 2000 μm)
Standard deviation	sd	Interpolated grainsize standard deviation measured in Phi
Skewness	skew	Interpolated grainsize skewness measured in Phi

6.2.1 Sediment data

A total of 166 sediment samples were obtained from 18 areas offshore from Gladstone and in Hervey Bay. The areas were targeted to provide a range of scallop habitats (e.g., high, medium, and low productivity) based on past commercial trawl fishing effort (see section 18.3.1, page 120). Acoustic mapping in the 18 areas identified areas of acoustically homogenous seabed that were then trawled and sampled. Two sediment samples were collected per trawl: one at the start and one at the end of each trawl. Sediment samples were collected using a 2 L Van Veen sediment grab and GPS coordinates were taken with each sample.

A sediment grainsize analysis was performed on each of the 166 samples (Wentworth 1922) and the data summarised through the G2sd package in Rstudio (Fournier *et al.* 2014) (section 18.3.2, page 123). Relationships were examined between 15 sediment grainsize variables, the percentage of calcium carbonate in each sample, seafloor backscatter intensity and scallop abundance. A Random Forest (RF) decision tree was used to predict backscatter values from the 15 summarised grainsize properties (see Figure 19-5, page 148). Correlation plots were used to identify significant explanatory variables. Line plots of the grainsize frequency distributions of each sediment sample were plotted by location, and sediment samples linked to the five most productive scallop trawls in each location were highlighted to identify potential patterns. Further details of the statistical methods can be found in section 19.3.5, page 146.

6.2.2 Modelling sediment distributions

A detailed description of the methods used to model sediment distributions is provided in section 20.3, page 158. The modelling was based on over 2000 sediment samples obtained from the Geoscience Australia's MARine Sediment (MARS) database, previous studies, and the 166 recently acquired samples (Table 20-1, page 161). Inverse Distance Weighted (IDW), three variants of RF, three variants of Generalised Boosting Method (GBM), and four variants of hybrid methods were used to predict the distribution of six seabed sediment properties (mud, sand, gravel, calcium carbonate, mean grainsize and fine sand) in southeast Queensland. Predictions using a simple IDW method were used as a baseline to be compared against RF, GBM, and their hybrid methods. RF, GBM and their hybrid methods used up to 11 covariates to aid predictions of sediment distribution (Table 20-2, page 163). The best performing models for each sediment parameter were identified by ranking based on the Variance Explained by cross validation (VEcv) for each model (Li *et al.* 2017).

6.2.3 Modelling scallop distributions

Details of the methods used to model the distribution of scallops in southeast Queensland are provided in section 21.3, page 203. Model covariates included nine derivatives of the bathymetry and 17 sediment raster layers. In preliminary analyses, Pearson's correlation coefficient was used to estimate the strength of the linear relationships between scallops and predictor variables. Correlations between 0.3 and 0.4 were considered weak, greater than 0.4 were considered moderate, and correlations less than 0.3 were considered to indicate the absence of a linear correlation. Predictions of scallop density were undertaken for each year that a comprehensive scallop survey was undertaken (i.e., seven years, 1997–2000 and 2017–2019). The R package 'spm', which was used for the spatial predictive modelling (Li 2019a), implements IDW, geostatistical (OK) and machine learning (RF) methods as well as their hybrid methods for spatial predictions (Table 6-2).

The four variants of RF were designed to assess the impact of adding latitudinal and longitudinal, basic sediment grainsize parameters, and high-resolution sediment grainsize parameters. Ten-fold cross validation was used to assess the optimum model parameters for the IDW, OK, and RF models. In 10-fold cross validation the input data are resampled evenly into 10 data subsets. Of these subsets, one was retained for validation while the remaining nine are used for model training. The cross validation was then repeated 10 times using each of the data subsets for validation each time. The models were run using each combination of model parameters and the optimum model was selected on the basis of the largest VEcv metric (Li 2017).

Table 6-2. Models used to predict the distribution of saucer scallops. Each model was applied to each year of the seven years of full survey data (i.e., 1997–2000, 2017–2019).

Method	Test
IDWd	Default IDW interpolation
IDW	Optimised IDW interpolation
OK	Ordinary Kriging Interpolation
RF	Random Forest – excluding X/Y
RF_en	Random Forest – including X/Y
RF_en_sed	Random Forest – including X/Y and basic sediment grainsize statistics
RF_en_sed_phi	Random Forest – including X/Y and all sediment grainsize statistics

The best performing method over the seven years of scallop surveys was identified by ranking each year from 1–7 based on its highest rank, modal rank, and average rank. For all methods, the average scallop densities were calculated using the predictions for all years in the study. Visual inspection of the best methods was then undertaken to make comparisons between methods and identify artefacts.

6.3   OBJECTIVE 3. ESTIMATING THE SCALLOP'S NATURAL MORTALITY RATE

Details of the tag-recapture experiment and statistical methods used to analyse the data and quantify the natural mortality rate (M) of the scallops are provided in section 22.3, page 234. Three approaches were applied to the experimental design and data analyses. The new estimates of M were compared against those of Dredge (1985a).

The first approach was based on the Brownie *et al.* (1985) Model 1 for measuring the survival and recovery rate of birds that were banded and recovered annually (section 22.3.3, page 237). This method is based on the earlier work of Seber (1970) and Robson and Youngs (1971) which uses the ratio of recoveries from annual bandings, and can be applied to many species including fish. The general design of the experiment is shown in Table 6-3 using the following notation:

N_i is the number of animals banded and released at the start of ith episode, $i = 1,…,k$.
R_{ij} is the number animals recovered in year j from releases in episode i, $i = 1,…,k$, $j = 1,…,l$.

Table 6-3. General design of the Brownie *et al.* (1985) Model 1 to measure recovery and survival rates.

Episode of release	Number tagged	1	2	3	4	5 = l
1	N_1	R_{11}	R_{12}	R_{13}	R_{14}	R_{15}
2	N_2		R_{22}	R_{23}	R_{24}	R_{25}
3	N_3			R_{33}	R_{34}	R_{35}
4 = k	N_4				R_{44}	R_{45}

To ensure the tagged population was not affected by fishing mortality (F), the experiment was conducted inside two SRAs (Hervey Bay A and Yeppoon B) which have been closed to trawling since late 2016 (see Figure 7-7, page 21). Batches of scallops were tagged, released and recaptured inside the closures over a period of 15 months from May 2018 to August 2019. The tagging and recapture episodes were conducted in May 2018 (trip 1), October 2018 (trip 2), March 2019 (trip 3), May 2019 (trip 4) and August 2019 (trip 5). No recaptures were made immediately after release, meaning that $R_{ii} = 0$. Also, no recaptures were made until trip 3, so $R_{12} = 0$.

The second approach to analysing the tagging data was a modification of the Brownie *et al.* (1985) Model 1 which avoided using annual ratios and assumed a constant daily rate for M (section 22.3.4, page 238). The third approach was based on a binomial logistic regression model of the probability of

recapturing tagged scallops over time and included fixed categorical terms and covariates (section 22.3.5, page 239).

All field work for the experiment, including the initial capture of the scallops by beam trawling, tagging, releases and recaptures, was undertaken on board the DAF 14.5 m *RV Tom Marshall* out of the ports of Bundaberg and Yeppoon. For each trip, it took 1–2 days to complete trawl sampling of the recaptured scallops, followed by another 2–3 days to catch, tag and release additional scallops at each SRA. Between 1335 and 2059 scallops were tagged and released inside each SRA each trip. The shell height (SH) of scallops was measured to the nearest millimetre at the time of tagging and recapture. Individually numbered Hallprint FPN glue-on 8 mm yellow tags were glued onto the left valve (i.e., brown valve, Figure 22-1, page 236) of each scallop using cyanoacrylate glue.

The methods addressed the following assumptions to make inferences from the tagging data:
1) Recaptured tagged scallops are representative of the scallop population.
2) The survival rate of the scallops was not affected by the tagging process, including being recaptured one or more times.
3) Emigration of scallops from inside to outside of the recapture grid was negligible.
4) Tag loss throughout the experiment was negligible.
5) The decline in the tagged population over time was not affected by fishing.
6) Scallops released during different tagging trips were well mixed by the time they were recaptured.
7) The logistic model accounted for variation in catchability of recaptured tagged scallops.

7 Results

The following are summaries of the results for each objective. Further results can be found in the relevant Appendices using the hyperlinked sections and page numbers provided (press control+click).

7.1 OBJECTIVE 1. FISHERY-INDEPENDENT SURVEY

The size-frequency distributions of measured scallops from the surveys show a bimodal distribution in most years and are consistently dominated by the 1+ age class (i.e., $\geq$ 78 mm SH). The relatively low number of 0+ scallops (i.e., < 78 mm SH) is consistent with previous studies (Dichmont *et al.* 2000; Courtney *et al.* 2008; Campbell *et al.* 2010b) and suggests that the survey is relatively inefficient at sampling this age class, possibly due to the behaviour and catchability of small scallops in relation to the trawl gear. There was no evidence to suggest a decline in the maximum size of the scallops, however, even though the catchability of the 0+ age class is low, the relative contribution of the 0+ scallops may be declining over the survey time series and this was particularly reflected in the 2019 size-frequency (Figure 7-1).

Density maps of the 0+ and 1+ age classes and total scallops, based on kriging, are provided in Figures 16-17 to 16-29. By focusing on those years when the survey was comprehensively implemented (i.e., omitting 2001–2006, when the survey design was scaled back), it is apparent that densities have declined from the early surveys (1997–2000) to recent years (2017–2019). Note the declining amount of red areas (i.e., high density) over time in the maps. An example is provided below in Figure 7-2 comparing total scallop densities in 1997 and 2019.

The weighted mean densities for the 0+ and 1+ age classes (i.e., Haddon 1997 method), and total scallops are provided in Table 16-5, page 78. Scallop densities were highest in 2001 for the total number of scallops and the 1+ age class, while the 0+ age class density peaked in 1997. Densities for total scallops and the 0+ age class were both at a minimum in 2019, while the 1+ age class experienced its lowest density in 2017.
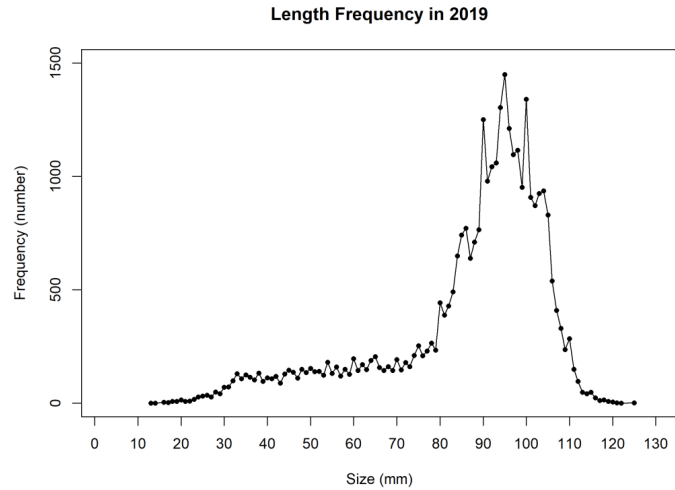
Figure 7-1. Size-frequency plot of saucer scallops measured in October 2019. The mode for the 0+ age class (i.e., 30–70 mm SH) is weak and may be indicative of a poor commercial catch in the 2021 fishing year (i.e., Nov 2020–Oct 2021). Adjusted mean densities for the 0+ age class in 2019 were the lowest in the survey time series.
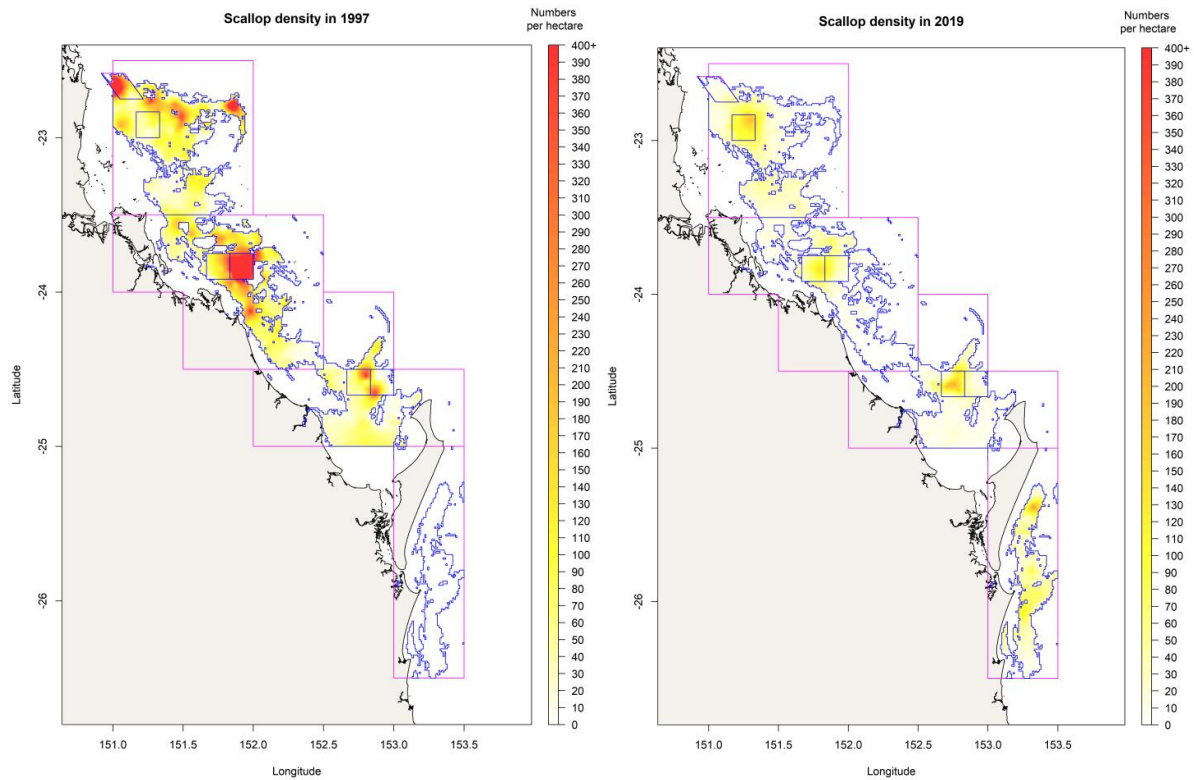
Figure 7-2. Total scallop densities in 1997 (left) and 2019 (right) derived from kriging the calibrated scallop survey data. The blue boundary outlines the extent of the fishery. Note the lack of high densities (red) in 2019 compared 1997. The southern extent of the scallop fishery east of Fraser Island was not included in the survey prior to 2017.

While the kriging maps and the weighted means provide information on the scallop population size, they are based on the raw calibrated catch rates, which don't consider some significant factors affecting the catch rates within and between survey years. In contrast, the adjusted mean densities are from a GLM that considers the influence of several explanatory terms (e.g., year, strata, lunar phase and time-of-night) and provides a more reliable measure for comparing densities across years. Adjusted mean scallop densities for each survey year and strata are provided below for 0+ age class (Table 7-1), 1+ age class (Table 7-2) and total scallops (Table 7-3). The two survey strata labelled MNP-24-1173 and MNP-23-1169 are green zones and were only sampled in 2017 at the request of industry and with approval from the GBRPMA. Similarly, grid W32 was only sampled in 2002.

In general, the adjusted means indicate that the density of 0+ age class, 1+ age class and total scallops have declined by about half from the early survey years 1997–2000 to the recent years 2017–2019. The density of the 1+ age class is typically 4–5 times higher than the 0+ age class. The adjusted mean 0+ densities in 2019 were the lowest for the survey time series, and indicate that the commercial catch for the 2021 fishing year (i.e., Nov 2020 to Oct 2021) is likely to be low.

7.1.1 Potential of a towed camera survey

A total of 14,657 useable images of the seafloor was obtained from the 11 trawl transects inside the HBA SRA in May 2019 from the towed camera pilot study. Approximately 1300 images were obtained for each transect (see section 17.3, page 97). Data on scallop presence, sediment type and macrobiota were recorded by manually examining each image (Figure 7-3). The overall mean density from the images was 657 scallops ha^{-1}, compared to a mean of 188 ha^{-1} from the trawl survey a few months earlier in October 2018. Although the two surveys were undertaken seven months apart, the results indicate that the towed camera system detects 3–4 times more scallops than the trawl survey and is therefore likely to produce a more accurate estimate of absolute scallop abundance. The AIMS autoclassification software grossly overestimated the presence of scallops in the images. Manual processing indicated scallops were present in about 1% of images, whereas the software incorrectly detected scallops in 26%. Because the scallops were comparatively rare in the images, the sample size of images used to train the software was quite small (i.e., 95 images with scallops present). The software could be improved with more training, but at present it is not suitable for processing images and any towed camera-based survey would still rely upon human annotation to quantify scallop catch rates.

Figure 7-3. Sample of seafloor images with scallops present from the towed camera pilot study in May 2019.

Table 7-1. Adjusted 0+ density of saucer scallops (number per hectare) for each stratum sampled throughout the fishery-independent scallop trawl surveys. Blank cells indicate that the stratum was not sampled in a given survey year. Standard errors are in italics.

Year	Strata																			
	BHA	BHB	HBA	HBB	Maheno	MNP-24 -1173	MNP-23 -1169	S28	S29	SUN	T28	T29	T30	U30	U31	V31	V32	W32	YA	YB
1997	77.9 *(20.7)*	106.4 *(25.8)*	81.1 *(22.4)*	28.1 *(14.0)*				83.4 *(7.6)*	23.3 *(4.6)*		27.8 *(4.6)*	45.4 *(7.3)*	59.2 *(7.4)*	45.3 *(9.3)*	19.8 *(3.8)*	15.2 *(4.1)*	17.7 *(3.4)*			18.4 *(8.2)*
1998	40.3 *(15.9)*	39.0 *(13.7)*	25.3 *(9.0)*	30.3 *(16.9)*				21.6 *(5.1)*	9.4 *(2.8)*		12.3 *(3.4)*	9.6 *(3.7)*	17.7 *(3.7)*	6.5 *(3.1)*	6.0 *(2.1)*	4.8 *(2.0)*	4.7 *(1.7)*		21.7 *(8.7)*	
1999	29.9 *(15.7)*	47.0 *(17.4)*	226.7 *(24.0)*	175.7 *(22.2)*				17.0 *(3.2)*	8.7 *(3.3)*		6.8 *(2.1)*	15.8 *(4.5)*	35.8 *(5.1)*	15.1 *(5.3)*	13.5 *(2.8)*	19.3 *(4.4)*	40.9 *(4.8)*		55.5 *(12.1)*	
2000	33.9 *(16.6)*	36.7 *(15.7)*	141.7 *(26.3)*	107.9 *(16.0)*				56.1 *(5.5)*	7.6 *(2.6)*		32.9 *(5.6)*	15.1 *(4.5)*	19.1 *(3.6)*	21.1 *(5.7)*	8.6 *(2.4)*	3.2 *(1.5)*	12.3 *(2.9)*		117.5 *(23.5)*	
2001	74.1 *(14.2)*	46.1 *(9.6)*	12.9 *(5.2)*	12.3 *(5.0)*									24.4 *(5.4)*						162.4 *(24.1)*	14.1 *(6.8)*
2002	24.1 *(6.8)*	24.6 *(7.0)*	12.3 *(4.9)*	2.1 *(1.9)*									11.4 *(3.3)*				23.8 *(19.3)*	8.2 *(13.8)*	111.5 *(18.9)*	51.1 *(11.9)*
2003	52.6 *(12.7)*	41.3 *(11.2)*	35.6 *(10.0)*	6.5 *(3.1)*									11.1 *(3.1)*						36.7 *(11.4)*	21.5 *(7.7)*
2004	38.5 *(9.3)*	71.5 *(16.9)*	83.6 *(14.0)*	14.3 *(5.0)*									21.4 *(4.7)*						62.4 *(14.5)*	31.4 *(10.5)*
2005	42.3 *(8.3)*	14.8 *(5.0)*	21.1 *(6.1)*	3.4 *(2.3)*									6.7 *(1.8)*						104.0 *(20.0)*	71.5 *(15.4)*
2006	19.3 *(5.3)*	11.2 *(5.6)*	7.8 *(4.2)*	36.4 *(9.9)*									9.9 *(2.5)*						49.1 *(14.6)*	12.5 *(6.4)*
2017	53.6 *(13.9)*	13.1 *(6.5)*	21.0 *(4.0)*	3.1 *(2.8)*	8.6 *(4.3)*	39.1 *(12.4)*	7.7 *(2.5)*	27.7 *(5.9)*	5.6 *(2.0)*	4.9 *(1.7)*	8.0 *(2.0)*	1.3 *(1.1)*	7.1 *(2.7)*	1.9 *(2.6)*	14.7 *(4.4)*	4.3 *(3.0)*	45.2 *(10.3)*		65.5 *(14.3)*	20.8 *(7.5)*
2018	24.5 *(10.8)*	60.1 *(11.4)*	35.8 *(6.5)*	1.8 *(2.3)*	19.2 *(4.1)*			23.1 *(4.2)*	27.8 *(5.0)*	21.9 *(3.7)*	5.1 *(1.4)*	12.9 *(3.1)*	6.1 *(3.0)*	5.0 *(2.3)*	18.8 *(6.3)*	8.9 *(4.3)*	6.7 *(3.4)*		47.4 *(12.3)*	40.4 *(10.7)*
2019	33.0 *(20.5)*	9.5 *(5.2)*	20.6 *(4.7)*	9.7 *(5.4)*	4.2 *(1.9)*			12.5 *(3.1)*	12.1 *(3.5)*	4.1 *(1.6)*	2.8 *(1.2)*	15.7 *(4.2)*	5.9 *(2.7)*	1.6 *(1.4)*	2.3 *(1.7)*	6.6 *(3.4)*	3.7 *(2.3)*		10.8 *(4.3)*	19.4 *(7.9)*

Table 7-2. Adjusted 1+ density of saucer scallops (number per hectare) for each stratum sampled throughout the fishery-independent scallop trawl surveys. Blank cells indicate that the stratum was not sampled in a given survey year. Standard errors are in italics.

Year	BHA	BHB	HBA	HBB	Maheno	MNP-24 -1173	MNP-23 -1169	S28	S29	SUN	T28	T29	T30	U30	U31	V31	V32	W32	YA	YB
1997	232.5 (*57.9*)	494.1 (*93.8*)	162.9 (*50.4*)	71.9 (*36.6*)				61.9 (*9.7*)	13.1 (*5.5*)		33.4 (*8.0*)	38.0 (*8.0*)	68.2 (*12.5*)	41.6 (*13.4*)	37.3 (*8.4*)	3.6 (*3.2*)	12.5 (*4.7*)			34.6 (*19.0*)
1998	653.3 (*180.9*)	470.2 (*145.8*)	413.2 (*112.7*)	382.7 (*189.5*)				180.9 (*37.0*)	70.3 (*17.4*)		65.0 (*18.6*)	50.1 (*14.3*)	161.2 (*23.3*)	35.1 (*20.3*)	115.0 (*23.2*)	30.8 (*14.9*)	104.7 (*24.9*)		211.0 (*79.1*)	
1999	124.6 (*52.4*)	260.5 (*66.4*)	212.1 (*35.2*)	49.6 (*18.4*)				36.8 (*7.4*)	37.7 (*11.0*)		4.8 (*2.7*)	33.6 (*8.9*)	68.0 (*9.5*)	51.0 (*15.5*)	41.2 (*7.8*)	8.2 (*4.4*)	36.6 (*7.2*)		71.5 (*20.9*)	
2000	485.9 (*107.0*)	216.2 (*64.0*)	361.9 (*70.1*)	82.6 (*22.6*)				87.4 (*10.9*)	16.1 (*6.2*)		56.9 (*11.7*)	48.4 (*13.4*)	60.2 (*9.5*)	49.6 (*14.3*)	15.3 (*5.2*)	2.6 (*2.1*)	34.7 (*7.9*)		401.9 (*71.1*)	
2001	358.6 (*56.1*)	237.0 (*36.2*)	198.8 (*33.5*)	9.5 (*7.1*)									66.0 (*14.0*)						416.1 (*59.4*)	326.9 (*53.9*)
2002	82.7 (*20.5*)	142.4 (*27.8*)	65.7 (*18.6*)	20.1 (*9.3*)									30.3 (*7.9*)				45.4 (*43.0*)	9.0 (*23.7*)	28.1 (*14.5*)	12.4 (*9.2*)
2003	81.3 (*31.7*)	318.8 (*83.5*)	100.5 (*41.3*)	17.5 (*15.1*)									193.1 (*38.7*)						121.9 (*52.6*)	456.1 (*115.2*)
2004	353.1 (*55.4*)	198.1 (*44.1*)	402.6 (*50.6*)	35.9 (*13.0*)									43.5 (*10.3*)						16.5 (*11.6*)	96.8 (*29.3*)
2005	19.4 (*8.2*)	44.3 (*14.8*)	116.1 (*26.1*)	6.3 (*5.3*)									43.7 (*8.1*)						71.0 (*23.7*)	135.4 (*34.2*)
2006	102.8 (*28.7*)	165.4 (*41.7*)	153.2 (*36.2*)	58.1 (*21.6*)									196.5 (*30.2*)						254.6 (*55.9*)	211.1 (*46.5*)
2017	26.4 (*12.6*)	42.1 (*17.0*)	133.5 (*20.6*)	36.2 (*30.1*)	2.2 (*6.3*)	17.7 (*20.2*)	27.0 (*12.4*)	85.9 (*18.2*)	64.1 (*20.3*)	115.3 (*14.2*)	38.3 (*9.9*)	4.8 (*4.9*)	12.1 (*5.6*)	0.4 (*1.7*)	18.0 (*12.2*)	1.3 (*4.3*)	134.6 (*35.6*)		1.6 (*3.2*)	260.3 (*81.9*)
2018	268.8 (*60.5*)	483.7 (*56.3*)	274.1 (*37.4*)	16.0 (*11.1*)	1.0 (*1.5*)			103.7 (*14.8*)	47.8 (*10.4*)	10.0 (*4.0*)	7.1 (*2.6*)	16.9 (*5.6*)	19.5 (*8.6*)	8.6 (*4.7*)	115.5 (*24.8*)	25.3 (*12.0*)	110.1 (*22.8*)		98.1 (*28.6*)	140.2 (*32.7*)
2019	24.3 (*22.2*)	130.5 (*34.7*)	235.1 (*33.7*)	29.0 (*15.3*)	64.2 (*12.3*)			37.1 (*8.3*)	30.4 (*9.0*)	78.7 (*12.8*)	2.6 (*1.9*)	22.6 (*7.8*)	29.4 (*10.0*)	2.5 (*2.9*)	3.0 (*3.0*)	7.0 (*5.8*)	12.6 (*6.8*)		66.6 (*17.7*)	253.5 (*45.5*)

Table 7-3. Adjusted total density of saucer scallops (number per hectare) for each stratum sampled throughout the fishery-independent scallop trawl surveys. Blank cells indicate that the stratum was not sampled in a given survey year. Standard errors are in italics.

Year	BHA	BHB	HBA	HBB	Maheno	MNP-24 -1173	MNP-23 -1169	S28	S29	SUN	T28	T29	T30	U30	U31	V31	V32	W32	YA	YB
1997	313.3 (*68.8*)	601.5 (*104.4*)	246.3 (*63.8*)	100.3 (*43.8*)				146.4 (*15.7*)	37.3 (*9.6*)		61.4 (*11.2*)	75.0 (*12.4*)	128.4 (*17.6*)	84.3 (*19.8*)	57.9 (*10.7*)	19.1 (*7.3*)	30.4 (*7.4*)			54.3 (*24.2*)
1998	717.4 (*182.5*)	542.6 (*148.0*)	449.0 (*110.9*)	435.0 (*191.4*)				230.0 (*40.4*)	84.6 (*18.8*)		92.0 (*21.8*)	60.7 (*15.9*)	201.0 (*25.2*)	51.3 (*23.9*)	121.9 (*22.9*)	42.9 (*16.6*)	108.0 (*23.6*)		256.4 (*83.7*)	
1999	171.6 (*65.6*)	336.5 (*79.3*)	443.9 (*53.3*)	230.5 (*41.3*)				55.1 (*9.4*)	51.7 (*13.8*)		11.3 (*4.3*)	90.5 (*12.9*)	105.1 (*12.3*)	66.6 (*18.1*)	55.3 (*9.3*)	29.2 (*8.8*)	77.7 (*10.8*)		124.0 (*28.5*)	
2000	524.8 (*112.5*)	252.5 (*70.0*)	507.1 (*84.1*)	191.1 (*35.1*)				144.4 (*14.3*)	23.8 (*7.7*)		89.9 (*15.1*)	64.4 (*15.7*)	73.7 (*9.3*)	71.0 (*17.5*)	24.1 (*6.6*)	5.8 (*3.2*)	47.4 (*9.4*)		521.8 (*82.4*)	
2001	500.9 (*62.8*)	302.5 (*37.1*)	211.3 (*31.2*)	21.9 (*9.9*)									92.1 (*14.4*)						615.5 (*62.1*)	364.6 (*48.2*)
2002	106.8 (*21.0*)	161.3 (*26.7*)	75.7 (*18.1*)	24.6 (*9.8*)									46.0 (*8.6*)				66.7 (*47.6*)	16.8 (*29.3*)	131.3 (*26.4*)	65.7 (*17.9*)
2003	231.7 (*50.8*)	404.7 (*84.0*)	206.6 (*53.9*)	38.9 (*19.8*)									221.5 (*36.2*)						234.8 (*61.3*)	471.7 (*95.8*)
2004	444.7 (*57.3*)	311.0 (*54.0*)	477.0 (*49.7*)	51.5 (*14.2*)									12.3 (*72.9*)						95.5 (*23.9*)	158.9 (*31.1*)
2005	63.5 (*15.8*)	60.2 (*17.5*)	138.6 (*28.3*)	9.9 (*6.8*)									50.9 (*8.8*)						178.1 (*40.2*)	211.1 (*43.9*)
2006	150.9 (*35.0*)	196.2 (*47.1*)	177.9 (*39.9*)	112.9 (*32.3*)									218.0 (*30.5*)						336.5 (*67.2*)	251.3 (*52.6*)
2017	78.1 (*24.5*)	61.1 (*22.4*)	156.0 (*21.4*)	42.1 (*30.8*)	30.1 (*22.4*)	138.6 (*56.7*)	48.8 (*16.4*)	167.0 (*27.5*)	74.7 (*20.9*)	121.0 (*14.6*)	60.5 (*12.3*)	7.8 (*6.5*)	21.5 (*8.1*)	2.3 (*4.5*)	64.8 (*23.1*)	12.0 (*12.9*)	268.0 (*52.5*)		218.8 (*45.3*)	297.4 (*82.6*)
2018	331.5 (*70.3*)	553.1 (*60.1*)	347.1 (*41.1*)	17.8 (*12.0*)	20.3 (*6.9*)			127.6 (*16.7*)	75.8 (*13.5*)	32.6 (*7.4*)	12.3 (*3.5*)	29.8 (*7.6*)	26.6 (*10.4*)	14.8 (*6.6*)	152.2 (*30.2*)	34.4 (*14.2*)	126.5 (*25.4*)		145.7 (*35.6*)	181.3 (*37.8*)
2019	48.7 (*33.7*)	141.0 (*35.9*)	287.1 (*36.3*)	38.9 (*18.1*)	68.6 (*12.9*)			49.8 (*9.9*)	42.9 (*11.0*)	83.4 (*13.0*)	5.4 (*2.8*)	37.9 (*10.4*)	35.6 (*11.2*)	4.3 (*4.0*)	5.4 (*4.2*)	13.6 (*8.2*)	17.3 (*8.3*)		78.0 (*19.5*)	280.7 (*49.06*)

7.2   OBJECTIVE 2. SAUCER SCALLOP-SUBSTRATE RELATIONSHIPS

7.2.1   Analysis of sediment, backscatter and scallop abundance samples

An analysis of the 166 sediment samples obtained offshore from Gladstone and in Hervey Bay is provided in section 18.4, page 124. Collectively, the previous studies (Maxwell and Maiklem 1964; Marshall 1977, 1980; Davies and Tsuji 1992) and the newly acquired samples indicate that sediments in southeast Queensland are dominated by sand, with a highly variable gravel component and generally low mud content (< 5%). The new samples a) showed a peak in carbonate concentration of 10–30% suggesting the sediments were dominated by terrigenous, land-based sources, and b) were dominated by 'fine sand' (125–250μm), which is similar to sediments from Fraser Island, and is thought to be due to the transportation of sediments by waves and longshore currents from further south (Boyd *et al.* 2004).

Analyses of the 166 co-located sediment, backscatter and scallop samples indicated that sediments at sites with the highest scallop abundance were mainly composed of fine sand (125–250μm) (Figure 7-4). Scallop abundance was significantly correlated with the percentage of fine sand in the sediments in the offshore Gladstone area ($R^2 = 0.5409$), possibly indicating preferred habitat. However, the relationship was not significant in Hervey Bay ($R^2 = 0.1187$).
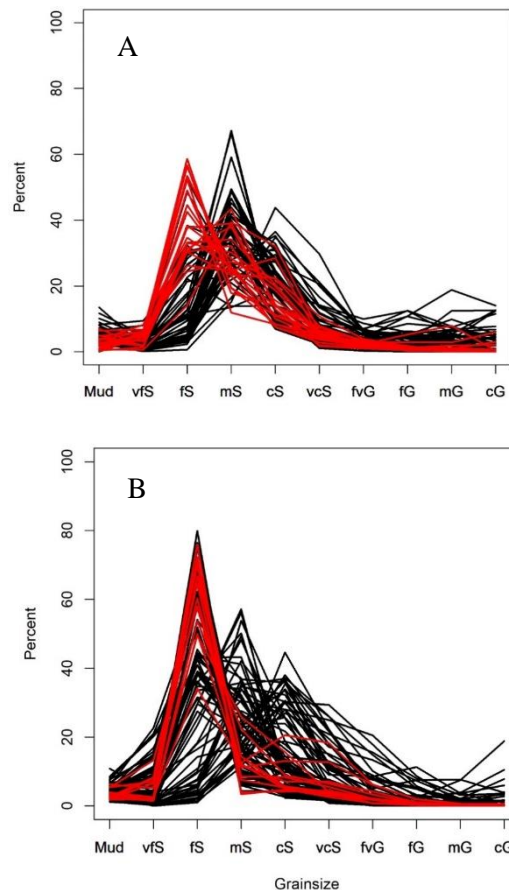
Figure 7-4. Grainsize-frequency distributions for all sediment samples from A) Gladstone offshore and B) Hervey Bay. The five trawls with the highest scallop abundance (in red) generally follow the same sediment grainsize distribution pattern with peak percentages of fine sand.

At both the Gladstone and Hervey Bay sites, saucer scallops primarily occurred on sediments that have a relatively narrow range of comparatively low backscatter intensity values (Figure 19-4, page 147). Of the 15 sediment variables considered, fine sand was the most important variable in predicting

backscatter values (Figure 19-5, page 148). Further details are provided in section 19.4, page 146. It is important to note that while analysis of the data from the 166 sites indicated that fine sand may be an important explanatory variable for scallop distribution, it was not the most important variable found when modelling scallop distribution at the regional level (see further results below).

7.2.2 *Modelling sediment distributions*

Comparisons of the sediment distribution models are provided in section 20.4, page 166. The results showed that: 1) sediment models improved when latitude and longitude were included as covariates, 2) models that used only sediment data that had co-located high-resolution bathymetry measures commonly outperformed models that used the entire sediment dataset which included interpolated bathymetry data, and 3) a hybrid model between IDW and GBM that only used samples that were co-located with high-resolution bathymetry measures was the most accurate on average.

Model predictions for the distribution of mud and calcium carbonate were the most accurate with a VEcv of 76.1 and 82.3, respectively. Predictions for gravel, using the highest-ranking model (i.e., IDW) were the least accurate with a VEcv of 33.0. Sampling of the 166 sites offshore from Gladstone and in Hervey Bay indicated scallop abundance was correlated with the sedimentary fraction of fine sand, possibly indicating details of the scallop's preferred habitat. The derived map for fine sand is provided in Figure 7-5 and additional maps showing the predicted distributions for all sediment types are provided on pages 193–198.
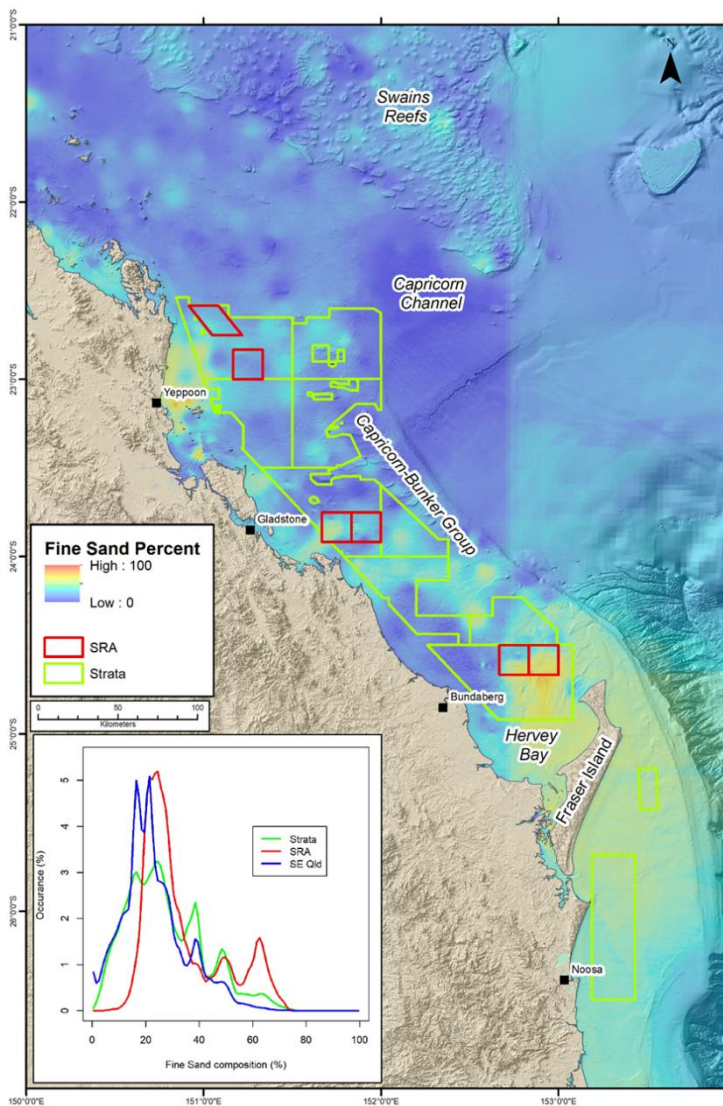
Figure 7-5. Example of the predicted distribution of seabed fine sand content in southeast Queensland using the GBMIDWb model overlaid on bathymetry. Also shown are key geographic areas, saucer scallop fishery survey strata and the scallop replenishment areas (SRAs). Distribution curves of interpolated pixel values indicate the percentage of fine sand predicted within the survey strata, SRAs and southeast Queensland.

7.2.3   *Modelling scallop distributions*

A comparison of the models used to predict saucer scallop distributions is provided in section 21.4, page 208. Inverse Distance Weighted (IDW), Ordinary Kriging (OK), and four variants of Random Forest (RF) were used to predict the distribution of saucer scallops within the scallop fishing grounds from 1997–2000 and 2017–2019. Two of the RF models contained regional sediment data layers to assess the degree to which sediment distribution data would improve predictions of scallop densities.

Pearson's correlation coefficients showed that very coarse sand, coarse sand, mean grainsize, skewness, medium sand2 (i.e., mean sand and finer sediment), and mud variables had low to moderate correlations with scallops in most years but commonly did not contribute greatly to improved model accuracy. The inclusion of sediment data improved the model predictions in some years but was generally outperformed by OK and a simple RF model using latitude, longitude and bathymetric derivatives only.

The RF_en and OK models were the two best scallop predictors. Predictions from both models for all years identified areas of high scallop densities in and around the SRAs, consistent with previous surveys (Jebreen *et al.* 2008). The OK model reproduced localised peaks and troughs in the sample datasets while the RF model produced a more generalised result (Figure 7-6).
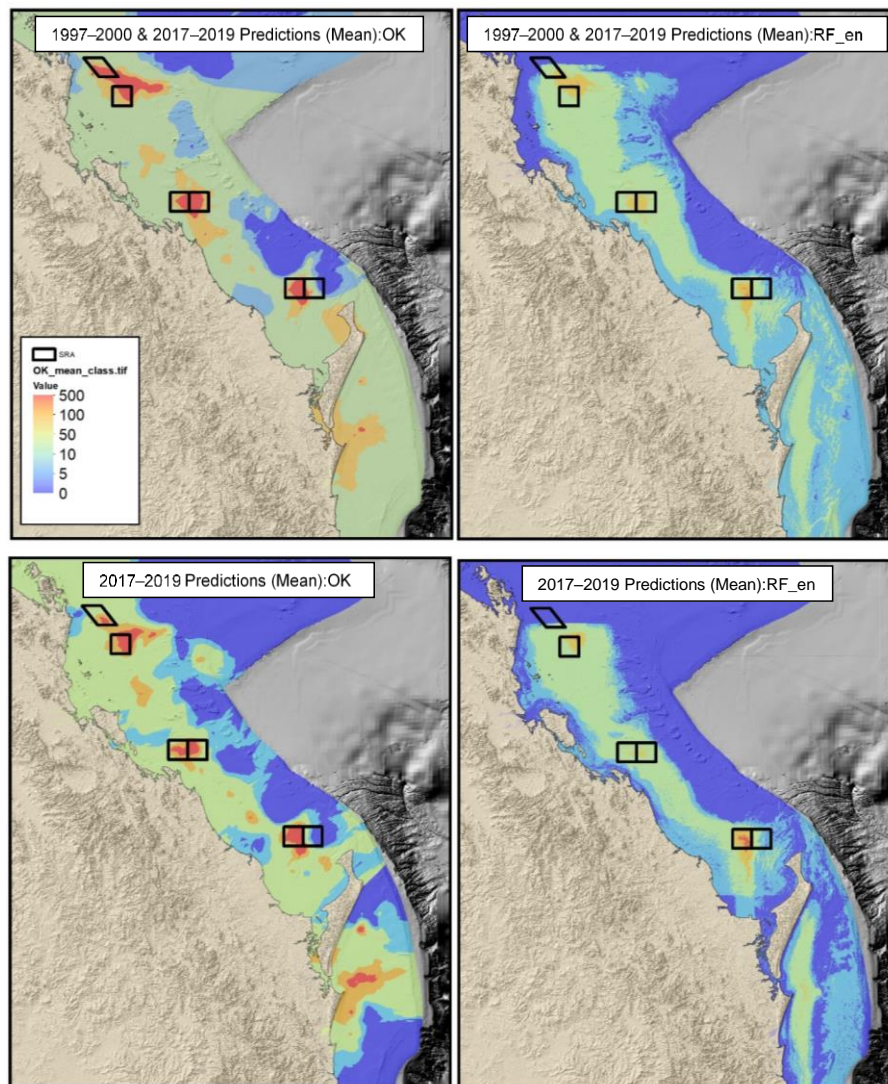
Figure 7-6. The maps show predicted mean scallop densities for the OK and RF_en models. The two upper maps use scallop survey data from 1997–2000 and 2017–2019, while the lower two maps use data from only the 2017–2019 surveys. Note the OK model tends to overestimate the spatial distribution of scallops close to the coast.

The RF predictions were comparatively smooth, with peaks of lower amplitude, compared to the OK predictions. The application of covariates within the RF_en models (i.e., RF model that includes latitude and longitude) results in a more spatially constrained and realistic model of scallop distribution with comparatively few scallops predicted towards the shelf-edge and near the coast (Figure 7-6), consistent with general observations of the scallop stock distribution. As a result, both the OK and RF_en models have strengths and weaknesses when predicting scallop distributions from yearly surveys. The predicted distributions for each survey year (i.e., 1997–2000 and 2017–2019) are provided on pages 226–229.

7.3   OBJECTIVE 3. ESTIMATING THE SCALLOP'S NATURAL MORTALITY RATE

Results from the tagging experiment are provided in section 22.4, page 240. A total of 13,295 scallops were tagged and released in the two SRAs during the four tagging trips (trip 1 May 2018, trip 2 October 2018, trip 3 March 2019 and trip 4 May 2019). A total of 526 tagged scallops were recaptured during the study (see Table 22-6, page 242). Periods at liberty for the 226 recaptured scallops in HBA ranged from 55 to 456 days, with a mean of 171.7 (s.e. 7.4) days, while periods at liberty for the 300 recaptures at YB ranged from 73 to 453 days, with a mean of 205.4 (s.e. 6.0) days. Details of the tagging study location, release sites and distribution of recaptured tagged scallops are provided in Figure 7-7.
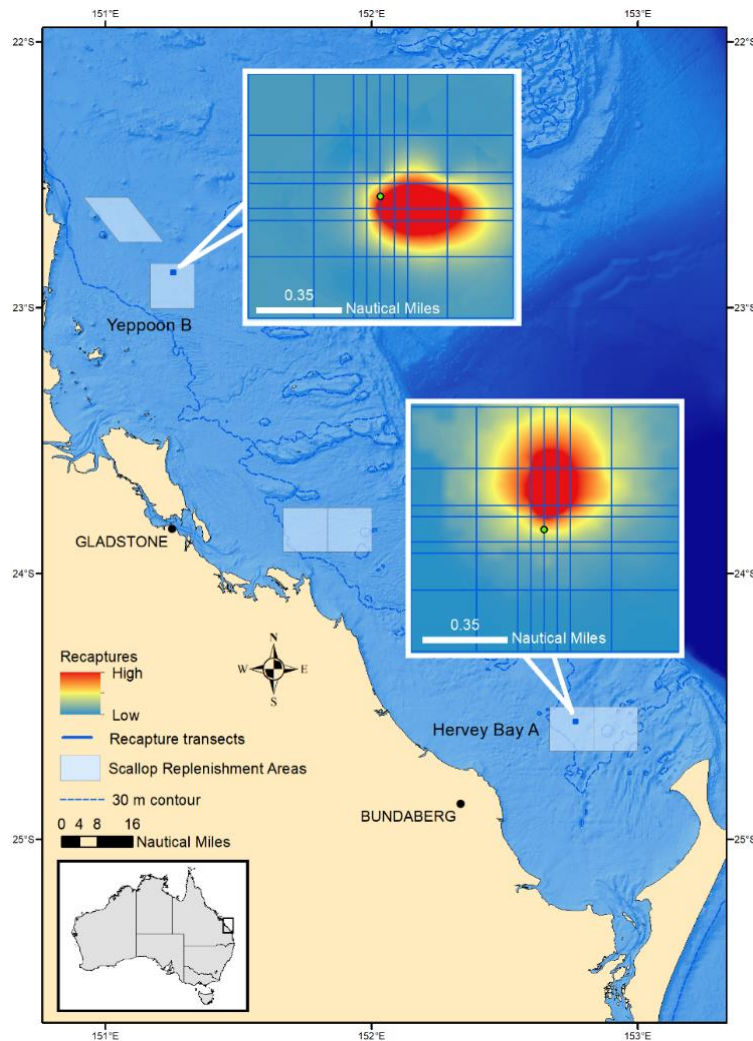
Figure 7-7. The map shows the location of the six SRAs, including Yeppoon B (YB) and Hervey Bay A (HBA), and the 1 nm square recapture grids within YB and HBA (i.e., small dark blue square). The recapture grids comprised about 1% of each SRA. The expanded insets show the recapture grids' details, including the 17 1-nm transects, the release site (green dot) and the general distribution of recaptures. All tagged scallops were released at the single release site located at the centre of each recapture grid.

The Brownie *et al.* (1985) Model 1 results indicated that *M* is higher for tagged scallops at liberty over warmer months (e.g. late spring and summer) than those at liberty over the cooler months (e.g. autumn, winter and early spring), possibly indicating seasonal variation (see Table 22-7, page 244), however further work may be required to confirm this. All three approaches indicated *M* was higher in the Hervey Bay closure (HBA) compared to the Yeppoon closure (YB). For each method, an average from the two locations was used to represent the whole fishery. The logistic model detected significant effects on the recapture rate of tagged scallops due to closure, scallop size, lunar phase at recapture, recapture trip, the number of days the scallops were at liberty and the interaction between days at liberty and closure (Table 22-10, page 246).

Annual mean estimates of *M* for the whole fishery ranged from a minimum of 1.461 year^{-1} for the logistic model, to 1.501 year^{-1} for the Brownie *et al.* (1985) Model 1, to 1.548 year^{-1} (variable recapture rate) and 1.594 year^{-1} (fixed recapture rate) for the modified Brownie *et al.* method. All three estimates were significantly higher than the previous estimate of 1.170 year^{-1} that was derived by Dredge (1985a) and based on a similar tagging study in the late 1970s.

8 Discussion

The following is a summary of the discussion addressing each objective. More detailed discussions are provided in the relevant Appendices, which can be viewed using the hyperlinked sections and page numbers provided (press control+click).

8.1 FISHERY-INDEPENDENT SURVEY

A detailed discussion of the survey is provided in section 16.5, page 88. All three approaches (i.e., interpolated densities, Haddon's weighted means and the GLM for adjusted means) indicated a decline in the scallop population from the early years (1997–2000) to the recent surveys (2017–2019). Based on the GLM adjusted mean densities, there has been a decline in scallop abundance of approximately 50% from the early years (1997–2000) to the recent years (2017–2019). Adjusted means for the 0+ age class in the 2019 survey were the lowest recorded. Findings from the survey time series (i.e., 1997–2019) were made widely available to the Queensland commercial fishing industry.

Investigating reasons for the decline was beyond the scope and objectives of the current study, which focused on deriving more reliable abundance indices. The brevity (i.e., 7 years of comprehensive survey data) and discontinuity of the survey dataset also limits its use for examining environmental influences on the stock. Continuous, multidecadal annual surveys of *Y. balloti* in Western Australia have shown that the catch rates of the 0+ age class decline with the strength of the Leeuwin Current and water temperature in winter (Joll and Caputi 1995a; Caputi *et al.* 1996; 2014; 2019). Rising SSTs in the Queensland saucer scallop fishing grounds may be contributing to the population's decline (see Figure 22-6, page 254). Analysis of Queensland's standardised commercial scallop catch rates revealed several significant correlations with Chlorophyll A, adjacent coastal river flows, SST and physical oceanographic properties of the adjacent Capricorn Eddy (Courtney *et al.* 2015).

The survey density estimates were incorporated in the most recent stock assessment model which concluded that the 2019 scallop spawning biomass was 14–17% of the unfished biomass (Wortmann *et al.* 2020). The model trajectories indicated that the stock could recover to 40% of unfished biomass in eight years if fishing effort was limited to 80,000 effort units annually (1454 boat-days). The modelling did not include environmental influences, but the authors noted that if rising SST has a negative impact on the scallop population, then potential yields may be lower than projected (Wortmann *et al.* 2020). Since the biomass is below 20% of the unfished biomass, the fishery would likely be closed under the Australian Government (2018) Commonwealth Fisheries Harvest Policy. Because the fishery remains open for several months of the year, it would be prudent keep the SRAs closed to constrain fishing mortality, especially since the 2019 survey indicated that 55% of the sampled scallop population was inside the SRAs.

8.2 RELATIONSHIPS BETWEEN SCALLOPS AND SEDIMENTS

8.2.1 *Modelling sediment distributions*

The project has made a significant contribution to mapping the seabed sediments in southeast Queensland, including the scallop fishery spatial domain. In general, hybrid Boosted Regression Tree (GBM) models outperformed simpler GBMs. However, hybrid Random Forest (RF) models did not improve upon simpler RF models. The best performing models included latitude and longitude, and those models that only used sediment data that were co-located with high-resolution bathymetry measures commonly outperformed models that used the entire sediment dataset which included interpolated bathymetry data. The resulting sediment maps can be used to examine relationships between scallop distribution and seabed properties, and hopefully to predict the distribution of scallops and other benthic fished species (e.g., prawns, Moreton Bay bugs, spanner crabs), and to better understand the scallop's habitat preferences and how trawl fishing effort is distributed.

8.2.2 *Modelling scallop distributions*

Analysis of the recently acquired co-located sediment, backscatter and scallop data from the 166 sites offshore from Gladstone and in Hervey Bay indicated an association between scallop distribution and the amount of fine sand (125–250μm) in the sediment (Figure 19-7, page 151). However, modelling scallop distribution at the regional scale was not always improved by including sediment properties. All the models trialed, except for the basic RF, could effectively predict scallop distributions, but model performance was improved by including latitude and longitude as covariates, although this resulted in artifacts in some predictions. Averaging the predictions across multiple years reduced the appearance of artefacts and could be an effective way to produce a generalized and artefact-free model of scallop predictions.

The two best models were RF_en (i.e., the RF model that included latitude and longitude) and OK. The most important variables for predicting scallop distribution for the RF models were latitude, longitude and distance to the coast. A detailed discussion comparing the models is provided in section 21.5, page 229. Modelling scallop distribution may improve by developing hybrid models, such as RFok and RFidw, and by implementing rigorous feature selection methods which omit noisy variables that have no significant influence (Li *et al.* 2019). The models could also be improved by including oceanographic variables from the Great Barrier Reef eReefs hydrodynamic model. Additional sediment data, which could be collected during the annual scallop trawl survey, may also improve model performance. Seafloor properties are used to improve survey monitoring and stock assessment of Atlantic sea scallops (*P. magellanicus*) (Miller *et al.* 2019), which make up the most valuable scallop fishery globally, and a better understanding of where, how and why saucer scallops are distributed could have similar benefits in Queensland.

8.3 SAUCER SCALLOP NATURAL MORTALITY RATE

A detailed discussion of the tagging experiment and resulting natural mortality rate estimates are provided in section 22.5, page 247. Queensland saucer scallops have a relatively high natural mortality rate and short life cycle compared to many commercially important scallops, including the Tasmanian scallop (*Pecten fumatus*) and the Atlantic sea scallop (*P. magellanicus*). If we assume that $M = 1.526$ year^{-1} based on an average obtained from the current study there would be 47 scallops surviving after two years (104 weeks) from an initial population of 1000, in the absence of fishing mortality. Using the Dredge (1985a) estimate of 1.170 year^{-1}, 96 scallops would be alive after two years – about twice as many compared to the current study average.

The Brownie *et al.* (1985) Model 1 estimates of *M* were much higher over spring–summer and lower over winter–spring, possibly indicating seasonal variation. This result supports the concept of a winter closure of the fishery, which is an element of current fishery management, because most scallops would survive the winter and still be available to the fishery when it typically opens in the spring (note that recent management changes have delayed the opening to December, i.e., summer). The study also

found *M* was significantly higher in the HBA SRA compared to the YB SRA. It is widely observed by fishers and researchers that saucer scallops in waters off Yeppoon are generally smaller than elsewhere and the spatial variation in *M* may be related to different environmental conditions in the two SRAs. The finding of lower *M* in YB combined with the observation of smaller scallops there (see Figure 22-2, page 241) helps to justify retaining a common minimum legal size across the whole fishery: scallops in YB, although they appear to grow more slowly, survive for longer and can still reach minimum legal size.

There is uncertainty in the Dredge estimate of *M* because it includes an unknown component of fishing mortality (*F*) and is therefore likely to be biased upwards. However, the Dredge estimate may be too low because the method did not consider the random variation in survival rate between release locations. The data (Dredge 1985a Table 3) show that some batches had recovery rates of more than 50% whereas others had no recoveries at all, even though the fishing mortality rate was thought to be very high once trawlers moved into the locality.

If the Dredge estimates were correct for the late 1970s, it is possible, although speculative, that multi-decadal warming of SST in the region has contributed to the increase in the scallops' natural mortality rate. Long-term monitoring of saucer scallops in Shark Bay WA strongly indicates that elevated SST during the winter spawning period has a detrimental impact on recruitment, possibly by lowering egg production, or increasing the mortality rate of scallop larvae, juveniles or adults (Joll and Caputi 1995a; Caputi *et al.* 2014; Caputi *et al.* 2019). Queensland saucer scallops also spawn mainly during winter (Dredge 1981) and it is noteworthy that winter SST in the fishing grounds has increased by 0.7–0.8°C since the 1950s (see Figure 22-6, page 254).

A recent saucer scallop stock assessment by Wortmann *et al.* (2020) included the logistic model estimate of the natural mortality derived herein (i.e., $M = 1.461$ year^{-1}), but found it resulted in relatively little overall effect on the assessment outputs compared to using Dredge's (1985a) estimate ($M = 1.170$ year^{-1}). Scallop biomass estimates for 2019 were very low (i.e., < 20% unfished biomass) in model outputs for both estimates of *M*. The assessment did not include environmental influences on the stock, although the authors noted that if *M* increases with SST then it may impact the target reference points used to manage effort and lower potential yields from the fishery. Future assessments may be improved by incorporating the seasonal and spatial variation in *M*.

9 Conclusion

9.1 OBJECTIVE 1. DESIGN AND CARRY OUT A COMPREHENSIVE FISHERY-INDEPENDENT SURVEY OF THE 0+ AND 1+ AGE CLASSES IN THE QUEENSLAND SAUCER SCALLOP FISHERY

The project improved the survey analyses and statistical methods which have resulted in more reliable abundance indices and the interpretation of long-term trends. The improvements include:
- incorporating survey sampling gear information on the number, configuration and size of nets deployed by each vessel during the survey, and net spread factors. This has enabled the estimation of swept area for each trawl sample and hence, calculation of scallop density (number of scallops caught per swept area, ha) which is a more precise measure of abundance than number of scallops per 20-minute shot,
- an improved calibration GLM used to adjust for differences between survey vessels (within each year),
- the application of kriging methods which were used to develop scallop density maps, and
- development of a second GLM for deriving adjusted mean scallop densities for each survey year and strata, which considers several explanatory factors, including lunar phase and time-of-night.

Adjusted mean total scallop density has declined by about 50% from the early survey years (i.e., 1997–2000) to recent years (i.e., 2017–2019). The decline is consistent with findings from recent quantitative assessments of the stock biomass (Yang *et al.* 2016; O'Neill *et al.* 2020; Wortmann *et al.*

2020). Survey densities in the northern strata (i.e., S28, S29, T28 and T29) have generally declined by more than 50%. While the scallop population has declined in the main fishing grounds (i.e., Yeppoon, Bustard Head, Hervey Bay), long-term trends in the logbook data indicate an increase in annual commercial catch in the southern extent of the fishery adjacent to Fraser Island. For this reason, two additional strata were added to the survey design in 2017 to include this southern part of the fishery. The overall declining trend in the survey data pertains to the main fishing grounds and excludes the recently-added strata since they were not sampled from 1997–2000. The decline in the population dominates and is not offset by the increased catch rates observed off Fraser Island in recent decades. The poor condition of the stock would likely require closure of the fishery under the Australian Government (2018) Commonwealth Fisheries Harvest Strategy Guidelines.

9.2   OBJECTIVE 2. UNDERTAKE EXPLORATORY ANALYSES ON THE RELATIONSHIP BETWEEN SAUCER SCALLOP ABUNDANCE AND BOTTOM SUBSTRATE

Analyses of the relationship between saucer scallop abundance and bottom substrate were undertaken at both 'regional' and 'vessel-based survey' scales. The vessel-based survey indicated a positive correlation between the percentage of fine sand (125–250 μm) in the sediment and the abundance of the 1+ scallop age class. Scallops were associated with sediments that had comparatively low acoustic backscatter values. Fine sand was the strongest predictor variable of backscatter at both the offshore Gladstone and Hervey Bay sites, and as a result, it may be possible to map the distribution of favourable scallop habitats using vessel-based acoustics. The acquisition of co-located sediment, acoustic, and scallop trawl data was of paramount importance in identifying these relationships.

At the regional scale (i.e., modelling scallop distribution), the relationship between scallops and substrates is less clear. Regional prediction of sediment distributions suggests that the SRAs generally contain more fine sand and mud than adjacent survey strata. To some degree this is broadly what was indicated by the vessel-based surveys. Regional correlations between scallop densities and seabed sediment characteristics indicate that the mud, mean grainsize, coarse sand and very coarse sand were more correlated with scallops than fine sand. It is possible that the saucer scallops prefer a habitat as broad as 'sand' as suggested by Welch *et al.* (2010). However, the vessel-based survey indicates that there might be more research to do to refine what constitutes an optimal scallop niche. This conclusion is based on the only existing set of co-located sediment sample and saucer scallop trawls in the entire fishery. Including co-located sediment sampling in the annual fishery-independent scallop survey would be one way to gain further insight into the relationship between scallops and seabed composition. Predictive modelling of sediments and scallops could be improved by including oceanographic parameters and tidal currents as covariates in the models.

9.3   OBJECTIVE 3. DERIVE ONE OR MORE TAGGING-BASED ESTIMATES OF THE SAUCER SCALLOP'S NATURAL MORTALITY RATE (M)

The new estimates of M were higher than the previous estimate by Dredge (1985a), which may have been high because it included a component of fishing mortality, or low because it was the minimum of many batch estimates and didn't account for different survival rates of different batches. The natural mortality rate estimates provided herein are reasonably robust because a) the experiment was conducted inside closures where the scallop population was not affected by fishing mortality, b) the study sites comprised two areas that were hundreds of kilometres apart, thus increasing the chance of encompassing any spatial variation in mortality, and c) three different methods were applied to analyse the tagging data, all of which converged on a relatively narrow range of M (1.461–1.594 year^{-1}). It is possible, however, that the value of M has increased since the late 1970s when Dredge's study was undertaken. In population modelling, a high value of M is likely to ascribe more importance to environmental effects and somewhat less to fishing mortality.

The Brownie *et al.* (1985) Model 1 batch tagging method estimates of M were higher over spring–summer than winter–spring, possibly indicating seasonal variation (Table 22-7). For fishery management, this finding supports the current fishery closure over the winter, insofar as many scallops

will survive until the fishery opens in the spring or early summer. Elevated natural mortality rates over the warmer months, combined with multidecadal rise in SST in the scallop fishing grounds, may indicate that M has increased because of rising SST. Incorporating seasonal and spatial variation in M could improve the scallop stock assessment and the design of temporal and spatial closures for maximising yield.

10   Implications

The trawl survey results indicate a significant long-term decline in scallop abundance, which has generated widespread concern in recent years. In addition, three separate quantitative assessments of the scallop stock have concluded that the spawning biomass has remained near or below 20% of the unfished biomass (Yang *et al.* 2016; O'Neill *et al.* 2020; Wortmann *et al.* 2020) for the last four years. Under the Australian Government (2018) Commonwealth Fisheries Harvest Strategy Policy, the poor stock status would likely require closure of the fishery, which has significant implications for Queensland scallop trawl fishers, seafood processors and exporters, especially those in southeast and central Queensland (i.e., Hervey Bay, Urangan, Bundaberg, Gladstone and Yeppoon).

The poor status of the stock may also have implications for securing WTO approval required to export saucer scallop meat under the Environment Protection and Biodiversity Conservation Act 1999. If the WTO considers the scallop fishery to "threaten any relevant ecosystem" then one possible implication is not only closure of the scallop fishery, but the entire QECOTF, as the approval process applies to the entire trawl fishery. This would have much wider and more severe impacts to several hundred trawler operators, crews, seafood businesses, processors and exporters state-wide and nationally.

The Queensland scallop fishery currently remains open to fishing for several months of the year. Given the poor status of the stock, and that 55% of the surveyed scallop population is inside the SRAs, the SRA's should remain closed indefinitely as a means of constraining fishing mortality.

Maps derived from modelling sediment (section 20, page 157) and scallop distributions (section 21, page 202) have provided a clearer understanding of scallop habitats. Measures of sediment type and scallop habitat can be used as explanatory terms to improve the analysis of scallop survey data and to standardise commercial catch rates, improving abundance indices for stock assessment.

The updated natural mortality rate (M) estimates, which have implications for stock assessment and management advice, have already been used in recent stock assessment models. Wortmann *et al.* (2020) noted that if M increases with SST then it may impact the target reference points used to manage effort and lower potential yields from the fishery. The new estimates indicate that M has increased compared to the previous estimate by Dredge about 40 years ago. The study also concluded that M appears to vary seasonally, increasing markedly in summer, possibly due to SST, and that rising SST in the scallop fishing grounds in winter may be contributing to the poor scallop stock status (Figure 22-6, page 254). Seasonal variation in M also has implications for seasonal closures.

11   Recommendations and further development

1. The annual scallop trawl survey should be continued and gaps in the time series, such as those from 2007 to 2016, should be avoided.
2. The survey results and previous field studies indicate the catchability of the 0+ age class (< 78 mm SH) in benthic trawls is low/poor, and as a result, these size classes are not well represented in the survey results. Research on the behaviour and selectivity of the scallops could lead to improved monitoring.
3. A weakness of the survey design is its reliance on chartering multiple and different vessels each year. Calibration of the data for differences between vessels is heavily reliant upon a single vessel (*FV C-King*) which has participated in all 13 surveys. Variation between vessels, within and between survey years, is difficult to account for completely. The use of wireless

net monitoring systems on survey vessels to measure and record net spread would improve swept area and scallop density estimates.

4. If the survey is continued, consideration should be given to developing a formal public 'living' document which periodically updates the analysis and results and can be used as a key reference of the survey.

5. While the study focused on improving the survey data analysis and the resulting abundance indices, the scope did not include research required to explain the changes in abundance. If the survey time series is continued, future research could focus on examining environmental influences on the survey density estimates.

6. Incorporating a towed camera system in the survey would likely produce more accurate estimates of scallop density and population size. Software required to detect and measure scallops is still under development, and therefore the images would need to be processed by human annotation for the foreseeable future.

7. Further surveys incorporating sediment sampling, seafloor acoustic measures and scallop sampling would provide additional data for mapping sediments, examining relationships between scallop and the seafloor, and predicting scallop distribution. Some of these additional data could be collected during the scallop fishery-independent trawl survey.

8. Predictive modelling of sediments and scallops could be improved by including oceanographic parameters as additional covariates. Tidal currents may provide an indication of sediment mobility, transport and deposition in southeast Queensland and further improve the sediment predictions. Further incorporation of hybrid interpolation/prediction methods such as RFok and RFidw, and optimal 'feature selection' into RF-based models which identifies the most instructive covariates, may also improve predictions.

9. If the tagging study was repeated, it would be productive to allow a minimum of 100 days at liberty. The timing of the tagging and recapture episodes could be standardised to spring and autumn to allow longer periods at liberty to estimate M, better capture of the strong seasonal variation detected in the current study, and avoidance of the tropical cyclone season.

10. A study of seasonal growth in scallops may provide further information on seasonal variation in M, based on the presumption that higher growth in winter reflects reduced stress and predation (i.e., low M), while low growth during summer reflects higher stress and mortality (i.e., high M). Such a study may be possible using existing length frequency and tagging data, and may not require new field work.

12   Extension and Adoption

The project findings were communicated to the end users, including the fishery managers, researchers, industry, and where applicable the broader community. The direct beneficiaries of the research are Fisheries Queensland, the trawl management working group and industry.

Project steering committee meetings
A combined extension strategy was developed for the current FRDC 2017-48 project and the associated FRDC 2017-057 project, as both addressed the needs for assessment and management of the Queensland saucer scallop fishery. As the two projects worked in close collaboration there was no benefit in developing separate extension strategies. Progress and results for both projects were overseen by a single joint project steering committee, which met three times at the Brisbane Airport Novotel on 8/9/17, 14/12/18 and 6/12/19. Detailed minutes and copies of presentations from each meeting were forwarded to all committee members and FRDC. Members of the committee include fishers, processors, Fisheries Queensland, the Great Barrier Reef Marine Park Authority, and scientists from DAF, Department of Environment and Heritage Protection, James Cook University and Western Australia Department of Fisheries. Further membership details are provided in section 1 Acknowledgements.

Dissemination of survey results
The project agreement and funding include the design and implementation of a fishery-independent survey in 2017. However, Fisheries Queensland provided additional funding for surveys in 2018 and

2019. The survey analyses in this report were therefore extended to include all years, thus delivering beyond the agreement. A PowerPoint presentation PDF file containing the 2017 survey results was uploaded onto a Fisheries Queensland server in January 2018 and an email link forwarded to all 300+ otter trawl license holders at the time. In this way, all Queensland trawler operators had access to the 2017 survey results within a few weeks of the survey being conducted in October 2017. Similarly, results from the 2018 survey were posted on the Fisheries Queensland server in December 2018, and all otter trawl license holders notified at that time. The 2019 survey results were posted online and fishers were notified in December 2019.

Scientific publications
Future extension and communication of the project includes publication of the survey analysis and results from 1997–2006 and 2017–2019 in the primary literature, which would complement the publication of the first survey in 1997 by Dichmont *et al.* (2000). Sections of the report on the scallop survey, sediment and scallop distribution models will contribute to chapters of Samara French's PhD thesis at James Cook University. The authors plan to publish findings from the natural mortality rate tagging experiment in the primary literature.

Presentations to working groups and expert panel
- Dr Courtney gave a presentation of the 2017 scallop survey results to the Queensland Trawl Working Group in February 2018.
- The survey and stock assessment modelling results were presented to the Queensland Government's Sustainable Fisheries Expert Panel on 18/4/2018.
- The scallop stock assessment findings, which include the scallop survey data, were presented by Dr Yang at the Southern Inshore (i.e., scallop fishers) Trawl Region Harvest Strategy Workshop 23–24 May 2019 at the Hervey Bay Boat Club. There were about 16 fishers and processors present, many of whom raised points and questions.
- Dr M. O'Neill presented scallop stock assessment results at the August 2019 Trawl Working Group.
- Dr Joanne Wortmann presented the most recent scallop stock assessment, forecast predictions and harvest strategy to the Trawl Working Group on 8/6/2020 via Teams teleconference, and repeated the presentation on 9/6/2020 to the Southern Inshore Harvest Strategy Working Group. The assessment included all available data, including the October 2019 survey results and an updated estimate of the scallop natural mortality rate (M) that was derived from the current FRDC project 2017-048. In both meetings there was considerable concern over the poor status of the stock.

Milestone reporting
The extension plan included the production of all Milestone reports, which have been provided to FRDC and Fisheries Queensland.

Conference presentations
Dr Daniell presented a paper at the 2018 Australian Marine Sciences Association annual conference in Adelaide entitled "Improving Fishing Mortality Rate Estimates for Management of the Queensland Saucer Scallop Fishery" by J. J. Daniell, A. J. Courtney, W.-H. Yang, M. J. Campbell and R. Beaman https://amsa18.amsa.asn.au/program/

Dr Yang presented mathematical aspects of the scallop modelling to the 'Biometrics by the Boarder' meeting in Kingscliff 2017, and the Satellite Workshop Applied^2 Probability event hosted by CARM, UQ in July 2019. https://informs-aps.smp.uq.edu.au/

Media releases
Dr Courtney's trip report, detailing the 2018 NOAA HabCam and dredge survey of the Atlantic sea scallop fishery near Georges Bank off the coast of Massachusetts in the USA was published by FRDC's FISH magazine (Volume 26 number 4) https://www.frdc.com.au/media-publications/fish/FISH-Vol-26-4/Pictures-of-abundance

DAF published a media release in January 2020 entitled "New technology scanning for scallops" which reports results from the towed camera pilot study. The article highlights the potential of towed camera systems as an alternative and improved method for monitoring the scallop stock.

13 Appendix 1. Staff

Matthew Campbell, Senior Fisheries Biologist, DAF
Tony Courtney, Senior Principal Fisheries Biologist, DAF
James Daniell, Lecturer, College of Science and Engineering, James Cook University
Samara French, Senior Fishery Resource Assessment Scientist, DAF, PhD candidate James Cook University
George Leigh, Principal Fishery Resource Assessment Scientist, DAF
Mark McLennan, Senior Fisheries Technician, DAF
Wen-Hsi Yang, Research Fellow, Centre for Applications in Natural Resource Mathematics, University of Queensland

14 Appendix 2. Intellectual property

No intellectual property has been generated by the project.

15 Appendix 3. References

Australian Government (2018) Guidelines for the Implementation of the Commonwealth Fisheries Harvest Strategy Policy Canberra, Australia.

Bolker, B. and R Development Core Team (2019). bbmle: Tools for General Maximum Likelihood Estimation. R package version 1.0.22. https://CRAN.R-project.org/package=bbmlebbmle.

Northeast Fisheries Science Center (2018). 65th Northeast Regional Stock Assessment Workshop (65th SAW) Assessment Summary Report. US Dept Commer, Northeast Fish Sci Cent Ref Doc. 18-08.

R Core Team (2019) R: A Language and Environment for Statistical Computing. (R Foundation for Statistical Computing: Vienna, Austria)

Anderson, J.T., Van Holliday, D., Kloser, R., Reid, D.G. and Simard, Y. (2008) Acoustic seabed classification: Current practice and future directions. *ICES Journal of Marine Science* **65**(6), 1004-1011.

Appelhans, T., Mwangomo, E., Hardy, D.R., Hemp, A. and Nauss, T. (2015) Evaluating machine learning approaches for the interpolation of monthly air temperature at Mt. Kilimanjaro, Tanzania. *Spatial Statistics* **14**, 91-113.

Beaman, R.J. (2010) Project 3DGBR: A high-resolution depth model for the Great Barrier Reef and Coral Sea.

Beaudoin, J., Clarke, J.E., Van den Ameele, E.J. and Gardner, J.V. (2002) Geometric and Radiometric correction of Multibeam Backscattter Derived from Reson 8101 Systems. *Canadian Hydrographic Conference Proceedings*, 1-22.

Benton, T. (2015) Can We Do Better than Using "Mean GCSE Grade" to Predict Future Outcomes? An Evaluation of Generalised Boosting Models. *Oxford review of education* **41**(5).

Biondo, M. and Bartholomä, A. (2017) A multivariate analytical method to characterize sediment attributes from high-frequency acoustic backscatter and ground-truthing data (Jade Bay, German North Sea coast). *Continental Shelf Research* **138**(December 2016), 65-80.

Blondel, P. and Sichi, O.G. (2009) Textural analyses of multibeam sonar imagery from Stanton Banks, Northern Ireland continental shelf. *Applied Acoustics* **70**(10), 1288-1297.

Bogazzi, E., Baldoni, A., Rivas, A., Martos, P., Reta, R., Orensanz, J.M., Lasta, M., Dell'Arciprete, P. and Werner, F. (2005) Spatial correspondence between areas of concentration of Patagonian scallop (Zygochlamys patagonica) and frontal systems in the southwestern Atlantic. *Fisheries Oceanography* **14**(5), 359-376.

Borgeld, J.C., Clarke, J.E.H., Goff, J.A., Mayer, L.A. and Curtis, J.A. (1999) Acoustic backscatter of the 1995 flood deposit on the Eel shelf. *Marine Geology* **154**(1-4), 197-210.

Bourgeois, M., Brethes, J.-C. and Nadeau, M. (2006) Substrate effects on survival, growth and dispersal of juvenile sea scallop, Placopecten magellanicus (Gmelin 1791). *Journal of Shellfish Research* **25**(1), 43-49.

Boyd, R., Ruming, K., Davies, S., Payenberg, T. and Lang, S. (2004) Fraser Island and Hervey Bay - a classic modern sedimentary environment. In PESA Eastern Australasian Basins Symposium II. pp. 511-521.

Brand, A.R. (2006) Scallop ecology: distributions and behaviour. In Developments in Aquaculture and Fisheries science. Vol. 35. pp. 651-744. (Elsevier)

Breiman, L. (2001) Random Forests. *Machine Learning* **45**, 5-32.

Brown, C., Beaudoin, J., Brissette, M. and Gazzola, V. (2019) Multispectral Multibeam Echo Sounder Backscatter as a Tool for Improved Seafloor Characterization. *Geosciences* **9**(3), 126.

Brown, C.E. (1998) Coefficient of variation. In Applied multivariate statistics in geohydrology and related sciences. pp. 155-157. (Springer)

Brown, C.J. and Collier, J.S. (2008) Mapping benthic habitat in regions of gradational substrata: An automated approach utilising geophysical, geological, and biological relationships. *Estuarine, Coastal and Shelf Science* **78**(1), 203-214.

Brown, C.J., Sameoto, J.A. and Smith, S.J. (2012) Multiple methods, maps, and management applications: purpose made seafloor maps in support of ocean management. *Journal of Sea Research* **72**, 1-13.

Brown, C.J., Smith, S.J., Lawton, P. and Anderson, J.T. (2011) Benthic habitat mapping: A review of progress towards improved understanding of the spatial ecology of the seafloor using acoustic techniques. *Estuarine, Coastal and Shelf Science* **92**(3), 502-520.

Brown, R., Fogarty, M., Legault, C., Miller, T., Nordahl, V., Politis, P. and Rago, P. (2007) Survey transition and calibration of bottom trawl surveys along the northeastern continental shelf of the United States. *International Council for the Exploration of the Sea, CM*.

Brownie, C., Anderson, D.R., Burnham, K.P. and Robson, D.S. (1985) Statistical inference from band recovery data-a handbook. Second edition. *Resource Publication - US Fish & Wildlife Service* **156**.

Burrough, P.A. and McDonnell, R.A. (1998) 'Principles of geographical information systems.' (Oxford Unviersity Press: New York)

Butler, I.R., Sommer, B., Zann, M., Zhao, J.X. and Pandolfi, J.M. (2013) The impacts of flooding on the high-latitude, terrigenoclastic influenced coral reefs of Hervey Bay, Queensland, Australia. *Coral Reefs* **32**(4), 1149-1163.

Campbell, A.B., O'Neill, M.F., Leigh, G.M., Wang, Y.-G. and J., J.E. (2012) Reference points for the Queeensland scallop fishery.

Campbell, M.J., Campbell, A.B., Officer, R.A., O'Neill, M.F., Mayer, D.G., Thwaites, A., Jebreen, E.J., Courtney, A.J., Gribble, N., Lawrence, M.L., Prosser, A.J. and Drabsch, S.L. (2010a) Harvest strategy evaluation to optimise the sustainability and value of the Queensland scallop fishery - FRDC Final Report Number 2006/024. Department of Employment, Economic Development and Innovation, Brisbane, Queensland.

Campbell, M.J., Officer, R.A., Prosser, A.J., Lawrence, M.L., Drabsch, S.L. and Courtney, A.J. (2010b) Survival of Graded Scallops Amusium balloti in Queensland's (Australia) Trawl Fishery. *Journal of Shellfish Research* **29**(2), 373-380.

Caputi, N., De Lestang, S., Hart, A., Kangas, M., Johnston, D. and Penn, J. (2014) Catch Predictions in Stock Assessment and Management of Invertebrate Fisheries Using Pre-Recruit Abundance—Case Studies from Western Australia. *Reviews in Fisheries Science and Aquaculture* **22**, 36-54.

Caputi, N., Feng, M., Pearce, A., Benthuysen, J., Denham, A., Hetzel, Y., Matear, R.J., Jackson, G., Molony, B.W., Joll, L. and Chandrapavan, A. (2015) Management implications of climate change effect on fisheries in Western Australia: Part 1 Environmental change and risk assessment. FRDC Project 2010/535. Fisheries Research Report 260, Department of Fisheries, Western Australia.

Caputi, N., Fletcher, W.J., Pearce, A. and Chubb, C.F. (1996) Effect of the Leeuwin Current on the recruitment of fish and invertebrates along the Western Australian coast. *Marine & Freshwater Research* **47**(2), 147-55.

Caputi, N., Kangas, M., Chandrapavan, A., Hart, A., Feng, M., Marin, M. and Lestang, S.d. (2019) Factors Affecting the Recovery of Invertebrate Stocks From the 2011 Western Australian Extreme Marine Heatwave. *Frontiers in Marine Science* **6**(484).

Caputi, N., Kangas, M., Denham, A., Feng, M., Pearce, A., Hetzel, Y. and Chandrapavan, A. (2016) Management adaptation of invertebrate fisheries to an extreme marine heat wave event at a global warming hot spot. *Ecology and Evolution* **6**(11), 3583-3593.

Chandrapavan, A., Kangas, M. and Caputi, N. (2020) Understanding recruitment variation (including the collapse) of saucer scallop stocks in Western Australia and assessing the feasibility of assisted recovery measures for improved management in a changing environment. FRDC Project 2015/026. Department of Primary Industries and Regional Development WA.

Chen, F.-W. and Liu, C.-W. (2012) Estimation of the spatial rainfall distribution using inverse distance weighting (IDW) in the middle of Taiwan. *Paddy and Water Environment* **10**(3), 209-222.

Cohen, J. (1988) 'Statistical power analysis for the behavioral sciences.' Second edn. (Lawrence Erlbaum Associates, Publishers: Hillsdale, NJ) 400

Collier, J.S. and Brown, C.J. (2005) Correlation of sidescan backscatter with grain size distribution of surficial seabed sediments. *Marine Geology* **214**(4), 431-449.

Courtney, A.J., Campbell, M.J., Roy, D.P., Tonks, M.L., Chilcott, K.E. and Kyne, P.M. (2008) Round scallops and square meshes: A comparison of four codend types on the catch rates of target species and by-catch in the Queensland (Australia) saucer scallop (*Amusium balloti*) trawl fishery. *Marine and Freshwater Research* **59**(10), 849-864.

Courtney, A.J., Campbell, M.J., Tonks, M.L., Roy, D.P., Gaddes, S.W., Haddy, J.A., Kyne, P.M., Mayer, D.G. and Chilcott, K.E. (2014) Effects of bycatch reduction devices in Queensland's (Australia) deepwater eastern king prawn (*Melicertus plebejus*) trawl fishery. *Fisheries Research* **157**, 113-123.

Courtney, A.J., Spillman, C.M., Lemos, R., Thomas, J., Leigh, G. and Campbell, A. (2015) Physical oceanographic influences on Queensland reef fish and scallops. FRDC Project #2013/020 Final Report.

Courtney, A.J., Tonks, M.L., Campbell, M.J., Roy, D.P., Gaddes, S.W., Kyne, P.M. and O'Neill, M.F. (2006) Quantifying the effects of bycatch reduction devices in Queensland's (Australia) shallow water eastern king prawn (*Penaeus plebejus*) trawl fishery. *Fisheries Research* **80**(2-3), 136-147.

Cressie, N.A.C. (1993) 'Statistics for spatial data.' (Wiley)

Cropp, D. (1992) Aquaculture of the saucer scallop *Amusium balloti* Fishing Industry Research and Development Corporation (FIRDC Project 1989-58) Final Report. Aquatech Australia Pty. Ltd., North Hobart, Tasmania.

Cutler, A., Cutler, D.R. and Stevens, J.R. (2009) Tree-based methods. In High-Dimensional Data Analysis in Cancer Research. pp. 1-19. (Springer)

Cutler, D.R., Edwards, T.C., Beard, K.H., Cutler, A., Hess, K.T., Gibson, J. and Lawler, J.J. (2007) Random Forests for Classification in Ecology.

Davies, P.J. and Tsuji, Y. (1992) Tropical and temperate carbonate environment: the effects of sea level, climate and tectonics on Facies Development. Record 1992/17. Bureau of Mineral Resources Geology and Geophysics.

Davis, K.S., Slowey, N.C., Stender, I.H., Fiedler, H., Bryant, W.R. and Fechner, G. (1996) Acoustic backscatter and sediment textural properties of inner shelf sands, northeastern Gulf of Mexico. *Geo-Marine Letters* **16**(3), 273-278.

De Falco, G., Tonielli, R., Di Martino, G., Innangi, S., Simeone, S. and Parnum, I.M. (2010) Relationships between multibeam backscatter, sediment grain size and Posidonia oceanica seagrass distribution. *Continental Shelf Research* **30**(18), 1941-1950.

Degraer, S., Verfaillie, E., Willems, W., Adriaens, E. and Vincx, M.a. (2008) Habitat suitability modelling as a mapping tool for macrobenthic communities: An example from the Belgian part of the North Sea. *Continental Shelf Research* **28**(3), 369-379.

Díaz-Uriarte, R. and De Andres, S.A. (2006) Gene selection and classification of microarray data using random forest. *BMC bioinformatics* **7**(1), 3.

Dichmont, C.M., Dredge, M.C.L. and Yeomans, K. (2000) The first large-scale fishery-independent survey of the saucer scallop, *Amusium japonicum balloti* in Queensland, Australia. *Journal of Shellfish Research* **19**(2), 731-739.

Donoghue, J.F. (2016) Phi Scale. In Encyclopedia of Estuaries. (Ed. MJ Kennish) pp. 483-484. (Springer Netherlands: Dordrecht)

Dredge, M. (2006) Scallop fisheries, mariculture and enhancement in Australia. In Developments in Aquaculture and Fisheries Science. Vol. 35. pp. 1391-1412. (Elsevier)

Dredge, M.C.L. (1981) Reproductive biology of the Saucer Scallop *Amusium japonicum balloti* (Bernardi) in Central Queensland Waters. *Australian Journal of Marine and Freshwater Research* **32**(5), 775-787.

Dredge, M.C.L. (1985a) Estimates of natural mortality and yield-per-recruit for *Amusium japonicum balloti* Bernardi (*Pectinidae*) based on tag recoveries. *Journal of Shellfish Research* **5**(2), 103-109.

Dredge, M.C.L. (1985b) Growth and mortality in an isolated bed of saucer scallops, *Amusium japonicum balloti* (Bernardi). *Queensland Journal of Agricultural and Animal Sciences* **42**(1), 11-21.

Dredge, M.C.L. (1994) Modelling management measures in the Queensland scallop fishery. *Memoirs of the Queensland Museum* **36**(2), 277-282.

Dredge, M.C.L., Marsden, I.D. and Williams, J.R. (2016) Chapter 30 - Scallop Fisheries, Mariculture, and Enhancement in Australasia. In Developments in Aquaculture and Fisheries Science. Vol. 40. (Eds. SE Shumway and GJ Parsons) pp. 1127-1170. (Elsevier)

Edgar, G.J., Stuart-Smith, R.D., Willis, T.J., Kininmonth, S., Baker, S.C., Banks, S., Barrett, N.S., Becerro, M.A., Bernard, A.T. and Berkhout, J. (2014) Global conservation outcomes depend on marine protected areas with five key features. *Nature* **506**(7487), 216-220.

Elith, J. and Leathwick, J. (2011) Boosted Regression Trees for ecological modeling.

Elith, J., Leathwick, J.R. and Hastie, T. (2008) A working guide to boosted regression trees. *Journal of Animal Ecology* **77**(4), 802-813.

ESRI (2018) ArcGIS Desktop: Release 10. (Environmental Systems Research Institute: Redlands, CA)

Ewing, G., Keane, J.P. and Semmens, J.M. (2018) Industry-independent video survey of commercial scallop (Pecten fumatus) densities in Great Oyster Bay – May 2017 survey. Institute for Marine and Antarctic Studies, University of Tasmania, Hobart, Tasmania.

Feng, M., Caputi, N., Chandrapavan, A., Chen, M., Hart, A. and Kangas, M. (2021) Multi-year marine cold-spells off the west coast of Australia and effects on fisheries. *Journal of Marine Systems* **214**, 103473.

Fenstermacher, L.E., Crawford, G.B., Borgeld, J.C., Britt, T., George, D.A., Klein, M.A., Driscoll, N.W. and Mayer, L.A. (2001) Enhanced acoustic backscatter due to high abundance of sand dollars, dendraster excentricus. *Marine Georesources and Geotechnology* **19**(2), 135-145.

Fernandes, L., Day, J., Lewis, A., Slegers, S., Kerrigan, B., Breen, D., Cameron, D., Jago, B., Hall, J., Lowe, D., Innes, J., Tanzer, J., Chadwick, V., Thompson, L., Gorman, K., Simmons, M., Barnett, B., Sampson, K., De'ath, G., Mapstone, B., Marsh, H., Possingham, H., Ball, I., Ward, T., Dobbs, K., Aumend, J., Slater, D. and Stapleton, K. (2005) Establishing representative no-take areas in the Great Barrier Reef: large-scale implementation of theory on marine protected areas. *Conservation biology* **19**(6), 1733-1744.

Ferrini, V.L. and Flood, R.D. (2006) The effects of fine-scale surface roughness and grain size on 300 kHz multibeam backscatter intensity in sandy marine sedimentary environments. *Marine Geology* **228**(1-4), 153-172.

Finch, T. (2009) Incremental calculation of weighted mean and variance. *University of Cambridge* **4**(11-5), 41-42.

Folk, R.L. (1954) The Distinction between Grain Size and Mineral Composition in Sedimentary-Rock Nomenclature. *The Journal of Geology* **62**(4), 344-359.

Folk, R.L. (1980) 'Petrology of sedimentary rocks.' (Hemphill Publishing Co: Austin, Texas)

Fonseca, L., Mayer, L., Orange, D. and Driscoll, N. (2002) The high-frequency backscattering angular response of gassy sediments: model/data comparison from the Eel River Margin, California. *The Journal of the Acoustical Society of America* **111**(6), 2621-2631.

Fournier, J., Gallon, R.K. and Paris, R. (2014) G2Sd: a new R package for the statistical analysis of unconsolidated sediments. *Géomorphologie: relief, processus, environnement* **20**(1), 73-78.

Franco, B.M., Hernández-Callejo, L. and Navas-Gracia, L.M. (2020) Virtual weather stations for meteorological data estimations. *Neural Computing and Applications* **8**, 1-12.

Galparsoro, I., Borja, n., Bald, J., Liria, P. and Chust, G. (2009) Predicting suitable habitat for the European lobster (Homarus gammarus), on the Basque continental shelf (Bay of Biscay), using Ecological-Niche Factor Analysis. *Ecological Modelling* **220**(4), 556-567.

GenStat (2016) 'VSN International (2016). *GenStat Reference Manual (Release 16.1), Part 1 Summary*. VSN International, Hemel Hempstead, UK.' (Laws Agricultural Trust)

Genuer, R., Poggi, J.M. and Tuleau-Malot, C. (2019) VSURF: Variable Selection Using Random Forests. R package version 1.1.0.

Goff, J.A., Olson, H.C. and Duncan, C.S. (2000) Correlation of side-scan backscatter intensity with grain-size distribution of shelf sediments, New Jersey margin. *Geo-Marine Letters* **20**(1), 43-49.

Gräler, B., Pebesma, E. and Heuvelink, G. (2016) Spatio-Temporal Interpolation using gstat. *The R Journal* **8**(1), 204-218.

Greenwell, B., Boehmke, B., Cunningham, J. and GBM Developers (2019) gbm: Generalized Boosted Regression Models. R package version 2.1.5.

Grimes, K.G. (1991) Shallow Stratigraphic Drilling in the Wide Bay and Maryborough 1:125000 Sheet Areas. Dept. of Resource Industries Queensland, Brisbane.

Guisan, A. and Zimmermann, N.E. (2000) Predictive habitat distribution models in ecology. *Ecological Modelling* **135**(2-3), 147-186.

Gwyther, D. and McShane, P.E. (1988) Growth rate and natural mortality of the scallop Pecten alba tate in Port Phillip Bay, Australia, and evidence for changes in growth rate after a 20-year period. *Fisheries Research* **6**(4), 347-361.

Haddon, M. (1997) FRDC Quantitative Fisheries Training Unit Introduction to Fisheries Methods. Institute of Marine Ecology University of Sydney, DPI, Brisbane.

Haris, K., Chakraborty, B., Ingole, B., Menezes, A. and Srivastava, R. (2012) Seabed habitat mapping employing single and multi-beam backscatter data: A case study from the western continental shelf of India. *Continental Shelf Research* **48**, 40-49.

Harris, P.T., Bridge, T.C., Beaman, R.J., Webster, J.M., Nichol, S.L. and Brooke, B.P. (2013) Submerged banks in the Great Barrier Reef, Australia, greatly increase available coral reef habitat. *ICES Journal of Marine Science* **70**(2), 284-293.

Heidemann, H. and Ribbe, J. (2019) Marine Heat Waves and the Influence of El Niño off Southeast Queensland, Australia. *Frontiers in Marine Science* **6**(56).

Hilborn, R. and Walters, C.J. (1992) 'Quantitative fisheries stock assessment: choice, dynamics and uncertainty.' (Chapman &Hall: New York)

Himmelman, J.H., Guderley, H.E. and Duncan, P.F. (2009) Responses of the saucer scallop Amusium balloti to potential predators. *Journal of Experimental Marine Biology and Ecology* **378**(1-2), 58-61.

Hjort, J. and Marmion, M. (2008) Effects of sample size on the accuracy of geomorphological models. *Geomorphology (Amsterdam, Netherlands)* **102**(3), 341-350.

Hopley, D. (2011) 'Encyclopedia of Modern Coral Reefs: Structure, Form and Process.' (Springer: Dordrecht, Netherlands) 1236

Huang, Z., Nichol, S.L., Siwabessy, J.P.W., Daniell, J. and Brooke, B.P. (2012) Predictive modelling of seabed sediment parameters using multibeam acoustic data: a case study on the Carnarvon Shelf, Western Australia. *International Journal of Geographical Information Science* **26**(2), 283-307.

Huang, Z., Siwabessy, J., Cheng, H. and Nichol, S. (2018) Using Multibeam Backscatter Data to Investigate Sediment-Acoustic Relationships. *Journal of Geophysical Research: Oceans* **123**(7), 4649-4665.

Huang, Z., Siwabessy, J., Nichol, S.L. and Brooke, B.P. (2014) Predictive mapping of seabed substrata using high-resolution multibeam sonar data: A case study from a shelf with complex geomorphology. *Marine Geology* **357**, 37-52.

Hughes-Clarke, J.E., Mayer, L.A. and Wells, D.E. (1996) Shallow-water imaging multibeam sonars: A new tool for investigating seafloor processes in the coastal zone and on the continental shelf. *Marine Geophysical Research* **18**(6), 607-629.

Iampietro, P.J., Young, M.A. and Kvitek, R.G. (2008) Multivariate prediction of rockfish habitat suitability in Cordell Bank National Marine sanctuary and Del Monte Shalebeds, California, USA. *Marine Geodesy* **31**(4), 359-371.

Jebreen, E.J., Whybird, O. and O'Sullivan, S. (2008) Fisheries Long Term Monitoring Program: Summary of scallop (*Amusium japonicum balloti*) survey results: 1997-2006. Department of Primary Industries and Fisheries, No. PR08-3519, Brisbane, Australia.

Joll, L.M. (1988) Daily growth rings in juvenile saucer scallops, *Amusium balloti* (Bernardi). *Journal of Shellfish Research* **7**(1), 73-76.

Joll, L.M. and Caputi, N. (1995a) Environmental influences on recruitment in the saucer scallop (*Amusium balloti*) fishery of Shark Bay, Western Australia. *International Council for the Exploration of the Sea Journal of Marine Science* **199**, 47-53.

Joll, L.M. and Caputi, N. (1995b) Geographic variation in the reproductive cycle of the saucer scallop, *Amusium balloti* (Bernardi, 1861) (Mollusca : Pectinidae), along the Western Australian coast. *Marine and Freshwater Research* **46**, 779-92.

Kangas, M., Sporer, E., Brown, S., Shanks, M., Chandrapavan, A. and Thomson, A. (2011) Stock assessment for the Shark Bay scallop fishery. Fisheries Research Report No. 226. Department of Fisheries, Western Australia.

Kingsford, C. and Salzberg, S.L. (2008) What are decision trees? *Nature Biotechnology* **26**(9), 1011-1013.

Kloser, R.J., Bax, N.J., Ryan, T., Williams, A. and Barker, B.A. (2001) Remote sensing of seabed types in the Australian South East Fishery; development and application of normal incident acoustic techniques and associated 'ground truthing'. *Marine & Freshwater Research* **52**(4), 475-489.

Kohavi, R. A study of cross-validation and bootstrap for accuracy estimation and model selection. In 'International Joint Conference on Articial Intelligence (IJCAI)', 1995, pp. 1137-1145

Kostylev, V.E., Courtney, R.C., Robert, G. and Todd, B.J. (2003) Stock evaluation of giant scallop (Placopecten magellanicus) using high-resolution acoustics for seabed mapping. *Fisheries Research* **60**(2-3), 479-492.

Kurina, F.G., Hang, S., Macchiavelli, R. and Balzarini, M. (2019) Spatial predictive modelling essential to assess the environmental impacts of herbicides. *Geoderma* **354**(July), 113874.

Kursa, M.B. and Rudnicki, W.R. (2010) Feature selection with the Boruta package. *Journal of Statistical Software* **36**(11), 1-13.

Lamarche, G. and Lurton, X. (2018) Recommendations for improved and coherent acquisition and processing of backscatter data from seafloor-mapping sonars. *Marine Geophysical Research* **39**(1-2), 5-22.

Lanier, A., Romsos, C. and Goldfinger, C. (2007) Seafloor habitat mapping on the Oregon continental margin: A spatially nested GIS approach to mapping scale, mapping methods, and accuracy quantification. *Marine Geodesy* **30**(1-2), 51-76.

Lenanton, R.C., Caputi, N., Kangas, M. and Craine, M. (2009) The ongoing influence of the Leeuwin Current on economically important fish and invertebrates off temperate Western Australia - has it changed? *Journal of the Royal Society of Western Australia* **92**, 111-127.

Li, J. Predicting the spatial distribution of seabed gravel content using random forest, spatial interpolation methods and their hybrid methods. In 'The International Congress on Modelling and Simulation (MODSIM)', 2013a, Adelaide, Australia, pp. 394-400

Li, J. Predictive modelling using random forest and its hybrid methods with geostatistical techniques in marine environmental geosciences. In 'The proceedings of the Eleventh Australasian Data Mining Conference (AusDM 2013), Canberra, Australia', 2013b,

Li, J. (2016) Assessing spatial predictive models in the environmental sciences: Accuracy measures, data variation and variance explained. *Environmental Modelling and Software* **80**, 1-8.

Li, J. (2017) Assessing the accuracy of predictive models for numerical data: Not r nor r2, why not? Then what? *PloS one* **12**(8).

Li, J. (2019a) A Brief Introduction to the spm Package.

Li, J. (2019b) A Critical Review of Spatial Predictive Modeling Process in Environmental Sciences with Reproducible Examples in R. *Applied Sciences* **9**(10), 2048.

Li, J. (2019c) spm: Spatial Predictive Modeling. R package version 1.2.0.

Li, J., Alvarez, B., Siwabessy, J., Tran, M., Huang, Z., Przeslawski, R., Radke, L., Howard, F. and Nichol, S. (2017) Application of random forest, generalised linear model and their hybrid methods with geostatistical techniques to count data: Predicting sponge species richness. *Environmental modelling & software* **97**, 112-129.

Li, J. and Heap, A.D. (2008) A review of spatial interpolation methods for environmental scientists.

Li, J., Heap, A.D., Potter, A. and Daniell, J.J. (2011a) Application of machine learning methods to spatial interpolation of environmental variables. *Environmental Modelling and Software* **26**(12), 1647-1659.

Li, J., Heap, A.D., Potter, A. and Daniell, J.J. (2011b) 'Predicting Seabed Mud Content across the Australian Margin II: Performance of Machine Learning Methods and Their Combination with Ordinary Kriging and Inverse Distance Squared.' (Geoscience Australia) 69

Li, J., Heap, A.D., Potter, A., Huang, Z. and Daniell, J.J. (2011c) Can we improve the spatial predictions of seabed sediments? A case study of spatial interpolation of mud content across the southwest Australian margin. *Continental Shelf Research* **31**(13), 1365-1376.

Li, J., Potter, A., Huang, Z., Daniell, J. and Heap, A. (2010) Predicting seabed mud content across the Australian margin: comparison of statistical and mathematical techniques using a simulation experiment. *Geoscience Australia* **11**.

Li, J., Potter, A., Huang, Z. and Heap, A. (2012) 'Predicting seabed sand content across the Australian margin using machine learning and geostatistical methods.' (Geoscience Australia: Canberra, ACT, Australia) 115

Li, J., Siwabessy, J., Huang, Z. and Nichol, S. (2019) Developing an Optimal Spatial Predictive Model for Seabed Sand Content Using Machine Learning, Geostatistics, and Their Hybrid Methods. *Geosciences* **9**, 180.

Li, J., Siwabessy, J.W., Tran, M., Huang, Z. and Heap, A.D. (2014) Predicting seabed hardness using random forest in R. In Data Mining Applications with R. (Eds. Y Zhao and Y Cen) pp. 299-329. (Elsevier: Amsterdam, The Netherlands)

Li, R., Zhang, C., Yang, Z., Li, G., Liu, H., Xie, Y., Zhang, A., Liu, H. and Feng, L. Gross Error Elimination of ICESat/GLAS Data in Typical Land Areas. In 'International Conference on Geo-informatics in Sustainable Ecosystem and Society', 2018, pp. 448-462

Liaw, A. and Wiener, M. (2002) Classification and Regression by randomForest. *R News* **2**(3), 18-22.

Lu, D. and Weng, Q. (2007) A survey of image classification methods and techniques for improving classification performance. *International journal of Remote sensing* **28**(5), 823-870.

Madden, R. (2016) A model of environmental drivers of the spatial-temporal population dynamics of the Queensland Saucer Scallop Fishery. The University of Queensland,

Maiklem, W.R. (1966) Recent Carbonate Sedimentation in the Capricorn Group of Reefs, Great Barrier Reef. University of Queensland,

Marmion, M., Parviainen, M., Luoto, M., Heikkinen, R.K. and Thuiller, W. (2009) Evaluation of consensus methods in predictive species distribution modelling. *Diversity and Distributions* **15**(1), 59-69.

Marshall, J.F. (1977) 'Marine geology of the Capricorn Channel area.' Bulletin 1 edn. (Bureau of Mineral Resources Geology and Geophysics) 81

Marshall, J.F. (1980) Continental shelf sediments: southern Queensland and northern New South Wales. *Bureau of Mineral Resources, Australia Bullentin 207* **137**, 1-39.

Mathews, E., Heap, A. and Woods, M. (2007) 'Inter-reefal seabed sediments and geomorphology of the Great Barrier Reef: A spatial analysis.' (Geoscience Australia)

Mauna, A.C., Franco, B.C., Baldoni, A., Acha, E.M., Lasta, M.L. and Iribarne, O.O. (2008) Cross-front variations in adult abundance and recruitment of Patagonian scallop (Zygochlamys patagonica) at the SW Atlantic Shelf Break Front. *ICES Journal of Marine Science* **65**(7), 1184-1190.

Maxwell, W.G.H. and Maiklem, W.R. (1964) Lithofacies analysis, Southern part of the Great Barrier Reef. Vol. Five. pp. 23. (The University of Queensland Press)

McGonigle, C. and Collier, J.S. (2014) Interlinking backscatter, grain size and benthic community structure. *Estuarine, Coastal and Shelf Science* **147**(June), 123-136.

McGonigle, C., Grabowski, J.H., Brown, C.J., Weber, T.C. and Quinn, R. (2011) Detection of deep water benthic macroalgae using image-based classification techniques on multibeam backscatter at Cashes Ledge, Gulf of Maine, USA. *Estuarine, Coastal and Shelf Science* **91**(1), 87-101.

Miller, T.J., Hart, D.R., Hopkins, K., Vine, N.H., Taylor, R., York, A.D. and Gallager, S.M. (2019) Estimation of the capture efficiency and abundance of Atlantic sea scallops (Placopecten magellanicus) from paired photographic–dredge tows using hierarchical models. *Canadian Journal of Fisheries and Aquatic Sciences* **76**(6), 847-855.

Monk, J., Ierodiaconou, D., Versace, V.L., Bellgrove, A., Harvey, E., Rattray, A., Laurenson, L. and Quinn, G.P. (2010) Habitat suitability for marine fishes using presence-only modelling and multibeam sonar. *Marine Ecology Progress Series* **420**, 157-174.

Moore, C. and Doherty, J. (2005) Role of the calibration process in reducing model predictive error. *Water Resources Research* **41**(5).

Mueller, U., Kangas, M., Sporer, E. and Caputi, N. (2012) Variability in the spatial and temporal distribution of the saucer scallop, Amusium balloti, in Shark Bay-management implications. *Marine and Freshwater Research* **63**(11), 1152-1164.

O'Neill, M.F., Courtney, A.J., Turnbull, C.T., Good, N.M., Yeomans, K.M., Staunton Smith, J. and Shootingstar, C. (2003) Comparison of relative fishing power between different sectors of the Queensland trawl fishery, Australia. *Fisheries Research* **65**(1-3), 309-321.

O'Neill, M.F. and Leigh, G.M. (2007) Fishing power increases continue in Queensland's east coast trawl fishery, Australia. *Fisheries Research* **85**(1-2), 84-92.

O'Neill, M.F., Yang, W.-H., Wortmann, J., Courtney, A.J., Leigh, G.M., Campbell, M.J. and Filar, J.A. (2020) Stock predictions and population indicators for Australia's east coast saucer scallop fishery. FRDC Project #2017/057 Final Report.

O'Neill, M.F., Yang, W.-H., Wortmann, J., Courtney, A.J., Leigh, G.M., Campbell, M.J. and Filar, J.A. (2020) Stock predictions and population indicators for Australia's east coast saucer scallop fishery FRDC Project No. 2017/057.

Oliver, E.C., Benthuysen, J.A., Bindoff, N.L., Hobday, A.J., Holbrook, N.J., Mundy, C.N. and Perkins-Kirkpatrick, S.E. (2017) The unprecedented 2015/16 Tasman Sea marine heatwave. *Nature communications* **8**(1), 1-12.

Oliver, E.C., Lago, V., Hobday, A.J., Holbrook, N.J., Ling, S.D. and Mundy, C.N. (2018) Marine heatwaves off eastern Tasmania: trends, interannual variability, and predictability. *Progress in Oceanography* **161**, 116-130.

Oliver, M.A. and Webster, R. (1990) Kriging: a method of interpolation for geographical information systems. *International Journal of Geographical Information System* **4**(3), 313-332.

Orensanz, J.L., Parma, A.M., Turk, T. and Valero, J. (2006) Dynamics, assessment and management of exploited natural populations. In Developments in Aquaculture and Fisheries Science. Vol. 35. pp. 765-868. (Elsevier)

Orensanz, J.M., Parma, A.M. and Iribarne, O.O. (1991) Scallops: biology, ecology and aquaculture. (Ed. SA Shunway) pp. 625-713. (Elsevier: Argentina)

Pebesma, E., J. (2004) Multivariable geostatistics in S: the gstat package. *Computers & Geosciences* **30**(7), 683-691.

Reinhardt, K. and Samimi, C. (2018) Comparison of different wind data interpolation methods for a region with complex terrain in Central Asia. *Climate Dynamics* **51**(9-10), 3635-3652.

Ribbe, J. (2014) Hervey Bay and its estuaries. In Estuaries of Australia in 2050 and beyond. pp. 185-201. (Springer)

Robins, J., Campbell, M. and McGilvray, J. (1999) Reducing prawn-trawl bycatch in Australia: An overview and an example from Queensland. *Marine Fisheries Review* **61**(3), 46-55.

Robson, D.S. and Youngs, W.D. (1971) Statistical analysis of reported tag-recaptures in the harvest from an exploited population. Biometrics Unit, Cornell University, Ithaca, NY. BU-369-M.

Rose, R.A., Campbell, G.R. and Sanders, S.G. (1988) Larval development of the saucer scallop *Amusium balloti* (Bernardi) (Mollusca : Pectinidae). *Australian Jounal Marine Freshwater Research* **39**, 153-60.

Ryan, W.B.F. and Flood, R.D. (1996) Side-looking sonar backscatter response at dual frequencies. *Marine Geophysical Research* **18**(6), 689-705.

Sanabria, L.A., Qin, X., Li, J., Cechet, R.P. and Lucas, C. (2013) Spatial interpolation of McArthur's Forest Fire Danger Index across Australia: Observational study. *Environmental Modelling and Software* **50**, 37-50.

Seber, G.A.F. (1970) Estimating time-specific survival and reporting rates for adult birds from band returns. *Biometrika* **57**, 313-318.

Semmens, J., Ewing, G. and Keane, J. (2019) Tasmanian Scallop Fishery Assessment 2018.

Shan, Y., Paull, D. and McKay, R.I. (2006) Machine learning of poorly predictable ecological data. *Ecological Modelling* **195**(1-2), 129-138.

Shears, N.T. and Bowen, M.M. (2017) Half a century of coastal temperature records reveal complex warming trends in western boundary currents. *Scientific reports* **7**(1), 1-9.

Siesser, W.G. and Rogers, J. (1971) An investigation of the suitability of four methods used in routine carbonate analysis of marine sediments. *Deep Sea Research and Oceanographic Abstracts* **18**(1), 135-139.

Siwabessy, P.J.W. (2001) An investigation of the relationship between seabed type and benthic and bentho-pelagic biota using acoustic techniques. Curtin University,

Smith, C.J., Banks, A.C. and Papadopoulou, K.N. (2007) Improving the quantitative estimation of trawling impacts from sidescan-sonar and underwater-video imagery. *ICES Journal of Marine Science* **64**(9), 1692-1701.

Smith, S.J., Lundy, M.J., Todd, B.J., Kostylev, V.E. and Costello, G. (2006) Incorporating bottom type information into survey estimates of sea scallop (*Placopecten magellanicus*) abundance.

Smith, S.J. and Rago, P. (2004) Biological reference points for sea scallops (Placopecten magellanicus): the benefits and costs of being nearly sessile. *Canadian Journal of Fisheries and Aquatic Sciences* **61**(8), 1338-1354.

Smith, S.J., Sameoto, J.A. and Brown, C.J. (2017) Setting biological reference points for sea scallops (Placopecten magellanicus) allowing for the spatial distribution of productivity and fishing effort. *Canadian journal of fisheries and aquatic sciences* **74**(5), 650-667.

Soria, G., Orensanz, J.L., Morsán, E.M., Parma, A.M. and Amoroso, R.O. (2016) Scallops biology, fisheries, and management in Argentina. In Developments in aquaculture and fisheries science. Vol. 40. pp. 1019-1046. (Elsevier)

Sparre, P. and Venema, S.C. (1992) 'Introduction to tropical fish stock assessment. Part 1. Manual.' (Food and Agricultural Organisation of the United Nations (FAO): Rome (Italy)) 376

Stephens, A.W., Holmes, K.H. and Jones, M.R. (1988) Modern sedimentation and Holocene shoreline evolution of the Hervey Bay coast: Australia. *Queensland Department of Mines, Marine and Coastal Investigations, Project report MA12*.

Sterling, D. (2000) 'The Physical Performance of Prawn Trawling Otter Boards and Low Opening Systems.' (Sterling Trawl Gear Services: Brisbane)

Sterling, D.J. (2005) Modelling the physics of prawn trawling for fisheries management. Ph.D. Thesis, Curtin University of Technology, Western Australia, Perth

Steven, A.D., Baird, M.E., Brinkman, R., Car, N.J., Cox, S.J., Herzfeld, M., Hodge, J., Jones, E., King, E., Margvelashvili, N., Robillot, C., Robson, B., Schroeder, T., Skerratt, J., Tickell, S., Tuteja, N., Wild-Allen, K. and Yu, J. (2019) eReefs: An operational information system for managing the Great Barrier Reef. *Journal of Operational Oceanography* **12**(sup2), S12-S28.

Sutherland, T.F., Galloway, J., Loschiavo, R., Levings, C.D. and Hare, R. (2007) Calibration techniques and sampling resolution requirements for groundtruthing multibeam acoustic backscatter (EM3000) and QTC VIEW™ classification technology. *Estuarine, Coastal and Shelf Science* **75**(4), 447-458.

Syvitski, J.P.M. (1991) 'Principles, Methods and Application of Particle Size Analysis.' (Cambridge University Press)

Tadić, J.M., Ilić, V. and Biraud, S. (2015) Examination of geostatistical and machine-learning techniques as interpolators in anisotropic atmospheric environments. *Atmospheric Environment* **111**, 28-38.

Tarabbia, P.J. (1990) 'Surficial Sediments of the Great Sandy Strait-Queensland, Australia.'

Taylor, B.M. and McIlwain, J.L. (2010) Beyond abundance and biomass: effects of marine protected areas on the demography of a highly exploited reef fish. *Marine Ecology Progress Series* **411**, 243-258.

Tobler, W.R. (1970) A computer movie simulating urban growth in the Detroit region. *Economic geography* **46**, 234-240.

Torgersen, C.E., Baxter, C.V., Li, H.W. and McIntosh, B.A. Landscape influences on longitudinal patterns of river fishes: spatially continuous analysis of fish-habitat relationships. In 'American Fisheries Society Symposium', 2006, p. 473

Tremblay, I., Samson-Dô, M. and Guderley, H.E. (2015) When Behavior and Mechanics Meet: Scallop Swimming Capacities and Their Hinge Ligament. *Journal of Shellfish Research* **34**(2), 203-212.

Tully, O., Hervas, A., Berry, A., Hartnett, M., Sutton, G., O'Keeffe, E. and Hickey, J. (2006) Monitoring and Assessment of scallops off the South East Coast of Ireland. Bord Iascaigh Mhara (Irish Sea Fisheries Board).

Ver Hoef, J.M. and Boveng, P.L. (2007) Quasi-Poisson vs. negative binomial regression: how should we model overdispersed count data? *Ecology* **88**(11), 2766-2772.

Verfaillie, E., Van Lancker, V. and Van Meirvenne, M. (2006) Multivariate geostatistics for the predictive modelling of the surficial sand distribution in shelf seas. *Continental Shelf Research* **26**(19), 2454-2468.

VSN International (2019) Genstat for Windows 20th Edition. (Hemel Hempstead, UK: VSN International)

Wang, S., Duncan, P.F., Knibb, W.R. and Degnan, B.M. (2002) Byssal attachment of Amusium balloti (Bernardi, 1861) (Bivalvia: Pectinidae) Spat. *Journal of Shellfish Research* **21**(2), 563-569.

Welch, D., Robins, J., Saunders, T., Courtney, T., Harry, A., Lawson, E., Moore, B., Tobin, A., Turnbull, C. and Vance, D. (2010) Implications of climate change impacts on fisheries resources of northern Australia. Part 2: Species profiles. (Final Report for FRDC Project)

Welch, D.J., Saunders, T., Robins, J., Harry, A., Johnson, J., Maynard, J., Saunders, R., Pecl, G., Sawynok, B. and obin, A. (2014) 'Implications of climate change impacts on fisheries resources of northern Australia Part 1 : Vulnerability assessment and adaptation options.' Project No edn. (Fisheries Research and Development Corporation)

Wentworth, C.K. (1922) A Scale of Grade and Class Terms for Clastic Sediments. *The journal of Geology* **30**(5), 377-392.

Wessel, P. and Smith, W.H. (1996) A global, self-consistent, hierarchical, high-resolution shoreline database. *Journal of Geophysical Research: Solid Earth* **101**(B4), 8741-8743.

Willcock, S., Martnez-Lpez, J., Hooftman, D.A.P., Bagstad, K.J., Balbi, S., Marzo, A., Prato, C., Sciandrello, S., Signorello, G., Voigt, B., Villa, F., Bullock, J.M. and Athanasiadis, I.N. (2018) Machine learning for ecosystem services. *Ecosystem Services* **33**, 165-174.

Williams, M.J. and Dredge, M.C.L. (1981) Growth of the Saucer Scallop, *Amusium japonicum balloti* Habe in Central Eastern Queensland. *Aust. J. Mar. Freshwater Res.* **32**(4), 657-666.

Wolanski, E. (1994) 'Physical oceanographic processes of the Great Barrier Reef.' (CRC Press: Boca Raton, Florida) 194

Wolff, M. (1987) Population dynamics of the Peruvian scallop Argopecten purpuratus during the El Niño phenomenon of 1983. *Canadian Journal of Fisheries and Aquatic Sciences* **44**(10), 1684-1691.

Wortmann, J., O'Neill, M.F., Courtney, A.J. and Yang, W.-H. (2020) Stock assessment of Ballot's saucer scallop (*Ylistrum balloti*) in Queensland. Department of Agriculture and Fisheries, Queensland.

Yang, W.-H., Wortmann, J., Robins, J.B., Courtney, A.J., O'Neill, M.F. and Campbell, M.J. (2016) Quantitative assessment of the Queensland saucer scallop (Amusium balloti) fishery, 2016 http://era.daf.qld.gov.au/5478/. Department of Agriculture and Fisheries, Queensland.

16 Appendix 4. Fishery-independent survey of the Queensland saucer scallop stock

This section of the report addresses Objective 1) *Design and carry out a comprehensive fishery-independent survey of the 0+ and 1+ age classes in the Queensland saucer scallop.*

16.1 ABSTRACT

This section of the report examined the 13 years of discontinuous fishery-independent saucer scallop trawl survey data (1997–2006, 2017–2019). Commercial trawlers were chartered to undertake a stratified random design survey of the fishery over about 10 nights in October each year, with scientific observers on board counting and measuring the scallops. The raw catch rates were calibrated to standardise for differences between vessels each year. A generalised linear model that considered the swept area of each trawl as an offset was used to derive adjusted mean catch rates (number ha^{-1}) for the 0+ and 1+ scallop age classes, as well as total scallops, for each strata and year. The model also considered lunar phase and time-of-night effects for each trawl. In general, adjusted mean scallop density has declined significantly over the sampling period. The 1+ age class numerically dominated survey catch rates. Using data from those years when the survey was comprehensively implemented, the density of scallops has declined by about half from the early survey years (1997–2000) to the recent years (2017–2019). The adjusted mean density of the 0+ age class was lowest in 2019 and there has been a general increase in the proportion of the scallop population inside the SRAs over the period. The calibrated scallop densities were interpolated using kriging methods to develop density maps. The survey catch rates have been used as an index of abundance in recent quantitative assessments of the stock. Recommendations on how the survey can be improved are also provided.

16.2 INTRODUCTION

The Queensland saucer scallop (*Y. balloti*) fishery is a significant component of the Queensland East Coast Otter Trawl Fishery (QECOTF) and mainly located in coastal waters between 21ºS and 27ºS in depths from about 20–70 m (Dredge 1994; Dichmont *et al.* 2000). From 1988–2017, mandatory logbook data indicate that the annual catch ranged from a maximum of 1930 t (meat weight) in 1993 to a minimum of 202 t in 2015. In 2016, a quantitative stock assessment concluded that the scallop biomass had fallen to less than 20% virgin stock biomass and that the stock was overfished (Yang *et al.* 2016).

Concern over the decline in the catch, combined with the findings and recommendations from the assessment, prompted management action and initiated further research on the stock. Management measures implemented in late 2016 included the indefinite closure of the six SRAs. These areas commonly contain relatively high scallop densities and were closed permanently in 1997 following a severe decline in the stock in 1996, as a means of lowering fishing mortality. However, since 2001 the SRAs have been rotationally opened and closed to fishing over a two-year cycle (i.e., closed for 15 months, open for nine months). In addition to closing the SRAs, the fishery managers implemented a complete closure of the fishery from May to October in 2017, which has been applied annually since.

Another management response was the reintroduction of an annual fishery-independent trawl survey of scallop abundance in 2017. This stratified random design survey was first implemented in 1997, following the 1996 collapse (Dichmont *et al.* 2000). The survey was comprehensively implemented from 1997–2000, however from 2001–2006 funding declined, reducing the number of strata and sample sites, and after 2006 the survey ceased. A summary of the survey data and results from 1997–2006 is provided by Jebreen *et al.* (2008). The survey is relatively expensive (~$150,000–$200,000 annually) and has always been funded entirely from Queensland consolidated revenue, which makes its current and future implementation tenuous and dependent on the priorities of the Government-of-the-day.

The reintroduced survey has now been implemented for the last three years (i.e., 2017, 2018 and 2019) and as a result the survey time series includes a total of 13 years, albethey discontinuous. This section of the report presents the survey results from all years and describes the survey design, including changes to the strata, and improvements to the statistical methods used to calibrate the survey catch rates and the resulting scallop density estimates. Of paramount importance is the need to be able to compare survey results between years to accurately interpret trends. Cautious interpretation of the results is required due to some changes in the survey over the years.

In addition to providing another fishery-independent source of information on the temporal and spatial distribution of the scallop population, the survey data are also used as an index of abundance in the scallop stock assessment model.

16.3 METHODS

16.3.1 *Survey design and sampling strata*

When the survey was reintroduced in 2017, significant attention was given to ensure the design was as close as possible to that of the first survey undertaken in 1997, described by Dichmont *et al.* (2000). This is imperative if results from recent years (i.e., 2017–2019) are to be comparable with those from the early years (i.e., 1997–2006). However, some significant changes have occurred since the survey was first implemented, including
1) loss of sampling strata area due to the introduction of closures (i.e., green zones) in 2004 in the Great Barrier Reef Marine Park under the Representative Areas Program (RAP) (Fernandes *et al.* 2005), which resulted in some previously-surveyed areas that could no longer be sampled,
2) the mandatory implementation of turtle excluder devices (TEDs) and a second bycatch reduction device (BRD) in all trawl nets, including survey nets, in the early 2000s (see Robins *et al.* 1999, Courtney *et al.* 2006, 2008, 2014 for further details on the devices),
3) changes to the shape and size of the SRAs in the early 2000s, and

In addition, two new strata were added to the design in 2017 in the southern part of the fishery adjacent to Fraser Island to reflect the increasing scallop catches in the area based on logbook data over the last two decades (see Figure 16 in O'Neill *et al.* 2020).

The first survey in 1997 was designed around CFISH logbook grids (30'x30') where the bulk of the scallop catch was historically reported from. These grids were located between approximately 22° S and 25° S in southern Queensland and are identified as S28, T28, S29, T29, T30, U30, U31, V31 and V32 (Figure 16-2). The survey domain consisted of 12 strata comprised of the nine grids and three permanently closed SRAs in the Yeppoon, Bustard Head and Hervey Bay regions, nested within the grids. From 1997–2006 the survey did not extend south of Hervey Bay or east of Fraser Island.

The survey is undertaken over approximately 10 days in early October, during the southern closure period (20 September to 31 October), when otter trawling in southern Queensland is prohibited in depths less than 50 fathoms (except for Moreton Bay). October is the optimum time for undertaking the survey because weather conditions are usually favourable and the population of the 0+ age class is relatively high following the winter spawning. Undertaking the survey in October also enhances the availability of vessels for chartering, as most vessels are not fishing at this time awaiting the closure opening.

The timing of the survey is centred around the neap tides to minimise the low scallop catch rates during the strong tidal currents associated with spring tides. From 1997–2000, the survey design remained relatively fixed and the SRAs permanently closed. In 1998 the boundaries for the Yeppoon SRA changed and in 2001 and 2002 there were further changes to the size, location and permanently-closed status of the SRAs, at the request of industry who argued for access to scallops inside the closed areas. As such, the function of the SRAs changed during this period, from being a permanently closed source of recruitment, to being subjected to fishing.

In 2001 and 2002 the number of SRAs were increased to create ten smaller SRAs that were rotationally opened and closed to trawling. In 2003 these smaller areas were merged to create two SRAs within each of the three areas (i.e., Yeppoon SRA A and B, Bustard Head SRA A and B, and Hervey Bay SRA A and B). Each A and B area was opened alternately for nine months and closed for 15 months (i.e., a 2-year rotational cycle) (Figure 16-1). The location, size and rotational opening of the six SRAs remained constant from 2003–2016. As a result of Yang *et al.* (2016) stock assessment, which concluded the stock to be overfished, and subsequent assessments (O'Neill *et al.* 2020; Wortmann *et al.* 2020) all six SRAs have been closed since September 2016.
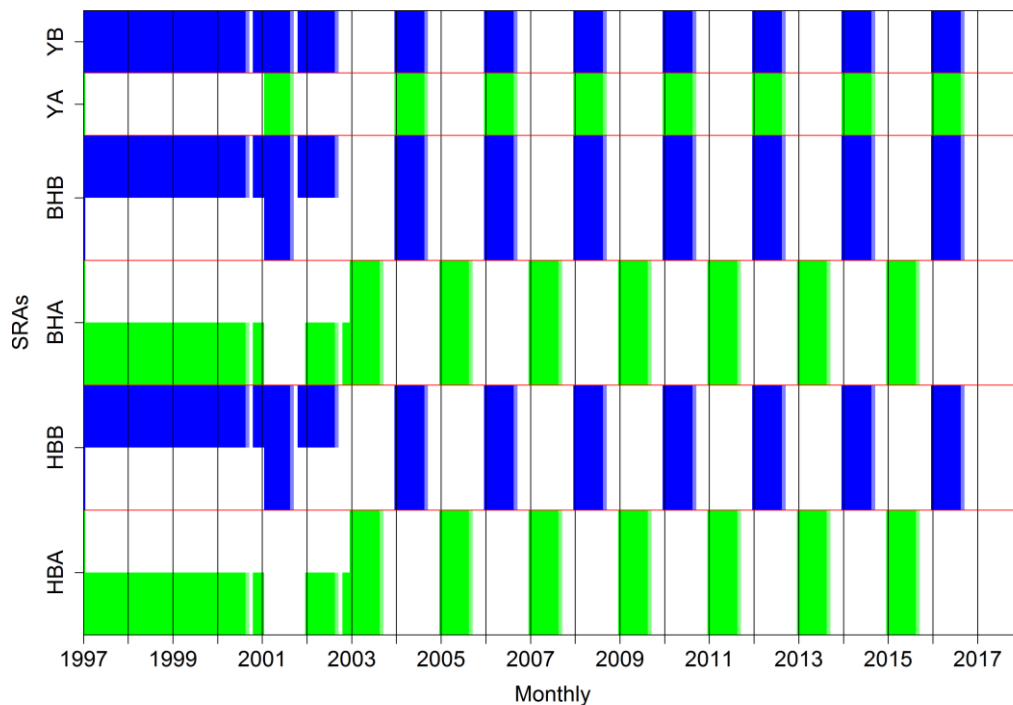
Figure 16-1. Diagram shows the opening and closing schedule applied to the SRAs from 1997–2017. Blue and green are periods open to trawling and white represents closed periods. Since September 2016 all six SRAs have remained closed. The figure is based on a similar diagram on page 38 of Campbell *et al.* (2012).

From 2001–2006 state government funding for the survey waned and eventually ceased. During this period the survey was downsized resulting in reductions in the number of participating chartered vessels, survey strata and sample sites. The only strata that were consistently sampled over this period were the SRAs and the T30 grid.

When the survey was reintroduced in October 2017 the original 1997 comprehensive design was implemented. Furthermore, examination of scallop catches in the Yang *et al.* (2016) report indicated increasing scallop catches and catch rates off Fraser Island over the last decade (~2007–2016). For this reason, two additional strata were added to the survey design in this region, referred to as the Maheno and Sunshine Coast Region.

The number of sites allocated to a given stratum is determined by a weighting method based on the summed product of stratum abundance index and stratum area. The total number of survey sites is largely governed by the funding available to charter commercial trawlers. Once the number of sites is estimated, a proportion of sites is allocated to each stratum, based on its contribution to the sum product, and the sites are randomly distributed within each stratum.

From 1997–2006, the abundance index was based on the logbook commercial mean annual catch per unit effort (CPUE, baskets per boat day) from 1988 onwards. In 2000, a high spatial resolution vessel monitoring system (VMS) was mandated for the Queensland trawl fleet and when these data were used in conjunction with the vessel's reported daily scallop catch, a much higher spatial resolution CPUE can be used as the abundance index in the survey design. This abundance index was based on the previous 10 years of logbook data. Marrying the high spatial resolution VMS data to the vessel's daily reported logbook catch is undertaken using TrackMapper software.

A decision rule was implemented by Dichmont *et al.* (2000) to ensure that each strata received a minimum of 2% of the total survey sampling effort. Prior to undertaking the survey, additional "spare" sites were identified for each stratum in the event that one or more sites could not be trawled due to problematic bottom type. In the early years between 1997 and 2000, the total number of sites that could be sampled ranged between 395 and 440. Due to the lack of funds reducing the number of vessels that could be chartered for each survey, the number of sites that could be sampled was halved between 2001 and 2006 and ranged between 135 and 155. In recent surveys, from 2017 to 2019, the number of sites that could be sampled was increased and ranged between 300 and 335.

The 1997–2000 surveys were carried out between north of Yeppoon to the south of Hervey Bay. The reduced funding from 2001–2006 resulted in a smaller survey spatial domain, but from 2017–2019 the survey area was increased to closely represent that of the early years (i.e.,1997–2000), and expanded southwards to include the Maheno and Sunshine Coast Region strata (Figure 16-2).
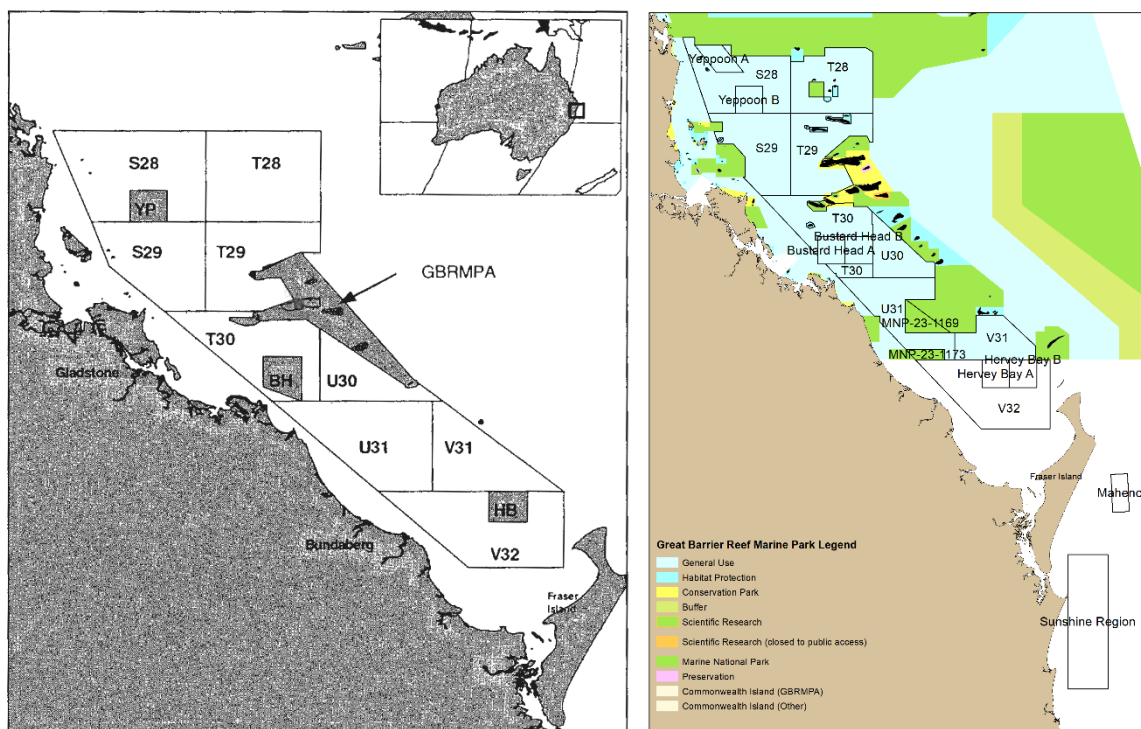
Figure 16-2. The left map shows the 12 survey strata in 1997, from Dichmont *et al.* (2000). The right map shows the strata in 2017. Some loss of strata sampling area occurred when the GBRMPA expanded their closed areas (green zones) in 2004, mainly in U31 and the far north of S28 and T28. The 2017 survey includes two additional strata (Sunshine Coast Region and Maheno) in the southern part of the fishery where scallop catches have increased over the last decade.

The survey has consistently chartered Queensland commercial otter trawlers and their crews to undertake the survey, with two scientific observers on board each vessel from the Queensland Department of Agriculture and Fisheries. In the early years, trawls were 20 min bottom time, but since

2017 all trawls have been set at 1 nm. Information on the size and number of nets deployed by each vessel has also been recorded. Across all years, all trawls have been undertaken in a straight line, transect lengths have ranged from 0.82–1.00 nm and trawl speed has ranged from 2.36–2.80 kn. Each trawl is generally referred to as a trawl shot.

16.3.2 Vessels and gear

Scallop surveys between 1997 and 2000 were completed by four commercial fishing vessels. After the reduction in funds in 2001 only two commercial fishing vessels were chartered until 2006 and when funding was available again in 2017, three commercial fishing vessels were chartered to undertake the survey in 2017, 2018 and 2019. The participation of the *FV C-King* has been consistent throughout all surveys. Table 16-1 provides a summary of the vessels chartered and their gear type for each survey. Prawn mesh ranging in size between 2.0 and 2.5 inches (50.8 and 63.5 mm) has been specified for use during each survey to increase the selectivity and retention of small (i.e., 0+ age class) scallops, rather than using the larger 3.5-inch (88.9 mm) scallop mesh.

In 2001, turtle exclusion devices (TEDs) and bycatch reduction devices (BRDs) were made mandatory on all commercial fishing vessels and required to be used in the survey. Table 16-1 details the implementation of TEDs and BRDs on the vessels during surveys. No TEDs or BRDs were deployed in the survey early years (1997–2000). There was a transitional period from 2001–2004 where the devices were trialled in some nets during the survey, and from 2005–2019 all survey nets have been fitted with both a TED and a second BRD. Statistical testing of the effects of TEDs and BRDs on the scallop catch rates was examined in section 16.4.5, page 77.

16.3.3 Data collection

Trawl sampling took place at night commencing at sunset and finishing at sunrise, with vessels trawling into the prevailing tidal current whenever possible. Each vessel was allocated a similar proportion of sites to sample, and each vessel allocated a specific region of the survey spatial domain.

At each trawl site the date, start time, shot number and site number were recorded. The following data were also recorded for each site from the vessel GPS; starting and ending latitude and longitude, distance trawled, bearing, depth, and trawl duration. Comments were also recorded during each shot in relation to any problems that may impact the scallop density estimate. Once a shot was complete, nets were pulled on board, the number of scallops from all nets was counted and a maximum subsample of 200 scallops measured. In 2001, scallops from each net were counted and measured separately. Between 2002 and 2004, scallops from the middle net-only were counted while scallops caught in the outer nets were counted and measured together. For all other surveys, nets were pooled before the scallops were counted and measured. Scallops were measured by recording the shell height (SH), which is the distance in millimetres (mm), between the auricles and the ventral margin of the scallop (Williams and Dredge 1981).

Table 16-1. Summary of survey vessels and gear setup. Total head rope length is derived by summing individual head rope lengths of all nets on a given vessel.

Year	Fishing vessel name	Gear setup		
		Number of nets	Total head rope length (metres)	TED and/or BRD
1997	C-King	5	38.95	No TED or BRD present in nets.
	Exodus	4	36.56	No TED or BRD present in nets.
	Rebecca Mae	3	40.23	No TED or BRD present in nets.
	Tamara	4	32.92	No TED or BRD present in nets.
1998	C-King	5	38.95	No TED or BRD present in nets.
	Rebecca Mae	3	42.06	No TED or BRD present in nets.
	Southern Intruder	4	36.56	No TED or BRD present in nets.
	Warlord	4	36.56	No TED or BRD present in nets.
1999	C-King	5	38.95	No TED or BRD present in nets.
	Chromatt	4	32.92	No TED or BRD present in nets.
	Rebecca Mae	3	38.40	No TED or BRD present in nets.
	Seadar Bay	3	38.40	No TED or BRD present in nets.
2000	C-King	5	38.95	No TED or BRD present in nets.
	Peggy D	4	36.58	No TED or BRD present in nets.
	Rebecca Mae	3	38.40	No TED or BRD present in nets.
	Seadar Bay	3	38.40	No TED or BRD present in nets.
2001	C-King	5	38.95	TED and BRD were present in one port and starboard net.
	Seadar Bay	3	38.40	TED and BRD were present in one outer net.
2002	C-King	5	38.95	TED and BRD were present in both outer nets.
	Seadar Bay	3	38.40	TED was present in both outer nets.
2003	C-King	5	38.95	TED and BRD were present in both outer nets.
	Seadar Bay	3	38.40	TED and BRD were present in both outer nets.
2004	C-King	5	38.95	TED and BRD were present in both outer nets.
	Seadar Bay	3	38.40	TED was present in both outer nets.
2005	C-King	5	38.95	TED and BRD were present in all nets.
	Seadar Bay	3	38.40	TED and BRD were present in all nets.
2006	C-King	5	38.95	TED and BRD were present in all nets.
	Gwendoline May	4	29.12	TED and BRD were present in all nets.
2017	C-King	5	38.40	TED and BRD were present in all nets.
	Benjamin	3	76.80	TED and BRD were present in all nets.
	Maddison	3	76.80	TED and BRD were present in all nets.
2018	C-King	5	40.00	TED and BRD were present in all nets.
	Silda	5	37.80	TED and BRD were present in all nets.
	Somatina	3	65.52	TED and BRD were present in all nets.
2019	C-King	5	40.00	TED and BRD were present in all nets.
	Silda	5	40.00	TED and BRD were present in all nets.
	Joseph-M	3	54.90	TED and BRD were present in all nets.

16.3.4 Queensland scallop survey data

Dichmont *et al.* (2000) reported the first (i.e., 1997) Queensland scallop survey catch rates as a density (i.e., number of scallops m^{-1}). However, Jebreen *et al.* (2008) reported subsequent years as number of scallops per 20-minute shot, which does not consider the area swept by each trawl and is therefore comparatively imprecise. To improve the precision of the survey catch rates, the analyses undertaken herein focused on quantifying the swept area of each trawl (in hectares, ha), thus enabling the calculation of density (i.e., number of scallops ha^{-1}). Swept area was estimated using detailed information on the gear used by each survey vessel each year, specifically 1) the head rope length of each net, 2) the length of each trawl, and 3) net spread factors, which vary with the configuration of the nets used (e.g. twin, triple or quad gear) (Sterling 2000). Other information recorded during the survey which was subsequently used to improve the catch rate analysis included 1) whether the catch from a specific net was included in the sample, 2) the position of the net (i.e., middle, inner port, outer starboard, etc.), 3) number of nets sampled from, 4) whether a trawl was for calibrating or a standard survey trawl, 5) how many scallops were measured and unmeasured in each trawl and 6) whether a TED and/or BRD was inserted in the net. Errors in the database were corrected to match the original survey hard copy datasheets.

16.3.5 Vessel calibration

Over the 13 years several different vessels have participated in the survey. The composition of participating vessels generally changed each year, and as a result, the trawl gear configurations and net sizes have also varied. This is partially addressed by calibrating for differences between vessels each year (but it does not address vessel differences between years). A calibration shot is defined as a shot in which all participating vessels trawl side-by-side keeping their starting location, heading, speed and duration consistent with each other. Calibration shots for all years were completed at randomly chosen sites within a stratum and conducted by all vessels completing 20 min or 1 nm side-by-side trawls, and counting all scallops caught upon completion of each shot. The number and location of calibration shots has changed for each survey (Table 16-2), with calibration shots completed during the day in the early surveys and during the night for later surveys.

Table 16-2. Summary of calibration shots. Strata indicates the location in which calibration shots were conducted for each survey. Survey day indicates which day the calibration shots were held on for each survey.

Year	Number of calibration shots	Strata	Time	Survey day
1997	10	T29	Day	Second
1998	19	T30	Day	First and second
1999	20	T30	Day	First and second
2000	21	T30	Day	First and second
2001	20	T30 and Bustard Head A	Night	First and second
2002	27	T30 and Bustard Head A	Night	First and second
2003	24	T30 and Bustard Head A	Night	First and second
2004	24	T30 and Bustard Head A	Night	First and second
2005	25	T30 and Bustard Head A	Night	First and second
2006	22	T30 and Bustard Head A	Night	First and second
2017	11	Bustard Head A	Night	First
2018	11	Bustard Head A	Night	First
2019	11	Bustard Head A	Night	First

The following model was used to derive calibration factors for differences between vessels each year. Let C_{yi} denote the total number of scallops caught in trawl i of year y from the calibration shots. For year y, C_{yi} was fitted to the Quasi-Poisson GLM, which assumes $E(C_{yi}) = \mu_{yi}$ and $var(C_{yi}) = \alpha_y \mu_{yi}$, where μ_{yi} and α_y represent the mean and overdispersion parameters, respectively, and $\mu_{yi} > 0$ and $\alpha_y > 0$ (Ver Hoef and Boveng 2007). For the sake of simplicity, let $\boldsymbol{\mu}_y$ denote the mean vector of μ_{yi}, and be modelled as:

$$\boldsymbol{\mu}_y = \exp{(\boldsymbol{W}_y\boldsymbol{\beta}_y + log(\boldsymbol{A}_y))},$$

where $\boldsymbol{W}_y$ is the design matrix of intercept, vessels and sample sites, $\boldsymbol{\beta}_y$ the vector of the associated coefficients, and $\boldsymbol{A}_y$ the vector of areas swept in year y, respectively. The logged $\boldsymbol{A}_y$ is the offset variable.

The area swept for each site was calculated as the product of the distance trawled and the effective net mouth spread width, where net spread was calculated as the product of the combined head rope length of all nets deployed on the vessel and a net spread factor. The net spread factors were based on research by Sterling (2005) and were 0.75, 0.70 and 0.80 for vessels towing triple gear (three nets), quad gear (four nets) and five nets, respectively.

The calibration model was fitted using the Generalised Linear Models function in Genstat (VSN International 2019). Each year, the mean scallop density (number of scallops ha^{-1}) was predicted for each vessel and used to derive proportions, or calibration factors, relative to the standard vessel (i.e., *FV C-King*). A calibration factor was applied to each trawl for each vessel, adjusting the catch rate for differences between vessels in such a way that it was analogous to each survey being undertaken by a single vessel.

16.3.6 Kriging

Scallop densities were obtained for each site sampled in each survey. To provide a visual representation of the scallop population size across the fishery, there is a need to predict scallop densities at unsampled locations. One way to approach this is through kriging, which is a geostatistical interpolation method developed from the regionalized variable theory (Oliver and Webster 1990; Cressie 1993). Predictions of unsampled locations produced by a kriging analysis are estimated based on the spatial arrangement of sampled sites. There are two steps involved when undertaking a kriging analysis: 1) the fitting of a variogram to the spatial structure of sampled sites, and 2) utilising the spatial structure through the use of weights to generate predictions at the unsampled sites. In addition, prediction errors are estimated, which are minimised by the kriging process.

This geostatistical model was used to estimate scallop densities within ten regions of the scallop fishery. The ten regions from north to south are the Yeppoon region, Yeppoon SRA A, Yeppoon SRA B, Bustard Head region, Bustard Head SRA A, Bustard Head SRA B, Hervey Bay region, Hervey Bay SRA A, Hervey Bay SRA B, and Sunshine Coast region. Within each region, the calibrated scallop densities were utilised in local kriging models to estimate scallop densities. Scallop density predictions were constructed for the 0+ age class, the 1+ age class and total scallops. The method is described in greater detail in the FRDC 2017-057 final report by O'Neill *et al.* (2020).

The kriging analyses for 2001–2006 should be considered with caution because the number of strata sampled was significantly reduced in these years to six SRAs and T30.

16.3.7 Strata weighted mean densities

The calibrated scallop densities for each site can also be utilised to produce mean densities for each stratum in each year by calculating weighted means. A weighted mean is a variation of the arithmetic mean which considers that each stratum may not replicate heterogeneity in the population distribution (Haddon 1997; Finch 2009). A weight for each stratum is based on the proportion of a given stratum area to the total strata area surveyed in the given year. A weight represents the importance of the stratum mean to the final analysis. Through weighting of the calibrated densities, uncertainty in the estimates produced is removed. For each survey year the following methodology was used to calculate a stratified mean density of scallops.

For each survey the stratum weighting, W_h, is calculated by the following:

$$W_h = \frac{A_h}{\sum A_h}$$

where, A_h represents the area of stratum h.

Each stratum h has n_h calibrated density samples, x_{hi}. The mean density of scallops within each stratum h is given by:

$$X_h = \frac{\sum x_{hi}}{n_h}$$

Stratified mean density, X_{st}, for scallops in each survey is obtained by taking the sum of all strata mean densities, X_h, weighted by their respective stratum weighting, W_h:

$$X_{st} = \sum W_h * X_h$$

The standard error of the estimate of the stratified mean density, X_{st}, is given by the square root of the variance:

$$SE_{X_{st}} = \sqrt{\sum W_h{}^2 * \frac{S_h{}^2}{n_h}}$$

where, S_h represents the calibrated standard deviation of the scallop density for stratum h, and is used to determine variance:

$$S_h{}^2 = \frac{\sum(x_{hi} - X_h)^2}{n_h - 1}$$

For the above equations, n_h represents the number of sites sampled within stratum h.

The coefficient of variation (CV) describes the dispersion of densities for each survey year and is given by a ratio of the stratified standard error to the stratified mean density of scallops (Haddon 1997). The higher the CV the greater the dispersion around the mean. The lower the CV, the more precise the mean. For each survey year the coefficient of variation will be obtained:

$$CV = \frac{SE_{X_{st}}}{X_{st}}$$

16.3.8 *Generalised linear model of scallop densities*

The following model was fitted to the calibrated number of scallops caught at each trawl site. Let C_{sj} denote the number of scallops caught in trawl j of size class s in the survey years 1997–2000 and 2017–2019, where size class s represents the 0+ age class, 1+ age class, or total scallops (i.e., all scallops caught – measured and unmeasured). By multiplying the corresponding calibration factor acquired at the previous stage, C_{sj} is calibrated to produce the calibrated number of scallops $\tilde{C}_{sj}$. For size class s, $\tilde{C}_{sj}$ was fitted to the Quasi-Poisson GLM, which assumes $E(\tilde{C}_{sj}) = \tilde{\mu}_{sj}$ and $\text{var}(\tilde{C}_{sj}) = \delta_s \tilde{\mu}_{sj}$, where $\tilde{\mu}_{sj}$ and δ_s represent the mean and overdispersion parameters, respectively, and $\tilde{\mu}_{sj} > 0$ and $\delta_s > 0$. For simplicity, let $\tilde{\boldsymbol{\mu}}_s$ denote the mean vector of $\tilde{\mu}_{sj}$, and it is modelled with the following form

$$\tilde{\boldsymbol{\mu}}_s = \exp(\boldsymbol{X}_s \boldsymbol{\theta}_s + log(\boldsymbol{A})),$$

where $\boldsymbol{X}_s$ is the design matrix of intercept, strata, year, time-of-night, lunar phase, TED/BRD, the interaction between strata and year, $\boldsymbol{\theta}_s$ the vector of the associated coefficients, and $\boldsymbol{A}$ the vector of areas swept in size class s, respectively. The logged $\boldsymbol{A}$ is the offset variable.

The explanatory variables had the following features:
(1) Year (categorical term, 13 levels representing each year the scallop trawl survey was conducted).
(2) Strata (categorical term, 20 levels representing each of the strata sampled from by each scallop trawl survey).

(3) Lunar phase (categorical term, four levels based on lunar luminance which ranged from 0–15% for the new moon phase, 85–100% for the full moon phase, the waxing phase was based on increasing luminance between 15 and 85% and the waning phase based on declining luminance between 85 and 15%).

(4) Time-of-night (categorical term, six levels representing two-hour blocks between 1800 hr and 0600 hr, and a level representing the day, 0600 hr to 1800 hr).

(5) TED/BRD (categorical term, four levels representing nets without devices, nets with only TEDs, nets with only BRDs, and nets with both devices).

The size-frequency distribution of all measured scallops from all survey years has a general bimodal appearance (Figure 16-3), with separation of the modes at approximately 78 mm shell height (SH) (Dichmont *et al.* 2000). The scallops can therefore be assigned into two age classes, 0+ age class or 1+ age class. Individuals that are < 78 mm are classed as younger than 1 year old (0+ age class), and individuals ≥ 78 mm are older than 1 year old (1+ age class). The above model was fitted separately for each age class, as well as the total number of scallops, using the Generalised Linear Models function in Genstat (VSN International 2019). The mean scallop density (number of scallops ha^{-1}) for each age class was calculated by fixing the time-of-night to 2200 hr to 0000 hr and the lunar phase to waxing, as these factor levels were associated with highest catch rates.

Other models were considered, including the negative binomial generalised linear model. While this type of model can be used to fit overdispersed count data, it cannot be used when the count data are non-integer. Once the calibration factors were applied to the raw survey data, the count data were converted to non-integers and a negative binomial model was no longer suitable. A two-step logistical model was also considered, but after problematic shots were removed the number of observations with zero scallop counts was very low (i.e., < 4%) and so the model was uninformative.

16.4 RESULTS

16.4.1 Size class frequency analysis

The size-frequency distributions of measured scallops from each survey are provided in Figures 16-3 to 16-16. A clear bimodal distribution is apparent in 1997, 2000, 2002, 2003 and 2017, however evidence of a 0+ modal peak is weak in several years, possibly suggesting relatively poor recruitment or low catchability of the smaller size class. The 0+ age class mode generally occurs at 50–60 mm SH, while the 1+ age mode occurs at approximately 90 mm SH. The trough separating the modes occurs at approximately 78 mm SH. The 1+ age class consistently dominate the size-frequency distribution. The number of scallops larger than 90 mm SH declines markedly, while the number of scallops larger than 120 mm SH is negligible. There is no evidence to suggest that the maximum size of the scallops is declining. In 1997 the modes for both age classes occurred at slightly larger sizes (Figure 16-4) compared to the remaining time series. In 2000 the 0+ mode and the trough occurred at a smaller size (Figure 16-7). In 2003 the modes for both age classes occurred at relatively small sizes (Figure 16-10).

Length Frequency
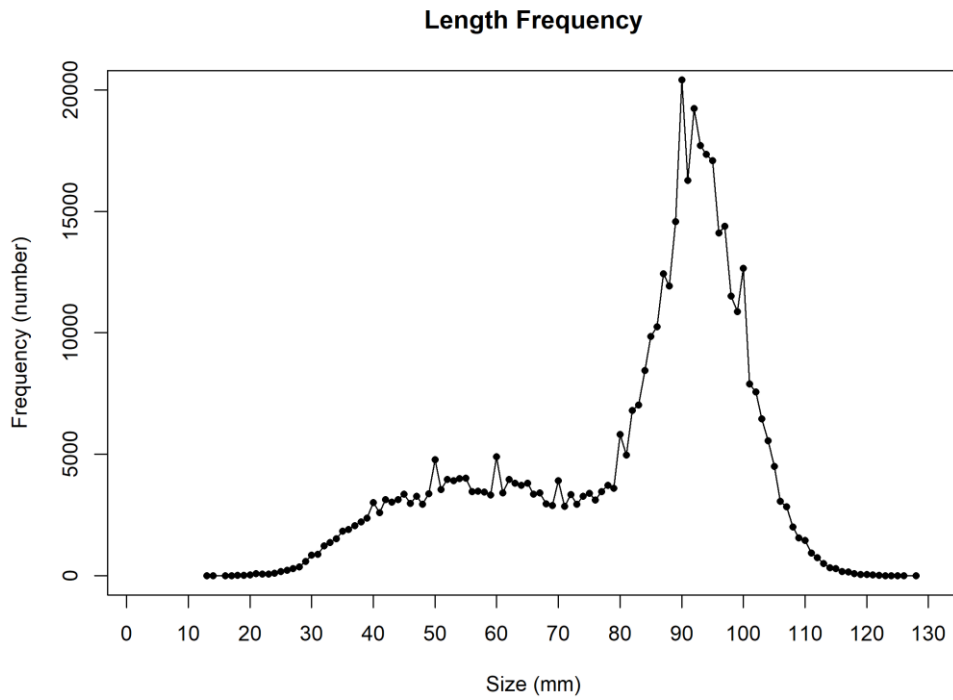
Figure 16-3. Size-frequency plot of all saucer scallops measured in all survey years (i.e., 1997–2006, 2017–2019).

Length Frequency in 1997
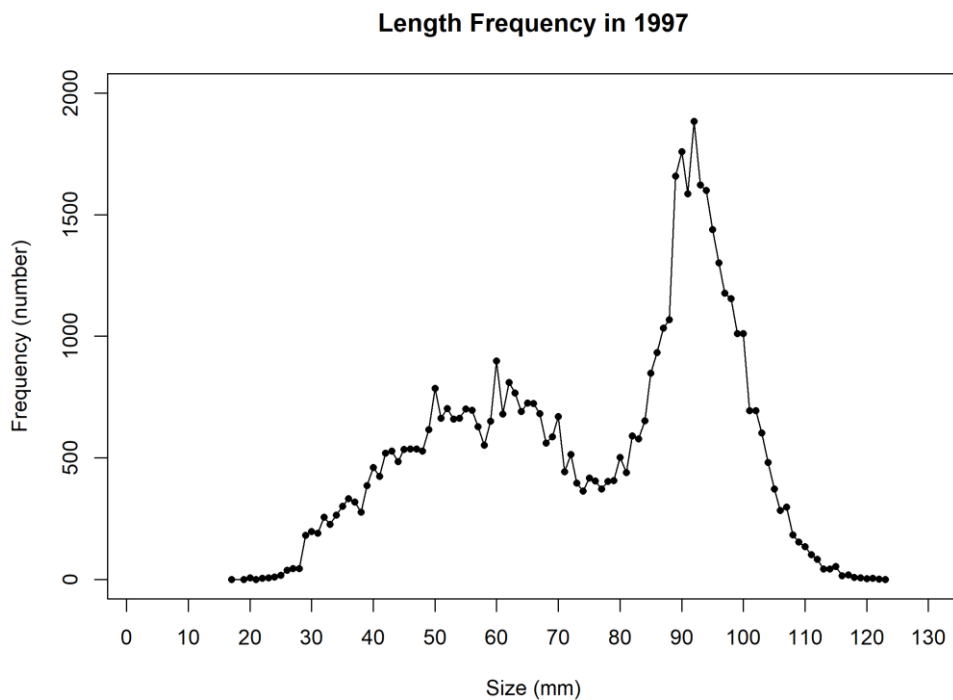
Figure 16-4. Size-frequency plot of saucer scallops measured in 1997.

Length Frequency in 1998
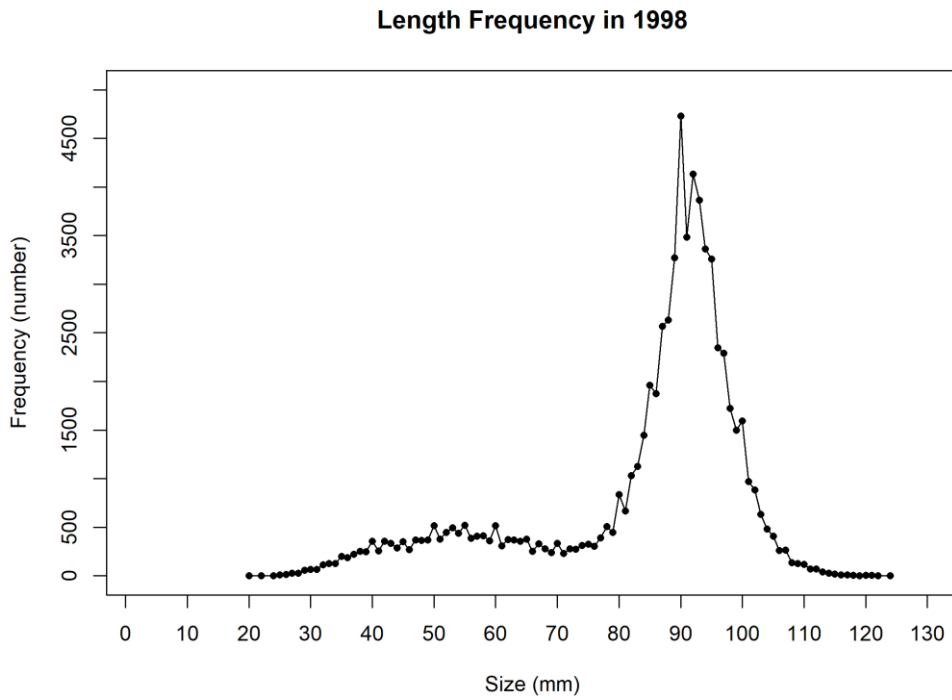
Figure 16-5. Size-frequency plot of saucer scallops measured in 1998.

Length Frequency in 1999
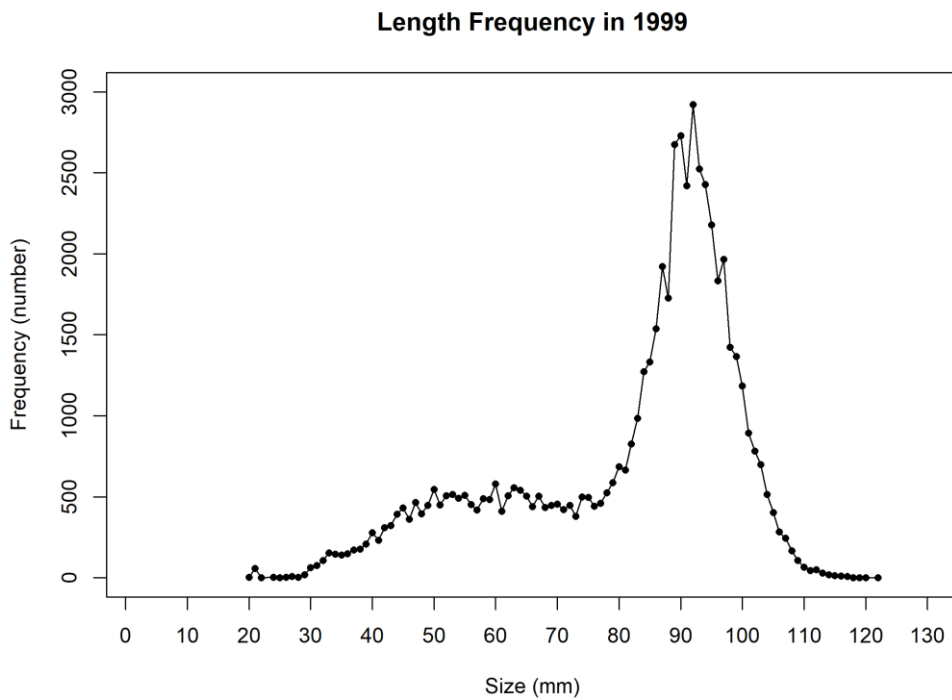
Figure 16-6. Size-frequency plot of saucer scallops measured in 1999.
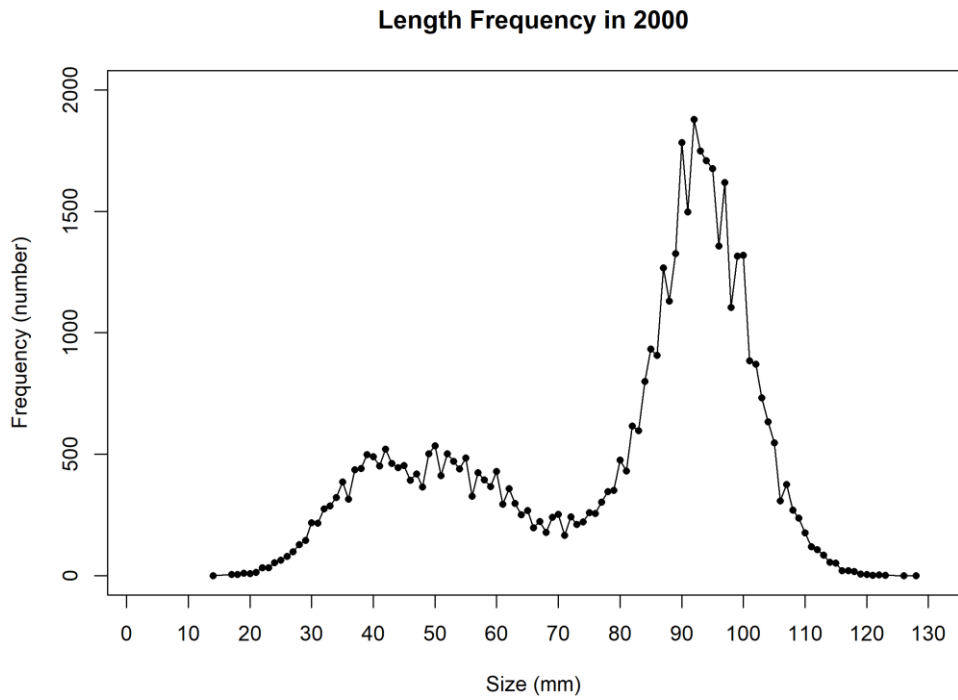
Figure 16-7. Size-frequency plot of saucer scallops measured in 2000.
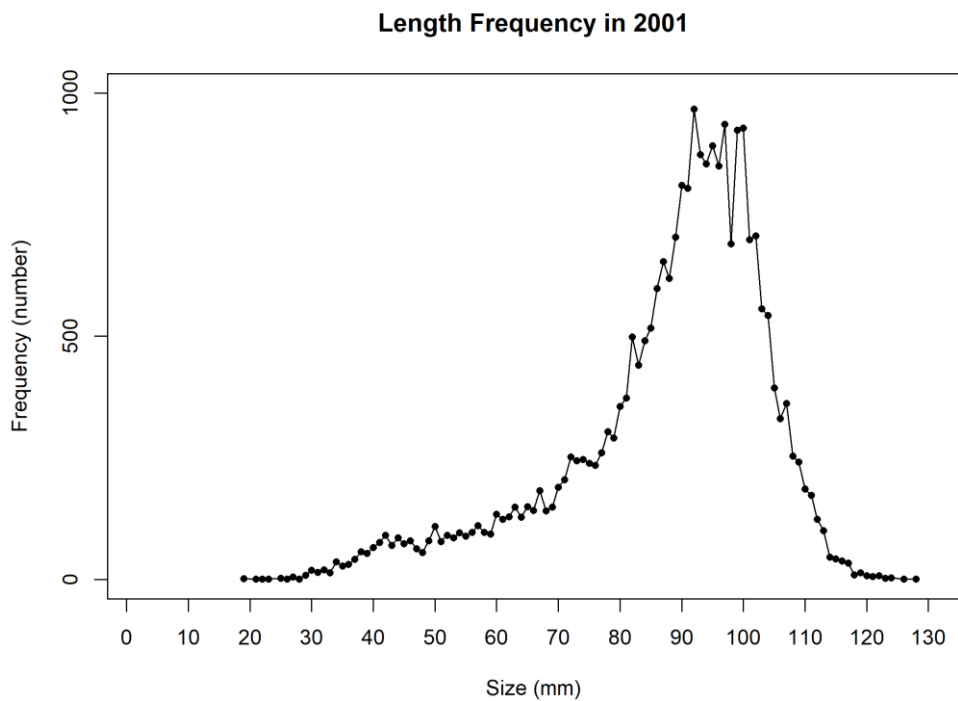
Figure 16-8. Size-frequency plot of saucer scallops measured in 2001.
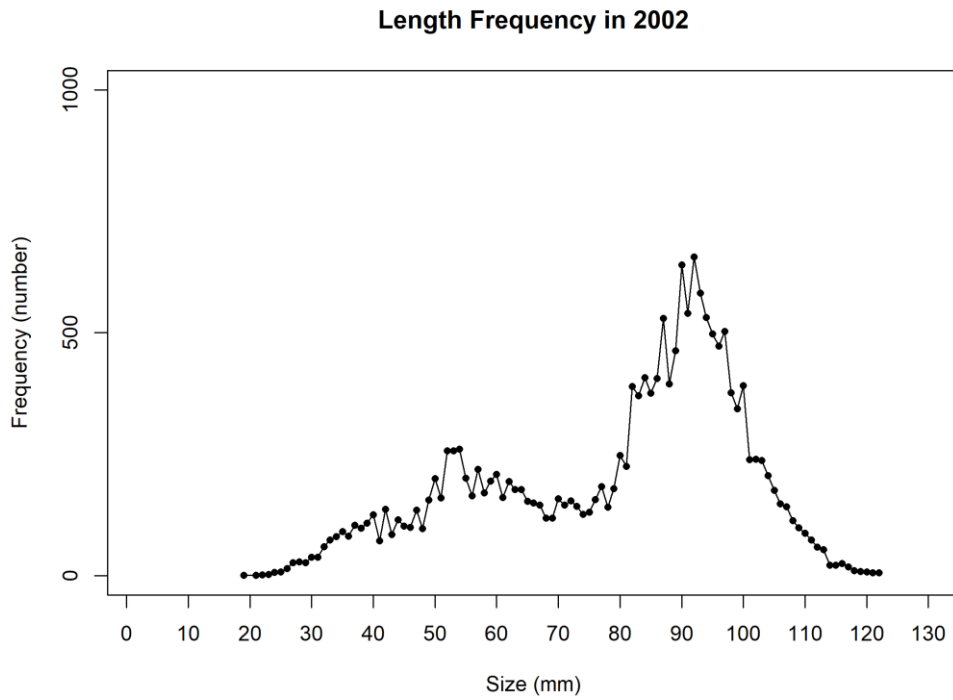
Figure 16-9. Size-frequency plot of saucer scallops measured in 2002.
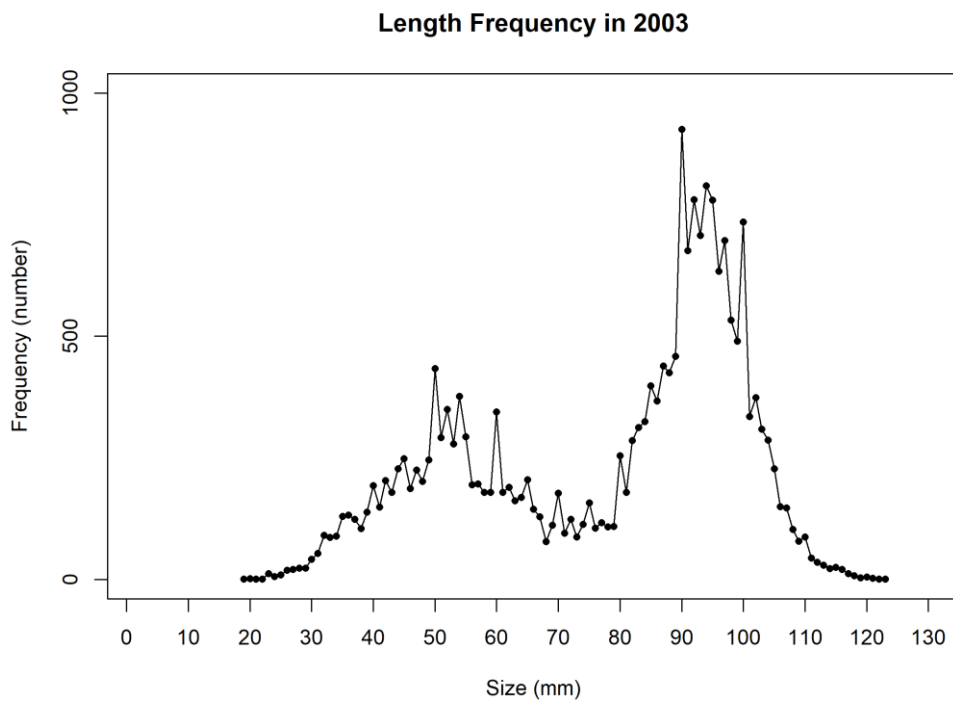
Figure 16-10. Size-frequency plot of saucer scallops measured in 2003.

Length Frequency in 2004
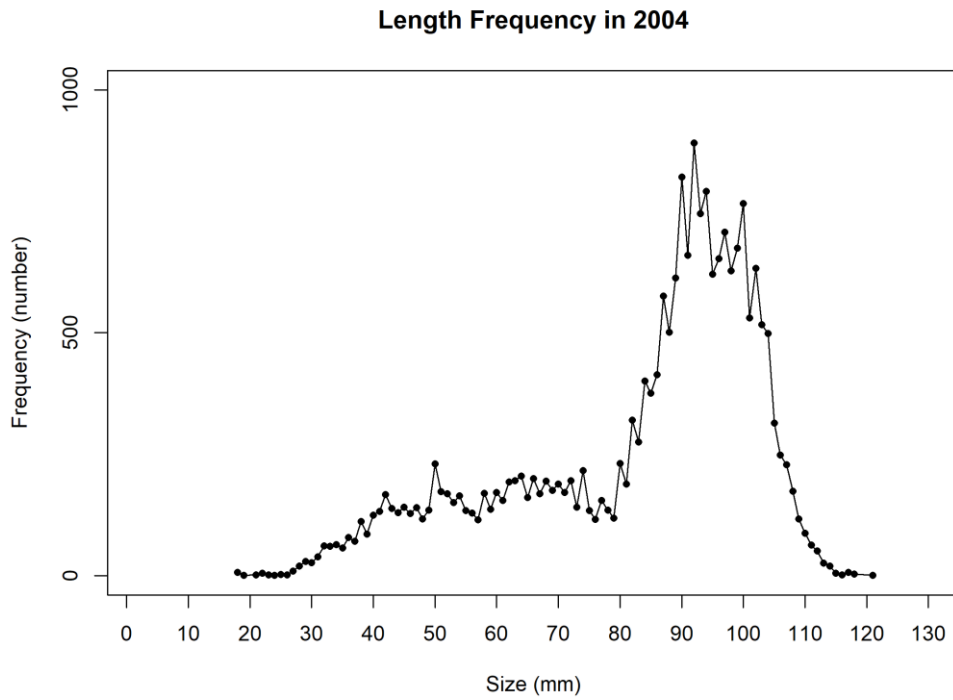
Figure 16-11. Size-frequency plot of saucer scallops measured in 2004.

Length Frequency in 2005
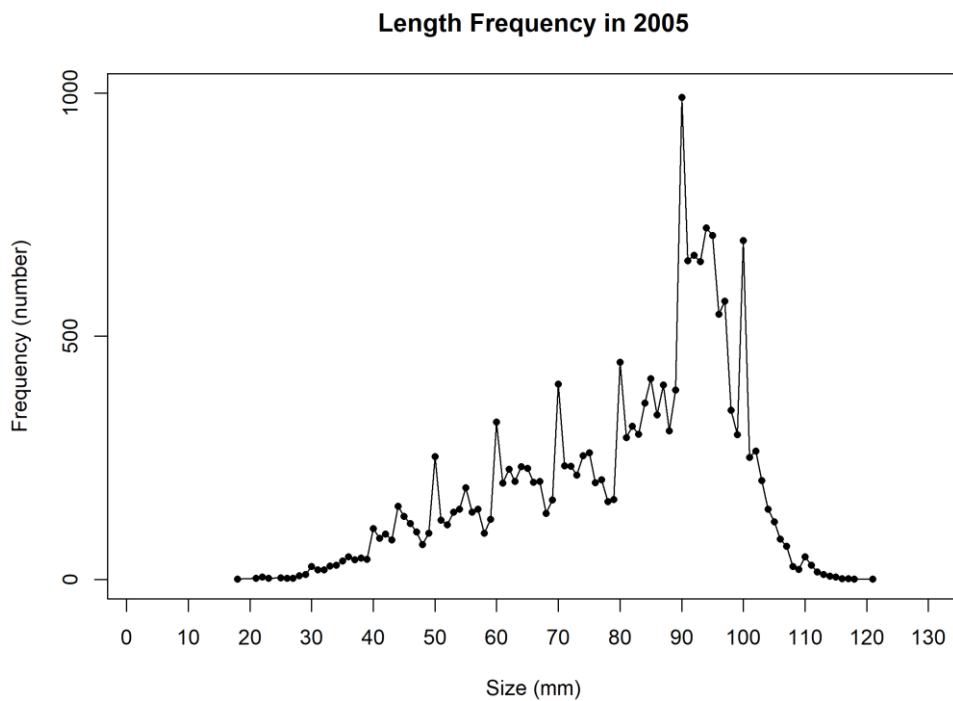
Figure 16-12. Size-frequency plot of saucer scallops measured in 2005.

Length Frequency in 2006
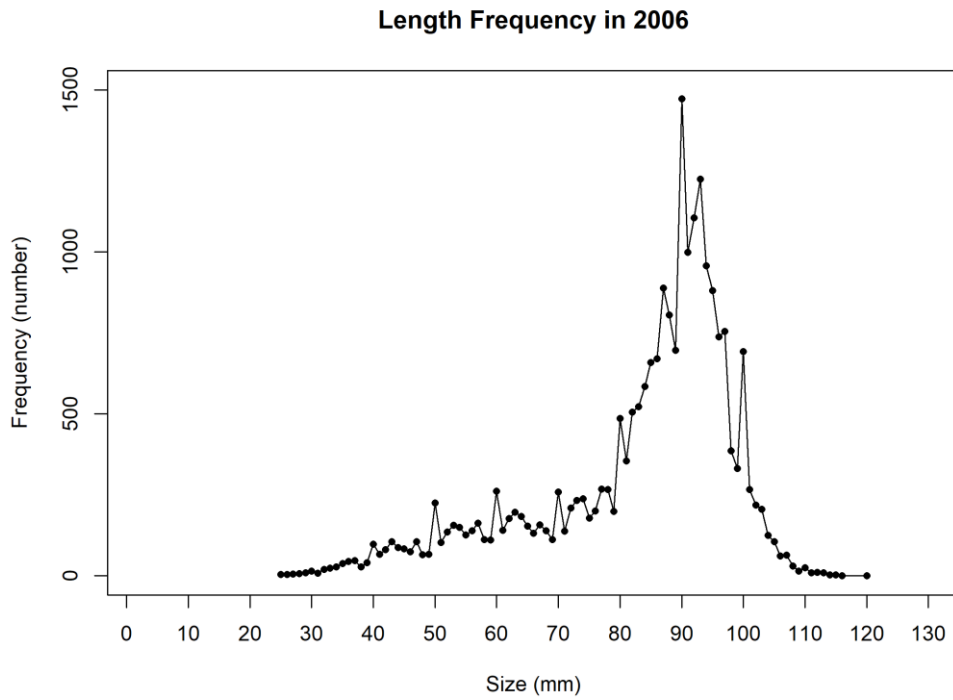
Figure 16-13. Size-frequency plot of saucer scallops measured in 2006.

Length Frequency in 2017
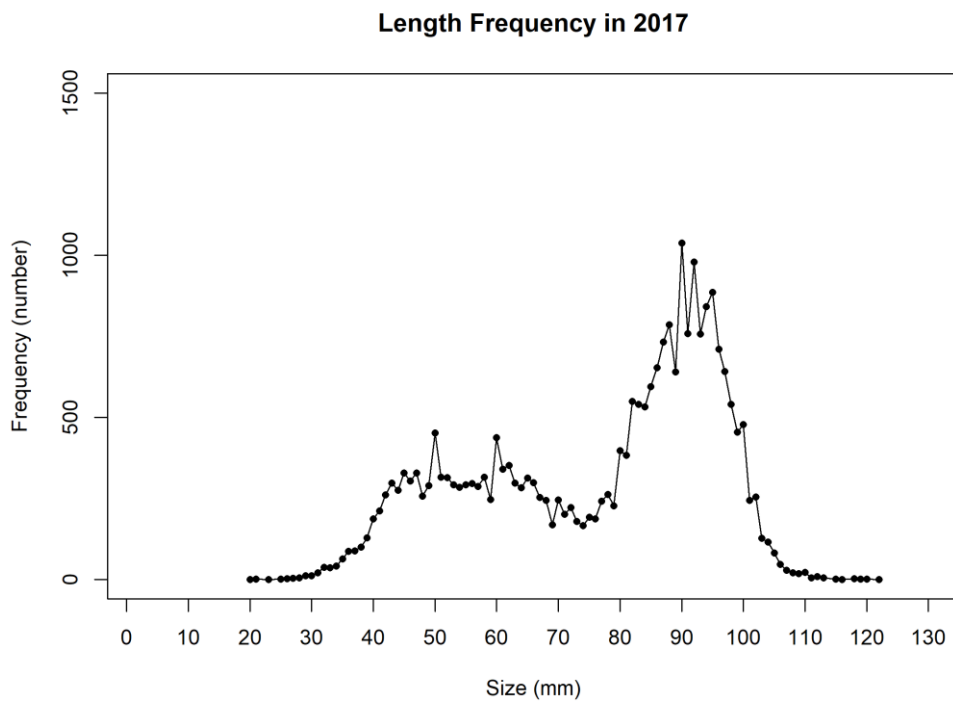
Figure 16-14. Size-frequency plot of saucer scallops measured in 2017.

Length Frequency in 2018
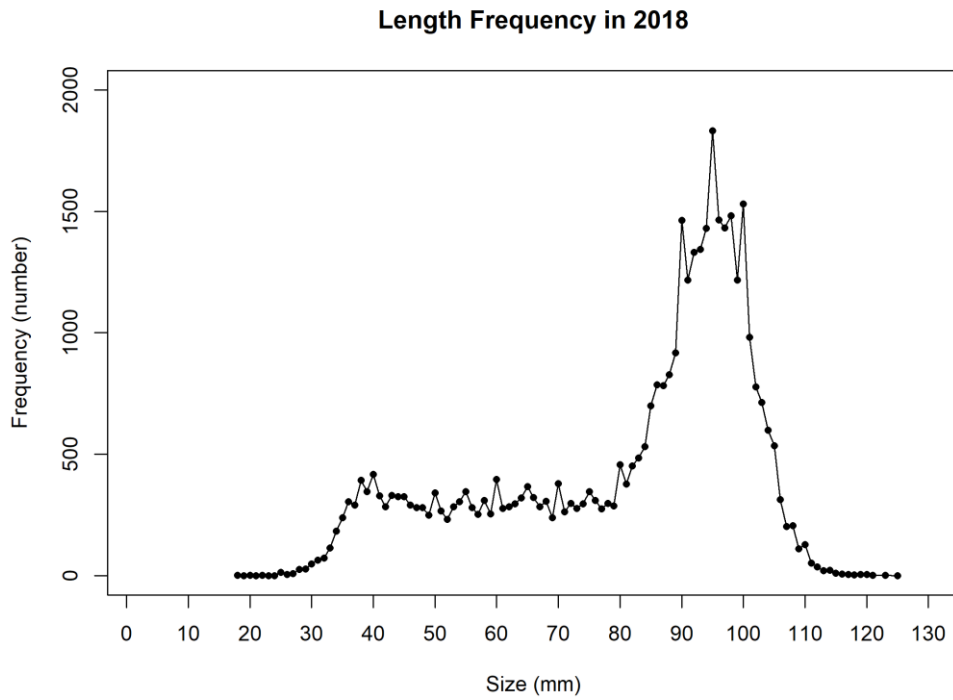
Figure 16-15. Size-frequency plot of saucer scallops measured in 2018.

Length Frequency in 2019
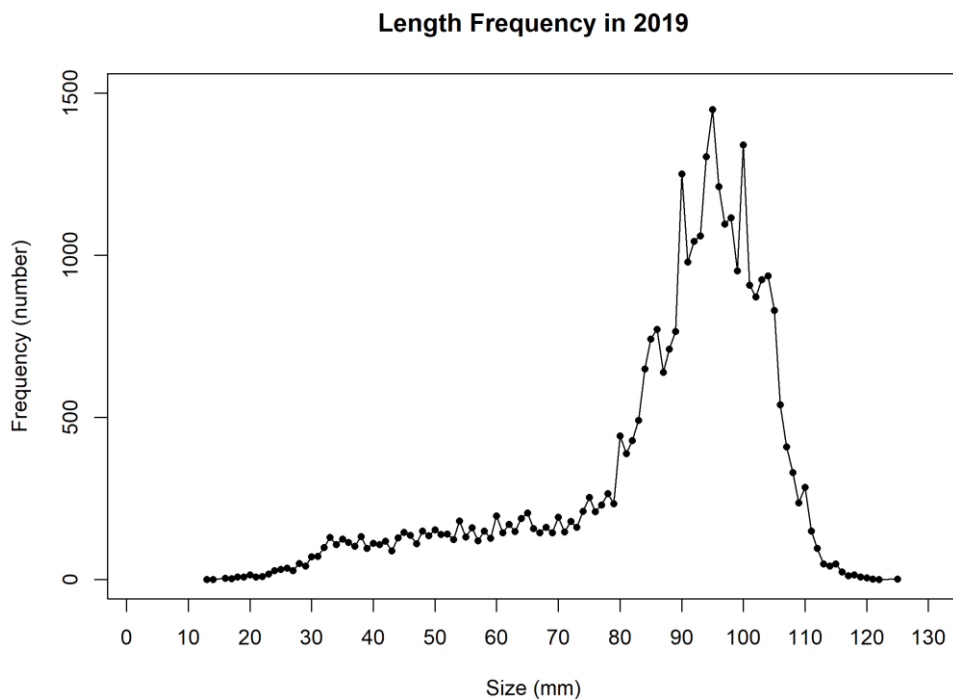
Figure 16-16. Size-frequency plot of saucer scallops measured in 2019.

16.4.2 *Vessel calibration analysis*

The generalised linear model used to calibrate the data included vessel and shot site as explanatory terms and explained between 49 and 99% of the variance between vessel catch rates (Table 16-3).

Although in 1997, 2001, 2004, 2005, and 2019, shot site was the only significant factor (P < 0.05) and explained 44%, 93%, 98%, 89% and 76% of the variance, respectively. In all other years, both vessel and shot site were significant (P < 0.05). For each of the survey years, the residuals were normally distributed.

Table 16-3. Variance explained between catch rates by 1) both the vessel and shot site, and 2) shot site only for each survey year.

Year	Variation explained by Vessel and Shot site (%)	Variation explained by Shot site (%)
1997	49	44
1998	78	67
1999	84	54
2000	52	11
2001	93	93
2002	92	87
2003	87	77
2004	98	98
2005	91	89
2006	99	92
2017	97	20
2018	71	50
2019	77	76

The mean density of scallops (all size classes) on the calibration sites was predicted for each vessel and year *y* and then used to produce proportions relative to the standard vessel, *FV C-King* which participated in every survey. A calibration factor is applied to each trawl for each vessel, adjusting the catch rate for differences between vessels in such a way that it is analogous to each survey being undertaken by a single vessel.

The mean densities produced by the calibration model indicate that within each survey year, there are differences between vessels. The resulting proportions relative to the standard vessel (*FV C-King*), and calibration factors, show that for most years the differences were not significant (Table 16-4). The *FV Seadar Bay* in 2001 and 2004 and the *FV Silda* in 2018 were similar to the *FV C-King*, while in 2017, *FV Benjamin* and *FV Maddison* were significantly different to the *FV C-King*.

Table 16-4. Vessel calibration factors. Estimates of calibrated mean density for total scallops and standard errors produced by the vessel calibration model. Proportion to standard vessel is calculated by dividing each vessel's calibrated mean density by the standard vessel calibrated mean density in the respective survey. Taking the reciprocal of each proportion derives a calibration factor.

Year	Fishing vessel name	Calibrated mean density (number/ha)	Standard errors	Proportion to standard vessel	Calibration factor
1997	*C-King*	45.45	4.20	1.00	1.00
	Exodus	39.67	4.02	0.87	1.15
	Rebecca Mae	37.80	3.61	0.83	1.20
	Tamara	41.84	4.29	0.92	1.09
1998	*C-King*	146.30	10.76	1.00	1.00
	Rebecca Mae	162.90	12.14	1.11	0.90
	Southern Intruder	166.10	12.91	1.14	0.88
	Warlord	247.40	15.79	1.69	0.59
1999	*C-King*	50.88	3.62	1.00	1.00
	Chromatt	36.29	3.83	0.71	1.40

Year	Fishing vessel name	Calibrated mean density (number/ha)	Standard errors	Proportion to standard vessel	Calibration factor
	Rebecca Mae	40.57	3.64	0.80	1.25
	Seadar Bay	94.73	5.53	1.86	0.54
2000	*C-King*	37.72	2.93	1.00	1.00
	Peggy D	27.14	2.62	0.72	1.39
	Rebecca Mae	60.70	4.33	1.61	0.62
	Seadar Bay	54.34	3.86	1.44	0.69
2001	*C-King*	246.40	6.92	1.00	1.00
	Seadar Bay	261.00	8.71	1.06	0.94
2002	*C-King*	37.71	1.79	1.00	1.00
	Seadar Bay	51.74	2.83	1.37	0.73
2003	*C-King*	87.64	4.98	1.00	1.00
	Seadar Bay	59.46	4.12	0.68	1.47
2004	*C-King*	131.00	5.08	1.00	1.00
	Seadar Bay	138.40	5.83	1.06	0.95
2005	*C-King*	40.28	2.75	1.00	1.00
	Seadar Bay	33.25	3.05	0.83	1.21
2006	*C-King*	45.49	2.05	1.00	1.00
	Gwendoline May	66.23	3.21	1.46	0.69
2017	*C-King*	110.31	6.88	1.00	1.00
	Benjamin	33.43	2.82	0.30	3.30
	Maddison	17.14	2.03	0.16	6.44
2018	*C-King*	217.00	30.54	1.00	1.00
	Silda	218.60	27.66	1.01	0.99
	Somatina	131.50	17.14	0.61	1.65
2019	*C-King*	174.20	23.59	1.00	1.00
	Silda	157.80	22.44	0.91	1.23
	Joseph-M	142.00	19.45	0.82	1.10

16.4.3 Kriging analysis

The density maps (Figures 16-17 to 16-29) show the distribution of scallops in the Queensland scallop fishery in survey years between 1997 and 2019. Maps illustrating the distribution of densities were partitioned into the four regions and the six SRAs. From north to south the regions are Yeppoon (including the Yeppoon SRAs), Bustard Head (including the Bustard Head SRAs), Hervey Bay (including the Hervey Bay SRAs, and the Sunshine Coast region (including the Maheno stratum). Between 1997 and 2006 no sampling was undertaken south of Fraser Island; hence spatial predictions of scallop densities were not calculated for the Sunshine Coast region during this period.

To assist with interpreting trends, the density scales of the maps were fixed across years and ranged from 0–250 scallops ha^{-1} for the 0+ and 1+ age classes, and 0–400 ha^{-1} for total scallops.

The density of scallops in 1997 was highest in the SRAs (Figure 16-17). Highest total scallop densities were observed in the Yeppoon SRA A, T28 and Bustard Head SRA B. The high densities in the Yeppoon SRA A were likely attributed to the 0+ age class, while the 1+ age class most likely contributed to the high densities observed in T28 and Bustard Head SRA B. Total scallop densities were lowest in the Hervey Bay region outside of SRAs and in the southern Yeppoon region.

In 1998 scallop densities peaked inside the SRAs and in areas outside that were open to fishing (Figure 16-18). Highest total scallop densities were observed in the Bustard Head SRAs and the northern Yeppoon region outside of the SRAs, and largely composed of the 1+ age class. The lowest total scallop densities were in the Hervey Bay region outside of the SRAs. The density of the 0+ age class was noticeably low across the whole fishery, while the 1+ densities were moderately high.

Scallop densities in 1999 were highest in both the SRA and fished areas (Figure 16-19). The highest total scallop densities were in W32 and Hervey Bay SRA A and mainly composed of the 0+ age class, while the 1+ age class densities were only high in the Hervey Bay SRA A. The density of 1+ scallops was also high in the Yeppoon region, close to the SRA A, and in the Bustard Head SRAs. The Yeppoon region had relatively low total scallop densities.

Scallop densities in 2000 were highest in the SRAs (Figure 16-20). All SRAs, and the Yeppoon region, contained high total scallop densities, which were largely composed of the 1+ age class. Densities of 0+ scallops were high in the Hervey Bay SRAs, moderately high in the Yeppoon region and low in other regions of the fishery. Total scallop densities were lowest in the southern Bustard Head region.

The kriging maps for 2001 to 2006 are less reliable due to the reduced scale of the surveys in these years. Specifically, the number of strata and the total number of sites were reduced due to decreased funding. As S29, S28, T29, T28, U30, U31, V31, V32 were not sampled from 2001–2006, the interpolated densities for these strata are most affected and the least accurate.

Scallop densities in 2001 were highest in both the SRA and fished areas of the fishery (Figure 16-21). Total scallop densities were highest in the Yeppoon region, Bustard Head SRAs and in Hervey Bay SRA A, largely due to the 1+ age class. Densities of 1+ and total scallops were also moderately high in the southern Bustard Head region. The 0+ densities were low for the whole fishery. The lowest total scallop densities were observed in the Hervey Bay SRA B.

Scallop densities in 2002 were highest in the SRAs (Figure 16-22) and relatively low across the whole fishery for both size classes. The highest total scallop densities were observed in Yeppoon SRA A and Bustard Head SRA B. The high density in Yeppoon SRA A was attributed to the 0+ age class, and the high density in Bustard Head SRA B was attributed to the 1+ age class. The lowest total scallop densities were observed in the southern Yeppoon region and the southern Bustard Head region. The southern Yeppoon region had moderately low 1+ scallop densities and very low 0+ densities.

In 2003 total scallop densities were highest in the northern Yeppoon region (Figure 16-23), largely attributed to the 1+ age class. Scallop densities generally declined from north to south and the 0+ age class density was low across the fishery.

Highest total scallop densities in 2004 were observed in the northern Yeppoon region, Bustard Head SRA A, Hervey Bay SRA A, and in an area north of Hervey Bay and south of Bustard Head (Figure 16-24). The high densities were attributed to 1+ age class. The lowest total scallop densities were observed in the southern Yeppoon region. Densities of 0+ scallops were moderately low across the fishery.

In 2005 total scallop densities were highest in the Yeppoon SRAs and Hervey Bay SRA A (Figure 16-25), mainly due to the 1+ age class, although the Yeppoon SRAs also had high 0+ densities. Total scallop densities were the lowest in the Bustard Head region, including inside the SRAs.

Scallop densities in 2006 were highest in areas outside of the SRAs (Figure 16-26). Total scallop densities were highest in S28, T30 and Hervey Bay SRA A, mainly attributed to the 1+ age class. Throughout the Yeppoon region and the southern Bustard Head region, the densities of 1+ scallops were moderately high. Total scallop densities were lowest in the Bustard Head SRAs and densities of the 0+ age class were very low across the fishery.

When interpreting the kriging maps for 2017–2019 it's helpful to be aware that all the SRAs have been closed to fishing since late 2016. In 2017 the highest total scallop densities were observed in the Sunshine Coast region and mainly attributed to the 1+ age class (Figure 16-27). The lowest total scallop densities were observed in the Bustard Head region. Densities inside the SRAs were very low, except for the 0+ age class in the Yeppoon SRA A. The density of 1+ scallops across the whole fishery, from northern Yeppoon to the north of Fraser Island, was very low.

Scallop densities in 2018 were highest in the SRAs (Figure 16-28). Total scallop densities were the highest in Bustard Head SRA B, Hervey Bay SRA A and a small area outside of Yeppoon SRA B. These high densities were mostly attributed to the 1+ age class. Total scallop densities were very low outside these areas. Densities of 1+ scallops were low outside of the SRAs. The density of 0+ scallops was moderately low in the SRAs and Sunshine Coast region but very low in all remaining areas.

Scallop densities in 2019 were highest in the Yeppoon SRA B, Bustard Head SRA A, Hervey Bay SRA A, and the Maheno and Sunshine Coast regions (Figure 16-29) and almost entirely attributed to 1+ age class. Lowest total scallop densities were observed in the Bustard Head and Hervey Bay regions outside of the SRAs. Densities of 1+ scallops were very low outside of the SRAs and the Sunshine Coast region, and densities of 0+ scallops were very low across the whole fishery.

To comment on long-term trends from the kriging maps it is useful to consider the relatively large red areas in the maps from 1997–2000 (Figures 16-17 to 16-20), indicating relatively large areas of high scallop density. In contrast, there is very little red in the maps from 2017–2019 (Figure 16-27 to Figure 16-29), indicating a decline in population size and scallop density between these two periods.
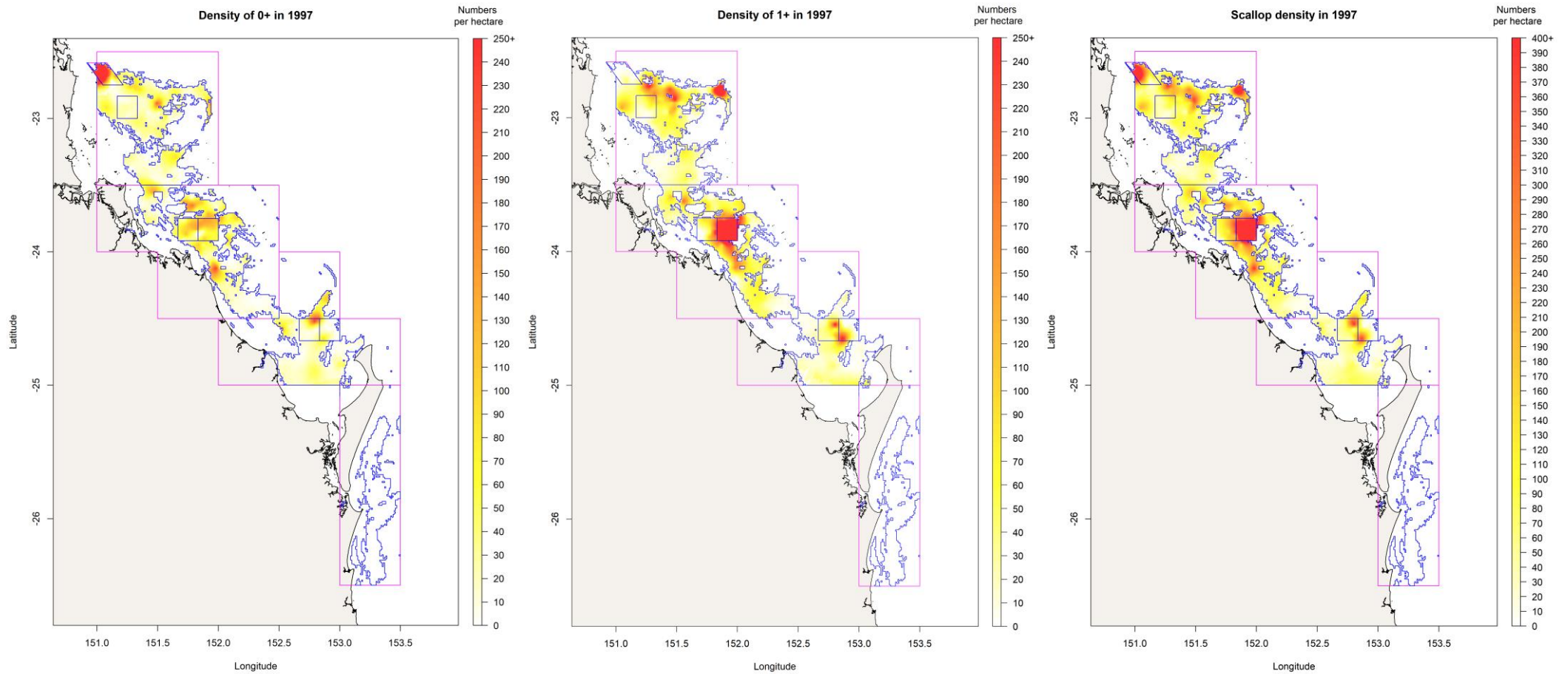
Figure 16-17. Estimate of scallop densities in 1997 derived from the local kriging model for ten regions in the Queensland saucer scallop fishery. The blue boundary outlines the extent of the fishery, based on monthly TrackMapper fishing effort from 2000 to 2018. The boundary was defined and based on including all monthly fishing effort for each 0.01° pixel that received more than one hour of scallop fishing effort. Estimates of scallop densities were produced for the 0+ age class (left), the 1+ age class (middle) and total scallops (right).
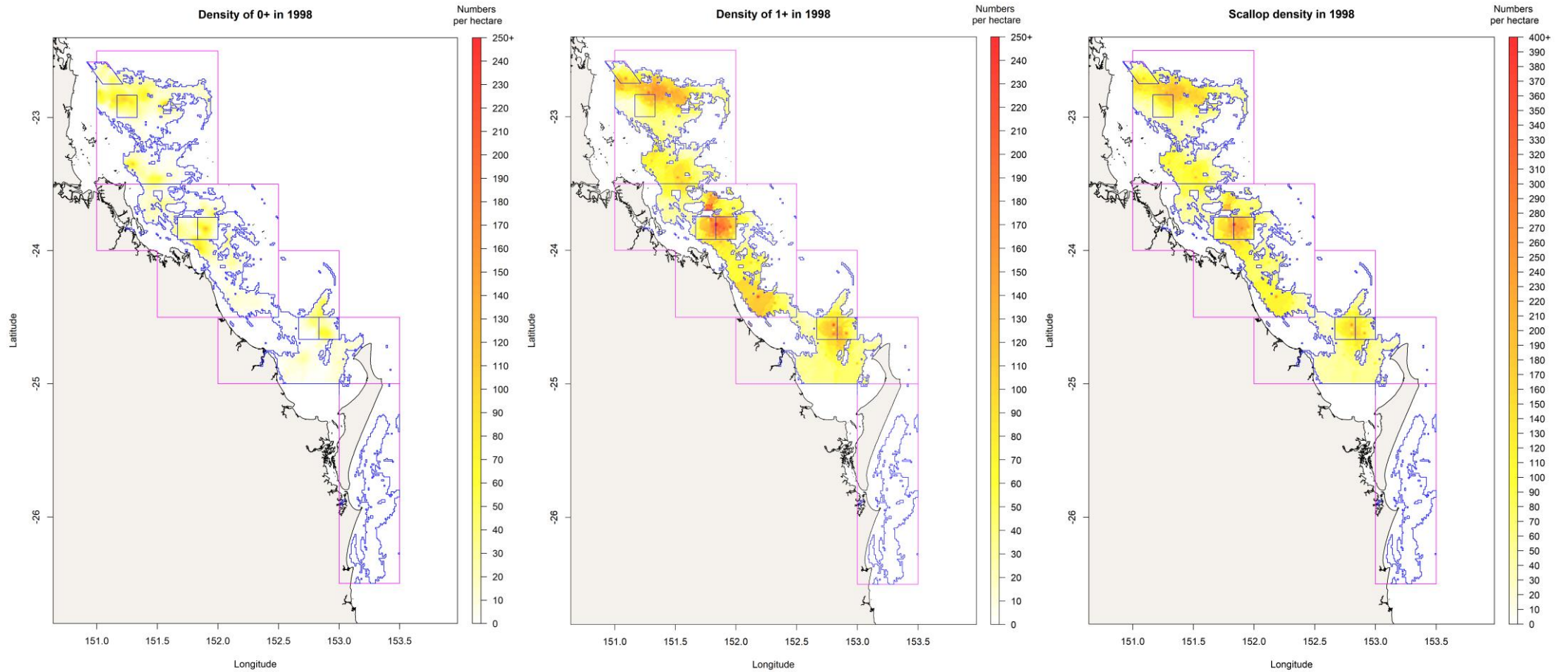
Figure 16-18. Estimate of scallop densities in 1998 derived from the local kriging model for ten regions within the Queensland saucer scallop fishery. The blue boundary outlines the extent of the fishery, based on monthly TrackMapper fishing effort from 2000 to 2018. The boundary was defined and based on including all monthly fishing effort for each 0.01° pixel that received more than one hour of scallop fishing effort. Estimates of scallop densities were produced for the 0+ age class (left), the 1+ age class (middle) and total scallops (right).
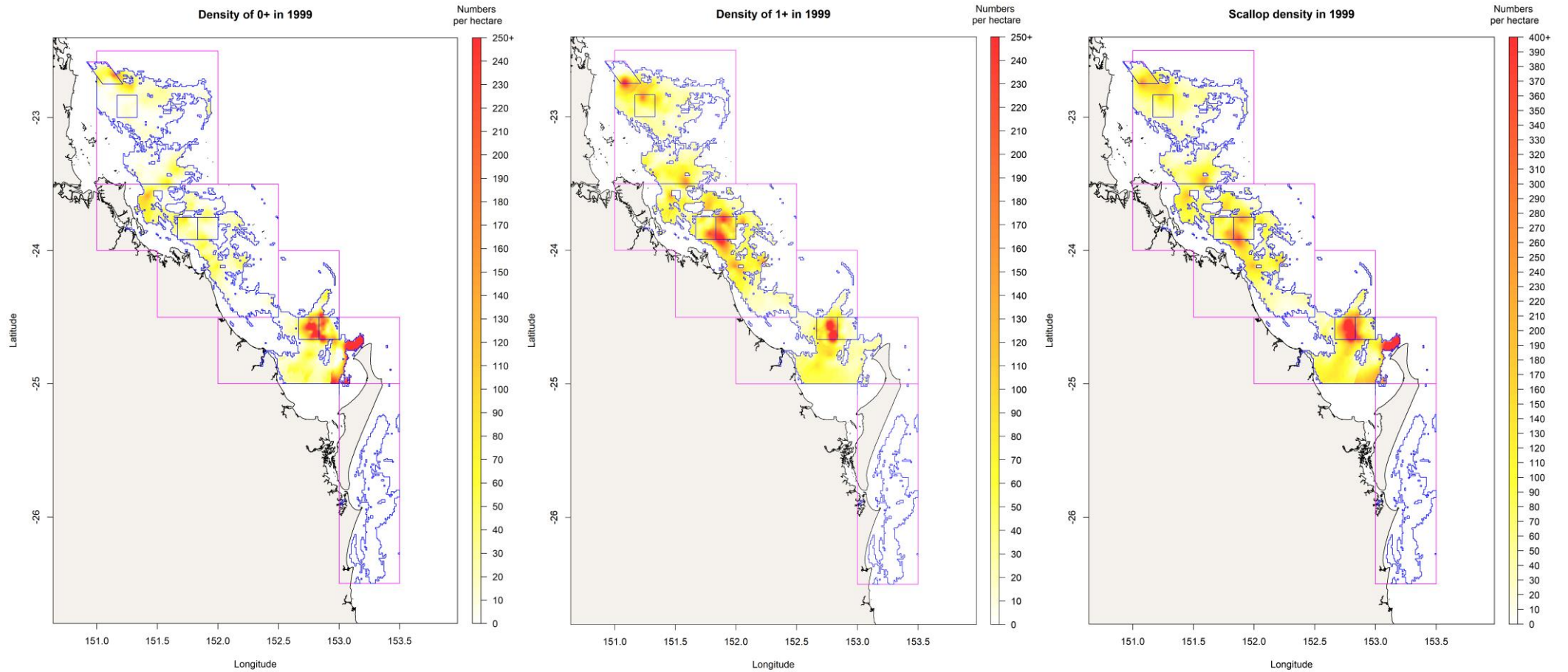
Figure 16-19. Estimate of scallop densities in 1999 derived from the local kriging model for ten regions within the Queensland saucer scallop fishery. The blue boundary outlines the extent of the fishery, based on monthly TrackMapper fishing effort from 2000 to 2018. The boundary was defined and based on including all monthly fishing effort for each 0.01° pixel that received more than one hour of scallop fishing effort. Estimates of scallop densities were produced for the 0+ age class (left), the 1+ age class (middle) and total scallops (right).
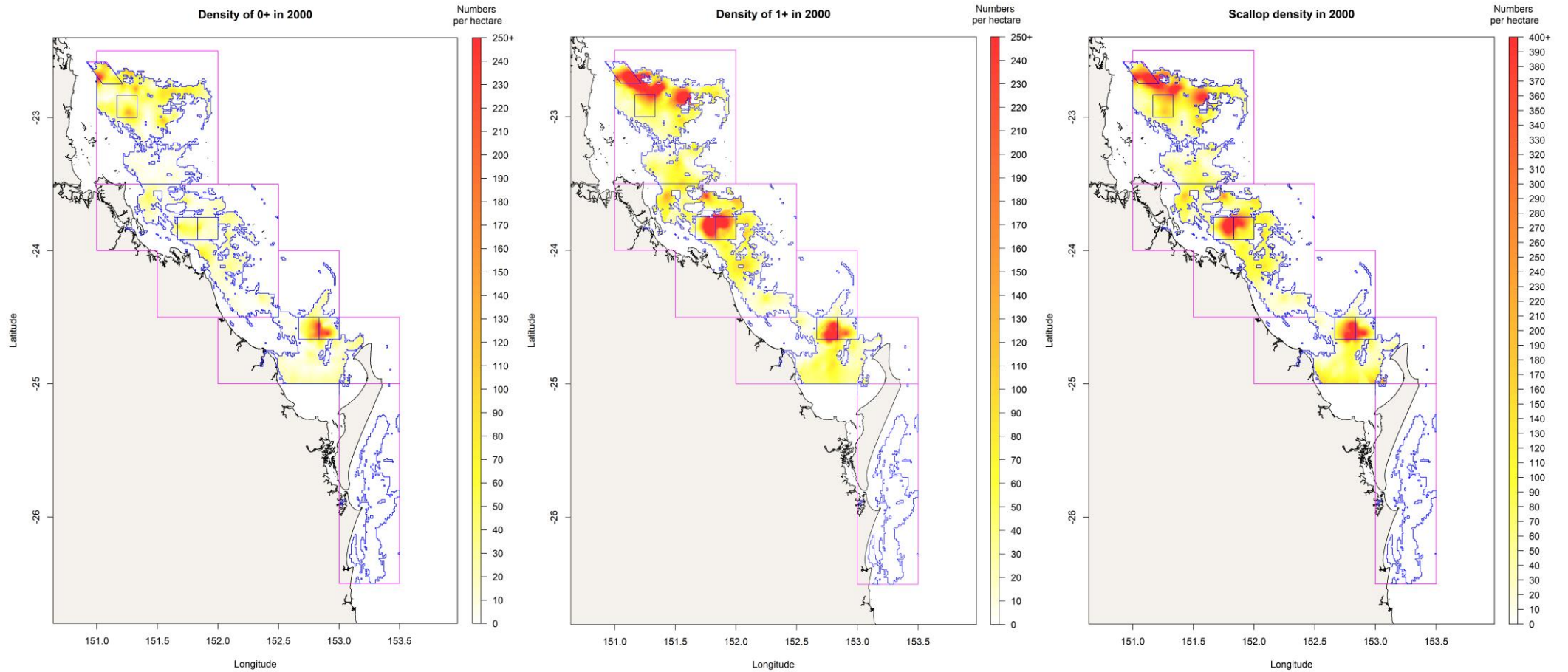
Figure 16-20. Estimate of scallop densities in 2000 derived from the local kriging model for ten regions within the Queensland saucer scallop fishery. The blue boundary outlines the extent of the fishery, based on monthly TrackMapper fishing effort from 2000 to 2018. The boundary was defined and based on including all monthly fishing effort for each 0.01° pixel that received more than one hour of scallop fishing effort. Estimates of scallop densities were produced for the 0+ age class (left), the 1+ age class (middle) and total scallops (right).
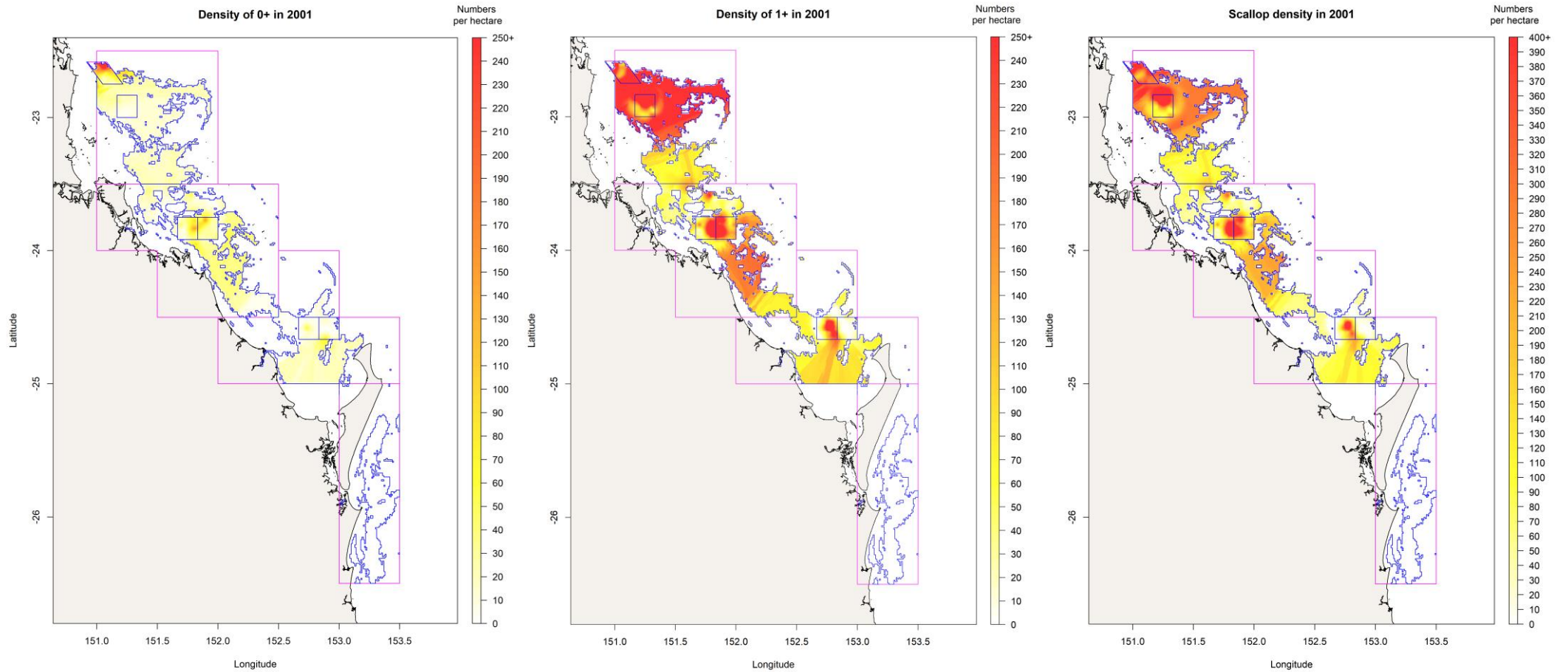
Figure 16-21. Estimate of scallop densities in 2001 derived from the local kriging model for ten regions within the Queensland saucer scallop fishery. The blue boundary outlines the extent of the fishery, based on monthly TrackMapper fishing effort from 2000 to 2018. The boundary was defined and based on including all monthly fishing effort for each 0.01° pixel that received more than one hour of scallop fishing effort. Estimates of scallop densities were produced for the 0+ age class (left), the 1+ age class (middle) and total scallops (right).
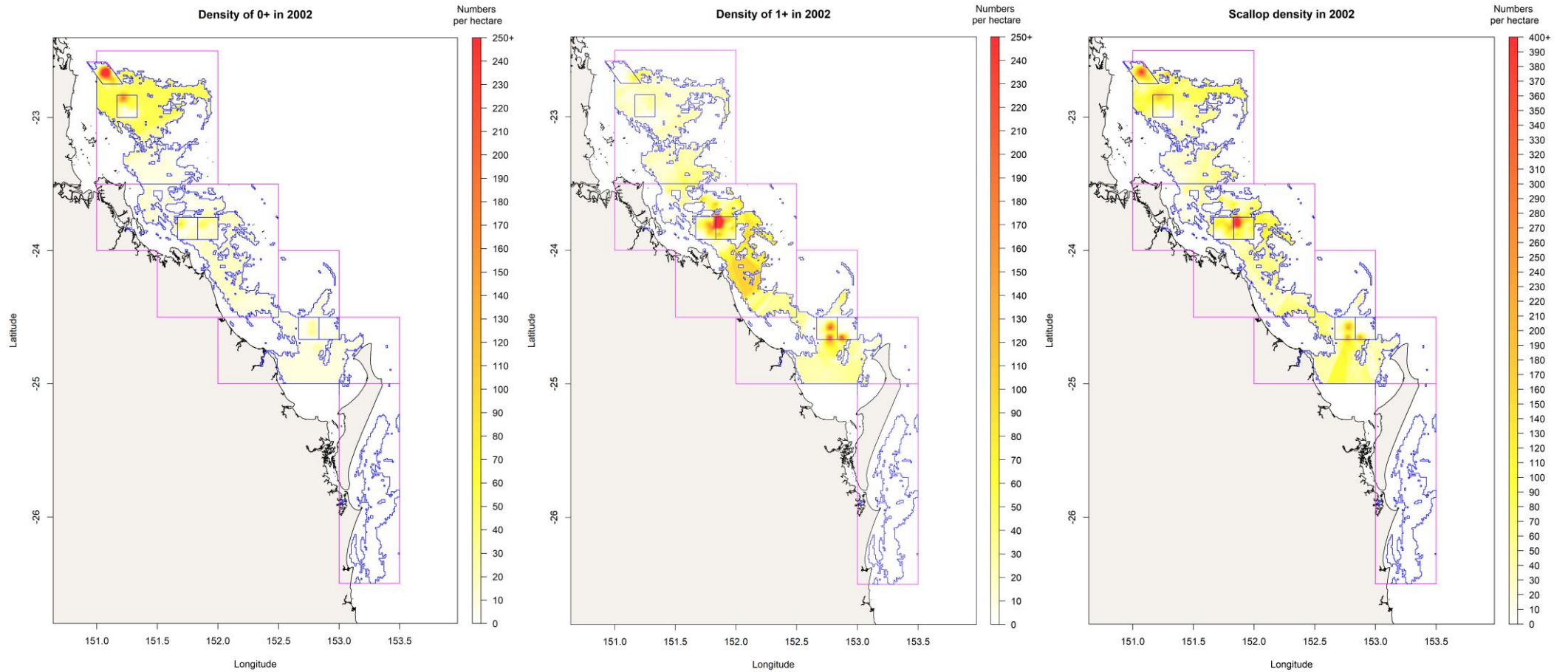
Figure 16-22. Estimate of scallop densities in 2002 derived from the local kriging model for ten regions within the Queensland saucer scallop fishery. The blue boundary outlines the extent of the fishery, based on monthly TrackMapper fishing effort from 2000 to 2018. The boundary was defined and based on including all monthly fishing effort for each 0.01° pixel that received more than one hour of scallop fishing effort. Estimates of scallop densities were produced for the 0+ age class (left), the 1+ age class (middle) and total scallops (right).
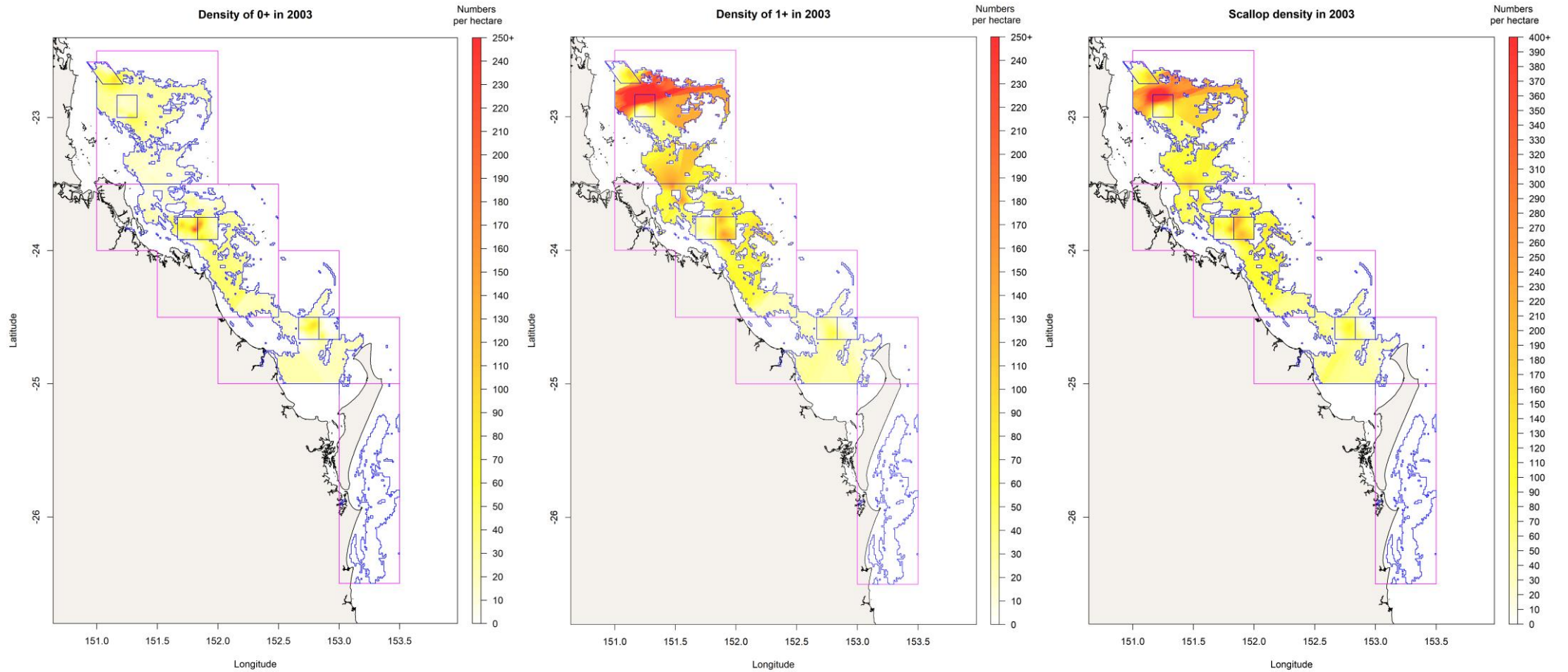
Figure 16-23. Estimate of scallop densities in 2003 derived from the local kriging model for ten regions within the Queensland saucer scallop fishery. The blue boundary outlines the extent of the fishery, based on monthly TrackMapper fishing effort from 2000 to 2018. The boundary was defined and based on including all monthly fishing effort for each 0.01° pixel that received more than one hour of scallop fishing effort. Estimates of scallop densities were produced for the 0+ age class (left), the 1+ age class (middle) and total scallops (right).
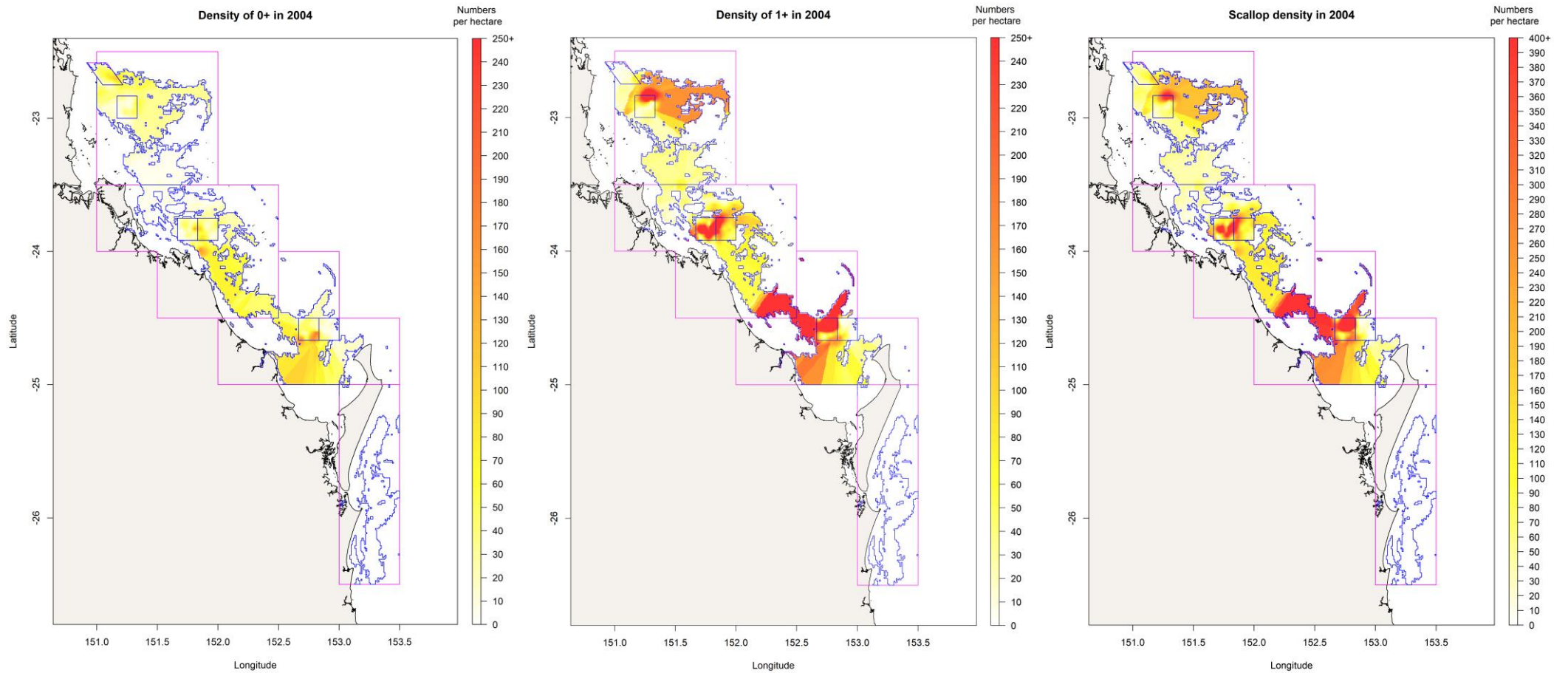
Figure 16-24. Estimate of scallop densities in 2004 derived from the local kriging model for ten regions within the Queensland saucer scallop fishery. The blue boundary outlines the extent of the fishery, based on monthly TrackMapper fishing effort from 2000 to 2018. The boundary was defined and based on including all monthly fishing effort for each 0.01° pixel that received more than one hour of scallop fishing effort. Estimates of scallop densities were produced for the 0+ age class (left), the 1+ age class (middle) and total scallops (right).
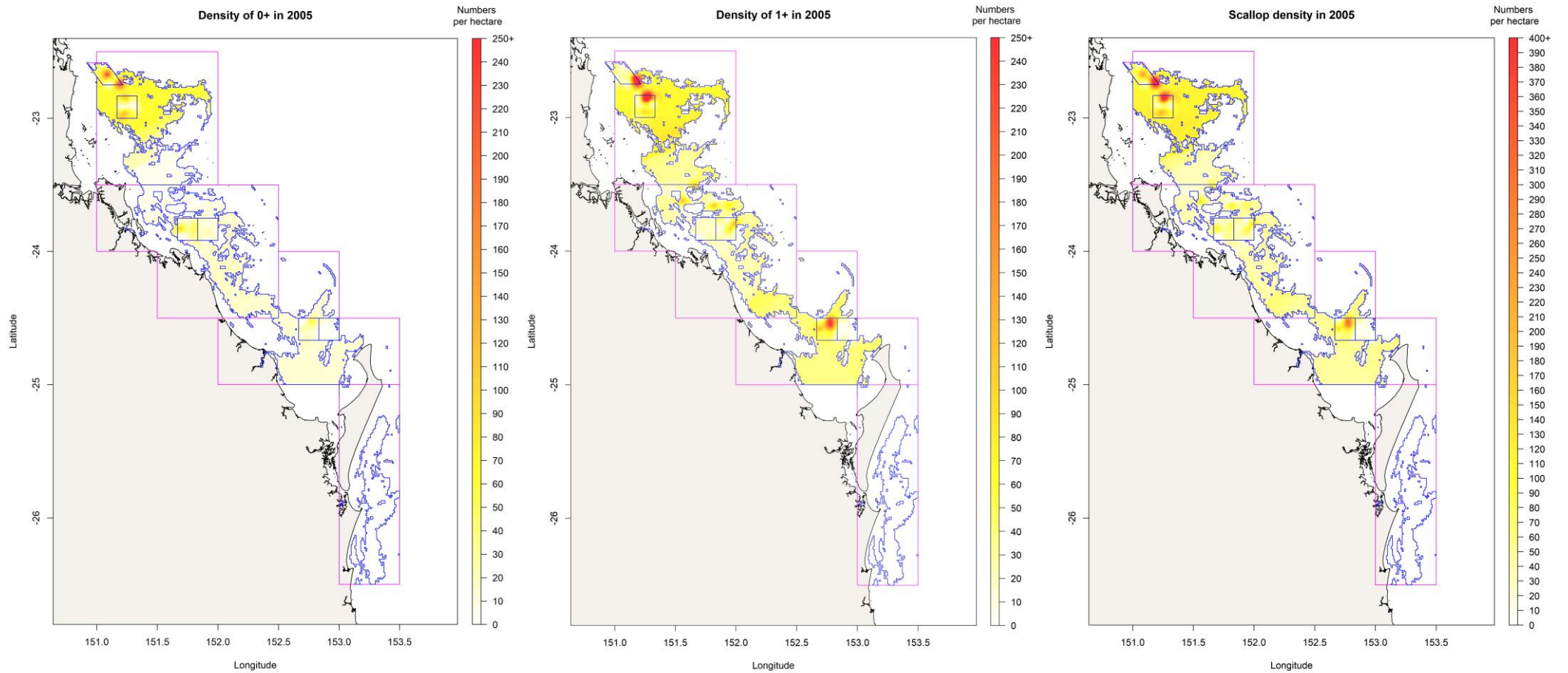
Figure 16-25. Estimate of scallop densities in 2005 derived from the local kriging model for ten regions within the Queensland saucer scallop fishery. The blue boundary outlines the extent of the fishery, based on monthly TrackMapper fishing effort from 2000 to 2018. The boundary was defined and based on including all monthly fishing effort for each 0.01° pixel that received more than one hour of scallop fishing effort. Estimates of scallop densities were produced for the 0+ age class (left), the 1+ age class (middle) and total scallops (right).
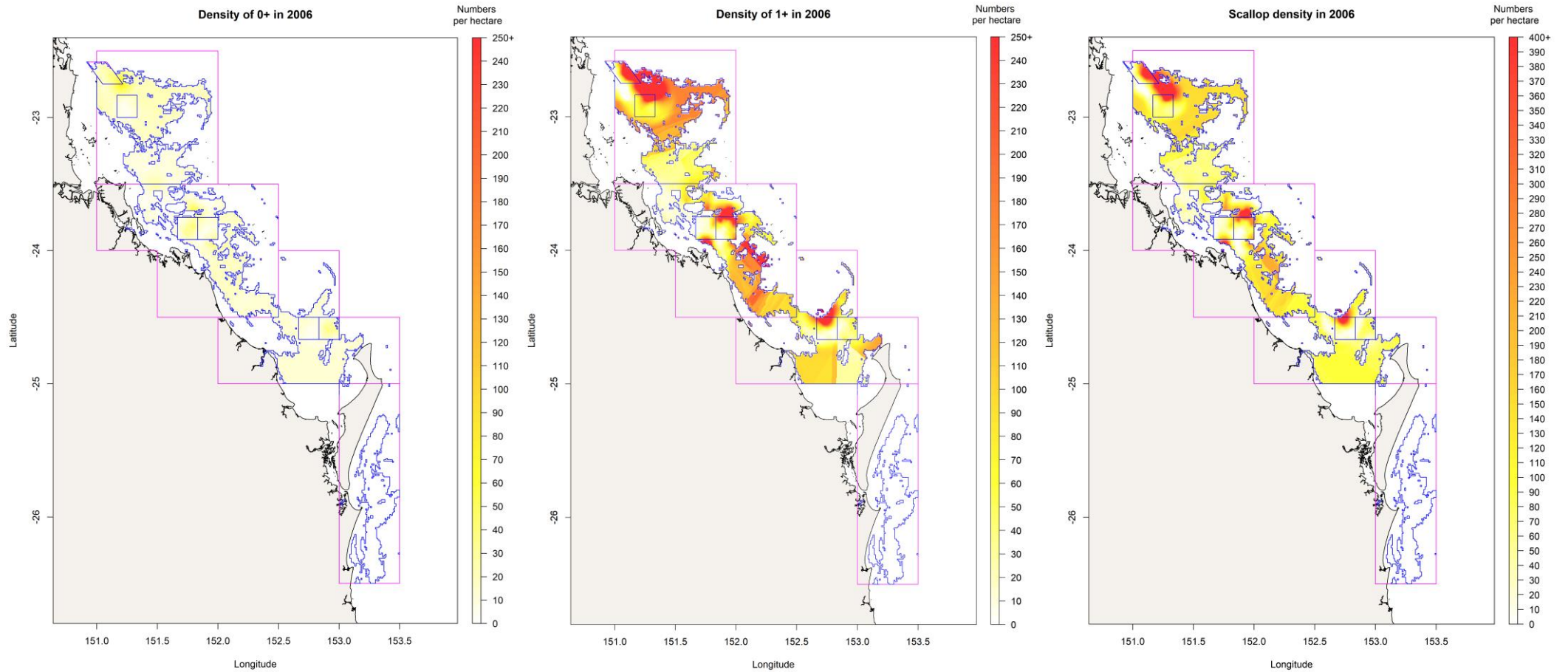
Figure 16-26. Estimate of scallop densities in 2006 derived from the local kriging model for ten regions within the Queensland saucer scallop fishery. The blue boundary outlines the extent of the fishery, based on monthly TrackMapper fishing effort from 2000 to 2018. The boundary was defined and based on including all monthly fishing effort for each 0.01° pixel that received more than one hour of scallop fishing effort. Estimates of scallop densities were produced for the 0+ age class (left), the 1+ age class (middle) and total scallops (right).
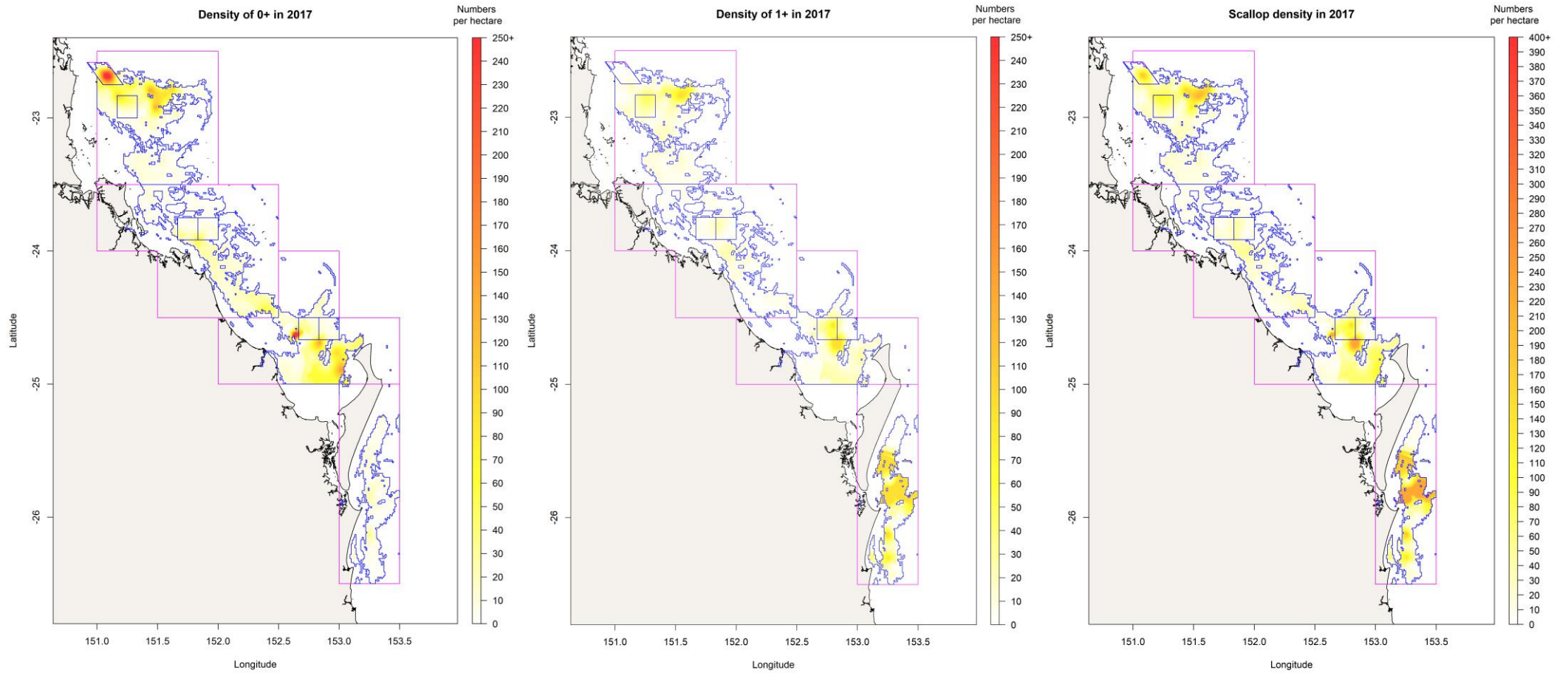
Figure 16-27. Estimate of scallop densities in 2017 derived from the local kriging model for ten regions within the Queensland saucer scallop fishery. The blue boundary outlines the extent of the fishery, based on monthly TrackMapper fishing effort from 2000 to 2018. The boundary was defined and based on including all monthly fishing effort for each 0.01° pixel that received more than one hour of scallop fishing effort. Estimates of scallop densities were produced for the 0+ age class (left), the 1+ age class (middle) and total scallops (right).
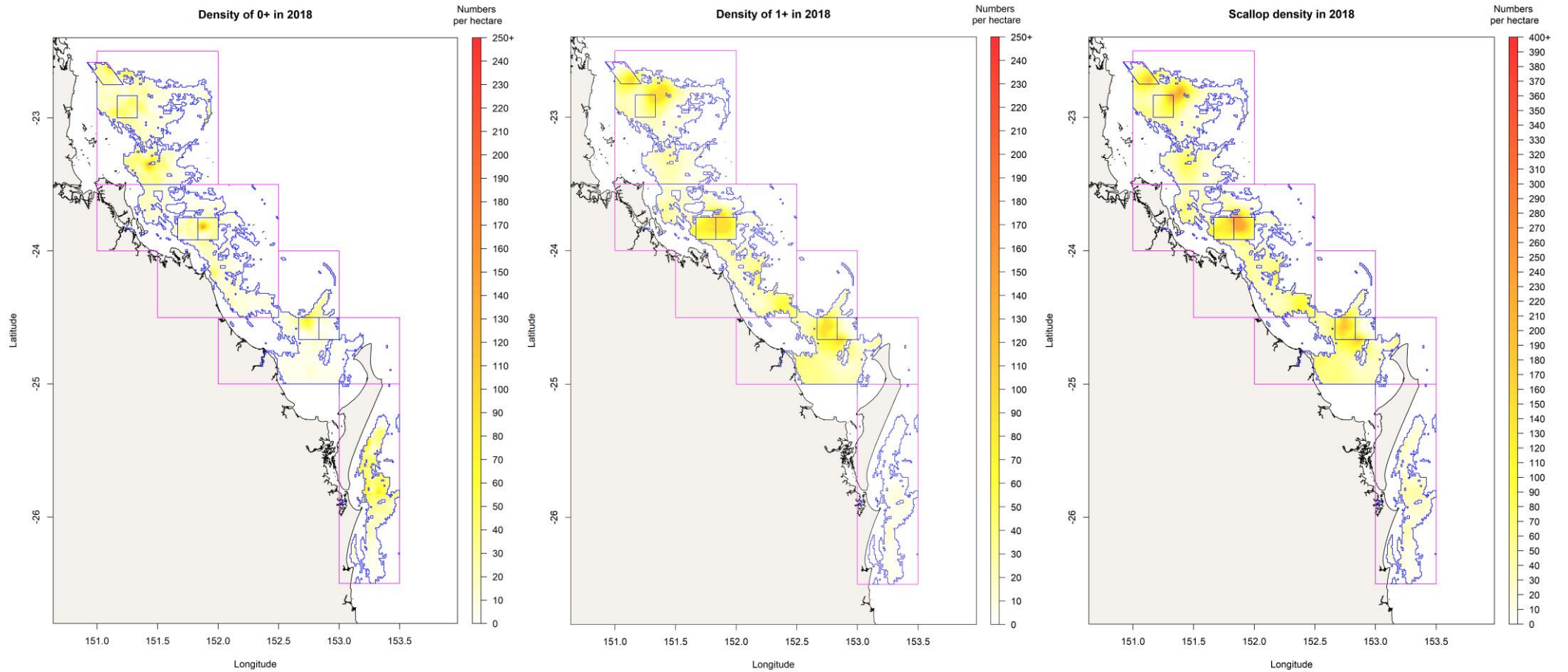
Figure 16-28. Estimate of scallop densities in 2018 derived from the local kriging model for ten regions within the Queensland saucer scallop fishery. The blue boundary outlines the extent of the fishery, based on monthly TrackMapper fishing effort from 2000 to 2018. The boundary was defined and based on including all monthly fishing effort for each 0.01° pixel that received more than one hour of scallop fishing effort. Estimates of scallop densities were produced for the 0+ age class (left), the 1+ age class (middle) and total scallops (right).
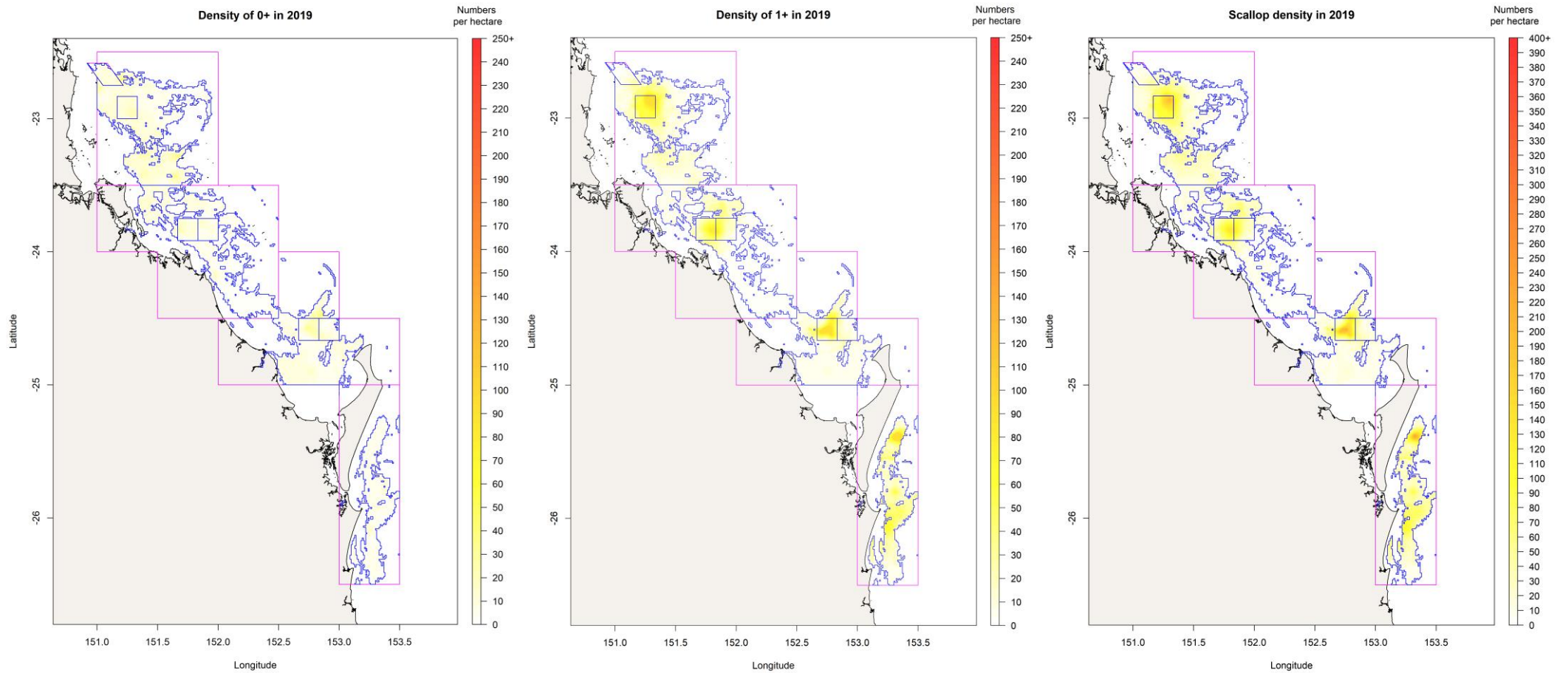
Figure 16-29. Estimate of scallop densities in 2019 derived from the local kriging model for ten regions within the Queensland saucer scallop fishery. The blue boundary outlines the extent of the fishery, based on monthly TrackMapper fishing effort from 2000 to 2018. The boundary was defined and based on including all monthly fishing effort for each 0.01° pixel that received more than one hour of scallop fishing effort. Estimates of scallop densities were produced for the 0+ age class (left), the 1+ age class (middle) and total scallops (right).

16.4.4 Strata weighted means

The weighted mean densities for the total number of scallops, the 0+ age class and the 1+ age class are provided in Table 16-5. Densities were highest in 2001 for the total number of scallops and the 1+ age class, at 170.16 and 134.38 scallops ha^{-1}, respectively. The 0+ age class density peaked in 1997 at 31.46 scallops ha^{-1}. Densities for total scallops and the 0+ age class were both at a minimum in 2019, at 33.60 and 5.89, respectively. The 1+ age class experienced its lowest density in 2017 at 27.17 scallops ha^{-1}.

Between 2001 and 2006, only the SRAs and T30 were sampled due to the reduced funding. Limiting the survey in these years to mainly the SRAs, which are associated with higher densities, generally resulted in elevated annual means, especially for total scallops and 1+ age class. For example, in 2001, 2004 and 2006 the stratified mean densities exceeded 100 ha^{-1} for total scallops. Caution is therefore required when interpreting the annual weighted mean densities, especially for those years when the number of strata was reduced (i.e., 2001–2006). The similar trends for total scallops and the 1+ age class reflect the relatively high proportion of this age class to the total number of scallops. The 0+ age class densities were relatively similar across all years. Commenting on the 0+ age class densities is challenging because the catchability of this age class appears to be low, both inside and outside the SRAs. Even though the abundance of the 0+ age class must be higher than the 1+ age class, the survey has always caught fewer of them.

16.4.5 Adjusted mean densities

Details on the deployment of TEDs and BRDs for each survey year are provided in Table 16-1. The influence of the devices, which was considered as a categorical term with levels (i.e., no device, TED only, BRD only, TED with BRD), was considered in the GLM described in section 16.3.8 using all survey data (1997–2019). The model indicated that nets fitted with a TED and/or a BRD had significant effect on the catch rate of the 0+ age class, but no effect on the catch rate of the 1+ age class or the total number of scallops caught, compared to the reference level (i.e., net without devices). Because the 0+ age class made up a minor proportion of the scallops caught (~30%) and the devices had no effect on the majority of the scallops, the TED and BRD variable was excluded from further analyses used to derive adjusted mean densities.

All other variables outlined in section 16.3.8 had a significant effect on the total number of scallops caught and were therefore included in the final model. The model treated 1997 as the reference level that all subsequent years were compared against because it was the first survey. The V32 stratum was used as the reference level that strata were compared against as it approximates the centre of the fishery. The waxing phase was used as the reference level for lunar phase influence because it produced the highest adjusted mean density of the lunar phases (Table 16-7). Similarly, the two-hour interval between 2200 hr and 0000 hr (midnight) was used as the reference level for the time-of-night effect because it also had the highest adjusted mean density for total scallops compared against the other time intervals (Table 16-6).

Total scallop densities in 1998, 1999, 2001, 2003, 2004, 2005, 2006, 2017 and 2018 were significantly higher than the 1997 reference survey year (Table 16-6). Compared to V32, total scallop densities were significantly higher for the following strata: Bustard Head SRA A, Bustard Head SRA B, Hervey Bay SRA A, Hervey Bay SRA B, Maheno, S28, Sunshine Coast, T28, T29, T30, U31, U30 and Yeppoon SRA A. For the green zone MNP231169 that was sampled in 2017, total scallop densities were significantly less than V32. The effect of lunar phase was significant, indicating that there was a decrease in total scallop densities between the waxing phase and the new moon, full moon and waning phases. Total scallop densities were significantly lower at 0400 hr – 0600 hr, 0600 hr –1800 hr, 1800 hr –2000 hr and 2000 hr – 2200 hr, compared to the 2200 hr – 00:00 hr (midnight) reference level.

Table 16-5. Summary of weighted mean densities for total scallops, 0+ age class and the 1+ age class from all survey years, based on the analysis described by Haddon (1997). Stratified standard error provides an indication of statistical accuracy of the stratified mean density estimate for each survey. The coefficient of variation indicates the distribution of densities for each survey.

Total Number		1997	1998	1999	2000	2001	2002	2003	2004	2005	2006	2017	2018	2019
Number of strata	N_h	14	14	14	14	7	8	7	7	7	7	19	17	17
Total number of observations	n_h	438	479	536	457	606	306	329	327	169	163	341	333	330
TED and/or BRD		No	No	No	No	Yes	Yes	Yes	Yes	Yes	Yes	Yes	Yes	Yes
Stratified mean density (number ha^{-1})	X_{st}	71.13	60.83	58.08	73.25	170.16	53.81	89.50	124.78	59.71	102.15	43.23	61.83	33.60
Stratified standard error	$SE_{X_{st}}$	5.06	4.24	3.66	5.65	8.89	10.23	5.13	8.46	5.75	16.24	6.18	6.05	2.49
Coefficient of variation	CV	7%	7%	6%	8%	5%	19%	6%	7%	10%	16%	14%	10%	7%

0+ Number		1997	1998	1999	2000	2001	2002	2003	2004	2005	2006	2017	2018	2019
Number of strata	N_h	14	14	14	14	7	8	7	7	7	7	19	17	17
Total number of observations	n_h	438	479	536	457	606	306	329	327	169	163	341	333	330
TED and/or BRD		No	No	No	No	Yes	Yes	Yes	Yes	Yes	Yes	Yes	Yes	Yes
Stratified mean density (number ha^{-1})	X_{st}	31.46	12.20	19.43	21.83	30.25	19.31	26.01	25.18	18.71	13.25	16.07	13.08	5.87
Stratified standard error	$SE_{X_{st}}$	3.18	1.02	1.68	1.55	1.98	5.37	1.47	1.78	2.18	1.68	2.81	1.23	0.54
Coefficient of variation	CV	10%	8%	9%	7%	7%	28%	6%	7%	12%	13%	18%	9%	9%

1+ Number		1997	1998	1999	2000	2001	2002	2003	2004	2005	2006	2017	2018	2019
Number of strata	N_h	14	14	14	14	7	8	7	7	7	7	19	17	17
Total number of observations	n_h	438	479	536	457	606	306	329	327	169	163	341	333	330
TED and/or BRD		No	No	No	No	Yes	Yes	Yes	Yes	Yes	Yes	Yes	Yes	Yes
Stratified mean density (number ha^{-1})	X_{st}	39.67	48.54	35.05	52.27	134.38	37.60	62.06	89.20	41.01	88.90	27.17	48.75	27.72
Stratified standard error	$SE_{X_{st}}$	3.67	3.58	2.48	4.99	7.95	8.85	4.69	8.17	4.59	15.67	4.88	5.70	2.31
Coefficient of variation	CV	9%	7%	7%	10%	6%	24%	8%	9%	11%	18%	18%	12%	8%

Table 16-6. Estimates of β coefficients, standard errors, t probabilities and back-transformed estimates of β coefficients produced by the model predicting mean total scallop densities. The reference level for year was 1997, for strata was V32, for lunar phase was the waxing phase and for time-of-night was 2200 hr to midnight. Coefficients are significantly different (bold) from the reference level if the p-value falls below 0.005, otherwise they are not significant.

Parameter	Constant	Estimate	Standard error	t pr.	Back-transformed estimate
		3.414	0.245	< 0.001	30.380
Year	**1998**	**1.268**	**0.324**	**< 0.001**	**3.555**
	1999	**0.940**	**0.279**	**< 0.001**	**2.559**
	2000	0.445	0.312	0.153	1.561
	2001	**1.905**	**0.463**	**< 0.001**	**6.716**
	2002	0.786	0.753	0.297	2.195
	2003	**2.162**	**0.477**	**< 0.001**	**8.689**
	2004	**1.074**	**0.485**	**0.027**	**2.927**
	2005	**1.358**	**0.473**	**0.004**	**3.888**
	2006	**1.532**	**0.487**	**0.002**	**4.629**
	2017	**2.177**	**0.310**	**< 0.001**	**8.822**
	2018	**1.427**	**0.313**	**< 0.001**	**4.166**
	2019	-0.564	0.540	0.296	0.569
Strata	**BHA**	**2.333**	**0.326**	**< 0.001**	**10.310**
	BHB	**2.986**	**0.296**	**< 0.001**	**19.800**
	HBA	**2.093**	**0.352**	**< 0.001**	**8.109**
	HBB	**1.195**	**0.500**	**0.017**	**3.302**
	Maheno	**1.380**	**0.517**	**0.008**	**3.973**
	MNP-24-1173	-0.660	0.416	0.113	0.517
	MNP231169	**-1.703**	**0.345**	**< 0.001**	**0.182**
	S28	**1.572**	**0.263**	**< 0.001**	**4.819**
	S29	0.204	0.353	0.563	1.227
	SUN	**1.574**	**0.505**	**0.002**	**4.828**
	T28	**0.704**	**0.302**	**0.020**	**2.022**
	T29	**0.903**	**0.292**	**0.002**	**2.467**
	T30	**1.441**	**0.278**	**< 0.001**	**4.227**
	U30	**1.020**	**0.337**	**0.002**	**2.774**
	U31	**0.644**	**0.303**	**0.034**	**1.905**
	V31	-0.463	0.451	0.305	0.629
	W32	-1.380	1.880	0.464	0.252
	YA	**1.507**	**0.542**	**0.005**	**4.513**
	YB	0.581	0.506	0.252	1.787
Lunar Phase	**Full Moon**	**-0.217**	**0.091**	**0.017**	**0.805**
	New Moon	**-0.357**	**0.083**	**< 0.001**	**0.700**
	Waning	**-0.882**	**0.123**	**< 0.001**	**0.414**
Time	2am to 4am	-0.059	0.050	0.238	0.943
	4am to 6am	**-0.440**	**0.065**	**< 0.001**	**0.644**
	6pm to 8pm	**-0.414**	**0.051**	**< 0.001**	**0.661**
	8pm to 10pm	**-0.107**	**0.048**	**0.026**	**0.898**
	Day (6am – 6pm)	**-0.223**	**0.083**	**0.007**	**0.800**
	Midnight to 2am	-0.079	0.049	0.108	0.924

Lunar phase had a marked influence on the survey catch rates. Adjusted mean total scallop density peaked at 135.3 scallops ha^{-1} during the waxing phase, which was about 3 times higher than during the waning phase (Table 16-7). The adjusted mean total scallop density peaked from 2200 hr – 0000 hr (midnight) (Table 16-8) at 127.1 scallops ha^{-1}. Adjusted means were low during periods associated with transitioning diel light conditions from 0400 hr – 0600 hr and 1800 hr – 2000 hr (Table 16-8).

Table 16-7. Adjusted total mean density of saucer scallops (total scallops from all size classes) within each lunar phase.

Lunar phase	Adjusted total mean density (number ha^{-1})	Standard error
Full Moon	109.0	12.1
Waxing	135.3	13.7
New Moon	94.7	9.8
Waning	56.0	6.6

Table 16-8. Adjusted total mean density of saucer scallops (total scallops from all size classes) within each 2-hour interval throughout the night.

Time-of-night (hr)	Adjusted total mean density (number ha^{-1})	Standard error
Day (0600 – 1800)	101.7	11.9
1800 – 2000	84.0	8.2
2000 – 2200	114.2	10.8
2200 – 0000 (midnight)	127.1	12.0
0000 (midnight) – 0200	117.5	11.1
0200 – 0400	119.9	11.4
0400 – 0600	81.9	8.5

The adjusted mean densities for each stratum for total scallops, the 0+ age class and the 1+ age class, over all survey years are presented in Figures 16-30, 16-31 and 16-32, respectively.

Across all years and strata, the adjusted mean total densities were highly variable, and the large number of strata complicates interpreting overall trends (Figure 16-30a).

Overall years, the peak adjusted mean total density was 717.4 scallops ha^{-1} in BHA in 1998. From 1997–2005, adjusted mean total densities for several strata exceeded 400 ha^{-1}. In recent years from 2017–2019 however, there has been only one stratum with an adjusted mean total density above 400 scallops ha^{-1} (i.e., BHB 2018, 553.1 scallops ha^{-1}).

Years that were associated with relatively high adjusted mean total densities were 1998, 2000 and 2001. In 2002 scallop densities were very low, with none of the strata means exceeding 200 scallops ha^{-1} (Figure 16-30a). Adjusted mean total scallop densities generally declined from 2018 to 2019.

Over the time series, marked declines in adjusted total mean densities occurred in YA (Figure 16-30b), BHA (Figure 16-30d) and HBB (Figure 16-30f).

The 1+ age class has consistently dominated the size class distribution and typically comprised 60–80% of scallops measured in the survey. There is some indication that the relative contribution of the 0+ age class has declined. Marked declines in the 0+ age class densities can be observed in the time series for YA (Figure 16-31b), HBA and HBB (Figure 16-31f). In 2019, adjusted mean densities for the 0+ age class were less than 35 scallops ha^{-1} in all strata, which is the lowest recorded (Figure

16-31a) and as a result, the 0+ age class made up only 12% of measured scallops in 2019. Densities of the 0+ age class were also consistently low across strata in 1999 (Figure 16-31a).

Commenting on the abundance of the 0+ age class is challenging because the catchability of this age class appears to be low. Even though the abundance of the 0+ age class must be higher than the 1+ age class, the survey has always caught fewer of them.

(a)
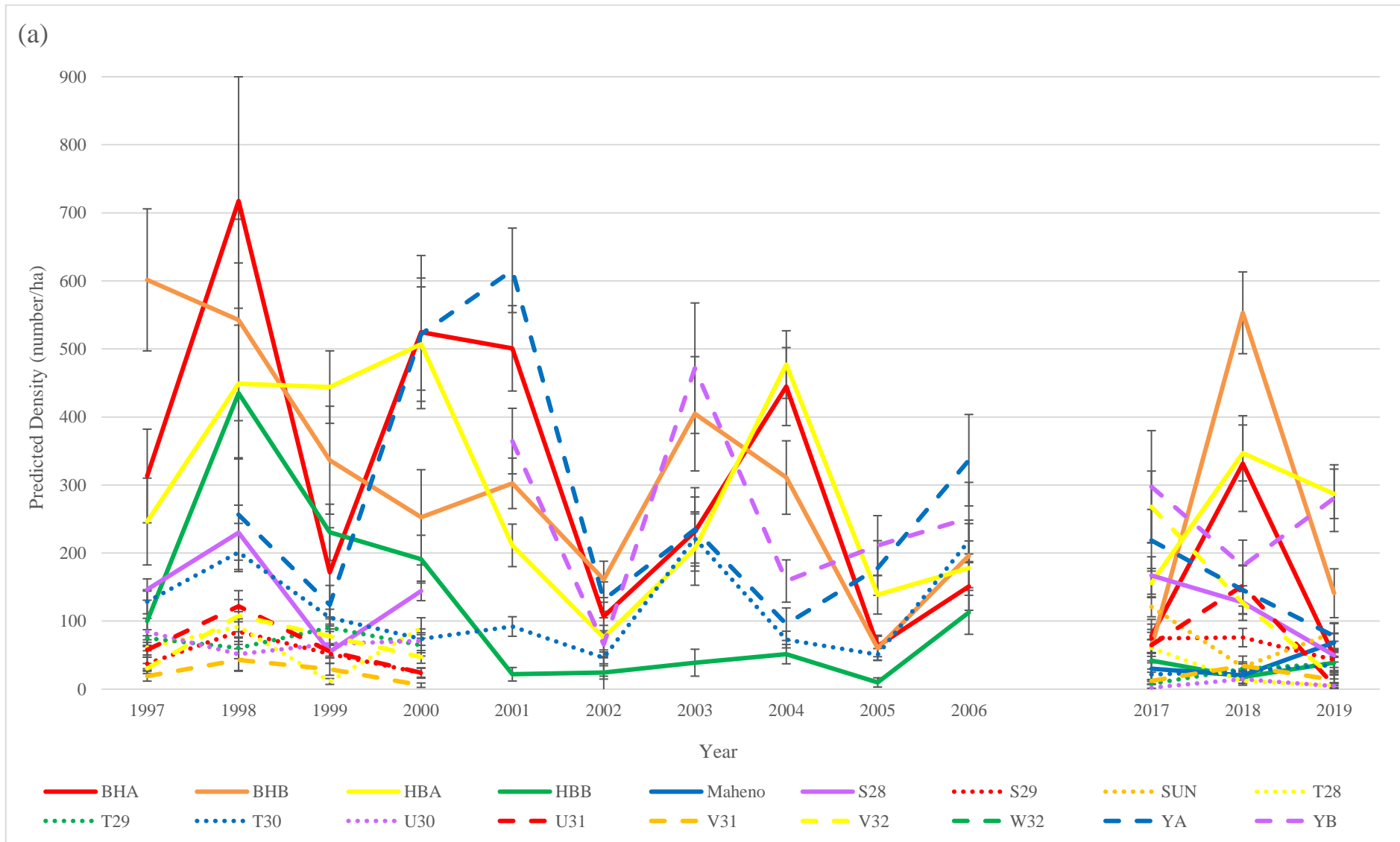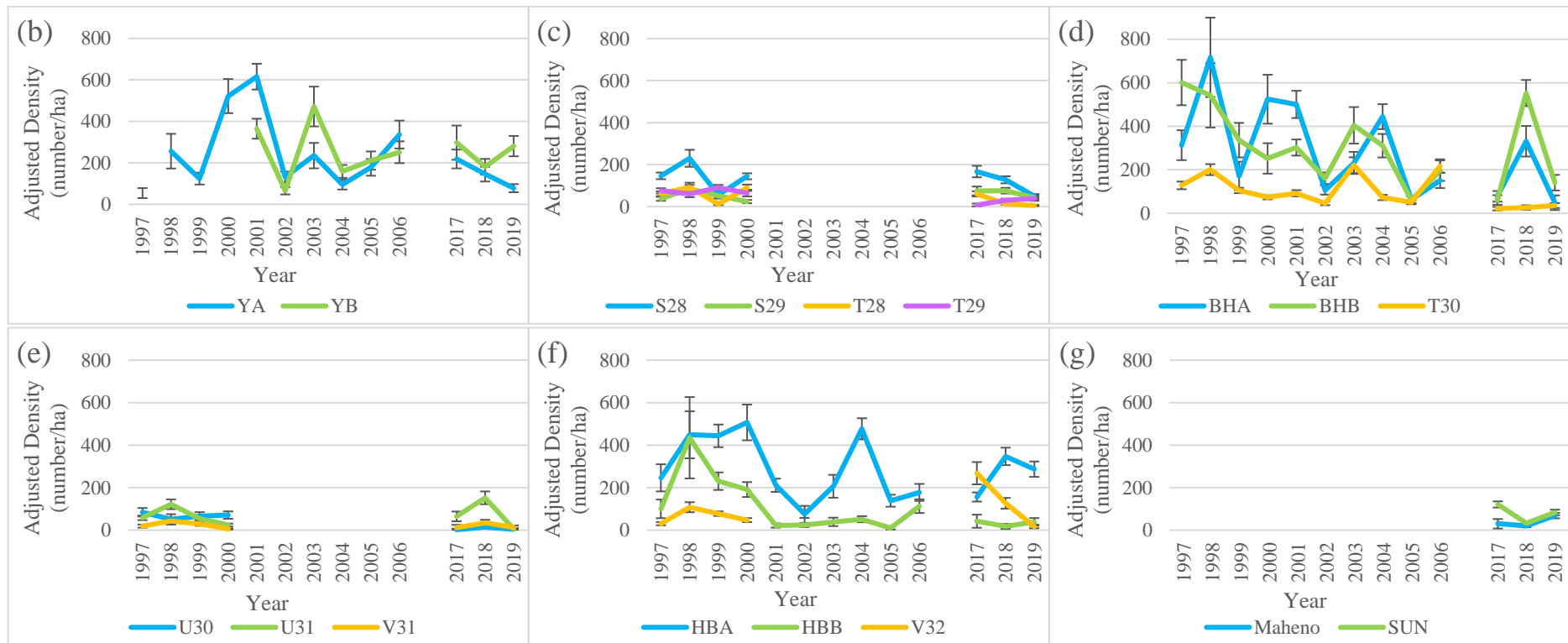
Figure 16-30. Adjusted total density of saucer scallops (number ha⁻¹) over the duration of the fishery-independent scallop survey within (a) all strata, (b) the Yeppoon SRAs, (c) S28, S29, T28 and T29 strata, (d) Bustard Head SRAs and T30 strata, (e) U30, U31 and V31 strata, (f) Hervey Bay SRAs and V32 strata, (g) the Maheno and Sunshine Coast strata. Vertical bars represent one standard error either side of the mean. No data for the two GBRMPA green zones (MNP-24-1173 and MNP231169) are provided because these two areas were only sampled once in 2017.

(a)
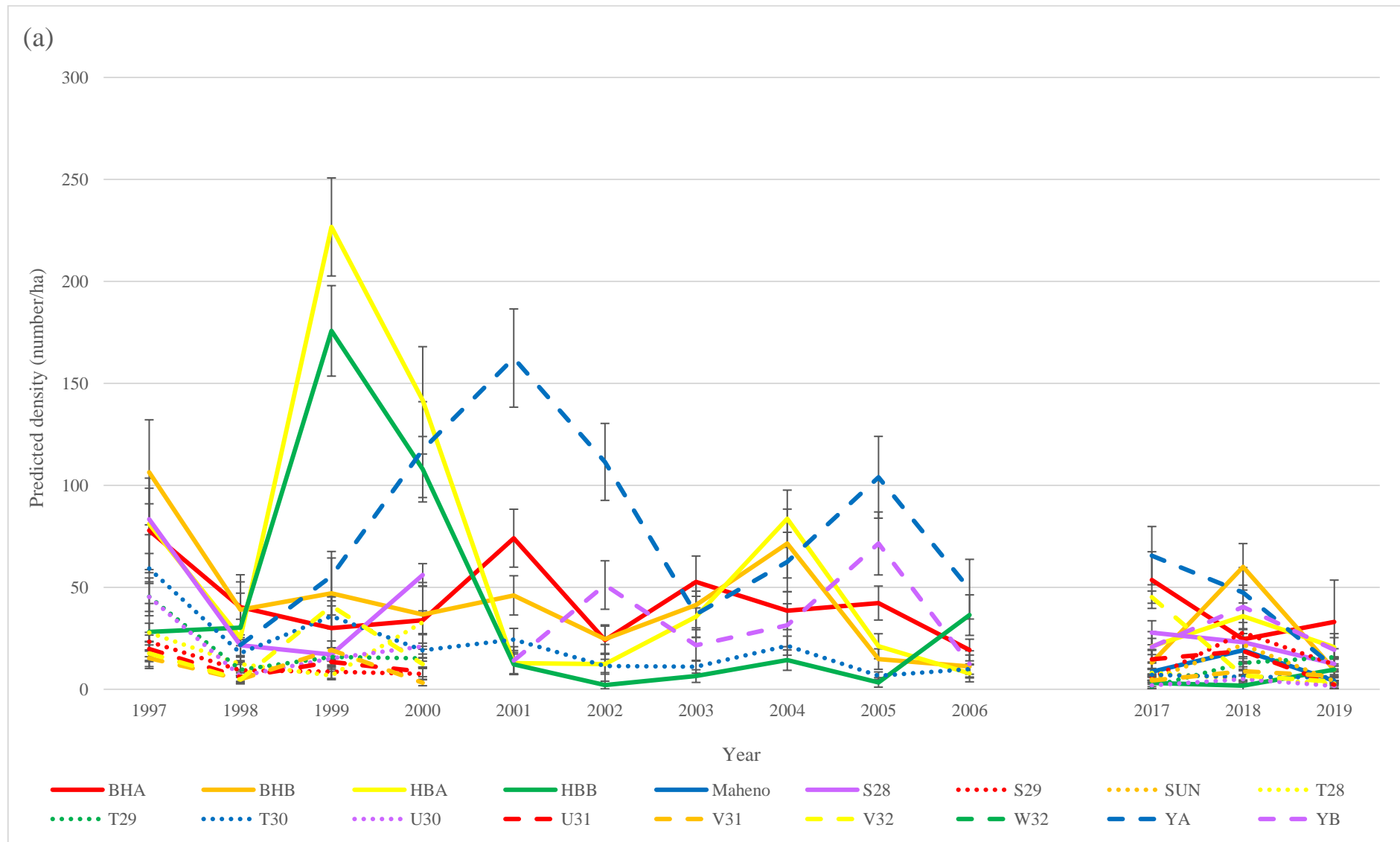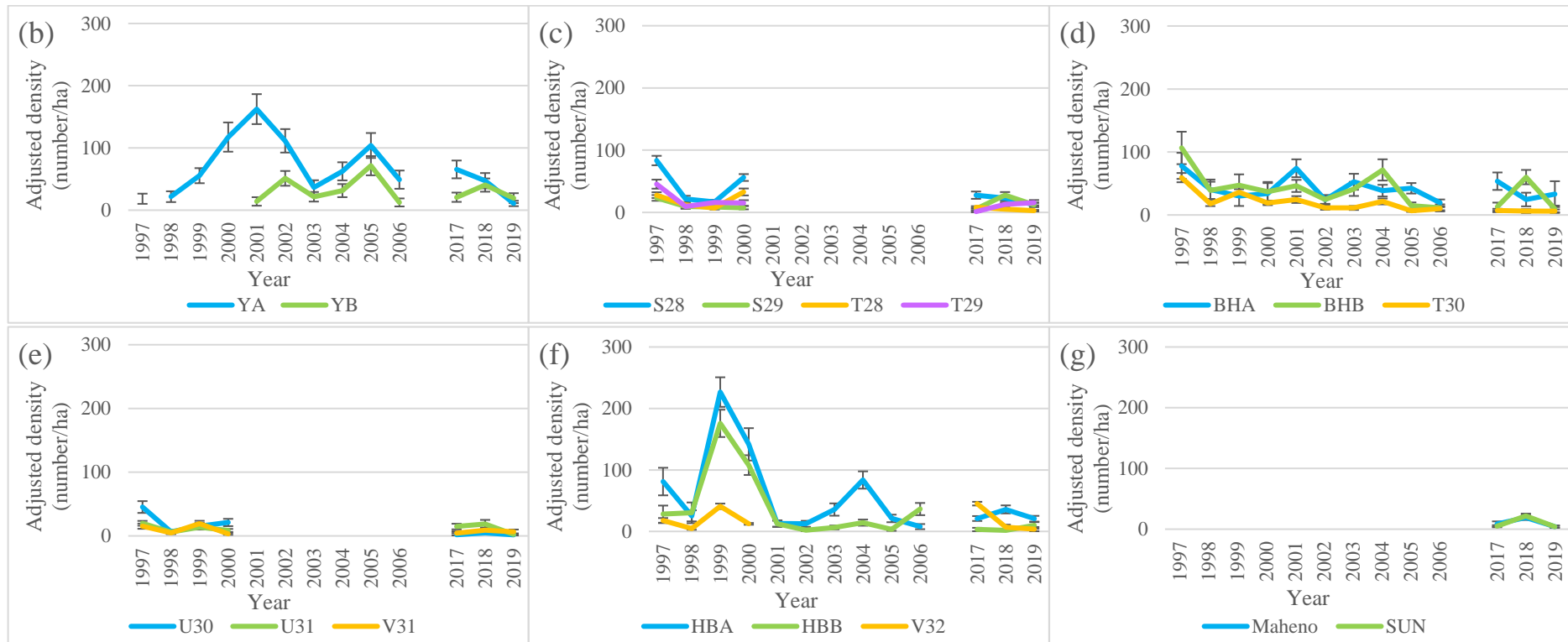
Figure 16-31. Adjusted 0+ density of saucer scallops (number ha⁻¹) over the duration of the fishery-independent scallop survey within (a) all strata, (b) the Yeppoon SRAs, (c) S28, S29, T28 and T29 strata, (d) Bustard Head SRAs and T30 strata, (e) U30, U31 and V31 strata, (f) Hervey Bay SRAs and V32 strata, (g) the Maheno and Sunshine Coast strata. Vertical bars represent one standard error either side of the mean. No data for the two GBRMPA green zones (MNP-24-1173 and MNP231169) are provided because these two areas were only sampled once in 2017.

(a)
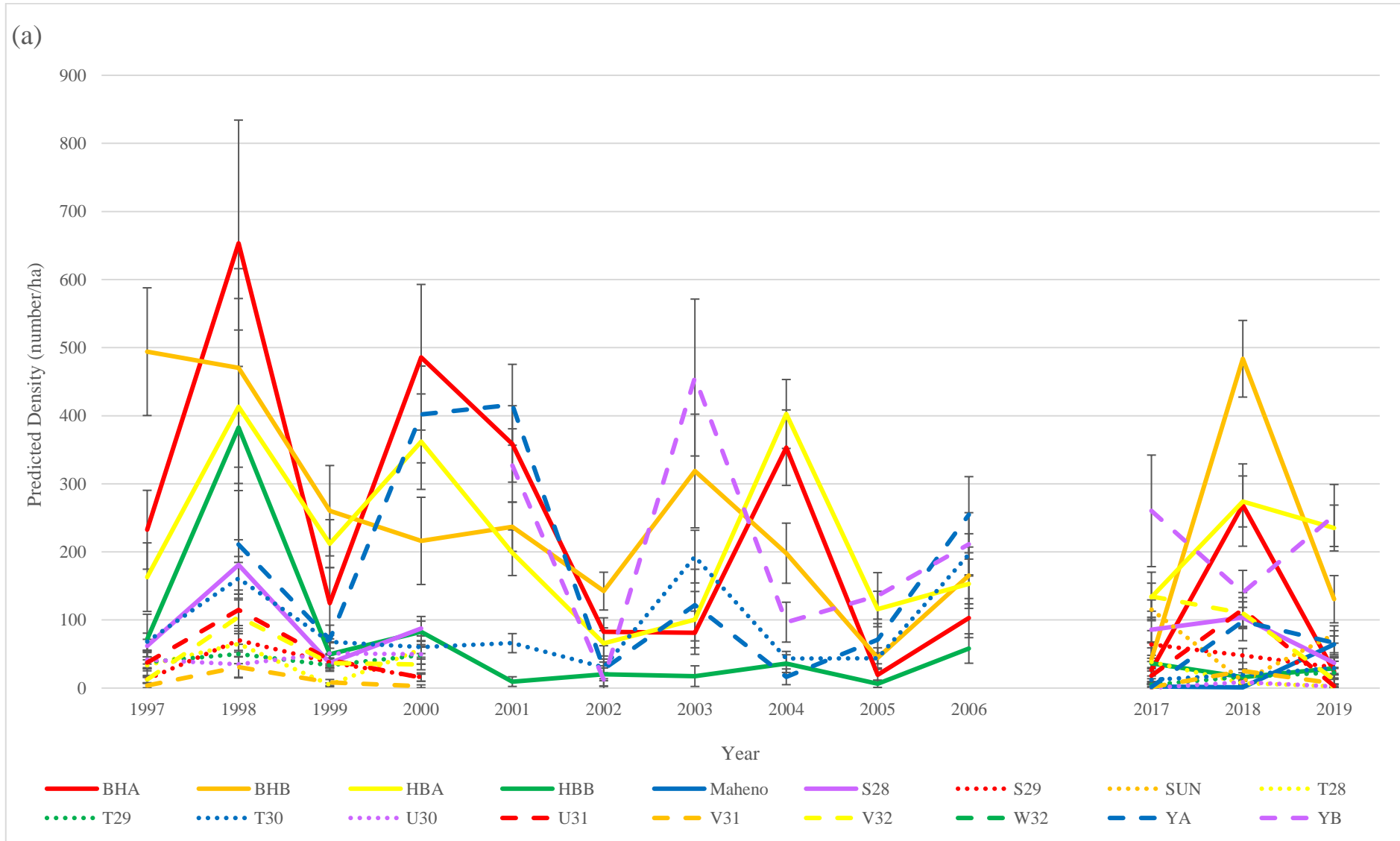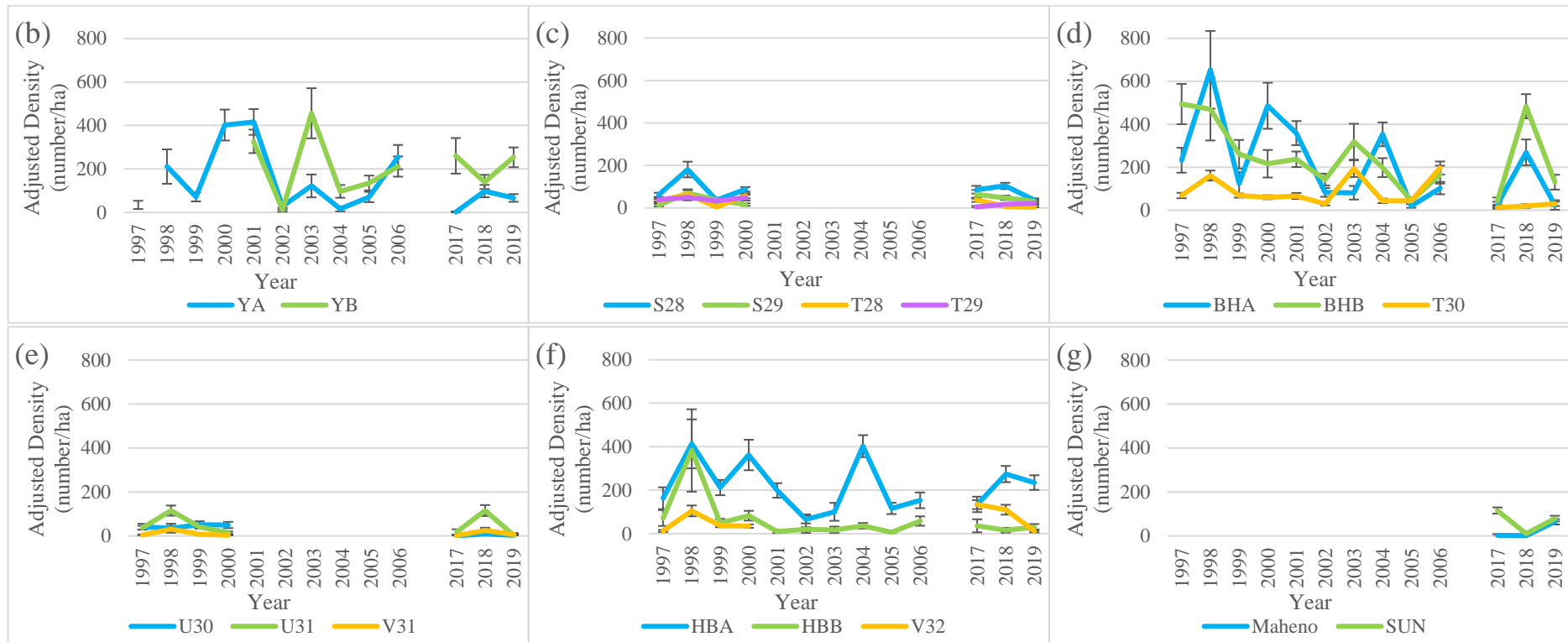
Figure 16-32. Adjusted 1+ density of saucer scallops (number ha^{-1}) over the duration of the fishery-independent scallop survey within (a) all strata, (b) the Yeppoon SRAs, (c) S28, S29, T28 and T29 strata, (d) Bustard Head SRAs and T30 strata, (e) U30, U31 and V31 strata, (f) Hervey Bay SRAs and V32 strata, (g) the Maheno and Sunshine Coast strata. Vertical bars represent one standard error either side of the mean. No data for the two GBRMPA green zones (MNP-24-1173 and MNP231169) are provided because these two areas were only sampled once in 2017.

16.5 DISCUSSION

A major decline in the Queensland saucer scallop commercial catch rates in 1996 prompted the first large-scale fishery-independent survey in 1997. The objectives of the survey were to provide an index of the relative abundance of the scallop population and the size class structure, including the relative abundance of the 0+ and 1+ age classes (Dichmont *et al.* 2000). This section of the report collated and analysed all the available survey data (i.e., 1997–2006, 2017–2019) to examine long-term trends in the scallop population. The results for 2001–2006 need to be considered with caution because the survey was scaled back in this period to mainly the SRAs, which are generally associated with higher scallop densities. A more robust assessment of the population can be obtained by comparing the early survey years from 1997–2000, against those from 2017–2019, when the survey was comprehensively implemented. The analyses a) calibrated catch rates for differences between participating vessels, b) considered the effects of TEDs and BRDs that were mandated part-way through the survey time series, c) adjusted catch rates due to variation in the lunar phase and time-of-night when the samples were obtained, and d) improved the precision of the survey by including the swept area of the trawls, enabling the catch rates to be reported as a density rather than number per trawl (Jebreen *et al.* 2008).

16.5.1 Calibrating for differences between vessels

For most survey years, a different group of trawlers participated in the survey, resulting in the size of the nets and net configurations (i.e., twin, triple, quad and five nets) used by vessels varying within and between survey years. Each year, differences in the catch rates between vessels were measured by undertaking several calibration trawls before or after the survey. Importantly, a single vessel, the *FV C-King* has participated in all 13 surveys and each year all vessels were calibrated against the *FV C-King*, effectively adjusting the catch rates to reflect a single vessel undertaking the survey. The calibration was undertaken after the swept area estimates of each trawl were calculated, and therefore differences between vessels due to net size and net spread factors were already considered.

Calibrating for differences between vessels remains heavily dependent on the *FV C-King* participating in any future surveys. However, the calibration procedure does not consider any changes to the catching efficiency of the *FV C-King* over the survey time series, apart from the size and configuration of the nets used each year. Hence, the calibration only considers within-year variation between vessels, and not between-year variation and therefore some variation in the catching efficiency of vessels between years is likely to remain unexplained. The parameter estimates obtained from the calibration model minimise the error associated with the predictions (Moore and Doherty 2005). The need to standardise among vessels is common in surveys (Brown *et al.* 2007) and the lack of control over participating vessels and their gear type and configuration has remained a significant problem for the Queensland scallop survey since it was first implemented in 1997.

One approach which could avoid the need to calibrate for differences between vessels each year involves adopting a towed camera system to quantify scallop densities, such as the towed camera system deployed by NOAA to survey the Atlantic sea scallop fishery, which is the most valuable commercial scallop fishery globally (https://habcam.whoi.edu/about/habcam-4/). Research undertaken by the Northeast Fisheries Science Centre (2018) and Miller *et al.* (2019) shows that the towed camera system detects more scallops than the NOAA dredge survey and therefore can be used to derive more accurate estimates of total scallop abundance (additional information provided in section 17.2, page 93).

16.5.2 Survey trends in abundance

When the 2001–2006 data are omitted, the overall trend in the kriging maps, based on a comparison of surveys from 1997–2000 (Figures 16-17 to16-20) against those from 2017–2019 (Figures 16-27 to 16-29), is a marked decline in total scallop abundance. For most years, the 0+ age class contributed relatively little to total scallop densities and the relative contribution of this age class to the size frequency distribution has declined over the time series. Extremely low 0+ densities in the 2019

survey are concerning and indicate that the commercial catch in the 2021 fishing year (December 2020 to April 2021) is likely to be low.

The weighted means CVs for total scallop densities from all strata for those years when the survey was comprehensively undertaken (i.e., 1997–2000 and 2017–2019) were relatively low and ranged from 6 to 14%, indicating relatively low dispersion and high precision of the means (Table 16-5) (Brown 1998). The weighted means method weights the contribution of each strata to the overall means, based on the area of each stratum. Hence, large strata have more influence on the means than small strata. Although the density of scallops in the SRAs was generally higher than elsewhere, the weighted means method reduced the influence of SRAs on the overall means because the SRAs are relatively small.

Weighting the strata may not be required because the amount of sampling sites allocated to each stratum is already weighted and based on the product of the stratum area and the commercial catch rate of the stratum. Hence, applying a second weighting in the analyses may be redundant.

Although the weighted means and kriging provide insight into the scallop population trends in the surveyed area, the adjusted means (Figures 16-30, 16-31 and 16-32) provide a more reliable index of abundance because the GLM considered the influence of lunar phase and the time-of-night when the samples were obtained, and as well as the year-strata interaction. Lunar phase and time-of-night increased the amount of variation explained by the model, resulting in more reliable indices of abundance and lower standard errors. Including swept area as an offset allowed the model to predict scallop density (number ha^{-1}), which is a more precise measure of abundance than the number of scallops per 20-minute shot, which has been reported previously. The first survey analyses by Dichmont *et al.* (2000) reported catch rates as a density. Density also enables total population size and biomass to be estimated by extrapolation and is therefore the preferred unit for reporting the survey catch rates, although it requires more data (i.e., net size, net configuration, net spread factors and trawl distance) and analysis.

16.5.3 *Environmental influences on scallop abundance*

Scallop fisheries are often characterised by large fluctuations in annual abundance that are linked to oceanographic conditions (Wolff 1987; Orensanz *et al.* 1991; Mauna *et al.* 2008; Caputi *et al.* 2015; Soria *et al.* 2016). Compared to other scallop fisheries, the amount of variation observed in the Queensland scallop commercial catches and survey data is relatively low. Notable large fluctuations in the survey data were attributed to peak densities in 1999, and the very low densities in 2002, 2005, 2017 and 2019 (Figure 16-30a), although caution is required when interpreting the 2002 and 2005 data due to the reduced sampling in those years.

Analyses of multi-decadal annual survey data from Western Australia (WA) have shown that recruitment of *Y. balloti* is heavily influenced by SST and the strength of the south-flowing Leeuwin Current off the WA coast (Joll and Caputi 1995a; Lenanton *et al.* 2009; Caputi *et al.* 2014; 2015; 2019). Investigating reasons for variation in the Queensland scallop survey densities was beyond the scope of the current project, but it should be the focus of future research if the survey is continued and more data become available. As the survey has only been undertaken comprehensively for seven years (i.e., 1997–2000, 2017–2019) it is unlikely that any meaningful environmental influences on the survey catch rates could be demonstrated.

When analysing the 1997 data, Dichmont *et al.* (2000) found densities were highest in northern inshore and central strata (i.e., S28 and T30), while southern strata (i.e., V31 and V32) had comparatively low densities. In contrast, the recent surveys indicate total scallop densities were highest in the central and southern strata, namely V32 in 2017, U31 in 2018 and the Sunshine Coast in 2019 (Figure 16-30). The southerly shift in the population may be related to rising sea surface temperature (SST) in the region. Winter SST in the scallop fishing grounds has risen by 0.7–0.8ºC since the 1950s (see Figure 22-6, page 254). Heidemann and Ribbe (2019) have shown that SST in

the East Australian Current adjacent to Hervey Bay and south of Fraser Island increased by 0.016°C per year between 1993 and 2016. The southerly shift is also reflected in a general increasing trend in the scallop fishery standardised logbook catch rates in some logbook grids adjacent to Fraser Island over the last two decades (see Figure 8-13 in Yang *et al.* 2016). Despite this regional trend, overall catch rates and annual catches for the fishery have declined markedly over the period.

Courtney *et al.* (2015) examined relationships between the commercial fishery standardised catch rates in November (the start of the scallop fishing year) and environmental variables, and found several significant correlations with Chlorophyll A, adjacent coastal river flows, SST and physical oceanographic properties of the adjacent Capricorn Eddy. The strongest correlation found was 0.85 for Chlorophyll A five months prior in June in logbook grid T30. When this relationship was subsequently updated with additional annual logbook data, however, it was not sustained.

The most recent quantitative assessment of the Queensland scallop stock included the survey catch rates as one of the data sources and concluded that current (i.e., 2019) spawning biomass was 17% of the unfished biomass (Wortmann *et al.* 2020), confirming the poor stock status. The modelling indicated that scallop biomass would increase from 17% to 40% in eight years if effort is constrained to 80,000 effort units annually (equates to 1454 boat days). The modelling did not include environmental influences on the stock, but the authors noted that if the scallops are adversely impacted by rising SST, then potential yields from the fishery may be lower than projected.

16.5.4 Trends in other scallop fisheries

The WA coastline experienced a severe marine heatwave in the summer of 2010–11 which had a severe and prolonged negative impact on the state's saucer scallop and other fisheries (Caputi *et al.* 2016; Chandrapavan *et al.* 2020). Prior to the heatwave, the northern Shark Bay fishery had fairly constant densities (i.e., number of scallops per nautical mile) for both the 0+ (< 86 mm SH) and 1+ (≥ 86 mm SH) age classes, while the Denham Sound fishery experienced frequent periods of poor recruitment and low spawning stock events. Following the heatwave, the 0+ densities from 2011–2013 were the lowest recorded in the survey time series for both fisheries. Recruitment (i.e., 0+ age class) densities for the northern Shark Bay fishery declined to less than 1% of the pre-heatwave abundance (Caputi *et al.* 2019).

From 2014–2017, 0+ and 1+ age class densities in the northern Shark Bay and Denham Sound fisheries increased (Kangas *et al.* 2011; Chandrapavan *et al.* 2020). In 2018 densities declined in both fisheries, although the Denham Sound stock remained largely recovered (Caputi *et al.* 2019). The cause of the declines is unknown, although SST increased briefly in the summer of 2017–18 before falling to its lowest level in the past decade in the summer of 2018–19 (Feng *et al.* 2021).

Mean SSTs off Tasmania increased at a rate of 0.2°C per decade between 1946–2016, which is four times the global average rate (Shears and Bowen 2017; Oliver *et al.* 2018). Tasmania also experienced a marine heat wave in the summer of 2015–16 which lasted 251 days and reached a peak intensity of 2.9°C above average (Oliver *et al.* 2017). The Tasmanian Scallop Fishery for the common scallop (*P. fumatus*) undertakes pre-season surveys in the White Rock region to estimate abundance and inform decision rules (Semmens *et al.* 2019). After a survey in 2011 indicated some stock had recovered (> 30 kilogram per square kilometre), the White Rock region reopened to fishing. However, average scallop densities have declined since. Estimates of abundance in the 2017 pre-season survey were produced for the White Rock, Marion Bay, Northwest (Circular Head) and Flinders Island regions, with average densities ranging from 2.4 to 4.7 kilograms per square kilometre.

Collectively the surveys for Queensland and other Australian scallop fisheries indicate a decline in the nation's scallop fisheries in recent years, based on surveys conducted in 2018 and 2019 for Queensland, 2017 and 2018 for Western Australia and 2016 and 2017 for Tasmania.

The NOAA Northeast Fisheries Science Centre has undertaken dredge surveys of abundance for the Atlantic sea scallop (*P. magellanicus*) on the Georges Bank and Mid-Atlantic regions since 1979. Since approximately 2000 the survey design has also incorporated a towed camera system (https://habcam.whoi.edu/projects/noaa-annual-scallop-survey/) and a drop camera system for additional information on scallop abundance. The survey data indicate that from the late 1970s to the early 1980s the biomass of Atlantic sea scallops declined, and thereafter remained stable but relatively low though to the mid-1990s. The biomass then increased markedly from the mid-1990s to the early 2000s and has remained high since.

Annual pre-season surveys for Tehuelche scallop (*Aequipecten tehuelchus*) populations in the San Matias Gulf (Argentina) commenced in 1986 (Soria *et al.* 2016). Annual landings indicate that the fishery is characterised by boom-and-bust periods, with short periods of exploitable stock (i.e., 1968–1972, 1983–1985, 1987–1990, and 2000–2004) and extended periods of depletion. During periods of exploitation, recruitment tends to be stronger when SST is above average in spring and summer, and weaker during cooler years (Soria *et al.* 2016). The first Tehuelche scallop survey was conducted in 1973 after the fishery expanded to the San Jose Gulf in 1972. Between 1995 and 2001 the biomass was negligible, and then slowly increased to peak in 2007. The biomass declined severely in 2009, increased in 2010 and declined rapidly between 2010 and 2013, leading to the collapse of the fishery. The abundance of sub-legal sized scallops has remained consistently low from 1997 to 2013, with a slight peak in 2005.

Surveys for Patagonian scallops (*Zygochlamys patagonica*) began in 1999 and estimate absolute biomass (Soria *et al.* 2016). Densities (number of whole scallops per square kilometre) have been declining since the opening of the fishery in 1996, except for a peak in 2006. Since 2012, the density has remained at approximately 20 scallops per square kilometre.

16.5.5 Recommendations

The SRAs were implemented in 1997 to reduce fishing mortality on the stock and permanently closed from 1997–2000. The 2-year rotational regime (15 months closed, 9 months open) was applied from 2001–2016, until September 2016 when the Queensland Government closed all six SRAs indefinitely due to the poor stock status (see Figure 16-1, page 45). The survey results indicate that the proportion of the scallop population inside the SRAs has increased. In 1997, about 20% of scallops sampled in the survey were from inside the SRAs (Dichmont *et al.* 2000), while 55% of scallops were from inside the SRAs in 2019.

Under the Australian Government (2018) Commonwealth Fisheries Harvest Strategy Policy, the Queensland saucer scallop stock would likely be closed to fishing because the biomass is less than 20% of the unfished biomass (Wortmann *et al.* 2020). Since 2016, the fishery managers have also implemented temporal/monthly total closures of the fishery, such that the fishery is currently open for five months annually (December to April). Given the poor status of the stock, and that fishing is still permitted each year, and that a high proportion of the proportion of the stock is within the SRAs, it would be prudent to keep the SRAs closed until stock recovery is evident. As the stock biomass declines the value of closed areas as spatial refugia becomes increasingly important to limit fishing mortality and assist recovery (Taylor and McIlwain 2010; Edgar *et al.* 2014).

The selectivity of the prawn nets used in the survey for scallops of different size classes is poorly understood. Since its commencement in 1997 the survey has specified the use of 2.0–2.5 inch mesh, even though the minimum mesh size specified for the commercial scallop fishing is 3.5-inch mesh or 80 mm square mesh. The reason for using the smaller mesh was to selectively catch and retain the 0+ age class, as well as the 1+ age class. Dichmont *et al.* (2000) concluded there was little difference in the selectivity of scallops ≥ 90 mm SH between the two mesh sizes. However, it is clear from the length frequency data (Figure 16-3) that scallops that are < 40 mm SH are poorly represented, and it is likely that the density of the 0+ size class is grossly underestimated. This problem is probably not

entirely attributed to mesh size, but also to the behavioural responses, reaction times and swimming speeds of the small scallops as they react to approaching trawl net ground chains.

Experiments could be conducted to trial sampling gear that has a higher selectivity for the 0+ age class. Courtney *et al.* (2008) found no significant decrease in the catch rates of legal size of scallops (≥ 95 mm SH) between the standard commercial net 3.5-inch (88.9 mm) diamond-mesh codend net and a 4-inch (101.6 mm) square-mesh codend net with TED. For undersized scallops (< 95 mm shell height) a 32% reduction in catch rates was reported for the square mesh codend with TED. Since this research was undertaken, square mesh codends have been made mandatory in the Queensland scallop fishery to reduce bycatch and lower the catch and incidental fishing mortality on undersize scallops and Moreton Bay bugs. Note that the legal size of scallops in Queensland has since been lowered to ≥ 90 mm SH and the square mesh codends that were mandated are 88 mm which is slightly smaller than what was trialled by Courtney *et al.* (2008).

The Queensland scallop survey may be able to incorporate a towed camera system as an additional and independent method for quantifying scallop abundance. The NOAA towed camera system has been used to estimate the dredge efficiency, which facilitates the estimation of absolute abundance of Atlantic sea scallops (Miller *et al.* 2019). A similar comparison between a towed camera system and a dredge survey was conducted for the Tasmanian scallop fishery in May 2017 (Ewing *et al.* 2018; Semmens *et al.* 2019). The Tasmanian trial results indicated that densities were similar, however the towed camera survey detected a greater number of smaller scallops than the dredge. A similar towed camera pilot study was undertaken in the Queensland saucer scallop fishery as part of this FRDC project (see section 17.3, page 97). Although there was uncertainty in the photographed image area sizes, results from the pilot study indicated that the towed camera system detects more scallops than the trawl survey. Scallop density estimates based on the camera images were about 3.5 times higher than those based on trawl sampling. The results are promising and suggest that a towed camera system could improve the current annual trawl survey density estimates.

The Queensland scallop survey should be continued annually and comprehensively implemented (i.e., not down scaled such as the period from 2001–2006) because it provides a robust, independent assessment of the scallop population and distribution, and the survey catch rates are incorporated in the quantitative assessment of the stock (O'Neill *et al.* 2020; Wortmann *et al.* 2020). The survey analyses could be improved further by incorporating physical properties of the seafloor (e.g., sediment composition and bottom hardness) as factors affecting scallop habitat which may be useful for explaining variation in the observed densities. If the survey is continued, research should investigate relationships between survey density estimates and environmental parameters, including SST, Chlorophyll A and physical oceanographic properties, including aspects of the Capricorn Eddy, similar to the analyses undertaken by Courtney *et al.* (2015) which used commercial logbook catch rates.

17   Appendix 5. Study tour and pilot study of a towed camera system for surveying abundance of Queensland saucer scallops (*Ylistrum balloti*)

17.1 ABSTRACT

This section of the report presents findings from a brief study tour of the NOAA Atlantic sea scallop annual survey off the northeast coast of the United States of America and a subsequent pilot study that evaluated a towed camera system as an alternative method for detecting, counting and surveying saucer scallop abundance in the Queensland fishery. The work was undertaken as part of this FRDC 2017-048 project but was not an objective of the project. The tour and pilot study were undertaken using savings from the project, specifically from the 2017 Queensland fishery-independent scallop survey, with approval from FRDC and Fisheries Queensland. The findings include 1) report on a brief study tour of the NOAA Atlantic sea scallop annual survey in June 2018 which utilises the towed camera HabCam system, 2) results from a towed camera pilot study conducted in the Queensland scallop fishery in May 2019, 3) assessment of the Australian Institute of Marine Science (AIMS) autoclassification software (BenthoBox, https://www.aims.gov.au/advanced-observation-technologies/image-analysis) as a means of processing the seafloor images obtained from the pilot study.

17.2 STUDY TOUR REPORT

T. Courtney, 4 July 2018

The purpose of this overseas travel was to participate in and evaluate a survey of Atlantic sea scallops (*Placopecten magellanicus*) in the vicinity of Georges Bank off the coast of Maine and Massachusetts.   The survey is designed and conducted by the USA National Oceanic and Atmospheric Administration (NOAA) Marine Fisheries Service. NOAA has been conducting scallop dredge surveys for decades, but since 2011 they have incorporated an innovative camera-based system (HabCam https://habcam.whoi.edu/projects/) into the survey design. HabCam takes photographs of the seafloor that are then used to derive scallop abundance estimates. The fishery extends across several USA northeast states and into Canadian waters and is one of the two most valuable commercial fisheries in the USA, valued at about USD$480 million annually.

On 10 June Dr Courtney flew from Brisbane to Los Angeles to Boston and travelled by bus to Woods Hole near

Figure 1. Northeast coast of the United States and Canada, showing the location of Georges Bank which was surveyed during the study tour trip. The Atlantic sea scallop fishery extents offshore from and adjacent to several northeast USA states and into Canadian waters. The study tour involved flying from Brisbane to Los Angeles to Boston, catching a bus down to Cape Cod and boarding the *RV Hugh R Sharp* which departed at Woods Hole (near Martha's Vineyard).

Martha's Vineyard (Figure 1). Prior to participating in the survey and at NOAA's invitation, Dr

Courtney gave a seminar on Queensland scallop research and assessment at the National Marine Fisheries Service laboratory at Woods Hole on Tuesday 12 June (copy of the presentation is available). The survey takes about 32 days and is conducted in three legs. Dr Courtney participated in the third leg over the last six days, boarding the vessel at Woods Hole on the 13 June when it came in to refuel.

NOAA charter the Research Vessel *Hugh R Sharp* for the survey (Figure 2). This is a 146-foot state of the art vessel that operates as a member of the University-National Oceanographic Laboratory System and is based at the University of Delaware. During the survey the ship had a crew of eight, including a cook, and 12 scientists, researchers and volunteers. The cost of the vessel charter is about US$16,000 per day or about US$512,000 for the whole survey. The survey continues 24 hours per day, with crew and two teams of six scientists and researchers undertaking 12-hour shifts. Dr Courtney participated in the night shift (12AM to 12PM) from 13–18 June, working on the HabCam survey and scallop dredge sampling.

About two-thirds of the survey (~21 days) is dedicated to obtaining HabCam photographs of the seafloor, processing, and manually annotating (i.e., counting scallops and other species) the images, while the remaining one-third (~11 days) is dedicated to dredge sampling.

HabCam takes six photographs of the seafloor per second while the vessel travels at about 6 knots, which equates to about 2 photographs per metre. As the survey continues 24 hours/day, the system generates about 500,000 photographs per day, or about 10 million photographs over the 21 days. NOAA aim at manually annotating about 2% of the images. Hence, their annual estimates of scallop abundance are based on about 200,000 photographs.

Figure 2. Top – *RV Hugh R Sharp* at Woods Hole prior to departing for the scallop survey. Middle – Inside the vessel's dry laboratory during the HabCam survey. Activities being undertaken here include piloting the HabCam, monitoring the sensors, outputs and equipment on the HabCam, annotating the images (i.e., counting scallops) and managing the large amount of data and files being generated. Bottom – running repairs on HabCam on the deck of the vessel. Note the lit-up area under the HabCam as the strobe lights continue to flash while on deck.

While NOAA has developed software to automatically process the images, manual annotation produces more accurate estimates of scallop abundance. As a result, they are still reliant on people to process the images, which is labour intensive. It was impressive to witness the skills, knowledge and speed of experienced NOAA staff annotators who have participated in several surveys. Trained annotators can process about 1000 images per day, which suggests that the survey requires about 200 person-days to annotate the 200,000 images each year. NOAA achieve this by relying upon a team of

about 15 staff and volunteers participating in the survey. About half of the images are processed at sea during the survey, while NOAA staff process the remaining images back in the lab after the survey ends. Four people in the middle photograph of Figure 2 were undertaking annotations.

A significant consideration for NOAA that resulted from the HabCam survey was the production of extremely large data sets. The system generates 2–3 terabytes of data daily, and about 70 terabytes during an annual survey. The system requires a fulltime data specialist on board to track, store, copy and access the images and other data, including sonar, temperature, conductivity, turbidity and oxygen data files. Data storage logistics would need to be considered if a similar monitoring program was adopted for the Queensland scallop fishery.

The leg of the survey that Dr Courtney participated in included several scallop dredge samples (Figure 3), each of which required deploying the dredge on the bottom for 20 minutes. The dredge was then brought to the surface and the catch processed to record the number and size of all scallops, as well as the number and weight of finfish and skates. The scallop estimates of density and abundance use data from both the HabCam and dredge samples.

The vessel returned to Woods Hole at about 6AM on Monday 18 June and much of the morning was spent disassembling computer workstations, washing down sampling gear and wet weather gear and packing equipment. Dr Courtney disembarked at 10AM and caught a bus back to Boston. On Tuesday 19 June he spent the day touring Boston and flew home from Boston to Los Angeles and onto Brisbane, landing at 6AM Friday 22 June.

Figure 3. Top – emptying the scallop dredge after a 20-minute haul. Middle – the catch includes skates, flatfish and hermit crabs, in addition to the sea scallops. Bottom – Atlantic sea scallop which is about 5–6 years old. This species grows slower and lives longer than the Queensland saucer scallop.

In summary, the trip was one of the most useful and stimulating experiences of Dr Courtney's career. The survey is extremely well organised by NOAA staff and the data derived from it are being directly used to assess the stock and make management decisions. There is strong potential to develop and apply a similar HabCam-type survey methodology in Queensland because we have a similar scallop species which inhabits the seafloor and has limited swimming ability. Saucer scallops appear well suited to being photographed via a similar towed camera system and the resulting data could be used to

derive an index of abundance which is more accurate than our current trawl survey estimates. The methodology imposes less impact on the seafloor than the current trawl surveys. Such a towed camera methodology would probably be supported by the GBRMPA, as an additional method for monitoring benthic ecosystems in the Park, and the system would probably be of significant interest to Western Australia, which has a trawl fishery for the same scallop species. Significant funding for the development, trialling and implementation of a towed camera-based system would be required, but this could be supported from a relatively broad user-base, that could include Western Australia, the GBRMPA and the FRDC, as well as Queensland. It may also be possible to raise industry support for such an initiative.

17.3 RESULTS FROM THE TOWED CAMERA PILOT STUDY IN MAY 2019

These results were presented to the joint FRDC 2017-048 and 2017-057 scallop research steering committee on 6/12/19.
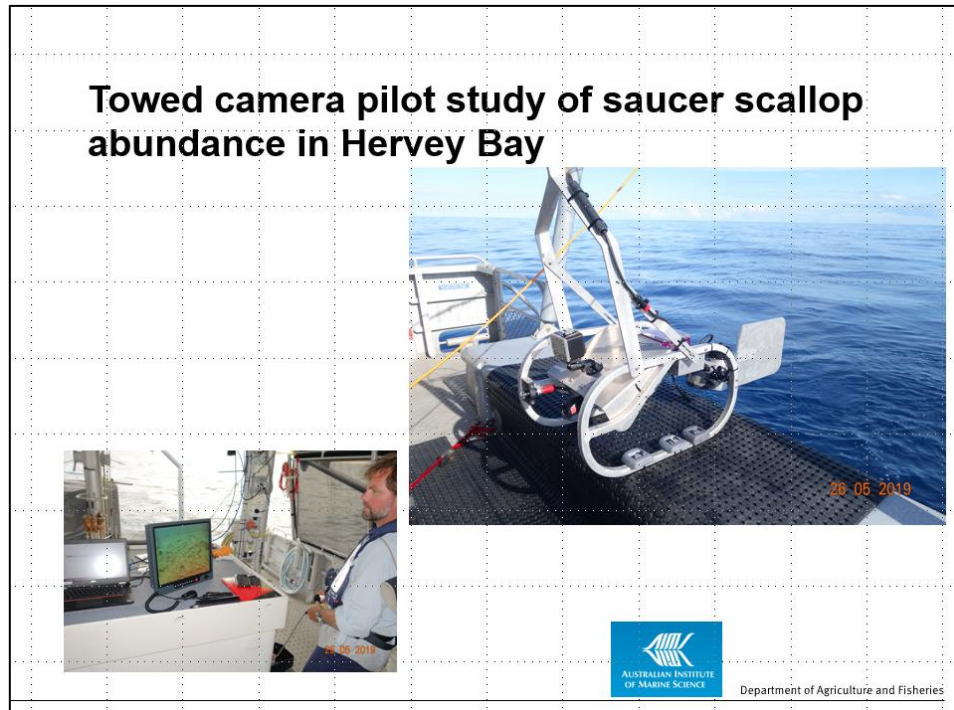
Why trial a towed camera system

➤ Towed camera may offer an additional and better approach for monitoring scallops
➤ NOAA (USA) use a towed system (HabCam) to survey Atlantic sea scallops annually in USA and Canada - largest scallop fishery in the world
➤ Camera detects more scallops than dredge survey (closer estimate of absolute abundance)
➤ Potential for automated software detection, counting and measurement of scallops in images (could enhance stock assessment)

2015 Mid-Atlantic Habcam Survey

Chang et al. 2017. *Limnology Oceanography: Methods, 15:480-494.*

Raw Habcam scallop observations

Geostatistical estimation of scallop density
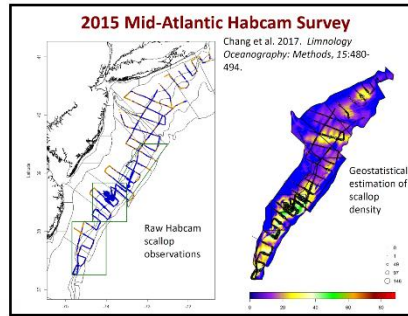
Department of Agriculture and Fisheries

Towed camera pilot study methods

- 11 1-nm transects in Hervey Bay HBA (survey calibration sites)

- Each transect sampled by 3 trawlers (C-King, Silda, Somatina) in October 2018 scallop survey (pink lines)

- AIMS camera system towed over each transect by *RV Tom Marshall* in May 2019 (black dot line)

  – Camera towed ~ 50 cm height (flies over seafloor)

  – ~ 1251 images per transect

  – ~ 1 image per second (frequency affected by strobe light battery)

  – 20 minutes per transect

  – 2.8 kn tow speed

  – Photo image area ~ 0.157 m^2 (450 mm x 350 mm) Area needs to be measurable and increased, too small

- Scallop density calculated for trawl and camera (number of scallops per hectare, ha)

- Applied AIMS "BenthoBox" image autoclassification software on all ~14,000 images to detect scallops

Queensland

Great Barrier Reef Marine Park

HBA   HBB

Camera tows May 2019
Scallop trawl survey October 2018

Department of Agriculture and Fisheries

Saucer scallop images

Department of Agriculture and Fisheries

Seafloor images
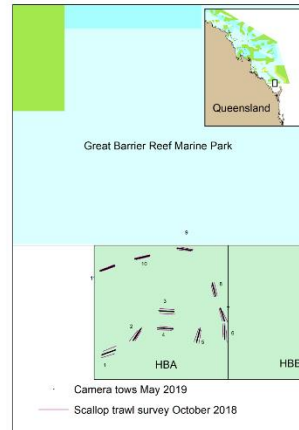
Department of Agriculture and Fisheries
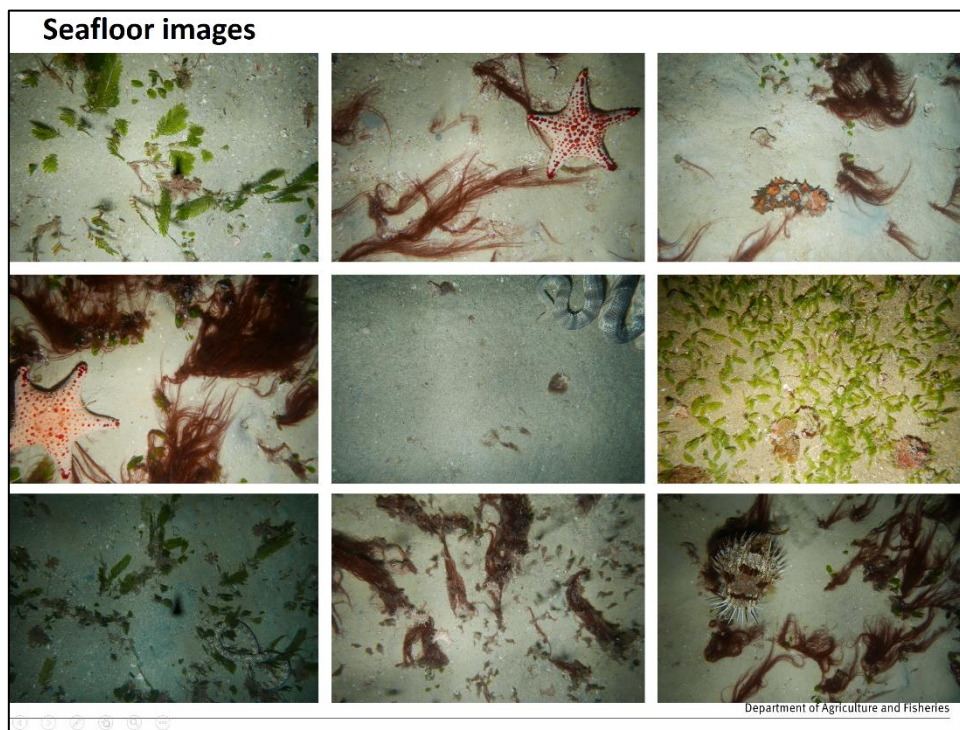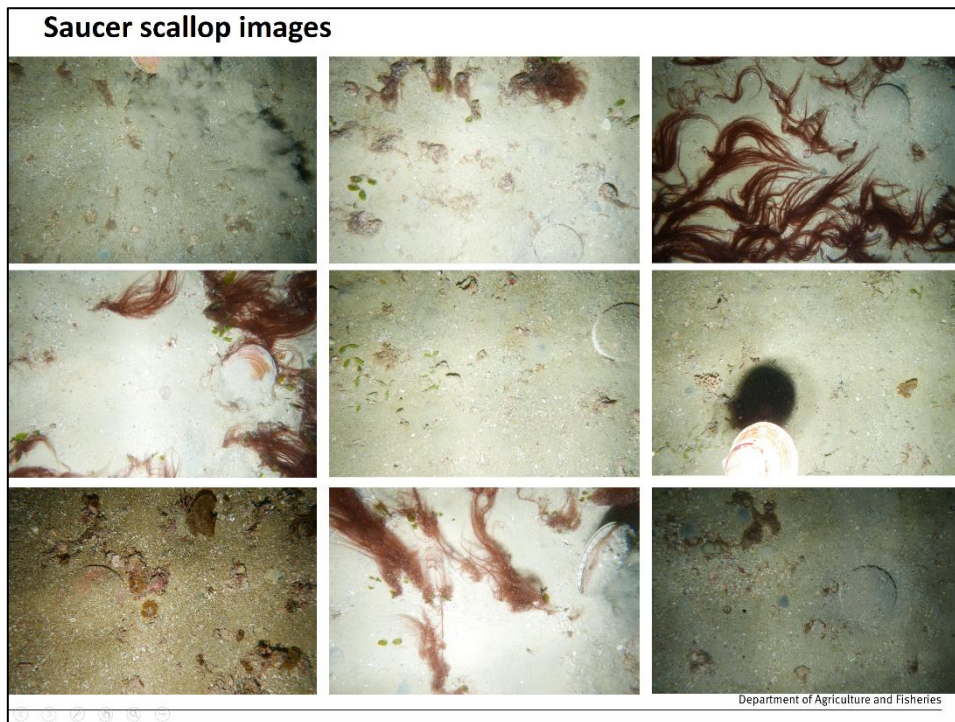
Results

Transect	Number of images	Number of useable images	Number live scallops seen	Camera scallop density (number per ha)	Mean trawl scallop density from 3 vessels (number per ha)
1	1550	1549	5	205	151
2	1311	1297	13	636	285
3	537	536	14	1658	349
4	1477	1476	7	301	171
5	1405	1401	18	816	78
6	1371	1352	24	1127	209
7	1257	1077	6	354	66
8	1190	1186	4	214	200
9	1222	1210	24	1259	162
10	1350	1345	11	519	326
11	1358	1339	3	142	72
Grand Total	14918	14657	155	Average = 657	Average = 188

Scallop density camera vs trawl

Average camera density = 657 scallops/ha
Average trawl density = 188 scallops/ha
Suggests that a trawl retains about 29% of scallops in its path

Department of Agriculture and Fisheries

Results

Camera vs trawl

$y = 2.3742x + 211.14$
$R^2 = 0.218$
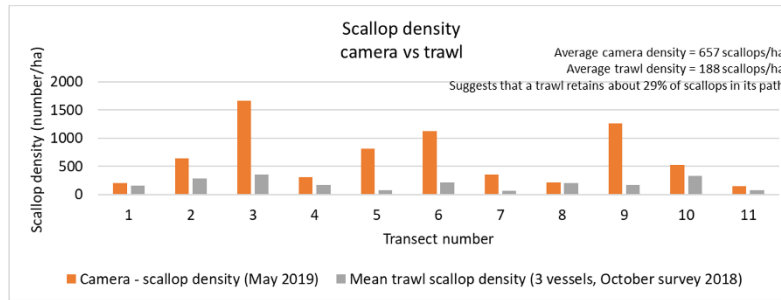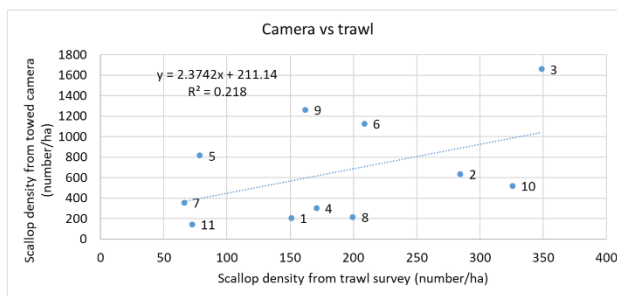
Weak correlation

Department of Agriculture and Fisheries

Associations between scallops, substrate and macrobiota

Substrate composition	Number of images	Substrate %		Number of scallops	Scallops %
GRAVEL	503	2		1	1
Gravelly SAND	12789	63		148	82
None	273	1			0
Rubble	694	3		1	1
SAND	4913	24		24	13
Sandy GRAVEL	1239	6		7	4
Grand Total (all images includes additional transects)	**20411**	**100**		**181**	**100**

Dominant structural macrobiota	Number of images	Structure %		Number of scallops	Scallops %
Anemone	4	0			0
Ascidian (incl. tunicates, sea squirts)	54	0			
Brown filamentous algae	5556	27		64	35
Green filamentous algae	54	0			0
Halimeda	283	1		1	1
Halophila ovalis	1655	8		24	13
Halophila ovata	1	0			0
Halophila spinulosa	717	4		3	2
Hard coral	6	0			0
None	3499	17		38	21
Padina	421	2		7	4
Red filamentous algae	7928	39		43	24
Soft coral (Octocorallian including gorgonians, sea pens, sea whips)	231	1		1	1
Sponge	1	0			
#N/A	1	0			
Grand Total (all images includes additional transects)	**20411**	**100**		**181**	**100**

Department of Agriculture and Fisheries

Results

➢ AIMS autoclassification software trial based on small training set of 95 images with scallops present

➢ Software incorrectly predicted scallop presence in 26% of images (actual observed presence is 1% - gross over prediction)

➢ Software could be useful with more training – see AIMS report

Example of a live saucer scallop labelled using the Visual Geometry Group (VGG) annotator used by AIMS

Example where objects were detected by autoclassification, when clearly no scallop exists

➢ Images forwarded to NOAA (Dr Dvora Hart) who have offered to pass them through the NOAA software used for Atlantic sea scallops. Watch this space.

Department of Agriculture and Fisheries

NOAA automated software annotations of Atlantic sea scallop
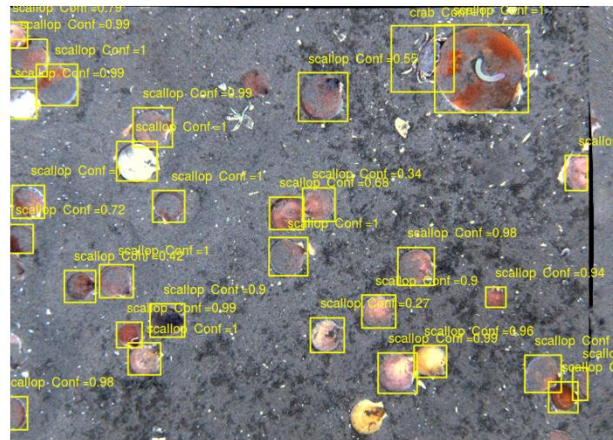
NOAA software is improving but still misses some Atlantic sea scallops

Department of Agriculture and Fisheries

Towed camera pilot study conclusions and recommendations

➢ Towed camera is potential additional and better form of monitoring Queensland scallop abundance
➢ Camera detects more scallops than trawl
➢ Results dependent on assumptions about swept area for both trawl and camera
➢ Swept area much smaller for camera (~250 m² per transect versus ~7 ha for trawl)
➢ Need to accurately measure image area
➢ Need to increase photographed image area (~0.157 m²) – fly camera higher off seafloor, needs stronger strobe light/s, water clarity
➢ Each image requires a scale to measure scallop size (shell height)
➢ Autoclassification software still some way off - still reliant on human counting
➢ Potential to examine seafloor properties (fauna/predators, flora, bottom hardness, sediment profile) influence on scallop abundance and habitat condition (relevant to GBRMPA?)
➢ Camera-based survey of whole scallop fishery would require significant funding, development, staffing, vessel and post-survey image processing (~20 boat-days, 100+ transects, 100,000-200,000 images annually)

Department of Agriculture and Fisheries

17.4 EVALUATION OF THE AIMS BENTHOBOX AUTOCLASSIFICATION SOFTWARE FOR DETECTING SAUCER SCALLOPS

Assessing the utility of AIMS towed video and BenthoBox software to count and measure scallops

Mathew Wyatt, Karen Miller & Neill Roberts

A report prepared for Queensland Department of Agriculture and Fisheries

July 2019

AIMS: Australia's tropical marine research agency.

www.aims.gov.au

Australian Institute of Marine Science

Australian Institute of Marine Science

PMB No 3   PO Box 41775   Indian Ocean Marine Research Centre
Townsville MC Qld 4810   Casuarina NT 0811   University of Western Australia, M096
                                                      Crawley WA 6009

This report should be cited as:
Wyatt, M., Miller, K., and Roberts N. (2019). Assessing the utility of AIMS towed video and BenthoBox software to count and measure scallops Report prepared for Queensland Department of Agriculture and Fisheries. Australian Institute of Marine Science, Perth. (13 pp)

DISCLAIMER

Revision History:		Name	Date
0	Revised by:	*Karen Miller*	*28/08/2019*
A	Prepared by:	*Mat Wyatt & Karen Miller*	*30/07/2019*
	Approved by:	*Michaela Dommisse*	*31/07/2019*

Cover photo:
AIMS towed video system being deployed from the RV Solander. Image: K. Miller, AIMS

CONTENTS

105

1 BACKGROUND

Assessment of the Queensland saucer scallop stock is based on modelling the population. The model includes several datasets, including data from an annual fishery-independent scallop trawl survey. While the survey provides an index of relative abundance, the absolute abundance of scallops has greater uncertainty. Towed camera-based survey methods can be used to derive more accurate estimates of absolute abundance of scallops. In addition, towed camera surveys have less impact on the seafloor and on the scallops than trawl surveys. In the USA, NOAA use a towed camera system, referred to as HabCam, to survey Atlantic sea scallop stocks, in addition to their dredge survey. The HabCam is deployed from a research vessel and collects high-resolution images of the sea floor. Images are processed manually to count and measure scallops, an approach that is very resource intensive and cost-prohibitive for most scallop fisheries. NOAA also utilise software to detect, count and measure the scallops, but it is not as accurate or reliable as human annotation.

AIMS routinely undertakes benthic surveys of reefs and other habitats using a purpose-built towed video system which collects forward-facing video as well as downward-facing high-resolution still images. To complement data collection with towed video, AIMS has developed an automated image analysis system (BenthoBox) for rapidly classifying biota from towed video images. These tools are now being used routinely for habitat classification and to determine cover of key organisms such as corals.

This project was developed in order to assess the utility of the AIMS towed video for collecting field data on scallops for stock assessment and of the BenthoBox system to detect and classify scallops from towed video still imagery.

2 TOWED VIDEO SURVEYS OF SCALLOPS

Field trials with the AIMS towed video were run from the DAF vessel FRV Tom Marshall. An initial inspection of the vessel was conducted to assess options for winch mounting, tow body launch, location of the operator station, power supply, as well as access to NMEA feeds for position data. Based on the initial assessment, it was determined that the AIMS towed video system with electric winch would be suitable for the survey.

Field work was undertaken from 24-30 May 2019, AIMS Trip #7209. During this trip, the electric tow video system was installed and tested on FRV Tom Marshall. A total of 11 one-nautical mile (nm) towed video transects was completed in the Qld Fisheries Scallop closure area (Hervey Bay A, HBA) located around 20 miles offshore from Bundaberg (Figure 1). In addition to the 11 transects, the camera system was deployed over a site where DAF has released a large number of tagged scallops over the last 12 months, to determine if any tagged scallops were visible. To optimise the amount of seabed surveyed, imagery was captured at 1 frame per second (FPS) (usually set at 1 image every 5 seconds) which required modification of an Inon Z240 strobe with an external lithium battery pack to enable imagery to be captured at this faster rate. Of note is that tows were conducted at

Australian Institute of Marine Science

~2.8knots because the vessel could not consistently tow the camera system at slower speeds. This is twice the speed normally used for towed video surveys.

A total of ~19,000 images of the seafloor and associated biota were collected from the tows. To facilitate training of the autoclassification software, DAF undertook a preliminary examination of about half of the images to provide a reference collection of ~100 images containing scallops. The reference collection was then provided to AIMS to train the autoclassification software. The reference images contained predominantly live scallops (~95%) but also included examples of dead individuals (~5%). This preliminary examination indicated that scallops were present in approximately 1% of images.

In the weeks after the reference collection was provided to AIMs, DAF undertook a more comprehensive examination of the full dataset (~19,000 images), recording scallop presence/absence, live/dead status, sediment composition, dominant structural macrobiota and presence/absence of starfish (which may be scallop predators) for each image. Analyses and results of this study, including a comparison of the image-based scallop densities against trawl-based density estimates from the same 11 transects, are provided in the associated FRDC 2017-048 final report.
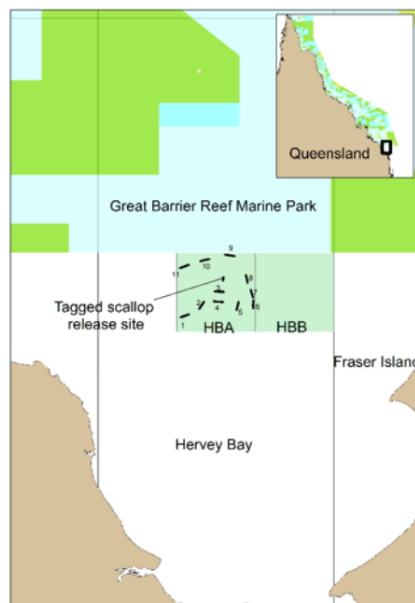
Figure 1 Location of the 11 transects and scallop tag release site where the towed video system was deployed in May 2019. The sites are located inside a scallop management area (HBA) which has been closed to commercial trawling for about three years.

107

3 AUTO-CLASSIFICATION OF SCALLOPS FROM TOWED VIDEO IMAGERY

The BenthoBox system of automation has been designed for use in the detection of corals from underwater imagery, and also designed around the automation of point sampled labels inside images. In the case of corals, we are looking at "stuff" and not "things". Whereas for scallops, we are really looking at "things", and not "stuff". This approach to detection of species lends itself to a style of image labelling and automation called **Object Detection** or **Object Classifiers**, which aims to localise and label multiple objects within an image. This contrasts with coral classification where we use a full image/patch **Classification** method (Figure 2). For these reasons we had to step outside of the standard BenthoBox system and use a more tailored approach to the automated detection of scallops.
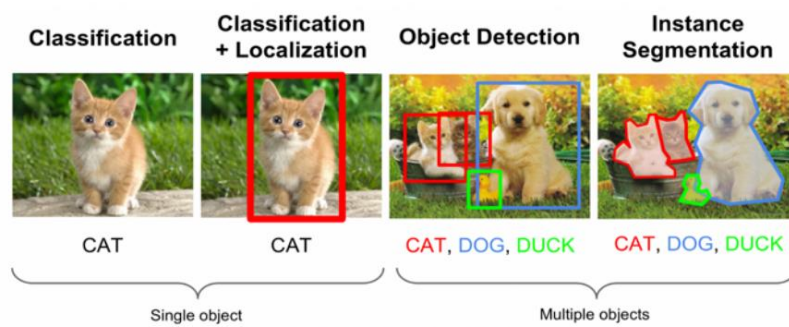
Figure 2 Different methods for automated image classification

3.1 Image Labelling

The images in the reference collection were subsequently processed manually using the VGG image annotator tool (http://www.robots.ox.ac.uk/~vgg/software/via/) whereby each image that contained a scallop was assessed and the scallop was traced with a bounding box and given an associated label (Figures 3 & 4.).

The labelled data was then exported from VGG annotator and modified using the open refine tool (http://openrefine.org/) to create a csv format with the following convention:

```
Image Path, X1, Y1, X2, Y2, Label
```

3

108

Australian Institute of Marine Science

Figure 3 Example of a live scallop labelled using the VGG annotator tool.

Figure 4. Example of a dead scallop labelled using the VGG annotator tool.

3.2 Automation Approach

To trial autoclassification of scallops from the towed video still images we used RetinaNet (https://arxiv.org/abs/1708.02002), a highly accurate one-stage object detection algorithm for detecting objects in images. More specifically we used the keras-retina package which can be found on Github (https://github.com/fizyr/keras-retinanet).

Traditionally in the assessment of a machine learning method we would split the data into a training set and a testing set and validate the accuracy of the method from the training data on an unseen dataset (the testing data). However due to the small number of images containing scallops, these metrics would unlikely represent the application of this method in the field. Hence, rather than determining the accuracy of the method on a known set of images, we tested whether training a model with the small number of images (n=95) would allow us to detect any scallops that may have been missed in the initial preliminary manual observation. Further, it was possible to determine if the model would get confused and start predicting scallops that were not scallops to provide an *indication* if the method had potential for scallop detection given a larger dataset.

3.3 Results

Unsurprisingly, due to the lack of training data for the object detection algorithm, the results of the autoclassification trials were poor. Out of ~19,000 images, the model predicted ~5000 images containing scallops (i.e. ~26%), of which a majority didn't contain any (Figures 4-16). Interestingly, however, even with very little training data the model is picking up on the round shape of the scallop and is picking up on objects in images when they resemble a scallop or scallop shell, suggesting the method could be useful with additional training data. It is noteworthy that the preliminary 'human' examination by DAF found that scallops were present in about ~1% of images.

Australian Institute of Marine Science

Figure 5. Example of an object incorrectly detected as a scallop by the autoclassification method

Figure 6. Example of an object incorrectly detected as a scallop by the autoclassification method

Australian Institute of Marine Science
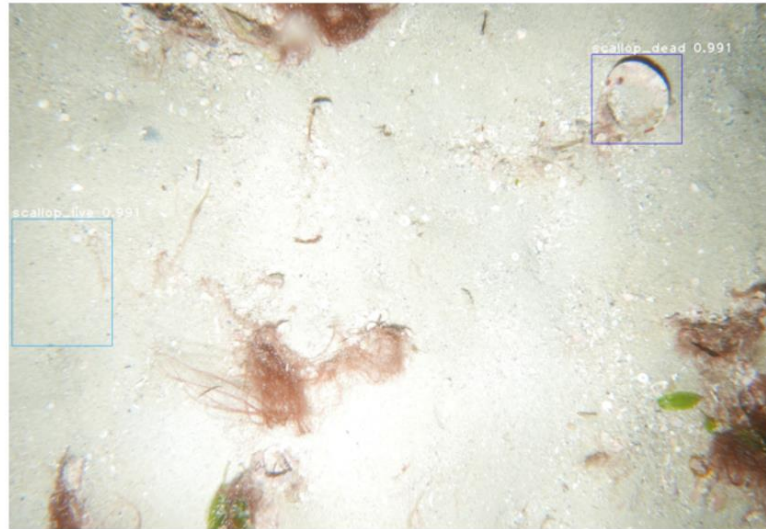
Figure 7. Example of an object incorrectly detected as a scallop by the autoclassification method
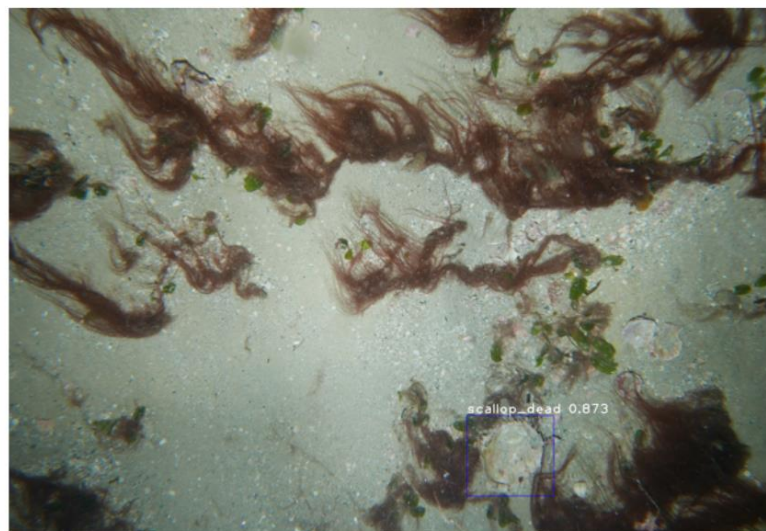
Figure 8. Example of an object incorrectly detected as a scallop by the autoclassification method

7

112

Australian Institute of Marine Science

Figure 9. Example of an object incorrectly detected as a scallop by the autoclassification method

Figure 10. Example of an object incorrectly detected as a scallop by the autoclassification method

Australian Institute of Marine Science
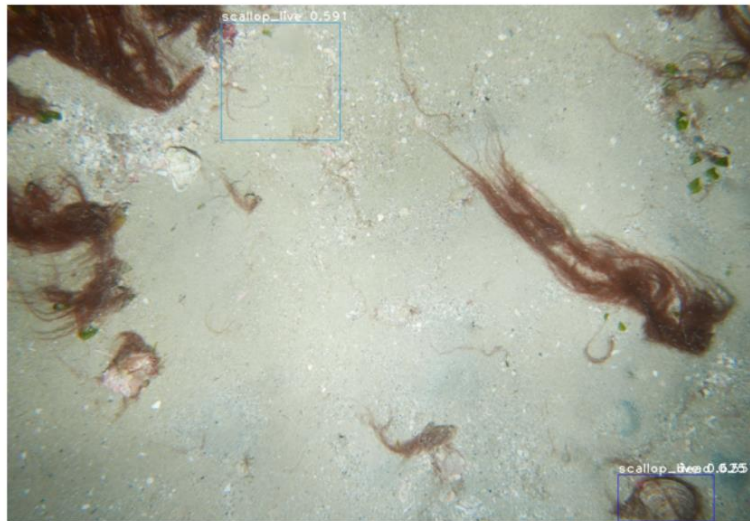
Figure 11. Example of an object incorrectly detected as a scallop by the autoclassification method

Figure 12. Example of an object incorrectly detected as a scallop by the autoclassification method

114

Australian Institute of Marine Science

Figure 13. Example of an object incorrectly detected as a scallop by the autoclassification method

Figure 14. Example where objects were detected by autoclassification, when clearly no scallop exists

Australian Institute of Marine Science

Figure 15. Example where objects were detected by autoclassification, when clearly no scallop exists

Figure 16. Example where objects were detected by autoclassification, when clearly no scallop exists

Australian Institute of Marine Science

Figure 17. Example where objects were detected by autoclassification, when clearly no scallop exists

4 CONCLUSIONS AND RECOMMENDATIONS

The test of the utility of the AIMS towed video and BenthoBox system indicates the approach has potential for generating estimates of scallop densities and abundance indices, although further refinement and testing would be necessary to optimise both the field collection and image classification. If DAF decide to continue to pursue development of this approach, based on the learnings from this trial we would recommend the following.

4.1 Field operations

1. Towed video transects need to be run at speeds no faster than 1.5knots to ensure good coverage of the seabed. At this speed and using a frame rate of 1FPS, full cover imagery would likely be achieved, optimising scallop detection.
2. The use of a modified strobe on the towed video to capture images at 1FPS was largely successful during the trial, although it is not considered a long-term solution to operate at the fast frame rate. The strobe started to struggle and the quality of the images degraded throughout the tows, especially towards the end of the trip. The AIMS deep towed video system uses LED lights powered by an on-board battery and this system where illumination is constant would be better suited to capturing fast frame rate images for scallop stock assessment. A system with multiple strobe lights, such as NOAA's Habcam which has four

Australian Institute of Marine Science

strobes, could also allow greater photographic frequency, although increases the complexity of the system (and associated costs). The Habcam system operates at six images per second.

3. The AIMS deep towed video system uses a large hydraulic winch, and it was not possible to modify this system for trials on the FRV Tom Marshall for this project. If future tests are planned it would be logical to use a vessel capable of running the hydraulic system and towing at slow speeds. The AIMs RV Cape Ferguson would be a feasible option.

4. The towed video has a live-feed forward-facing video which is used to "fly" the system. This footage can also be used for broad habitat classification of the seabed, at it may be worth considering if such information might be useful for the scallop survey in the future. Forward facing video may also provide an alternate way of assessing population density. All video is recorded, and hence post-hoc assessment of its usefulness and potential application would be possible.

5. The towed video is typically flown at 50cm above the seabed. This results in an image size of ~450x350mm which is optimum for providing the detail required for identification of epibiota to reasonable taxonomic resolution (which is what the system has been designed for). Given the low densities of scallops, flying the towed video at a greater height would cover more area and potentially capture more scallops. For example, at 120cm height the image size is increased to ~870x660mm, although this will also result in lower resolution/clarity, especially if water quality is poor. Further testing to optimise height against image and water quality would be important.

6. For application as a scallop survey, it is imperative to be obtain an area size measure for each photographic image. This is because the scallop stock assessment process requires density estimates (i.e. number of scallops per area). Therefore either a scaling system that would enable accurate calculation of image size (refer point 7 below) or, alternately, an altimeter-based system that was capable of maintaining the towed camera off the seafloor at a constant height, and therefore photographing a fixed area size, would be helpful.

7. The capacity to measure scallop size (mm, shell height) is also imperative. To do this accurately from images would require installation of lasers onto the towed video body to provide image size calibration. This would be an achievable modification in the future if it was required, for example we routinely use this approach for measuring fish from BRUVS video footage. The lasers may also be useful for deriving image area size measures.

4.2   Auto-classification of images

1. A larger corpus of scallop images is needed to train the machine learning algorithms for scallop detection. Even though the model for this study was trained on a very small set of images, the results showed potential for utilising this technology in future given a larger training set.

2. As a minimum, given the capacity of the system to detect scallop-like shapes in the images, even an initial screen could be used to reduce the number of images to be scored manually to a more manageable number.

3. In future, given the low number of scallops being detected in images, we could use a n-fold cross validation approach to testing the model accuracy, for example see https://en.wikipedia.org/wiki/Cross-validation_(statistics).

18   Appendix 6. Sediment grainsize analysis from the offshore Gladstone and Hervey Bay regions, southeast Queensland

This section of the report addresses Objective 2) *Undertake exploratory analyses on the relationship between saucer scallop abundance and bottom substrate*

18.1 ABSTRACT

This section of the report described the processing, grainsize distribution and calcium carbonate content of 166 sediment samples acquired from 18 areas located off Gladstone and in Hervey Bay in 2018 and 2019. Overall, the samples were dominated by sand with a highly variable gravel component and less than 5% mud. Fine sand (125–250 µm) was the dominant grainsize fraction. The sediments were similar to those reported previously from near Fraser Island and are thought to have a terrigenous origin and to have been transported by south-easterly winds, waves and longshore currents from southern coastal areas. The data add to existing coastal sediment datasets and were used for modelling sediment distributions and scallop distributions in subsequent sections of the report.

18.2 INTRODUCTION

The spatial distribution of scallop species has rarely been investigated using methods appropriate for the study of biological patterns, mainly because of the inherent problems in the methods for capturing or observing scallops in their natural habitats (Brand 2006). Multibeam sonar echo sounders (MBES) are fast becoming the survey tool of choice in the general field of seafloor habitat mapping, in part due to their ability to simultaneously collect seafloor bathymetry and backscatter information over a wide swath of the seafloor (Hughes-Clarke *et al.* 1996; Brown *et al.* 2011). Acoustic backscatter is a measure of the "seafloor backscatter strength". The backscatter strength has been shown by numerous authors to provide a useful proxy for seabed substrate and backscatter maps can limit the need for prohibitive exhaustive sampling programs and subjective mapping approaches. Acoustic backscatter data are by far the most widely used form of remote sensing data for marine habitat characterisation and mapping, and the majority of studies reported in the scientific literature utilise these data in some way (see Brown *et al.* (2011) for a review). Photos and physical sediment samples are commonly used to ground truth acoustic backscatter datasets. In the Browns Bank region of Canada, Kostylev *et al.* (2003) demonstrated a significant relationship between commercial size scallops and sediment type, by using acoustic backscatter as a proxy of sediment type. Identifying links between bottom type and scallop abundance can improve the estimation of scallop stock size and has been shown to be easily integrated with existing low-resolution proxies for scallop distribution such as fishing effort and oceanographic datasets (Smith *et al.* 2017).

Anecdotal evidence indicates that Queensland saucer scallops (*Y. balloti*) have a preference for substrates that are both soft (to enable the scallops to burrow) and have a high sand content (Welch *et al.* 2014). Existing sediment datasets, however, also demonstrate that substrate composition within the GBRMP can be highly variable and form 'patches' at a scale of tens of meters (Mathews *et al.* 2007). Currently, there is scant information on the relationship between sediment texture and saucer scallop distributions. An improved understanding of scallop habitats and factors influencing their distribution could help explain their patchy distribution and lead to improved assessment and management, including planning of reseeding/restocking areas, developing marine protected areas, and reducing impact on the seabed (Kostylev *et al.* 2003).

The Queensland saucer scallop fishery extends from approximately Noosa in the south at approximately 26º30' S to Yeppoon in the north at approximately 22º50' S (Figure 18-1). Within the fishery, areas of relatively high scallop productivity (known as scallop replenishment areas, SRAs) have been rotationally opened and closed to fishing to aid management of the stock (Jebreen *et al.* 2008). The fishery is located on the continental shelf with scallops typically occurring in depths between 20 and 60 m. There have been several marine sediment sampling surveys throughout

southeast Queensland, with the most extensive of these including Maxwell and Maiklem (1964), Marshall (1977, 1980) and Davies and Tsuji (1992) (Figure 18-1). The continental shelf of southeast Queensland is dominated by sand, however, the region's proximity to major river systems, such as the Fitzroy River, the Capricorn-Bunker Group, and deep water environments from the adjacent Capricorn Channel creates a region with spatially complex distributions of sediments (Marshall 1977). To assess the relationships between scallops and seabed texture, co-located sediment, trawl and acoustic data are required.

This section of the report presents an analysis of a recently acquired sediment dataset obtained from offshore of Gladstone and Hervey Bay and compares the sediment properties with those of existing sediment studies from southeast Queensland. The sediment samples were obtained with co-located measures of scallop abundance by trawl sampling and acoustic backscatter and investigations on the relationships between the sediments, acoustic backscatter and scallops are provided in section 19, page 139. Modelling sediment distributions is provided in section 20, page 157 and the predictive modelling of scallop distributions which utilises all of the available sediment data and sediment modelling is provided in section 21, page 202.

18.3 METHODS

18.3.1 Study area and sediment sampling

Sediment samples were obtained from 18 areas located offshore from Gladstone and in Hervey Bay within the fishery (Figures 18-1 and 18-2) on board the *RV Tom Marshall* over four cruises. The offshore Gladstone area was sampled in June and August of 2018 and Hervey Bay was sampled in June and July 2019. Sampling in both locations occurred during the winter seasonal closure of the saucer scallop fishery.

Six small survey areas were sampled from the Gladstone region in depths of 10–49 m and 12 areas in Hervey Bay were sampled in depths of 11–52 m (Figure 18-2). The location and depth of each sample are provided in Table 18-3. The 18 areas were targeted to provide a range of different scallop habitats (high, medium, and low productivity) based on advice from the Department of Agriculture and Fisheries (DAF) and the level of fishing activity in the area (see Table 19-1 and Table 19-2, page 143 for details). Between four and 16 sediment samples were obtained in each area resulting in a total of 166 sediment samples. Acoustic mapping within the 18 study areas identified areas of acoustically homogenous seabed that were then trawled and sampled. Two sediment samples were collected per trawl: one at the start and end of each trawl. Sediment samples were collected using a 2 L Van Veen sediment grab. GPS coordinates were taken with each sediment sample.
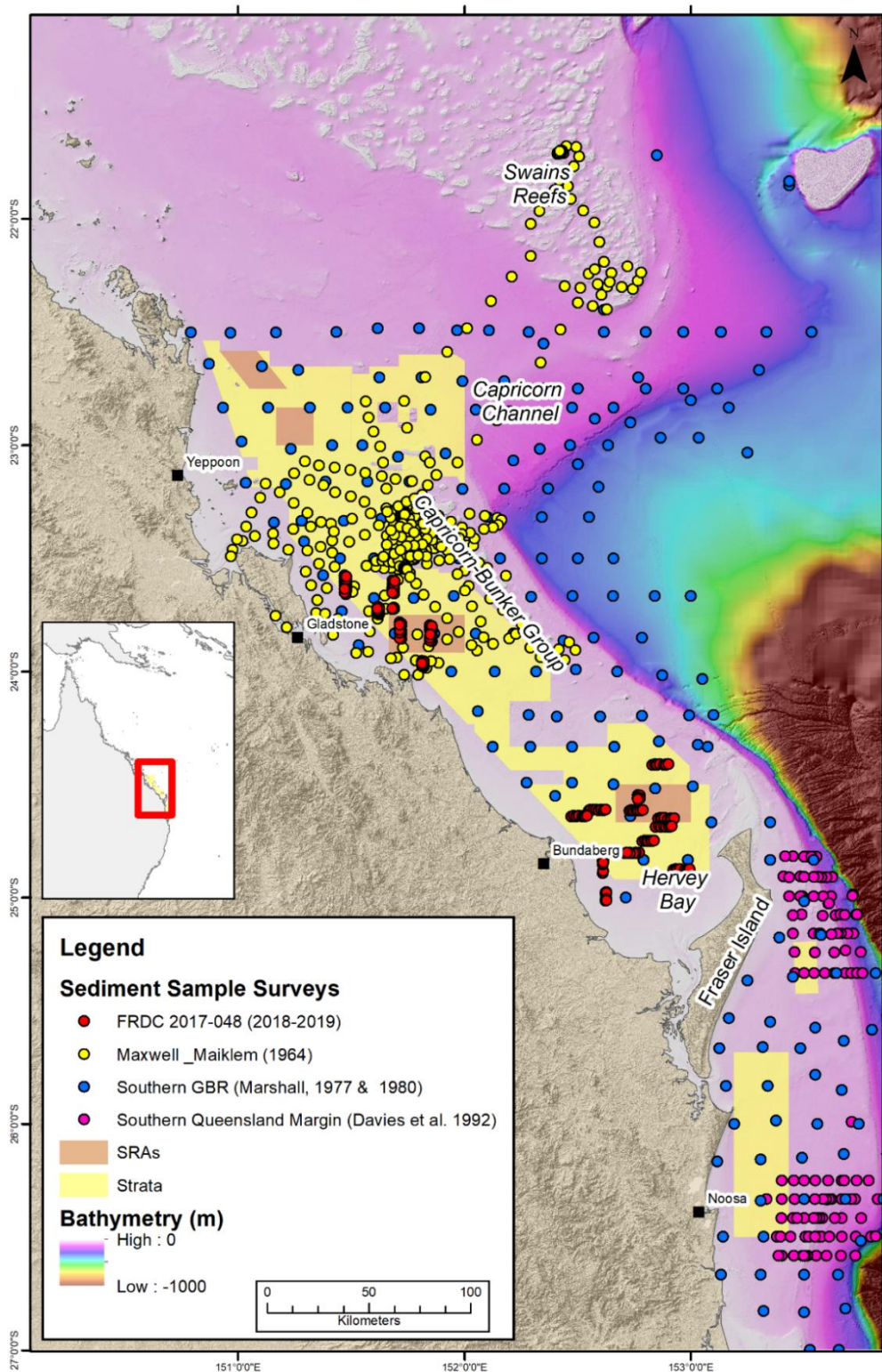
Figure 18-1. Regional map of southeast Queensland showing the location of historic sediment sampling surveys by Maxwell and Maiklem (1964), Marshall (1977, 1980) and Davies and Tsuji (1992). Also shown are the locations for the 166 sediment samples from the current FRDC 2017-048 study, the scallop fishery SRAs and scallop survey sampling strata.
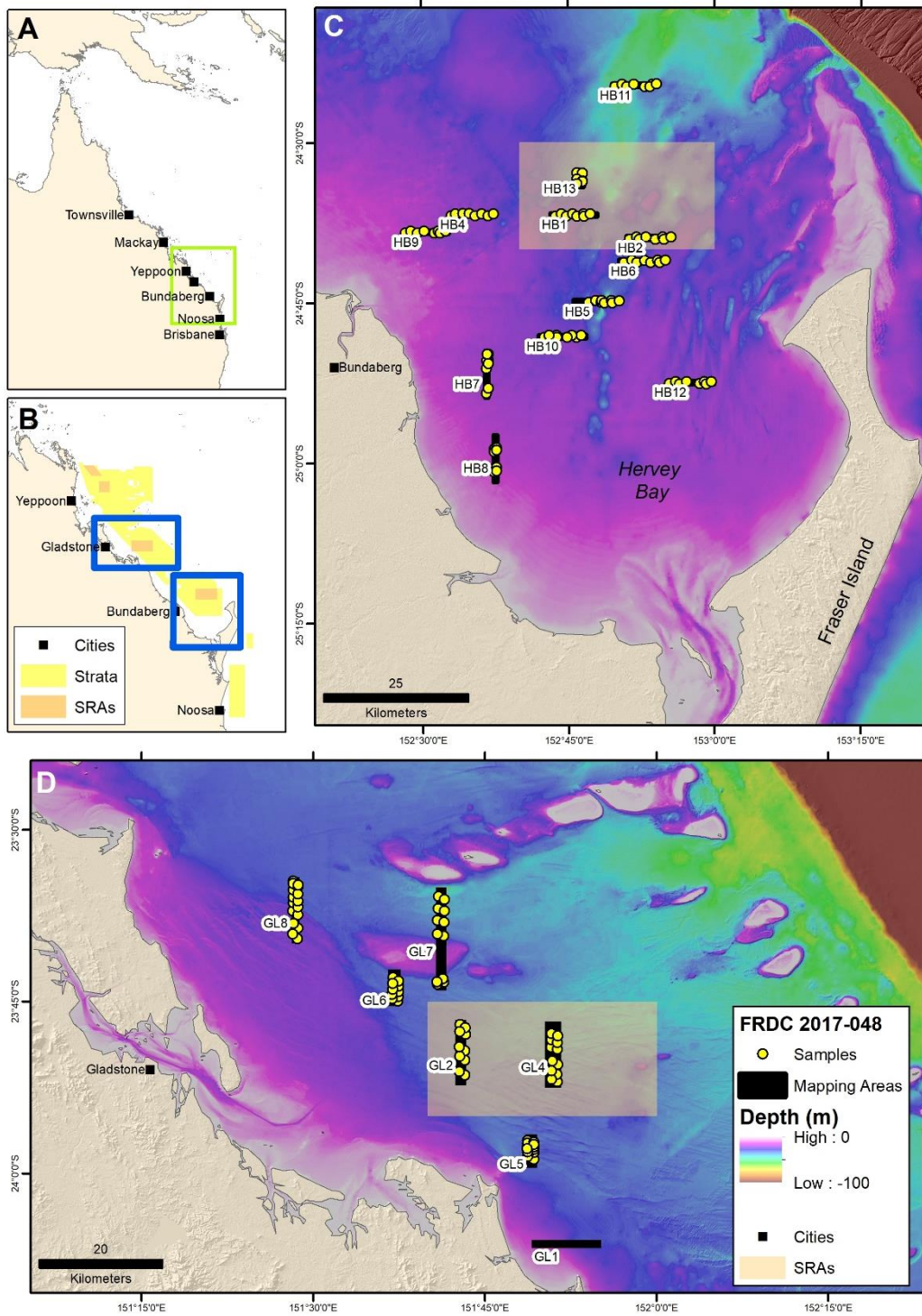
Figure 18-2. The sediment sample locations in the 18 areas in Hervey Bay (2019) and offshore from Gladstone (2018).

.

18.3.2 Grainsize analysis

A sediment grainsize analysis was performed on all 166 sediment samples. A process of wet sieving and dry sieving was used to accurately measure the sand (63 to 2000 µm) and gravel (2000 to 64,000 µm) components of the sediment at 1 Phi intervals and the quantity of mud (< 63 µm) (Folk 1980). Further analysis of the mud required to quantify the amount of silt (4 to 63 µm) and clay (< 4 µm) components was not undertaken as it was only a minor component of sediments in the region (Maxwell and Maiklem 1964; Marshall 1977, 1980)

18.3.3 Sample pre-treatment

Initially, all samples were treated with 5% Calgon solution to disaggregate the mud within the sediment. Approximately 100 g of sample was transferred into a 500 ml beaker and then 100 ml Calgon was added. The sample was then stirred to aid the breakdown and left to disaggregate for 1 to 2 hr.

18.3.4 Wet sieving

The sediment sample was then washed through a 63 µm sieve using deionised water to separate the mud (clay and silt) from the sand and gravel. Washing continued until all the mud had been removed from the sample. The volume of mud sample was recorded, stirred for 30 seconds and then subsampled (50 ml) three times. The three sub samples were transferred to beakers and dried overnight in an oven. Based on the weight of the dry sample the volume of mud was calculated. The median of the three replicate measures was used as the final estimate of mud in the sample.

18.3.5 Dry sieving

The beaker containing the sand and the gravel was transferred to an oven and dried overnight at 80 to 100ºC for 24 to 48 hr. Sieves were stacked together in ascending sieve size on a sieve shaker. A base pan was used to collect sediment passing through the 63 µm sieve. Above the base pan, and in increasing sieve diameters, were 63, 125, 250, 500, 1000, 2000, 4000, 8000 and 16,000 µm sieves. The sand/gravel fraction was poured into the top of the sieve. The shaker lid was placed on the top sieve and secured with clamps. The samples were shaken for 15 minutes at an amplitude setting of 60 to pass the grains through each sieve consequently capturing the fractions in the relevant sieve size.

18.3.6 Sample post processing

Once the sieve was finished each grainsize fraction was weighed to give a histogram of sediment grainsize fraction for each sample. The sediment/sieve grainsize (µm) fractions were assigned size terms and Phi scales based on Wentworth (1922) (Table 18-1). Sediment data were then summarised through the G2sd package in Rstudio (Fournier *et al.* 2014) to provide measurement of geometric mean, geometric standard deviation, skewness and Folk sediment sample classifications.

Table 18-1. Sediment size terms, grainsizes and their Phi conversions based on Wentworth (1922).

	Size Terms	Grainsize (µm)	Phi
Gravel	Very Coarse Gravel (VCG)	32,000–64,000	–5
	Coarse Gravel (CG)	16,000–32,000	–4
	Medium Gravel (MG)	8000–16,000	–3
	Fine Gravel (FG)	4000–8000	–2
	Very Fine Gravel (VFG)	2000–4000	–1
Sand	Very Coarse Sand (VCS)	1000–2000	0
	Coarse Sand (CS)	500–1000	1
	Medium Sand (MS)	250–500	2
	Fine Sand (FS)	125–250	3
	Very Fine Sand (VFS)	63–125	4
Clay and Silt	Mud	< 63	> 4

18.3.7 Percentage carbonate analysis

Most marine sediments contain some 'shelly' material. This material is composed of calcium carbonate ($CaCO_3$) and will react with strong acid. However, most other common rock forming minerals such as quartz, feldspar, mica, etc. do not react with acid. As a result, if sediment samples are dry (i.e., containing no water) acid can be used to dissolve the shelly material and the difference in dry weight (before and after) can be used to provide a measure of the amount of shelly material in the sediment. This was used to provide an estimate of the relative amounts of terrigenous (land-derived) and biological (shelly) material in each sample.

Approximately 10 g of sample was spooned into a beaker and dried for 24 hr in an oven at 80 to 100ºC. The dry sample was then broken up using a spatula and its weight recorded. 10% hydrochloric acid was slowly added to each sample to avoid a violent reaction. The sample was left overnight to ensure the reaction was complete. Once the reaction was complete, the sample was rinsed and decanted three times with deionised water to remove the HCl from the sample. The sample was again dried overnight, reweighed and the percentage of carbonate calculated.

18.3.8 Comparison with other studies

There have been numerous localized studies of sediment distributions within the Great Barrier Reef and are included in Mathews *et al.* (2007). In southeast Queensland, the most expansive sediment sample surveys are by Maxwell and Maiklem (1964), Marshall (1977, 1980) and Davies and Tsuji (1992) (Table 18-2). These surveys provide the percentage of gravel, sand, mud and carbonate in the sediment samples and can therefore be used as a comparison with samples acquired under the current FRDC project.

Table 18-2. Datasets for comparative grainsize analysis.

Location	Number of samples	Reference
Southeast Queensland, Swains Reefs, Capricorn Channel, and Capricorn-Bunker reefs	336	Maxwell and Maiklem (1964)
Southeast Queensland, Capricorn Channel, Capricorn-Bunker reefs, offshore Fraser Island	202	Marshall (1977, 1980)
Offshore of Fraser Island and areas further south	195	Davies and Tsuji (1992)

18.4 RESULTS AND DISCUSSION

18.4.1 Grainsize histograms

Details of the location, depth (m) and composition for each of the 166 sediment samples are provided as supplementary material in Table 18-3. The grainsize fractions and geometric mean grainsize for each sample are provided in Table 18-4.

Sediments were split into 11 grainsize fractions based on the size classes defined by Wentworth (1922). The sediment fraction that was finer than 63 μm was not analyzed further and classed as mud. The sediment grainsize fractions with the highest frequencies were medium sand (250–500 μm) and fine sand (125–250 μm) (Figure 18-3). These were also the most common fractions in samples obtained from Fraser Island (Grimes 1991) and indicate that sediments from these locations (i.e., Hervey Bay, offshore from Gladstone and Fraser Island) were sourced from terrigenous material. Boyd *et al.* (2004) suggested that the sediments are likely sourced from the south and transported by the prevailing south-easterly winds, waves and longshore currents. The average histogram for all the

samples (Figure 18-3, shown in red) indicated that approximately 85% of the sediments are sand (i.e., ranging in size 63–2000 μm), 10% are gravel (> 2000 μm) and less than 5% mud. The low mud content is considered to be a function of distance (generally tens of kilometers) from modern sources of mud, such as rivers.
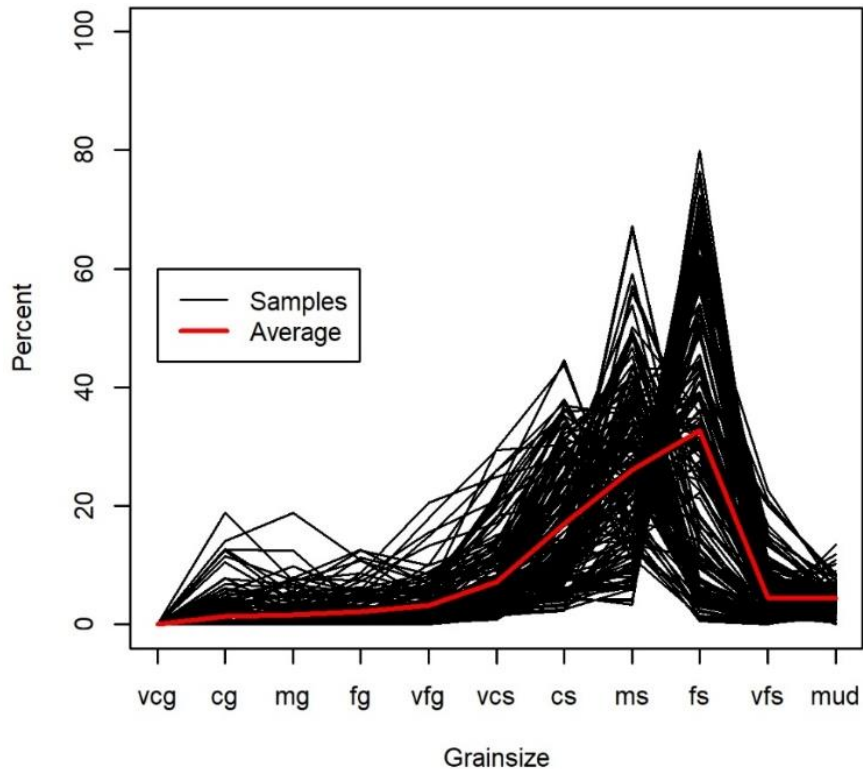
Figure 18-3. Histograms of the 166 sediment grainsize fractions based on the classification scheme of Table 18-1 and Wentworth (1922).

18.4.2 Folk classification

The samples were classified using the method of Folk (1954) based on relative percentages of gravel, sand and mud (Figure 18-4). Samples were found to be dominantly Slightly Gravely Sand (91) and Gravelly Sand (62) with amounts of Sandy Gravel (8), Gravelly Muddy Sand (3) and Slightly Gravelly Muddy Sand (2) (Figure 18-4).
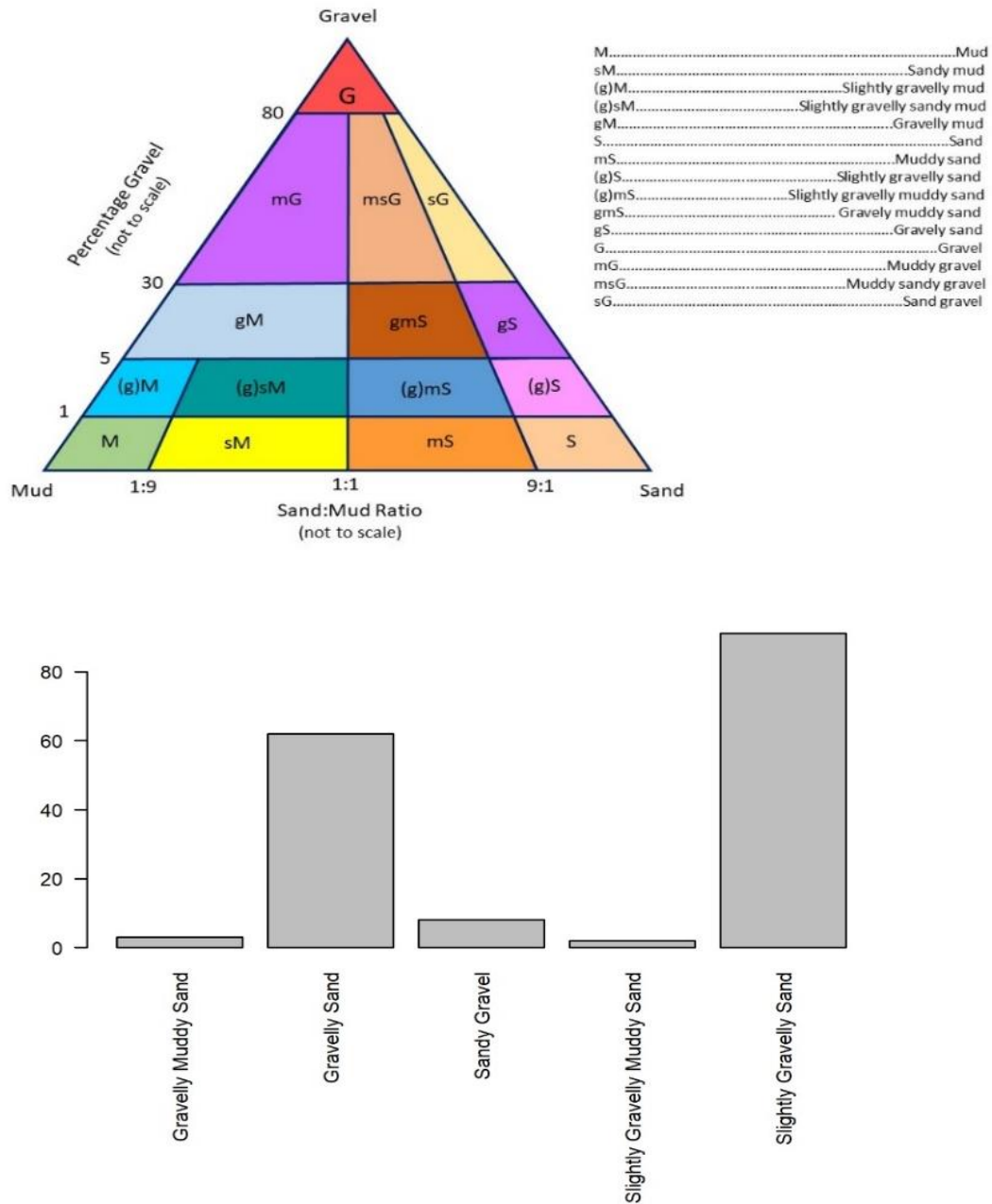
Figure 18-4. Classification of sediment samples based on relative percentages of gravel sand and mud, based on Folk (1954).

18.4.3 Ternary plots

The 166 sediment samples were compared to the samples of Maxwell and Maiklem (1964), Marshall (1977, 1980), and Davies and Tsuji (1992) (Figure 18-5). Samples from the project were dominated by sand (greater than 60% in all but one sample and averaging 87%). Mud was a minor component (maximum of 13%) while gravel was commonly also a minor component but reached a maximum of 48%. Sediments from all four surveys were dominated by sand, with lower proportions of gravel. The Southern Queensland Margin survey of Davies and Tsuji (1992) showed sediments were predominantly sand with gravel and a minor component of mud and are therefore very similar to the new samples analysed herein. Sediments from the southern Great Barrier Reef surveys of Marshall (1977, 1980) had a similar high content of sand/gravel, however, many samples also had high contents of mud and sand, reflecting the relatively deep locations (> 100 m) that were sampled. None of the

sediment samples obtained by Maxwell and Maiklem (1964) had mud content exceeding 5%. This is likely a result of their survey focussing on reefal environments around the Capricorn-Bunker and Swains reefs.
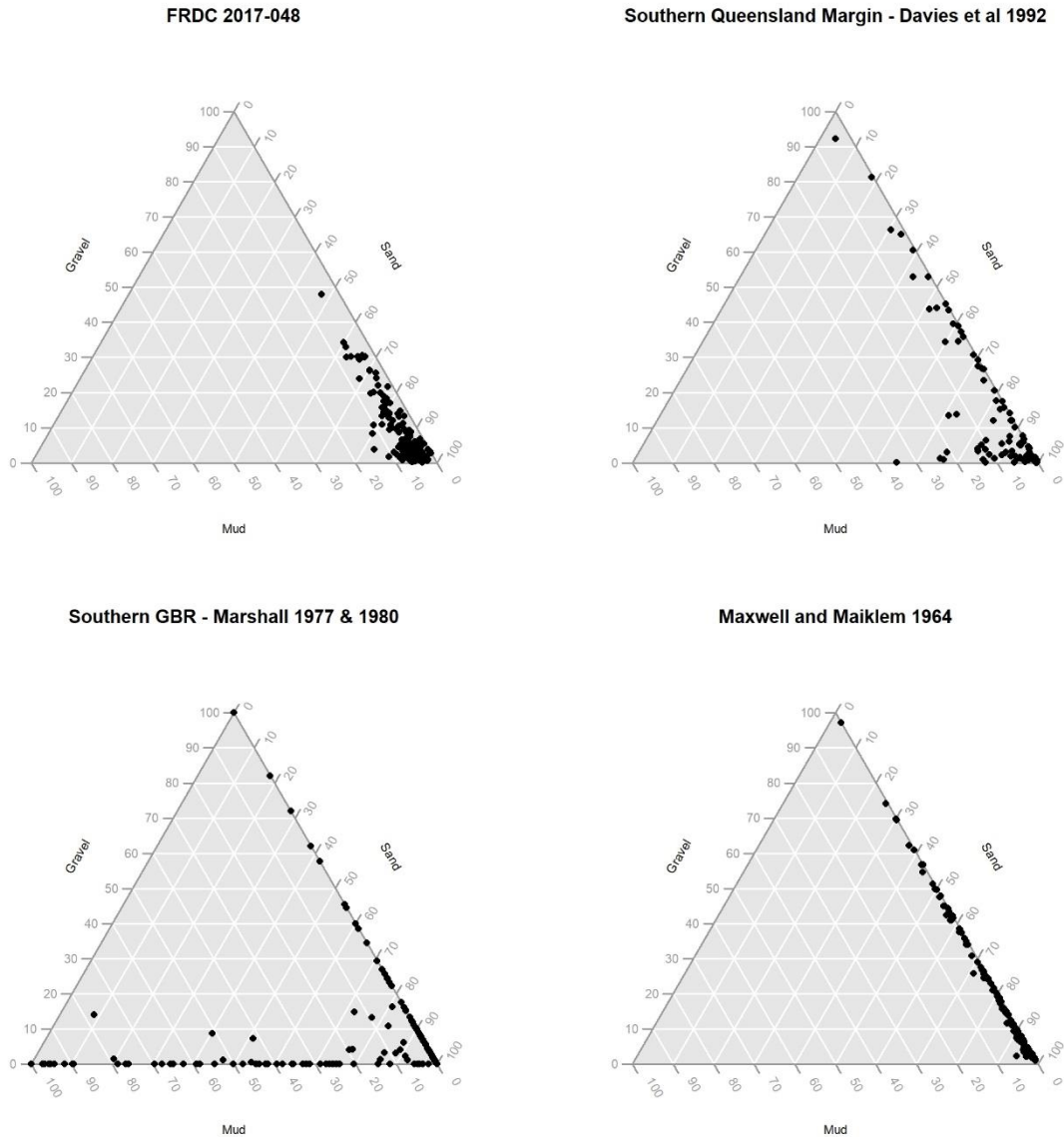
Figure 18-5. Classification of sediment samples based on relative percentages of gravel, sand and mud, based on Folk (1954) for the current FRDC project, Davies and Tsuji (1992), Marshall (1977, 1980) and Maxwell and Maiklem (1964).

18.4.4 Percent carbonate

All surveys contained samples with carbonate content ranging from low (0–10%) to high (90–100%) (Figure 18-6). A relatively high proportion of the sediments processed herein had low carbonate content of 10–30%, suggesting that they were dominated by terrigenous, land-based sources. The sediments sampled by Marshall (1977, 1980) and Davies and Tsuji (1992) generally had higher carbonate content than the sediments acquired in the current study reflecting environments with a stronger reefal influence. However, they also included a significant number of samples with low range carbonate content, suggesting a terrigenous source. A high proportion of the samples from Maxwell and Maiklem (1964) had high carbonate content (i.e., 90–100%) reflecting the survey's focus on coral reef environments.
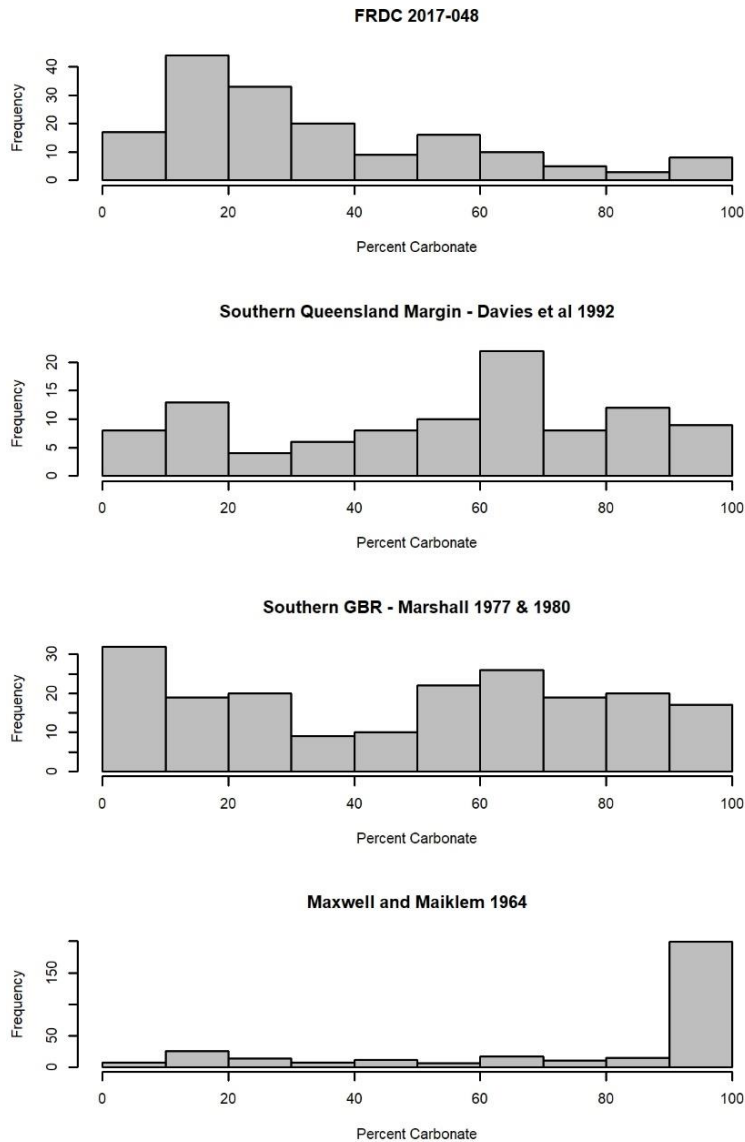
Figure 18-6. Histograms of sediment sample carbonate content for the current FRDC project, Davies and Tsuji (1992), Marshall (1977, 1980) and Maxwell and Maiklem (1964).

In conclusion, the sediments acquired from 166 locations offshore from Gladstone and in Hervey Bay in 2018 and 2019 were dominated by sand with a highly variable gravel component and low (<5%) mud content, similar to the sediments sampled by Davies and Tsuji (1992). The low mud content is consistent with sediments located at a significant distance from modern river systems. The sediments contained a wide range of calcium carbonate content, but sediments with low carbonate (10–30%) were the most common. The most common sediment grain size was fine sand (i.e., 125–250 µm) which is similar to sediments located near Fraser Island and is thought to be the result of transportation by waves and longshore currents of terrigenous material from further south (Boyd *et al.* 2004).

The samples were co-located with acoustic data and scallop trawl samples and used in the following sections of the report to examine the relationship between scallop abundance and seabed composition (section 19, page 139) and to model the regional distribution of sediments (section 20, page 157) and scallops (section 21, page 202).

18.5 SUPPLEMENTARY DATA

Table 18-3. Location and percentage of carbonate, gravel, sand and mud for 166 samples.

ID	Grab	Trawl	Longitude	Latitude	Bathy	Percent Carbonate	Percent Gravel	Percent Sand	Percent Mud
1	GLAD_AREA2_GR1	GLAD_AREA2_TR1	151.85553	-23.86695	-27.5	24.5	6.7	92.4	0.8
2	GLAD_AREA2_GR10	GLAD_AREA2_TR4	151.84626	-23.81666	-34.4	42.8	5.5	90.7	3.8
3	GLAD_AREA2_GR11	GLAD_AREA2_TR5	151.84653	-23.80584	-34.5	78.6	30.0	62.7	7.3
4	GLAD_AREA2_GR12	GLAD_AREA2_TR6	151.84680	-23.79652	-35.6	57.6	6.2	92.7	1.0
5	GLAD_AREA2_GR2	GLAD_AREA2_TR2	151.85483	-23.85598	-30.3	34.3	5.5	94.1	0.4
6	GLAD_AREA2_GR3	GLAD_AREA2_TR3	151.85605	-23.84141	-31.9	33.8	2.7	97.1	0.2
7	GLAD_AREA2_GR4	GLAD_AREA2_TR4	151.85540	-23.81959	-34.0	43.0	14.8	83.5	1.6
8	GLAD_AREA2_GR5	GLAD_AREA2_TR5	151.85534	-23.80977	-33.5	62.4	29.7	66.4	3.9
9	GLAD_AREA2_GR6	GLAD_AREA2_TR6	151.85566	-23.79976	-33.9	59.9	5.1	88.5	6.4
10	GLAD_AREA2_GR7	GLAD_AREA2_TR1	151.84653	-23.86324	-32.0	30.3	4.4	93.8	1.8
11	GLAD_AREA2_GR8	GLAD_AREA2_TR2	151.84694	-23.85064	-31.8	38.2	3.9	92.1	4.1
12	GLAD_AREA2_GR9	GLAD_AREA2_TR3	151.84790	-23.83639	-33.1	33.1	5.3	89.9	4.8
13	GLAD_AREA4_GR1	GLAD_AREA4_TR1	151.72081	-23.85695	-30.3	20.8	2.5	94.9	2.6
14	GLAD_AREA4_GR10	GLAD_AREA4_TR5	151.71370	-23.78320	-30.0	62.6	13.3	80.0	6.8
15	GLAD_AREA4_GR2	GLAD_AREA4_TR2	151.72089	-23.83504	-31.2	27.6	2.4	96.8	0.8
16	GLAD_AREA4_GR3	GLAD_AREA4_TR3	151.72081	-23.82138	-31.0	36.6	4.5	93.8	1.7
17	GLAD_AREA4_GR4	GLAD_AREA4_TR4	151.72161	-23.79780	-30.8	35.7	1.6	94.9	3.4
18	GLAD_AREA4_GR5	GLAD_AREA4_TR5	151.72129	-23.78787	-30.8	64.4	26.3	70.3	3.4
19	GLAD_AREA4_GR6	GLAD_AREA4_TR1	151.71273	-23.85214	-30.1	19.5	3.9	95.9	0.2
20	GLAD_AREA4_GR7	GLAD_AREA4_TR2	151.71315	-23.82948	-30.7	29.2	6.0	91.6	2.4
21	GLAD_AREA4_GR8	GLAD_AREA4_TR3	151.71287	-23.81566	-31.3	32.7	2.8	93.7	3.5
22	GLAD_AREA4_GR9	GLAD_AREA4_TR4	151.71301	-23.79383	-29.9	52.2	3.2	96.8	0.0
23	GLAD_AREA5_GR1	GLAD_AREA5_TR1	151.82120	-23.97947	-30.6	11.2	1.4	90.3	8.3
24	GLAD_AREA5_GR10	GLAD_AREA5_TR4	151.81211	-23.95902	-29.4	19.5	8.3	80.0	11.7
25	GLAD_AREA5_GR11	GLAD_AREA5_TR5	151.81191	-23.95215	-30.5	12.4	2.6	93.9	3.5
26	GLAD_AREA5_GR12	GLAD_AREA5_TR6	151.81184	-23.95626	-26.9	11.3	9.9	84.0	6.2
27	GLAD_AREA5_GR2	GLAD_AREA5_TR2	151.82157	-23.96965	-26.3	8.6	8.7	86.4	4.9
28	GLAD_AREA5_GR3	GLAD_AREA5_TR3	151.82091	-23.96567	-28.8	9.1	3.0	88.0	9.0
29	GLAD_AREA5_GR4	GLAD_AREA5_TR4	151.82157	-23.96169	-30.6	14.2	10.7	79.1	10.2
30	GLAD_AREA5_GR5	GLAD_AREA5_TR5	151.82120	-23.95468	-30.9	13.6	4.4	92.1	3.5
31	GLAD_AREA5_GR6	GLAD_AREA5_TR6	151.82135	-23.95792	-27.5	13.5	9.6	87.2	3.2
32	GLAD_AREA5_GR7	GLAD_AREA5_TR1	151.81218	-23.97593	-29.4	16.8	2.4	91.2	6.5
33	GLAD_AREA5_GR8	GLAD_AREA5_TR2	151.81184	-23.96912	-27.6	7.5	12.0	83.2	4.8
34	GLAD_AREA5_GR9	GLAD_AREA5_TR3	151.81137	-23.96400	-27.5	10.4	3.8	82.7	13.5
35	GLAD_AREA6_GR1	GLAD_AREA6_TR1	151.62315	-23.74906	-27.8	60.4	48.0	47.7	4.4
36	GLAD_AREA6_GR10	GLAD_AREA6_TR5	151.61633	-23.71465	-31.1	66.8	26.2	70.3	3.5

ID	Grab	Trawl	Longitude	Latitude	Bathy	Percent Carbonate	Percent Gravel	Percent Sand	Percent Mud
37	GLAD_AREA6_GR2	GLAD_AREA6_TR2	151.62353	-23.74273	-29.7	49.7	14.2	81.3	4.5
38	GLAD_AREA6_GR3	GLAD_AREA6_TR3	151.62449	-23.73572	-29.9	59.4	19.7	73.8	6.4
39	GLAD_AREA6_GR4	GLAD_AREA6_TR4	151.62411	-23.72757	-31.5	72.2	25.6	72.2	2.2
40	GLAD_AREA6_GR5	GLAD_AREA6_TR5	151.62440	-23.71980	-30.7	60.1	20.0	74.4	5.5
41	GLAD_AREA6_GR6	GLAD_AREA6_TR1	151.61480	-23.74564	-27.9	47.1	30.2	63.8	6.0
42	GLAD_AREA6_GR7	GLAD_AREA6_TR2	151.61475	-23.73933	-29.5	53.6	14.8	80.3	4.9
43	GLAD_AREA6_GR8	GLAD_AREA6_TR3	151.61571	-23.73181	-29.7	75.1	33.0	61.1	5.9
44	GLAD_AREA6_GR9	GLAD_AREA6_TR4	151.61554	-23.72332	-30.4	59.1	19.0	77.5	3.5
45	GLAD_AREA7_GR1	GLAD_AREA7_TR1	151.69004	-23.72202	-30.0	59.8	17.5	78.2	4.3
46	GLAD_AREA7_GR10	GLAD_AREA7_TR4	151.68089	-23.63156	-33.4	95.2	14.4	79.8	5.8
47	GLAD_AREA7_GR11	GLAD_AREA7_TR5	151.68189	-23.61423	-36.0	96.3	18.3	78.5	3.2
48	GLAD_AREA7_GR12	GLAD_AREA7_TR6	151.68231	-23.59703	-37.3	94.6	19.9	76.3	3.9
49	GLAD_AREA7_GR2	GLAD_AREA7_TR2	151.68873	-23.71677	-30.2	62.9	10.9	81.1	8.0
50	GLAD_AREA7_GR3	GLAD_AREA7_TR3	151.68974	-23.65467	-28.3	97.2	7.9	89.4	2.7
51	GLAD_AREA7_GR4	GLAD_AREA7_TR4	151.69022	-23.63439	-32.9	93.4	10.4	85.3	4.3
52	GLAD_AREA7_GR5	GLAD_AREA7_TR5	151.69070	-23.61805	-36.3	94.4	17.0	79.3	3.7
53	GLAD_AREA7_GR6	GLAD_AREA7_TR6	151.69118	-23.60111	-35.5	95.4	13.1	84.1	2.8
54	GLAD_AREA7_GR7	GLAD_AREA7_TR1	151.68068	-23.72437	-31.0	61.8	17.0	80.1	3.0
55	GLAD_AREA7_GR8	GLAD_AREA7_TR2	151.68018	-23.72117	-31.7	58.3	9.5	83.5	6.9
56	GLAD_AREA7_GR9	GLAD_AREA7_TR3	151.68068	-23.65139	-30.1	98.8	14.0	80.8	5.2
57	GLAD_AREA8_GR1	GLAD_AREA8_TR1	151.47705	-23.65815	-20.5	21.0	0.5	94.4	5.1
58	GLAD_AREA8_GR10	GLAD_AREA8_TR3	151.47025	-23.61814	-22.6	32.3	0.3	96.2	3.5
59	GLAD_AREA8_GR11	GLAD_AREA8_TR4	151.47053	-23.60609	-26.6	51.2	1.6	94.3	4.1
60	GLAD_AREA8_GR12	GLAD_AREA8_TR5	151.47075	-23.59800	-26.6	47.3	7.4	89.6	2.9
61	GLAD_AREA8_GR13	GLAD_AREA8_TR6	151.47087	-23.58701	-28.1	72.2	1.5	93.9	4.6
62	GLAD_AREA8_GR14	GLAD_AREA8_TR7	151.47081	-23.57451	-27.8	84.5	15.8	78.6	5.6
63	GLAD_AREA8_GR15	GLAD_AREA8_TR8	151.47740	-23.58281	-28.4	81.3	5.0	88.6	6.4
64	GLAD_AREA8_GR16	GLAD_AREA8_TR8	151.47097	-23.57809	-28.8	79.1	6.5	88.5	5.0
65	GLAD_AREA8_GR2	GLAD_AREA8_TR2	151.47751	-23.64283	-22.7	56.5	30.3	65.4	4.3
66	GLAD_AREA8_GR3	GLAD_AREA8_TR3	151.47751	-23.62383	-22.7	46.1	7.4	89.1	3.5
67	GLAD_AREA8_GR4	GLAD_AREA8_TR4	151.47782	-23.61203	-27.6	60.2	2.5	90.5	7.0
68	GLAD_AREA8_GR5	GLAD_AREA8_TR5	151.47782	-23.60375	-27.2	50.9	16.0	79.0	5.0
69	GLAD_AREA8_GR6	GLAD_AREA8_TR6	151.47782	-23.59318	-28.3	69.2	3.3	91.4	5.3
70	GLAD_AREA8_GR7	GLAD_AREA8_TR7	151.47828	-23.58031	-28.8	84.3	4.2	90.6	5.2
71	GLAD_AREA8_GR8	GLAD_AREA8_TR1	151.47025	-23.65168	-21.1	19.9	3.1	92.3	4.5
72	GLAD_AREA8_GR9	GLAD_AREA8_TR2	151.47142	-23.63589	-22.5	38.9	4.3	92.4	3.4
73	HB_AREA1_GR1	HB_AREA1_TR1	152.72836	-24.61522	-25.8	29.4	4.3	93.0	2.6
74	HB_AREA1_GR2	HB_AREA1_TR1	152.73828	-24.61171	-26.6	19.4	2.8	93.2	4.0

ID	Grab	Trawl	Longitude	Latitude	Bathy	Percent Carbonate	Percent Gravel	Percent Sand	Percent Mud
75	HB_AREA1_GR3	HB_AREA1_TR2	152.74726	-24.61554	-26.8	41.4	1.0	97.2	1.8
76	HB_AREA1_GR4	HB_AREA1_TR2	152.75750	-24.61177	-29.5	58.2	8.7	88.1	3.2
77	HB_AREA1_GR5	HB_AREA1_TR3	152.76504	-24.61535	-23.9	8.2	1.0	97.3	1.7
78	HB_AREA1_GR6	HB_AREA1_TR3	152.77634	-24.61177	-24.8	10.3	1.4	96.9	1.8
79	HB_AREA1_GR7	HB_AREA1_TR4	152.77728	-24.61548	-25.7	13.0	1.6	94.9	3.4
80	HB_AREA1_GR8	HB_AREA1_TR4	152.78808	-24.61171	-26.5	51.3	9.3	88.6	2.2
81	HB_AREA10_GR1	HB_AREA10_TR1	152.76429	-24.80466	-20.4	18.9	2.0	93.5	4.5
82	HB_AREA10_GR2	HB_AREA10_TR1	152.77183	-24.80139	-22.1	30.7	4.5	90.8	4.7
83	HB_AREA10_GR3	HB_AREA10_TR2	152.75625	-24.80128	-26.6	36.1	4.1	91.0	4.9
84	HB_AREA10_GR4	HB_AREA10_TR2	152.74826	-24.80466	-25.9	30.0	1.8	92.9	5.3
85	HB_AREA10_GR5	HB_AREA10_TR3	152.72990	-24.80110	-29.0	57.1	3.5	89.8	6.7
86	HB_AREA10_GR6	HB_AREA10_TR3	152.73080	-24.80450	-27.9	50.9	2.3	92.5	5.1
87	HB_AREA10_GR7	HB_AREA10_TR4	152.70927	-24.80455	-23.2	24.9	2.2	93.6	4.1
88	HB_AREA10_GR8	HB_AREA10_TR4	152.71732	-24.80123	-24.0	30.1	2.0	93.6	4.4
89	HB_AREA11_GR1	HB_AREA11_TR1	152.83044	-24.41331	-46.0	14.3	6.3	89.2	4.6
90	HB_AREA11_GR2	HB_AREA11_TR1	152.84260	-24.40961	-48.9	25.7	5.2	90.2	4.6
91	HB_AREA11_GR3	HB_AREA11_TR2	152.85041	-24.41325	-48.3	14.7	7.7	89.2	3.0
92	HB_AREA11_GR4	HB_AREA11_TR2	152.86233	-24.40967	-46.1	6.9	1.2	96.2	2.6
93	HB_AREA11_GR5	HB_AREA11_TR3	152.88100	-24.41337	-36.7	3.8	0.6	97.5	2.0
94	HB_AREA11_GR6	HB_AREA11_TR3	152.89340	-24.40949	-34.5	4.9	1.0	95.4	3.6
95	HB_AREA11_GR7	HB_AREA11_TR4	152.89000	-24.41325	-34.2	3.8	0.5	96.0	3.4
96	HB_AREA11_GR8	HB_AREA11_TR4	152.90103	-24.40931	-33.8	5.3	2.9	93.6	3.5
97	HB_AREA12_GR1	HB_AREA12_TR1	152.92262	-24.87698	-19.9	20.1	1.6	94.2	4.2
98	HB_AREA12_GR2	HB_AREA12_TR1	152.93341	-24.87373	-21.2	21.2	1.8	94.3	3.9
99	HB_AREA12_GR3	HB_AREA12_TR2	152.94001	-24.87709	-20.2	20.2	2.7	92.1	5.2
100	HB_AREA12_GR4	HB_AREA12_TR2	152.95253	-24.87373	-20.1	24.9	2.4	94.3	3.3
101	HB_AREA12_GR5	HB_AREA12_TR3	152.97432	-24.87698	-24.3	21.7	1.5	91.8	6.7
102	HB_AREA12_GR6	HB_AREA12_TR3	152.98244	-24.87379	-23.7	0.0	0.9	93.2	5.8
103	HB_AREA12_GR7	HB_AREA12_TR4	152.98579	-24.87703	-22.2	22.6	3.3	92.0	4.7
104	HB_AREA12_GR8	HB_AREA12_TR4	152.99454	-24.87373	-21.8	24.3	1.8	90.7	7.4
105	HB_AREA13_GR1	HB_AREA13_TR1	152.76545	-24.54746	-35.0	27.2	4.6	88.8	6.5
106	HB_AREA13_GR2	HB_AREA13_TR1	152.77461	-24.54804	-35.0	21.8	4.4	88.4	7.2
107	HB_AREA13_GR3	HB_AREA13_TR2	152.76558	-24.55754	-31.8	45.0	24.0	68.8	7.1
108	HB_AREA13_GR4	HB_AREA13_TR2	152.77458	-24.56033	-32.2	13.4	10.7	83.4	6.0
109	HB_AREA13_GR5	HB_AREA13_TR3	152.77470	-24.56142	-32.1	14.8	6.2	89.3	4.5
110	HB_AREA13_GR6	HB_AREA13_TR3	152.76548	-24.56465	-31.1	52.2	13.9	81.4	4.8
111	HB_AREA2_GR1	HB_AREA2_TR1	152.85482	-24.65154	-35.4	16.9	1.1	92.7	6.2
112	HB_AREA2_GR2	HB_AREA2_TR1	152.86702	-24.64787	-31.7	14.8	2.5	92.0	5.5

ID	Grab	Trawl	Longitude	Latitude	Bathy	Percent Carbonate	Percent Gravel	Percent Sand	Percent Mud
113	HB_AREA2_GR3	HB_AREA2_TR2	152.87162	-24.65149	-33.6	21.1	3.1	94.9	2.0
114	HB_AREA2_GR4	HB_AREA2_TR2	152.88292	-24.64792	-31.2	21.9	5.2	92.9	1.9
115	HB_AREA2_GR5	HB_AREA2_TR3	152.89863	-24.65166	-24.9	10.9	1.6	95.6	2.8
116	HB_AREA2_GR6	HB_AREA2_TR3	152.91180	-24.64804	-25.2	13.4	3.9	91.9	4.2
117	HB_AREA2_GR7	HB_AREA2_TR4	152.91350	-24.65177	-24.7	15.3	3.0	94.7	2.3
118	HB_AREA2_GR8	HB_AREA2_TR4	152.92560	-24.64815	-25.6	11.9	1.5	95.4	3.0
119	HB_AREA4_GR1	HB_AREA4_TR1	152.55037	-24.61447	-21.1	11.2	11.3	86.0	2.7
120	HB_AREA4_GR2	HB_AREA4_TR1	152.55805	-24.61124	-19.3	7.7	21.7	77.1	1.2
121	HB_AREA4_GR3	HB_AREA4_TR2	152.57092	-24.61092	-22.5	18.3	1.3	94.8	3.9
122	HB_AREA4_GR4	HB_AREA4_TR2	152.58140	-24.61113	-21.4	14.0	0.9	97.0	2.2
123	HB_AREA4_GR5	HB_AREA4_TR3	152.59127	-24.61436	-20.0	7.3	13.4	85.3	1.3
124	HB_AREA4_GR6	HB_AREA4_TR3	152.60253	-24.61130	-21.3	7.5	12.9	81.8	5.3
125	HB_AREA4_GR7	HB_AREA4_TR4	152.61335	-24.61465	-22.7	13.8	4.4	88.9	6.6
126	HB_AREA4_GR8	HB_AREA4_TR4	152.62293	-24.61144	-24.9	22.3	4.8	92.7	2.5
127	HB_AREA5_GR1	HB_AREA5_TR1	152.78519	-24.75031	-25.0	21.2	1.9	93.9	4.2
128	HB_AREA5_GR2	HB_AREA5_TR1	152.79688	-24.74715	-24.2	17.3	2.6	93.7	3.6
129	HB_AREA5_GR3	HB_AREA5_TR2	152.80630	-24.75020	-50.4	32.8	1.3	95.6	3.1
130	HB_AREA5_GR4	HB_AREA5_TR2	152.80734	-24.74720	-49.1	18.9	0.7	95.3	4.0
131	HB_AREA5_GR5	HB_AREA5_TR3	152.81155	-24.75045	-32.5	49.3	14.0	83.4	2.6
132	HB_AREA5_GR6	HB_AREA5_TR3	152.82365	-24.74729	-28.7	22.1	2.8	92.5	4.6
133	HB_AREA5_GR7	HB_AREA5_TR4	152.82509	-24.75052	-26.3	19.5	2.1	92.5	5.4
134	HB_AREA5_GR8	HB_AREA5_TR4	152.83712	-24.74742	-24.8	25.2	3.6	92.5	3.9
135	HB_AREA6_GR1	HB_AREA6_TR1	152.84501	-24.68755	-35.2	19.9	2.1	95.2	2.7
136	HB_AREA6_GR2	HB_AREA6_TR1	152.85861	-24.68418	-36.1	20.1	3.1	91.6	5.3
137	HB_AREA6_GR3	HB_AREA6_TR2	152.86742	-24.68755	-36.9	20.3	2.6	92.5	4.9
138	HB_AREA6_GR4	HB_AREA6_TR2	152.88050	-24.68444	-29.3	17.7	1.4	94.9	3.7
139	HB_AREA6_GR5	HB_AREA6_TR3	152.89047	-24.68794	-23.3	12.5	1.3	94.1	4.5
140	HB_AREA6_GR6	HB_AREA6_TR3	152.90291	-24.68418	-24.3	11.6	1.4	95.6	3.1
141	HB_AREA6_GR7	HB_AREA6_TR4	152.90627	-24.68781	-26.5	12.1	1.9	95.8	2.3
142	HB_AREA6_GR8	HB_AREA6_TR4	152.91599	-24.68444	-23.0	11.2	3.0	93.5	3.5
143	HB_AREA7_GR1	HB_AREA7_TR1	152.61325	-24.84026	-20.6	16.8	9.7	85.2	5.1
144	HB_AREA7_GR2	HB_AREA7_TR1	152.61329	-24.83022	-19.2	38.6	34.3	59.9	5.8
145	HB_AREA7_GR3	HB_AREA7_TR2	152.61088	-24.84055	-20.5	38.1	1.9	93.7	4.4
146	HB_AREA7_GR4	HB_AREA7_TR2	152.61122	-24.83022	-19.2	36.4	22.0	74.6	3.4
147	HB_AREA7_GR5	HB_AREA7_TR3	152.60972	-24.89153	-19.4	23.7	1.4	92.1	6.5
148	HB_AREA7_GR6	HB_AREA7_TR3	152.61300	-24.88357	-19.8	29.5	2.4	89.1	8.6
149	HB_AREA7_GR7	HB_AREA7_TR4	152.60972	-24.85325	-20.2	28.7	1.8	87.3	10.9
150	HB_AREA7_GR8	HB_AREA7_TR4	152.61315	-24.84509	-20.8	32.4	2.0	91.6	6.5

ID	Grab	Trawl	Longitude	Latitude	Bathy	Percent Carbonate	Percent Gravel	Percent Sand	Percent Mud
151	HB_AREA8_GR1	HB_AREA8_TR1	152.62290	-24.97850	-15.9	23.5	2.3	92.6	5.0
152	HB_AREA8_GR2	HB_AREA8_TR1	152.62690	-24.97650	-16.2	33.6	0.7	91.3	8.1
153	HB_AREA8_GR3	HB_AREA8_TR2	152.62290	-24.98229	-15.6	19.4	4.7	89.4	5.8
154	HB_AREA8_GR4	HB_AREA8_TR2	152.62690	-24.98011	-16.0	24.7	6.5	88.1	5.4
155	HB_AREA8_GR5	HB_AREA8_TR3	152.62300	-25.00908	-15.0	22.9	0.3	93.7	6.0
156	HB_AREA8_GR6	HB_AREA8_TR3	152.62690	-25.00704	-15.2	25.9	0.6	93.2	6.2
157	HB_AREA8_GR7	HB_AREA8_TR4	152.62290	-25.01453	-13.9	15.0	0.2	96.4	3.5
158	HB_AREA8_GR8	HB_AREA8_TR4	152.62690	-25.01256	-14.9	34.5	2.0	90.3	7.7
159	HB_AREA9_GR1	HB_AREA9_TR1	152.47227	-24.64133	-15.6	4.7	30.2	67.2	2.5
160	HB_AREA9_GR2	HB_AREA9_TR1	152.48190	-24.63816	-16.1	9.8	8.8	89.3	1.9
161	HB_AREA9_GR3	HB_AREA9_TR2	152.49324	-24.64109	-16.7	7.2	30.1	67.1	2.8
162	HB_AREA9_GR4	HB_AREA9_TR2	152.50445	-24.63820	-17.8	6.1	30.5	66.4	3.1
163	HB_AREA9_GR5	HB_AREA9_TR3	152.52161	-24.64129	-19.9	10.7	1.8	95.6	2.6
164	HB_AREA9_GR6	HB_AREA9_TR3	152.52834	-24.63846	-20.6	12.7	16.8	79.0	4.2
165	HB_AREA9_GR7	HB_AREA9_TR4	152.53142	-24.64101	-20.8	14.7	29.4	66.3	4.3
166	HB_AREA9_GR8	HB_AREA9_TR4	152.54133	-24.63831	-20.8	9.1	24.2	73.0	2.8

Table 18-4. Sediment grainsize fractions and further statistics for 166 samples.

ID	Grab	% > 16000µm	% 8000-16000µm	%4000-8000µm	% 2000-4000µm	% 1000-2000µm	% 500-1000µm	% 250-500µm	% 125-250 µm	% 63-125µm	% < 63µm	Geometric Mean µm	Geometric Std. Dev µm	Geometric Skewness µm	Geometric Kurtosis µm
1	GLAD_AREA2_GR1	2.2	1.9	1.3	1.4	6.3	32.1	39.3	14.1	0.6	0.8	521.5	2.8	1.0	8.1
2	GLAD_AREA2_GR10	0.0	0.2	1.8	3.5	6.6	15.6	25.6	34.7	8.2	3.8	296.6	3.2	-0.4	5.3
3	GLAD_AREA2_GR11	1.9	5.7	12.4	9.9	14.2	19.2	13.5	11.1	4.7	7.3	738.5	6.4	-0.7	3.5
4	GLAD_AREA2_GR12	0.0	0.6	1.7	3.9	10.7	22.4	23.4	30.4	5.8	1.0	397.5	2.8	0.1	4.5
5	GLAD_AREA2_GR2	0.7	1.1	1.3	2.4	5.2	20.5	34.2	32.9	1.3	0.4	390.1	2.6	1.2	7.0
6	GLAD_AREA2_GR3	0.0	0.1	1.0	1.6	5.6	10.9	19.4	56.7	4.5	0.2	272.5	2.2	1.2	5.6
7	GLAD_AREA2_GR4	6.0	2.9	2.9	3.1	5.5	8.4	11.9	52.4	5.4	1.6	396.9	4.8	1.1	4.2
8	GLAD_AREA2_GR5	4.7	7.3	10.8	7.0	9.8	14.0	13.8	22.2	6.5	3.9	730.4	6.2	-0.1	2.8
9	GLAD_AREA2_GR6	0.0	0.6	1.1	3.3	7.8	22.1	27.4	24.4	6.8	6.4	310.8	3.7	-0.9	5.0
10	GLAD_AREA2_GR7	0.0	0.5	1.4	2.5	4.6	18.7	28.5	38.3	3.7	1.8	323.5	2.7	0.0	6.5
11	GLAD_AREA2_GR8	0.0	0.3	1.2	2.3	5.7	19.8	30.1	33.2	3.2	4.1	311.7	3.0	-0.8	6.4
12	GLAD_AREA2_GR9	0.0	1.3	1.2	2.8	4.5	28.5	24.6	26.1	6.2	4.8	333.5	3.5	-0.7	5.6
13	GLAD_AREA4_GR1	0.0	0.4	0.5	1.5	2.8	7.6	25.8	53.4	5.3	2.6	236.1	2.5	-0.2	8.6
14	GLAD_AREA4_GR10	0.0	2.9	4.1	6.2	11.6	27.4	26.3	10.6	4.0	6.8	480.2	4.6	-0.8	4.7
15	GLAD_AREA4_GR2	0.0	0.2	0.3	1.9	3.6	7.6	23.1	56.3	6.2	0.8	246.7	2.2	0.7	7.6
16	GLAD_AREA4_GR3	0.0	0.0	1.3	3.2	7.4	14.0	17.8	49.0	5.6	1.7	293.0	2.7	0.1	5.3
17	GLAD_AREA4_GR4	0.0	0.0	0.6	1.1	2.3	6.9	27.0	52.3	6.4	3.4	219.7	2.5	-0.9	8.4
18	GLAD_AREA4_GR5	7.7	6.7	5.3	6.5	9.9	21.0	24.1	11.6	3.7	3.4	832.4	5.7	0.0	3.4
19	GLAD_AREA4_GR6	0.0	0.1	1.3	2.5	4.1	8.4	19.4	58.6	5.5	0.2	263.4	2.3	1.5	6.3
20	GLAD_AREA4_GR7	0.0	1.0	1.4	3.7	6.3	11.3	24.6	44.6	4.8	2.4	301.0	3.0	0.2	5.9
21	GLAD_AREA4_GR8	0.0	0.0	0.4	2.4	6.3	13.9	24.7	42.6	6.2	3.5	267.2	2.8	-0.7	6.1
22	GLAD_AREA4_GR9	0.0	0.1	1.1	2.0	4.4	12.3	37.5	38.1	4.6	0.0	315.1	2.2	1.2	5.1
23	GLAD_AREA5_GR1	0.1	0.1	0.4	0.8	2.3	17.1	36.9	24.6	9.4	8.3	227.9	3.5	-1.3	5.3
24	GLAD_AREA5_GR10	0.0	0.2	5.6	2.5	2.8	9.8	35.6	26.6	5.2	11.7	239.5	4.8	-0.6	3.9
25	GLAD_AREA5_GR11	0.0	0.1	1.0	1.5	4.0	22.4	37.1	26.2	4.3	3.5	317.1	2.8	-1.2	7.4
26	GLAD_AREA5_GR12	1.8	2.6	2.7	2.7	5.0	27.7	43.9	6.3	1.2	6.2	459.3	4.2	-0.6	6.0
27	GLAD_AREA5_GR2	0.0	2.2	4.7	1.8	5.6	30.8	45.2	3.9	0.9	4.9	482.2	3.6	-0.9	7.1
28	GLAD_AREA5_GR3	0.0	0.0	1.4	1.6	3.8	24.8	49.4	7.4	2.6	9.0	308.1	3.7	-1.6	6.0
29	GLAD_AREA5_GR4	0.0	3.4	6.0	1.2	2.1	8.4	33.0	30.7	5.1	10.2	267.4	5.1	-0.2	4.0
30	GLAD_AREA5_GR5	0.0	1.1	1.2	2.0	4.7	18.8	34.1	29.8	4.7	3.5	319.0	3.0	-0.5	6.7
31	GLAD_AREA5_GR6	0.0	1.8	5.3	2.4	7.4	32.9	41.1	5.0	0.8	3.2	540.6	3.2	-0.7	7.5
32	GLAD_AREA5_GR7	0.0	0.1	0.8	1.5	3.0	12.8	34.2	33.1	8.0	6.5	235.3	3.2	-1.1	5.9
33	GLAD_AREA5_GR8	0.0	4.9	4.9	2.2	4.2	20.6	48.8	7.7	1.9	4.8	470.8	4.0	-0.4	5.6
34	GLAD_AREA5_GR9	0.0	0.3	2.0	1.5	3.2	23.7	48.7	5.3	1.8	13.5	268.7	4.7	-1.3	4.3
35	GLAD_AREA6_GR1	14.0	18.8	10.9	4.3	4.9	14.2	24.5	3.4	0.6	4.4	1734.9	7.4	-0.6	3.1
36	GLAD_AREA6_GR10	12.7	5.3	4.4	3.8	8.3	23.6	30.6	7.0	0.7	3.5	960.9	5.9	0.1	3.5

ID	Grab	% > 16000um	% 8000-16000µm	%4000-8000µm	% 2000-4000µm	% 1000-2000µm	% 500-1000µm	% 250-500µm	% 125-250 µm	% 63-125µm	% < 63µm	Geometric Mean µm	Geometric Std. Dev µm	Geometric Skewness µm	Geometric Kurtosis µm
37	GLAD_AREA6_GR2	6.2	4.4	1.6	2.1	3.9	8.8	36.3	29.3	2.9	4.5	426.4	5.2	0.6	4.4
38	GLAD_AREA6_GR3	12.5	3.8	1.5	2.0	4.4	10.9	20.9	32.4	5.3	6.4	486.4	7.5	0.4	3.1
39	GLAD_AREA6_GR4	5.4	9.8	5.1	5.3	11.5	27.5	26.7	5.3	1.2	2.2	989.4	4.7	0.1	3.9
40	GLAD_AREA6_GR5	6.8	6.2	4.2	2.8	4.5	19.1	40.0	9.4	1.3	5.5	626.0	5.8	0.0	3.9
41	GLAD_AREA6_GR6	12.6	12.5	2.6	2.5	5.3	24.2	29.3	4.2	0.8	6.0	1010.9	7.4	-0.2	3.2
42	GLAD_AREA6_GR7	3.6	6.8	2.2	2.1	3.1	8.2	39.4	28.3	1.2	4.9	425.8	5.1	0.4	4.4
43	GLAD_AREA6_GR8	11.5	7.5	8.6	5.4	4.8	10.6	23.0	21.4	1.4	5.9	813.9	7.8	-0.1	2.7
44	GLAD_AREA6_GR9	2.4	5.4	6.3	5.0	9.4	28.2	32.3	6.3	1.2	3.5	707.2	4.3	-0.2	4.9
45	GLAD_AREA7_GR1	5.2	4.5	5.0	2.8	7.7	27.3	37.4	4.7	1.0	4.3	678.6	4.8	-0.1	4.8
46	GLAD_AREA7_GR10	2.7	5.0	3.0	3.8	14.0	35.3	27.9	2.3	0.4	5.8	673.2	4.6	-0.7	5.7
47	GLAD_AREA7_GR11	0.0	3.8	6.0	8.6	13.8	28.7	30.1	5.3	0.6	3.2	708.9	3.7	-0.7	5.9
48	GLAD_AREA7_GR12	3.6	5.1	4.4	6.8	21.1	34.8	16.4	3.0	1.0	3.9	906.7	4.3	-0.7	5.8
49	GLAD_AREA7_GR2	0.0	3.5	4.1	3.3	7.2	18.2	36.6	17.0	2.1	8.0	379.8	4.7	-0.6	4.5
50	GLAD_AREA7_GR3	0.0	1.2	1.2	5.5	29.7	43.8	15.2	0.6	0.1	2.7	783.3	2.7	-2.2	12.8
51	GLAD_AREA7_GR4	0.0	2.8	2.3	5.3	11.9	28.6	40.8	3.6	0.4	4.3	548.0	3.5	-1.0	7.2
52	GLAD_AREA7_GR5	4.3	2.4	4.3	6.1	16.6	31.6	26.0	4.6	0.5	3.7	765.7	4.2	-0.4	5.8
53	GLAD_AREA7_GR6	2.0	1.0	3.9	6.2	20.0	36.6	23.6	3.4	0.5	2.8	748.0	3.4	-0.8	7.7
54	GLAD_AREA7_GR7	4.6	3.0	5.0	4.4	7.8	24.7	38.4	7.8	1.4	3.0	653.8	4.3	0.2	5.0
55	GLAD_AREA7_GR8	2.6	0.5	2.4	4.0	6.8	20.5	39.0	14.5	2.7	6.9	393.7	4.4	-0.4	5.3
56	GLAD_AREA7_GR9	2.5	3.3	2.2	6.0	20.6	27.2	29.6	3.2	0.2	5.2	680.0	4.3	-0.8	6.0
57	GLAD_AREA8_GR1	0.0	0.0	0.2	0.3	1.1	12.9	67.2	12.5	0.7	5.1	296.0	2.6	-2.7	11.5
58	GLAD_AREA8_GR10	0.0	0.0	0.1	0.3	1.5	11.8	66.5	15.8	0.5	3.5	306.6	2.3	-2.8	14.3
59	GLAD_AREA8_GR11	0.0	0.1	0.4	1.0	1.7	14.1	39.0	37.7	1.8	4.1	263.9	2.6	-1.4	8.7
60	GLAD_AREA8_GR12	3.1	0.9	1.7	1.8	4.1	14.3	38.0	31.4	1.9	2.9	366.3	3.6	0.6	7.0
61	GLAD_AREA8_GR13	0.0	0.0	0.4	1.1	2.5	17.8	32.4	38.4	2.8	4.6	262.6	2.8	-1.4	7.5
62	GLAD_AREA8_GR14	2.4	3.7	3.1	6.7	13.4	29.5	21.9	10.2	3.5	5.6	586.6	4.8	-0.6	4.7
63	GLAD_AREA8_GR15	0.2	0.1	2.1	2.6	7.0	23.4	33.7	22.6	1.9	6.4	337.5	3.6	-1.1	5.9
64	GLAD_AREA8_GR16	0.0	1.9	1.9	2.7	6.7	22.0	46.7	11.3	1.8	5.0	400.5	3.4	-0.9	6.8
65	GLAD_AREA8_GR2	3.2	7.8	12.5	6.8	8.1	17.5	26.7	10.6	2.6	4.3	826.9	5.6	-0.3	3.5
66	GLAD_AREA8_GR3	1.0	2.9	1.4	2.1	6.8	18.1	49.2	14.7	0.4	3.5	433.1	3.4	-0.1	7.2
67	GLAD_AREA8_GR4	0.0	0.5	0.8	1.2	2.0	13.0	43.5	30.4	1.6	7.0	255.6	3.2	-1.3	6.8
68	GLAD_AREA8_GR5	0.4	8.0	5.3	2.4	4.5	10.0	32.1	30.4	2.0	5.0	425.5	4.9	0.2	4.0
69	GLAD_AREA8_GR6	0.0	0.9	0.9	1.4	4.0	9.1	25.5	48.5	4.2	5.3	236.8	3.1	-0.5	6.6
70	GLAD_AREA8_GR7	0.0	0.3	1.5	2.4	7.0	30.8	31.2	17.9	3.8	5.2	364.7	3.3	-1.3	6.4
71	GLAD_AREA8_GR8	0.0	0.8	1.0	1.3	2.0	17.8	59.2	12.8	0.5	4.5	341.0	2.8	-1.4	9.7
72	GLAD_AREA8_GR9	0.0	0.4	1.4	2.4	8.4	31.4	42.0	9.5	1.1	3.4	444.0	2.8	-1.5	9.0

ID	Grab	% > 16000µm	% 8000-16000µm	%4000-8000µm	% 2000-4000µm	% 1000-2000µm	% 500-1000µm	% 250-500µm	% 125-250 µm	% 63-125µm	% <63µm	Geometric Mean µm	Geometric Std. Dev µm	Geometric Skewness µm	Geometric Kurtosis µm
73	HB_AREA1_GR1	0.0	0.4	0.6	3.3	6.5	8.8	22.5	53.8	1.5	2.6	274.1	2.8	-0.1	6.7
74	HB_AREA1_GR2	0.0	0.0	0.7	2.2	3.9	5.7	14.4	66.7	2.5	4.0	213.4	2.7	-0.5	7.8
75	HB_AREA1_GR3	0.0	0.0	0.2	0.7	4.1	15.6	25.9	49.6	2.0	1.8	271.0	2.3	-0.7	8.0
76	HB_AREA1_GR4	0.0	0.5	1.9	6.2	18.2	20.6	12.5	34.2	2.5	3.2	429.6	3.5	-0.6	4.5
77	HB_AREA1_GR5	0.0	0.0	0.1	0.8	1.7	2.3	17.2	75.0	1.1	1.7	202.7	1.9	-0.7	15.0
78	HB_AREA1_GR6	0.0	0.0	0.1	1.2	2.6	4.1	13.6	75.0	1.6	1.8	207.8	2.1	-0.3	11.9
79	HB_AREA1_GR7	0.0	0.3	0.5	0.9	2.6	4.9	14.4	71.4	1.7	3.4	203.5	2.4	-0.5	10.3
80	HB_AREA1_GR8	0.6	0.6	2.0	6.1	12.7	13.0	11.2	50.0	1.6	2.2	365.3	3.4	0.2	4.5
81	HB_AREA10_GR1	0.0	0.0	0.6	1.4	3.4	5.9	10.5	65.3	8.4	4.5	190.3	2.7	-0.6	7.5
82	HB_AREA10_GR2	0.0	0.3	1.2	3.0	7.6	9.9	5.8	60.0	7.5	4.7	229.3	3.3	-0.1	5.3
83	HB_AREA10_GR3	0.0	0.3	0.8	3.0	7.6	10.9	13.0	42.6	16.8	4.9	225.5	3.4	-0.2	4.6
84	HB_AREA10_GR4	0.0	0.1	0.5	1.2	3.8	12.6	23.6	39.0	13.7	5.3	216.8	3.0	-0.8	5.7
85	HB_AREA10_GR5	0.3	0.0	0.8	2.4	6.1	17.8	26.4	31.6	7.9	6.7	262.3	3.6	-0.8	5.2
86	HB_AREA10_GR6	0.0	0.2	0.3	1.8	6.4	13.6	21.0	40.9	10.5	5.1	237.3	3.2	-0.7	5.4
87	HB_AREA10_GR7	0.0	0.0	0.5	1.7	5.3	10.8	17.4	54.2	5.9	4.1	230.2	2.8	-0.7	6.4
88	HB_AREA10_GR8	0.0	0.1	0.4	1.5	11.3	25.8	22.7	29.6	4.2	4.4	334.3	3.1	-1.2	5.9
89	HB_AREA11_GR1	2.8	0.9	1.4	1.1	2.6	11.3	27.0	45.5	2.8	4.6	285.4	3.8	0.5	6.9
90	HB_AREA11_GR2	0.0	1.2	1.3	2.8	5.3	10.7	26.4	44.1	3.6	4.6	273.2	3.3	-0.3	6.1
91	HB_AREA11_GR3	1.1	2.1	2.9	1.7	3.2	14.5	34.0	34.8	2.7	3.0	344.6	3.4	0.4	6.4
92	HB_AREA11_GR4	0.0	0.0	0.2	0.9	1.5	2.4	36.5	54.0	1.8	2.6	226.4	2.2	-1.4	12.1
93	HB_AREA11_GR5	0.0	0.0	0.1	0.5	0.8	10.5	56.1	29.6	0.5	2.0	290.6	2.0	-2.2	14.8
94	HB_AREA11_GR6	0.0	0.0	0.2	0.8	1.4	7.3	43.3	43.0	0.5	3.6	247.0	2.3	-1.8	10.9
95	HB_AREA11_GR7	0.0	0.0	0.1	0.5	1.0	8.1	57.2	29.5	0.2	3.4	272.0	2.3	-2.5	13.0
96	HB_AREA11_GR8	0.0	0.5	1.1	1.3	1.7	6.6	41.1	43.6	0.6	3.5	259.5	2.6	-0.7	9.5
97	HB_AREA12_GR1	0.0	0.0	0.3	1.2	3.3	5.8	6.0	68.0	11.2	4.2	40.7	5.5	0.3	1.6
98	HB_AREA12_GR2	0.0	0.0	0.3	1.5	2.8	6.1	7.1	64.4	13.9	3.9	178.9	2.5	-0.4	7.6
99	HB_AREA12_GR3	0.0	0.4	1.0	1.4	3.1	5.1	6.8	67.2	9.9	5.2	181.3	2.9	-0.2	7.4
100	HB_AREA12_GR4	0.0	0.2	0.5	1.7	5.3	7.7	8.0	64.7	8.8	3.3	208.6	2.7	-0.1	7.0
101	HB_AREA12_GR5	0.0	0.0	0.4	1.2	2.9	4.6	6.2	62.3	15.8	6.7	156.9	2.8	-0.8	6.5
102	HB_AREA12_GR6	0.0	0.1	0.0	0.8	2.9	4.1	4.3	59.2	22.7	5.8	147.9	2.7	-0.7	7.0
103	HB_AREA12_GR7	0.0	0.8	0.9	1.6	4.1	5.5	8.9	58.5	15.0	4.7	188.4	3.0	0.1	6.7
104	HB_AREA12_GR8	0.0	0.0	0.6	1.2	3.8	5.9	9.2	50.8	21.0	7.4	158.3	3.1	-0.5	5.4
105	HB_AREA13_GR1	0.0	0.6	1.0	3.1	6.7	16.6	27.0	35.7	3.0	6.5	281.9	3.6	-0.9	5.4
106	HB_AREA13_GR2	0.0	1.3	0.8	2.3	4.6	13.0	30.2	38.0	2.7	7.2	258.6	3.6	-0.7	5.6
107	HB_AREA13_GR3	3.9	7.6	7.5	5.0	10.5	23.9	23.9	9.5	1.0	7.1	709.6	6.2	-0.5	3.8
108	HB_AREA13_GR4	0.4	0.7	1.8	7.7	19.5	30.6	17.6	14.2	1.5	6.0	519.6	4.1	-1.2	5.6
109	HB_AREA13_GR5	1.7	0.0	0.9	3.6	18.0	36.4	22.7	10.8	1.4	4.5	529.6	3.6	-1.1	7.2
110	HB_AREA13_GR6	0.0	1.8	3.2	8.9	15.1	18.7	17.5	27.5	2.6	4.8	458.1	4.2	-0.6	4.3

ID	Grab	% > 16000um	% 8000-16000μm	%4000-8000μm	% 2000-4000μm	% 1000-2000μm	% 500-1000μm	% 250-500μm	% 125-250 μm	% 63-125μm	% <63μm	Geometric Mean μm	Geometric Std. Dev μm	Geometric Skewness μm	Geometric Kurtosis μm
111	HB_AREA2_GR1	0.0	0.0	0.2	0.8	3.5	4.8	3.4	75.9	5.1	6.2	167.7	2.7	-1.1	7.6
112	HB_AREA2_GR2	0.0	0.0	0.5	2.0	4.5	4.2	4.0	72.3	7.0	5.5	179.9	2.8	-0.5	7.0
113	HB_AREA2_GR3	0.0	0.3	0.7	2.1	5.5	8.4	8.5	64.6	8.0	2.0	227.6	2.6	0.4	6.9
114	HB_AREA2_GR4	0.0	0.0	1.0	4.2	7.0	7.1	11.9	60.2	6.5	1.9	253.4	2.8	0.4	5.6
115	HB_AREA2_GR5	0.0	0.0	0.5	1.0	2.1	3.4	19.1	68.6	2.3	2.8	205.5	2.2	-0.7	11.1
116	HB_AREA2_GR6	0.0	1.0	1.1	1.8	2.9	4.0	24.8	58.2	1.9	4.2	229.9	2.9	-0.1	8.1
117	HB_AREA2_GR7	0.0	0.1	0.5	2.4	4.6	4.9	14.5	68.3	2.5	2.3	226.4	2.4	0.1	8.4
118	HB_AREA2_GR8	0.0	0.3	0.2	1.0	2.4	3.5	17.0	69.5	3.1	3.0	202.0	2.3	-0.5	11.0
119	HB_AREA4_GR1	3.3	2.2	2.9	3.0	12.4	32.3	34.7	6.1	0.6	2.7	641.1	3.6	0.0	6.6
120	HB_AREA4_GR2	0.0	1.8	5.0	14.8	26.0	35.4	12.9	2.5	0.3	1.2	1009.3	2.7	-1.0	8.3
121	HB_AREA4_GR3	0.0	0.3	0.6	0.4	1.4	7.3	37.2	44.5	4.5	3.9	231.2	2.5	-1.2	9.3
122	HB_AREA4_GR4	0.0	0.2	0.3	0.3	1.0	8.1	50.2	35.8	1.9	2.2	269.5	2.1	-1.4	12.9
123	HB_AREA4_GR5	0.0	0.5	2.8	10.1	26.0	37.3	19.7	2.1	0.2	1.3	833.5	2.5	-1.3	9.9
124	HB_AREA4_GR6	0.0	0.5	4.9	7.6	11.6	30.2	35.0	4.6	0.3	5.3	550.3	3.7	-1.3	6.6
125	HB_AREA4_GR7	0.4	1.7	1.3	1.0	2.0	12.1	49.4	23.3	2.1	6.6	288.7	3.5	-0.7	6.8
126	HB_AREA4_GR8	0.0	1.2	0.7	2.9	11.3	35.8	36.8	7.4	1.3	2.5	507.3	2.7	-1.2	9.3
127	HB_AREA5_GR1	0.0	0.0	0.5	1.4	4.7	7.3	9.2	65.8	6.9	4.2	200.0	2.7	-0.5	7.1
128	HB_AREA5_GR2	0.0	0.4	0.9	1.3	2.7	5.9	9.7	69.1	6.4	3.6	199.0	2.6	-0.1	8.6
129	HB_AREA5_GR3	0.0	0.1	0.3	0.9	2.3	10.9	31.6	43.2	7.5	3.1	238.7	2.5	-1.0	8.0
130	HB_AREA5_GR4	0.0	0.0	0.2	0.5	2.3	4.8	16.3	57.5	14.4	4.0	178.4	2.4	-1.0	8.0
131	HB_AREA5_GR5	0.0	0.6	5.4	8.1	13.0	14.3	15.7	31.1	9.3	2.6	416.7	3.9	-0.1	3.5
132	HB_AREA5_GR6	0.3	0.0	0.8	1.7	5.9	8.7	14.5	51.9	11.4	4.6	215.7	3.1	-0.3	6.0
133	HB_AREA5_GR7	0.0	0.0	0.5	1.5	6.1	10.7	16.3	54.2	5.2	5.4	223.4	3.0	-0.8	6.0
134	HB_AREA5_GR8	0.0	0.0	0.9	2.7	6.7	7.8	9.2	61.2	7.6	3.9	222.6	2.9	-0.2	5.9
135	HB_AREA6_GR1	0.0	0.0	0.4	1.7	4.2	5.3	7.5	69.9	8.3	2.7	199.3	2.4	0.0	8.2
136	HB_AREA6_GR2	0.0	0.2	1.1	1.8	3.2	5.0	12.2	58.0	13.3	5.3	184.6	3.0	-0.3	6.6
137	HB_AREA6_GR3	0.0	0.4	0.5	1.7	4.5	6.2	6.4	64.8	10.7	4.9	188.1	2.9	-0.2	6.8
138	HB_AREA6_GR4	0.0	0.0	0.3	1.2	3.4	5.3	11.4	66.5	8.4	3.7	190.7	2.5	-0.7	8.3
139	HB_AREA6_GR5	0.0	0.0	0.1	1.2	2.1	2.6	6.0	79.9	3.6	4.5	172.5	2.4	-1.2	10.4
140	HB_AREA6_GR6	0.0	0.1	0.1	1.2	2.4	3.0	10.4	76.5	3.3	3.1	189.2	2.2	-0.8	11.4
141	HB_AREA6_GR7	0.0	0.5	0.2	1.3	2.4	3.5	16.4	69.4	4.2	2.3	206.7	2.3	0.0	11.4
142	HB_AREA6_GR8	0.0	0.5	0.4	2.1	3.1	3.0	8.0	76.3	3.1	3.5	197.3	2.5	0.0	9.6
143	HB_AREA7_GR1	4.1	0.0	1.1	4.6	22.2	44.6	13.6	3.5	1.3	5.1	693.2	4.0	-1.0	7.2
144	HB_AREA7_GR2	18.8	7.5	2.4	5.6	14.6	28.0	13.2	3.2	0.9	5.8	1390.5	7.4	-0.5	3.5
145	HB_AREA7_GR3	0.0	0.8	0.2	0.9	3.7	25.6	42.1	18.4	4.0	4.4	328.6	2.9	-1.4	8.0
146	HB_AREA7_GR4	10.4	3.8	1.9	5.8	17.8	34.0	17.7	4.0	1.1	3.4	1011.0	5.0	-0.2	4.6
147	HB_AREA7_GR5	0.0	0.0	0.4	0.9	2.3	13.4	22.4	38.2	15.8	6.5	196.9	3.1	-1.0	5.3
148	HB_AREA7_GR6	0.0	0.0	1.0	1.4	3.4	9.3	15.0	41.0	20.4	8.6	169.1	3.5	-0.6	4.6

ID	Grab	% > 16000um	% 8000-16000μm	%4000-8000μm	% 2000-4000μm	% 1000-2000μm	% 500-1000μm	% 250-500μm	% 125-250 μm	% 63-125μm	% < 63μm	Geometric Mean μm	Geometric Std. Dev μm	Geometric Skewness μm	Geometric Kurtosis μm
149	HB_AREA7_GR7	0.0	0.4	0.4	1.1	6.6	28.1	30.6	18.1	3.9	10.9	271.3	4.2	-1.3	4.6
150	HB_AREA7_GR8	0.0	0.0	1.1	0.9	2.1	11.9	31.1	39.1	7.3	6.5	221.7	3.1	-1.1	6.2
151	HB_AREA8_GR1	0.0	0.6	0.3	1.4	9.6	33.5	24.7	16.5	8.3	5.0	353.3	3.4	-1.3	5.8
152	HB_AREA8_GR2	0.0	0.0	0.1	0.6	1.5	11.8	21.6	36.3	20.2	8.1	169.7	3.2	-1.1	4.8
153	HB_AREA8_GR3	0.0	0.1	0.5	4.1	21.6	36.4	23.8	5.6	2.1	5.8	509.0	3.5	-1.9	7.3
154	HB_AREA8_GR4	0.0	0.0	0.6	5.8	22.1	38.0	17.8	6.2	4.0	5.4	528.7	3.6	-1.8	6.8
155	HB_AREA8_GR5	0.0	0.0	0.0	0.2	0.8	8.0	32.3	42.5	10.1	6.0	193.6	2.7	-1.7	7.1
156	HB_AREA8_GR6	0.0	0.0	0.0	0.6	2.0	12.9	35.8	33.5	9.0	6.2	220.4	2.9	-1.5	6.4
157	HB_AREA8_GR7	0.0	0.0	0.1	0.1	1.1	18.8	48.2	25.3	2.9	3.5	289.1	2.4	-2.2	10.5
158	HB_AREA8_GR8	0.0	0.0	0.3	1.7	3.6	11.0	22.6	38.4	14.6	7.7	193.6	3.3	-0.9	4.9
159	HB_AREA9_GR1	3.6	3.2	8.0	15.5	20.9	27.0	17.0	2.2	0.2	2.5	1131.7	3.9	-0.7	6.1
160	HB_AREA9_GR2	0.0	3.9	2.0	2.9	11.6	37.0	35.2	5.4	0.2	1.9	616.0	2.9	-0.3	8.0
161	HB_AREA9_GR3	0.0	1.0	8.7	20.5	24.9	28.1	13.1	1.0	0.1	2.8	1088.3	3.3	-1.7	8.8
162	HB_AREA9_GR4	7.8	2.1	7.3	13.3	17.1	29.9	17.9	1.4	0.2	3.1	1163.7	4.5	-0.5	5.3
163	HB_AREA9_GR5	0.0	0.1	0.4	1.3	5.3	25.7	53.8	9.9	0.8	2.6	395.5	2.4	-1.9	12.1
164	HB_AREA9_GR6	1.5	1.9	5.3	8.0	10.9	25.6	33.7	7.7	1.1	4.2	607.7	4.1	-0.6	5.6
165	HB_AREA9_GR7	5.9	3.7	11.3	8.5	9.1	21.6	27.6	5.6	2.3	4.3	874.9	5.4	-0.3	3.9
166	HB_AREA9_GR8	0.0	0.5	5.8	17.9	29.4	30.3	11.3	1.5	0.6	2.8	1000.3	3.2	-1.9	9.5

19 Appendix 7. Relationships between sediment grainsize, acoustic backscatter and saucer scallop (*Ylistrum balloti*) distribution in southeast Queensland

This section of the report addresses Objective 2) *Undertake exploratory analyses on the relationship between saucer scallop abundance and bottom substrate*

19.1 ABSTRACT

Seabed mapping with acoustics provides information on both structure (depth) and composition (backscatter). The backscatter strength is primarily influenced by seabed roughness, sediment grainsize and density contrasts. As a result, acoustic backscatter is often used as a proxy for benthic habitats. Saucer scallops (*Y. balloti*) are an important component of the multispecies Queensland East Coast Otter Trawl Fishery, but in recent years, scallop landings and catch rates have declined and the fishery is currently classed as overfished. Studies on the Atlantic sea scallop (*P. magellanicus*) have shown that sediment properties and geomorphological data can be used to help explain variation in the scallop's distribution and abundance. The current study investigated relationships between saucer scallop abundance, sediment grainsize properties and acoustic backscatter. Vessel-based surveys acquiring sediment grabs, seabed acoustic data and scallop abundance from trawls were undertaken within the QECOTF offshore from Gladstone and Hervey Bay. The results showed that 1) saucer scallops were found primarily on sediments that have a small range of comparatively low backscatter intensity values, 2) fine sand (125–250 µm) had the highest correlation with backscatter, and 3) saucer scallop abundance was correlated with the percentage of fine sand. The findings indicate that it may be possible to map scallop habitat in high-resolution using vessel-based techniques and that sediment composition could be a useful proxy for mapping scallop habitat throughout the fishery.

19.2 INTRODUCTION

The saucer scallop (*Y. balloti*) is an important component of the multispecies QECOTF and was valued around $30 million dollars from 1988–2000 (Campbell *et al.* 2010a). Since this time the stock has seen significant declines in annual landings and is currently classed as overfished (Yang *et al.* 2016). Current management strategies include a number of input controls including limited entry, tradeable effort units and spatial and temporal closures (i.e., SRAs) (Courtney *et al.* 2015; Madden 2016). However, further insight into the dynamics of the fishery is needed to improve management and to rebuild the stock.

Studies on the Atlantic sea scallop (*P. magellanicus)* have shown that sediment properties and geomorphological data can be used to explain variation in the scallop's distribution and abundance, thus improving stock assessment (Smith *et al.* 2017; Miller *et al.* 2019). Associations between scallops, sediment properties and acoustic backscatter intensity have been used to map scallop habitat suitability in this fishery (Smith *et al.* 2006; Brown *et al.* 2012; Smith *et al.* 2017). There is a strong relationship between Atlantic sea scallop abundance and sediment with high percentages of gravel, which is also highly correlated with acoustic backscatter (Smith *et al.* 2017). Most scallops are caught in aggregations, and by combining knowledge on the spatial distribution of scallop habitat with high spatial resolution fishing effort data, improved estimates of fishing mortality and exploitation rates can be derived (Smith *et al.* 2017).

Associating saucer scallops with substrate type through the use of acoustics and sediment sampling could allow for more robust predictions of scallop habitat distribution and better estimates of fishing mortality (Smith *et al.* 2006). However, in order to incorporate these data into models of the saucer scallop stock, it is important to first identify correlations between saucer scallop abundance and substrate composition.

19.2.1 Sediment-acoustic relationships

Side scanning sonar and multibeam echosounders are remote sensing devices routinely used for benthic habitat mapping (Brown and Collier 2008). These sonar systems record two important pieces of information; the time in which a transmitted signal is received (bathymetric data) and the strength of the returned signal (backscatter data) (Lamarche and Lurton 2018). While bathymetric data indicate depth and shape of the seafloor, backscatter data can convey important information pertinent to the nature of the seabed (Siwabessy 2001; Lanier *et al.* 2007; Blondel and Sichi 2009; McGonigle *et al.* 2011; McGonigle and Collier 2014). Acoustic sensors are well suited to habitat mapping because acoustic backscatter can provide a proxy for seabed substrate (Anderson *et al.* 2008; Huang *et al.* 2018).

Backscatter intensity is a product of the incident angle and a broad range of physical properties of the seabed including sediment grainsize, seabed roughness and substrate density (i.e., hardness) (Ryan and Flood 1996; Ferrini and Flood 2006; Biondo and Bartholomä 2017; Huang *et al.* 2018). The incident angle refers to the angle at which the transmitted signal interacts with the seabed (Huang *et al.* 2018), however, the influence of grazing angle on backscatter is removed in most studies to provide a mosaic that is indicative of substrate only (Ferrini and Flood 2006). Associating backscatter intensity with seabed characteristics is complex. Many studies have attempted to determine specific variables controlling backscatter response through the comparison of acoustic and ground-truthed data (Davis *et al.* 1996; Ryan and Flood 1996; Goff *et al.* 2000; Kloser *et al.* 2001; Collier and Brown 2005; Sutherland *et al.* 2007; De Falco *et al.* 2010; Haris *et al.* 2012; Huang *et al.* 2012; Huang *et al.* 2014), however, there has yet to be a universal consensus on the nature of these relationships.

One of the most common seabed characteristics used to investigate backscatter intensity is sediment grain size (Huang *et al.* 2018). In general, mud, sand and gravel have been the principle sediment types differentiated by acoustic backscatter (Ferrini and Flood 2006; Huang *et al.* 2014). In certain studies, the percentage of gravel was responsible for the majority of the backscatter response (Collier and Brown 2005; Biondo and Bartholomä 2017), yet in others the percentage of mud was more important (Huang *et al.* 2018). This complexity highlights the need for accurate ground truthing and that local facies may be more important in controlling backscatter intensity than mud, sand or gravel alone.

Relationships between backscatter and higher-resolution sediment grain size fractions (i.e., Phi intervals) have also been shown to be important (Collier and Brown 2005), however, these studies are rarely undertaken. It remains unclear whether the percentage of individual grainsize fractions in sediments are important determinates of backscatter intensity. Many studies have also found strong positive correlations between the mean grainsize and backscatter intensity (Davis *et al.* 1996; Goff *et al.* 2000; Collier and Brown 2005; Huang *et al.* 2018). This correlation reflects an expected result as denser material (i.e., coarse sediment) generally has a higher acoustic impedance (hardness) (Anderson *et al.* 2008). Conversely, finer sediments (i.e., mud) have low density thus, they generally have a low backscatter signal (Ryan and Flood 1996). Correlations between backscatter intensity and grainsize have been found to be disproportionately influenced by a low abundance of coarse material (Goff *et al.* 2000).

Other factors have also been reported to influence backscatter. Biological factors including bioturbation and the presence of benthic species, including vegetation, have been shown to affect substrate density (Fenstermacher et al. 2001; De Falco et al. 2010; Lamarche and Lurton 2018). Fenstermacher et al. (2001) found a strong positive correlation between the presence of sand dollars and backscatter intensity. Physical processes have also been reported to affect substrate density and seabed roughness including geological layering and undissolved gas in the sediment (Fonseca et al. 2002; Lamarche and Lurton 2018). Gas bubbles within the seabed substrate can increase volume scattering of acoustic waves, and thus dominate the backscatter response (Fonseca et al. 2002). The roughness of the seabed has been shown to have a greater influence over backscatter intensity than substrate density and sediment grainsize. A rough seabed (i.e., ripples) will scatter a signal in many

directions resulting in high backscatter, while a smooth seabed will reflect a signal at oblique angles resulting in low backscatter (Borgeld et al. 1999; Ferrini and Flood 2006).

The sediment-acoustic relationship has been analyzed using physical geoacoustic models, however, one model is not sufficient to describe the global variability of seabed characteristics (Huang et al. 2018). Instead, this relationship is explored within individual surveys using various statistical techniques. Correlations between sediment properties and backscatter intensity have been made using univariate statistical analyses (i.e., regressions) (Ferrini and Flood 2006), however, multivariate techniques and spatial predictions using machine learning algorithms have become more common (Huang et al. 2018). Multivariate analyses including Principle Component Analysis (PCA) (Ferrini and Flood 2006) and supervised linear discriminant analysis (LDA) (Biondo and Bartholomä 2017) enable an understanding of the sediment properties which make the most significant contribution to the variation in sediment samples.

19.2.2 Scallops and sediments

While commercial scallop species (i.e., Pectinidae spp.) have generally been associated with hard substrata (gravel and coarse sand) (Brand 2006), studies have identified different habitat preferences based on particular scallop species life history traits (Bourgeois et al. 2006). All juvenile scallops secrete a byssal thread which allows them to attach to the substrate, however, many species like the saucer scallop lose this ability as adults, rather living freely on the seabed (Brand 2006). Once the byssal threads are lost, free living species use jet propulsion to create depressions in the substrate in which they subsequently settle in a process called 'recessing' (Orensanz et al. 2006). Recessing into depressions is an important functional requirement for these sea scallop species as it increases food availability through the entrapment of detritus and provides predation avoidance from visual predators (Tremblay et al. 2015). However, some species of scallop (*Chlamys distorta, Hinnites multirugosa*) retain the ability to secrete byssal threads, and remain attached to the substrate throughout their life cycle (Brand 2006).

These two opposing life history traits (free swimming and sessility) may have major implications on species benthic habitat preferences. This is reflected in the range of bottom substrates upon which scallop species have been observed. *Mimachlamys varia*, a common scallop species distributed around the British Isles is found byssally attached to hard substrata (rocks, boulders, shells etc.) (Brand 2006). Likewise, the European *C. distorta* and the North Pacific *H. multirugosa* require a coarse seabed to attach as they lose their ability to swim freely later in life (Brand 2006).

However, many free-living species also occur on gravel bottoms. *Aequipecten opercular* occurs along the eastern coast of the North Atlantic in hard gravel and shelly bottoms as it does not recess into the seabed (Brand 2006). *Pecten maximus*, while sharing a similar geographic distribution as *A. opercular*, occurs on bottoms of fine or sandy gravel (Brand 2006). This substrate preference may reflect their need to recess into the seabed to avoid predation (Brand 2006; Himmelman *et al.* 2009). Similarly, the North Atlantic sea scallop (*P. magellanicus*) and the North Pacific or Yesso scallop (*Mizuhopecten yessoensis*) occur in hard, gravelly substrates with little mud content (Smith and Rago 2004). However, certain southern hemisphere species, (*Amusium pleuronectes, Argopecten gibbus, Argopecten irradians*) tolerate the presence of mud (Brand 2006; Dredge 2006).

Unlike certain scallop species found in the northern hemisphere, comparatively little information is known about the habitat preferences of southern hemisphere scallop species, including the saucer scallop (Brand 2006). Saucer scallops (*Y. balloti)* are found from Hervey Bay, Queensland to Esperance, Western Australia around the northern coast of Australia (Dichmont *et al.* 2000; Mueller *et al.* 2012). This species is free-living and known for its superior swimming ability, as individuals are able to swim for significantly longer periods of time than other species of similar size (Brand 2006). While saucer scallops have previously been associated with 'sand' (Welch *et al.* 2014), very little is known about their benthic habitat preferences compared to species in the North Atlantic such as *P. magellanicus* (Brand 2006).

19.2.3 Aims and objectives

This section of the report aims to investigate relationships between seabed substrate, acoustic backscatter and the distribution of saucer scallops in two locations within the QECOTF: Gladstone and Hervey Bay. By establishing these relationships through seabed mapping and sampling surveys, this study can provide the foundation for future modelling of scallop distributions within the fishery. Specifically, this study aims to:

1. investigate the relationship between saucer scallop abundance and acoustic backscatter,
2. explore the relationship between sediment properties and acoustic backscatter,
3. examine correlations between sediment properties and saucer scallop abundance, and
4. assess the importance of incorporating sediment grainsize data at 1 Phi resolution into studies of acoustic backscatter.

19.3 METHODS

19.3.1 Study location: Southern Great Barrier Reef

This study was conducted in two locations within the QECOTF: offshore from Gladstone and in Hervey Bay (Figure 19-1). Gladstone is situated on the central coast of Queensland adjacent to the southern edge of the Great Barrier Reef (23.8416° S, 151.2498° E). Six areas were sampled from 10 km to 40 km offshore. These areas ranged from 10–49 m deep and lay exposed to the predominant south-easterly winds. Hervey Bay is 228 km south of Gladstone and is located slightly north of the Great Sandy Straits (25.00°S, 152.85°E). The bay is shallow and approximately 4000 km^2 in total area (Butler *et al.* 2013). The northern mouth of the bay is about 80 km wide and subject to a tidal range of 4 m. The bay is protected from the south-easterly winds and oceanic swell by Fraser Island to the south (Butler *et al.* 2013). Twelve areas within Hervey Bay were sampled and ranged in depth from 11–52 m.

Sampling took place on the *RV Tom Marshall* over four cruises. Mapping and sampling of the six survey areas offshore from Gladstone were conducted in June and August of 2018, while mapping and sampling of the 12 areas in Hervey Bay were conducted in June and July 2019. Sampling in both locations occurred during the winter seasonal closure of the scallop fishery. Survey areas from Gladstone and Hervey Bay were identified based on regional bathymetry data and historic fishing effort data from the Queensland Department of Agriculture and Fisheries (DAF). The fishing effort data were acquired using TrackMapper software (http://era.daf.qld.gov.au/id/eprint/5479/), which uses high spatial resolution satellite-based Vessel Monitoring System (VMS) data to quantify the location and amount of fishing effort. Survey areas were typically 0.5–1 km x 7.5–15 km and represented regions of high, medium and low fishing effort. The narrow rectangular survey design for both the Gladstone area (Figure 19-2) and Hervey Bay (Figure 19-3) was chosen so areas could reflect a range of historic fishing effort within individual survey areas (Table 19-1 and Table 19-2).
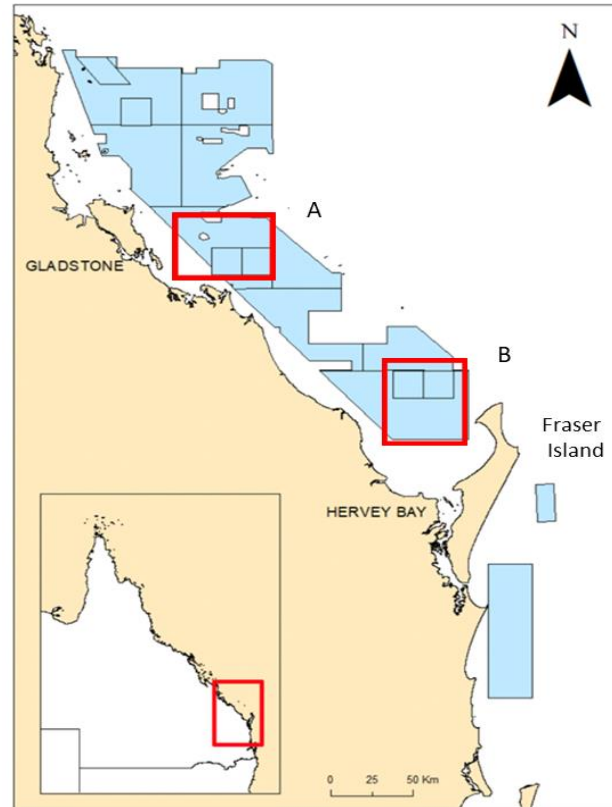
Figure 19-1. Regional map of the QECOTF: saucer scallop stock geographic extent with co-located management areas; A) Gladstone survey area extent, B) Hervey Bay survey area extent.

Table 19-1. Gladstone survey areas with size (area), relative fishing effort and depth.

Area	Size (km^2)	Effort	Depth (m)
Area 2	12.0	High	23–47
Area 4	12.4	High	20–47
Area 5	4.6	Low-Med	23–49
Area 6	12.0	Low-Med	15–35
Area 7	27.2	Medium	10–39
Area 8	15.1	Med-High	18–36

Table 19-2. Hervey Bay survey areas with size (area), relative fishing effort and depth.

Area	Size (km^2)	Effort	Depth (m)
Area 1	4.7	High	23–30
Area 2	5.0	High-Med	24–36
Area 4	4.4	Medium	18–25
Area 5	4.8	Medium	22–52
Area 6	5.1	Medium	22–41
Area 7	4.5	Medium	18–21
Area 8	4.7	Medium	11–17
Area 9	4.1	Low	14–21
Area 10	4.9	Medium	20–29
Area 11	4.9	Med-High	33–50
Area 12	4.1	Med-High	18–26
Area 13	3.3	High	28–36

19.3.2 Geophysical data

The Gladstone survey sites were mapped using a 240 kHz Reson 8101 multibeam sonar system. The surveys were conducted at a speed of 5–6 knots. The Reson 8101 system (Beaudoin *et al.* 2002) produced 101 acoustic beams that were 1.5° x 1.5° with up to 20 pings per second. Pitch, roll, and heave were corrected using a Kongsberg Seatex motion reference unit while the acoustic sound velocity profile was acquired using a Sontek CastAway CTD system. The geographic position was recorded by a Fugro MarineStar9200-SP GPS system. The Caris HIPS/SIPS software was used for tide and sound velocity profile corrections and removing spikes in bathymetry data. The final dataset had a resolution of 1 m and was adjusted to be relative to mean sea level. The error of estimation for the depth soundings was a maximum of +/– 0.2 m.

The Hervey Bay survey sites were mapped using a Lowrance HDS LIVE unit with an Active Imaging Transducer due to a malfunction in the Reson multibeam sonar system used in Gladstone. The surveys were conducted at a speed of 5–6 knots. The Lowrance unit provided 400 kHz sidescan imaging at a range of up to 80 m and single beam bathymetry beneath the transducer. The geographic position was recorded by a Fugro MarineStar9200-SP GPS system and these positioning data were used to update the original non-differential positioning of the Lowrance sonar. The SonarTRX software (http://www.sonartrx.com/web/) was used to update the survey positioning and generate beam angle corrected raster images from the Lowrance S2D data format files. The final sidescan raster datasets had a resolution of 0.25 m.

Sonar systems operating at different sonar frequencies are likely to respond to sediment composition in different ways due to relative signal penetration into the seabed; high frequency has a low penetration while low frequency has a high penetration (McGonigle and Collier 2014; Huang *et al.* 2018). As a result, comparisons of sediment composition and scallop distributions with backscatter were undertaken separately.

19.3.3 Scallop trawls

Between four and eight trawls were conducted in each area with a 4.2 m wide beam trawl net. Each trawl was approximately 1 km in length. Trawl sites were acquired from the full range of backscatter intensity values to represent the full range of sediment types within the study areas. Trawl sites were chosen based on areas of similar backscatter intensity to ensure individual trawls was conducted over homogeneous areas of the seabed (Figure 19-2 and Figure 19-3). Scallops from each trawl were measured, classed as either the 0+ age class (< 78 mm SH) or 1+ age class (≥ 78 mm SH), counted and recorded. Scallop abundance was summarised as number of scallops per hectare (ha^{-1}) for each trawl.

19.3.4 Sediment samples

Sediment samples were collected using a 2 L Van Veen sediment grab. Two sediment samples were collected per trawl: one at the start and end of each trawl. The samples were collected in depths ranging from 10–50 m. GPS coordinates were taken with each sediment sample along with the co-located trawl and backscatter intensity data.

A sediment grainsize analysis was performed using all 166 sediment samples collected from Gladstone and Hervey Bay. Details of how the sediments were processed are provided in section 18.3, page 120. The proportion of sediment in each sieve was then weighed. Sediment data were summarised through the G2sd package in Rstudio (Fournier *et al.* 2014). Fifteen sediment grainsize variables were used in the statistical analysis. These include the percentage content of gravel, sand, mud, 1600 µm fraction, 8000 µm fraction, 4000 µm fraction, 2000 µm fraction, 1000 µm fraction, 500 µm fraction, 250 µm fraction, 125 µm fraction, 63 µm, geometric mean, geometric standard deviation and skewness. The six sediment grainsize properties in addition to the Phi increments were chosen based on similar studies (Ferrini and Flood 2006; Huang *et al.* 2018).
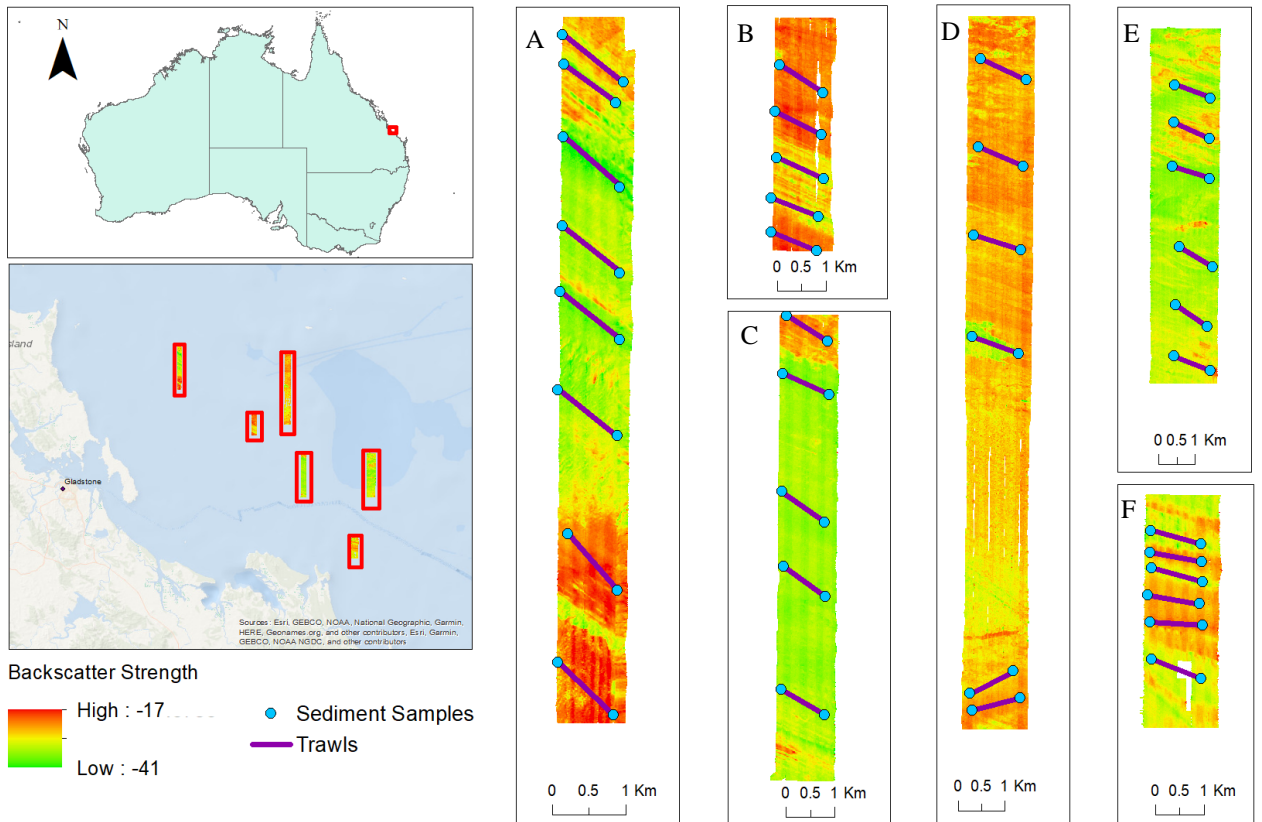
Figure 19-2. Gladstone survey areas with co-located sediment grabs, trawls and backscatter values A) Area 8, B) Area 6, C) Area 4, D) Area 7, E) Area 2, F) Area 5.
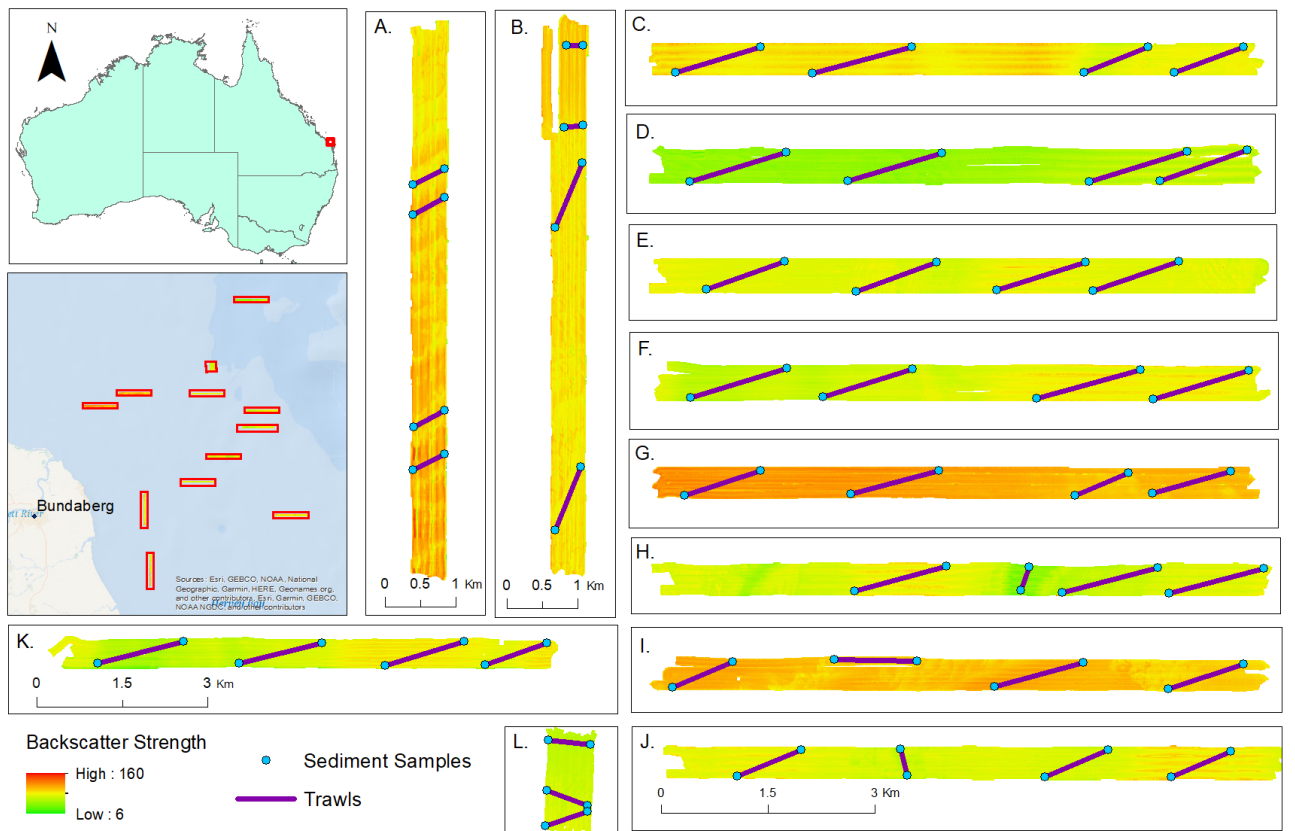
Figure 19-3. Hervey Bay areas with co-located sediment grabs, trawls and backscatter data A) Area 8, B) Area 7, C) Area 12, D) Area 11, E) Area 1, F) Area 2, G) Area 9, H) Area 5, I) Area 4, J) Area 10, K) Area 6, L) Area 13.

19.3.5 *Statistical analysis*

19.3.5.1 Scallop/backscatter relationships

Univariate analysis was used to investigate the relationship between backscatter intensity and saucer scallop abundance. Average backscatter intensity values were calculated within a 25 m buffer of each sediment sample. Relative homogeneity of sediment within each buffer was assumed (Huang *et al.* 2018). The mean backscatter value was taken from each pair of sediment samples to produce one average backscatter value per trawl. Each trawl corresponded to an average number of scallops ha^{-1}.

19.3.5.2 Sediment/backscatter relationships

Predictive statistical modelling was undertaken to determine the relationship between backscatter intensity and sediment properties. A Random Forest (RF) decision tree method was used to predict backscatter values from the 15 summarised grainsize properties. A separate model was used to predict backscatter values from the percentage content of mud, sand, gravel and geometric mean to identify potential differences in the model's prediction ability with 1 Phi fraction increments. All backscatter values within a 25 m buffer of each sediment grab were used and the models were separated by location.

Random Forest is a robust machine learning algorithm which creates many independent categorical or regression decision trees trained on 3/4 of a dataset (training dataset) (Huang *et al.* 2018). Prediction accuracy is then calculated by how well the model correctly identifies relationships from the remaining data (testing dataset). This multivariate approach enables a better understanding of the complexity surrounding the relationships between acoustic backscatter (response variable) and sediment properties (explanatory variables). The RF method also produces an importance value for each predictor variable in the model (Breiman 2001). Using this value, it is possible to identify the most important variables influencing the backscatter response. This model was chosen based on this importance measurement and the model's ability to handle non-parametric data.

19.3.5.3 Sediment/scallop relationships

Correlation plots were used to identify significant explanatory variables. Line plots of the grainsize-frequency distributions of each sediment sample were plotted by location. The sediment samples linked to the five most productive trawls in each location were highlighted to identify potential patterns in the sediment.

19.4 RESULTS

19.4.1 *Backscatter and saucer scallops*

The relationship between acoustic backscatter intensity and saucer scallop abundance was similar in both Gladstone and Hervey Bay. There was no significant correlation between the number of scallops ha^{-1} and mean backscatter values in both Gladstone (R^2 = 0.2433, p < 0.001) and Hervey Bay (R^2 = 0.1247, p < 0.01). However, in both locations, trawls with relatively high scallop density (i.e., > 15 scallops ha^{-1}) were consistently associated with a discrete narrow range of relatively low backscatter (Figure 19-4). In Gladstone, trawls with more than 30 scallops ha^{-1} were associated with backscatter values ranging between –29 and –31, while trawls with more than 5 scallops ha^{-1} were associated with backscatter ranging between 60 and 80 in Hervey Bay. Trawls with no scallops were associated with a broad range of backscatter, including the scallops 'preferred' lower than average backscatter values (Figure 19-4). It should also be noted, the different backscatter scales reflect the two types of sonar systems used in each location (backscatter ranges from –33.01 and –24.97 for Gladstone and 39.60 and 119.99 for Hervey Bay).
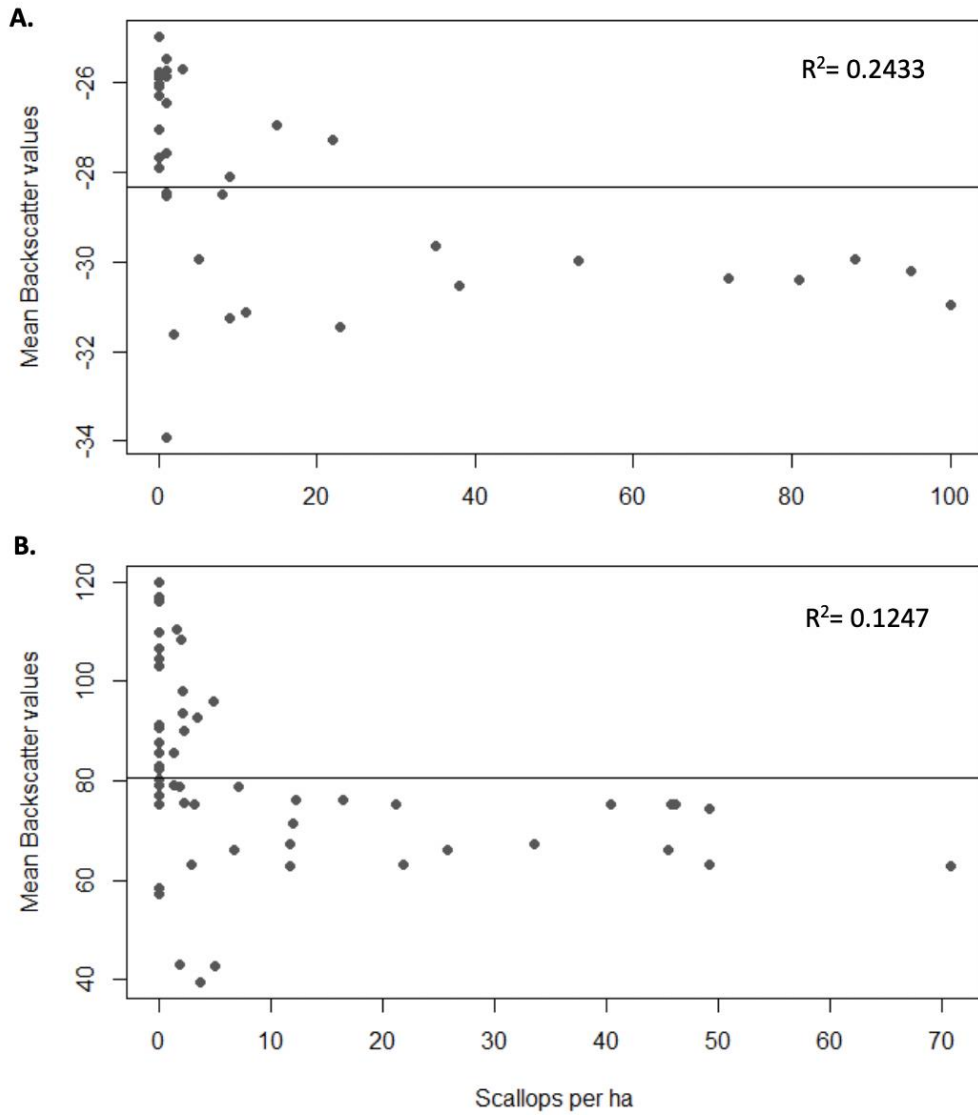
Figure 19-4. The relationship between mean backscatter values and scallop abundance offshore from Gladstone (A) and in Hervey Bay (B). Average backscatter values for each survey, –28.3 in Gladstone and 80.5 in Hervey Bay, are shown. The trawls with the higher abundances of scallops in both locations occur within a restricted range of lower-than-average backscatter values.

19.4.2 Sediment properties and backscatter

The RF models used to predict backscatter intensity from sediment properties achieved a good performance on the training dataset with 97% of the variance between sediment samples explained in both Gladstone and Hervey Bay. The Gladstone model with an input of 15 explanatory variables (including 1 Phi fractions) had a good prediction performance on the testing dataset with a low root-mean-square error (RMSE) (0.416). However, the model had a comparably poorer prediction performance (RMSE = 2.133) using only the percentage content of mud, sand, gravel and geometric mean as explanatory variables. In the Hervey Bay model, the model using 15 explanatory variables had a RMSE of 2.586, while the model achieved a slightly higher RMSE (poorer performance) of 2.588 using only 4 explanatory variables. While the models from both locations had better prediction accuracies with 15 explanatory variables the Gladstone model achieved a higher overall prediction performance on the testing data when compared to the Hervey Bay model.

Individual variable importance was identified using the models from both locations with the higher prediction performance (models including 1 Phi fractions). The 125 µm fraction (125–250 µm or fine sand) was the most important sediment grainsize variable in controlling the backscatter response in both models (Figure 19-5). However, the 125 µm fraction was twice the importance of the next variable (2000 µm fraction) in the Gladstone model, while only slightly higher than the second (geometric mean) in the Hervey Bay model. While the remaining variables differed in the importance values between the two models, the smaller grainsize fractions (63 µm fraction and percentage content of mud) were generally more important in both models (Figure 19-5).
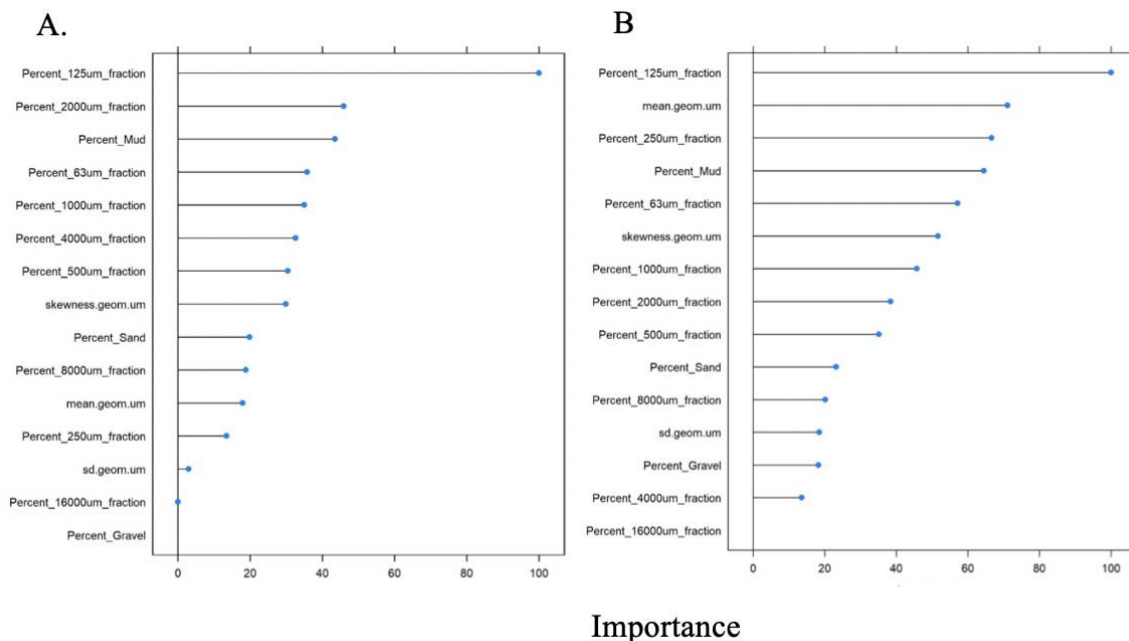
Figure 19-5. Importance values from Random Forest models predicting backscatter intensity from sediment properties in A) Gladstone and B) Hervey Bay. The 125 µm fraction was the most important variable in both models.

The relationships between backscatter intensity and the most important variable (125 µm fraction) from Gladstone and Hervey Bay were fitted with a linear function and shown in Figure 19-6. The correlation between fine sand and backscatter reflects slightly different relationships in each location. There is a strong negative correlation between mean backscatter values and the 125 µm fraction (fine sand) from the Gladstone data ($R^2 = 0.5929$, $p < 0.001$) (Figure 19-6). However, the Hervey Bay data reflects a comparably weaker negative relationship between mean backscatter values and the 125 µm fraction ($R^2 = 0.2648$, $p < 0.001$) (Figure 19-6).
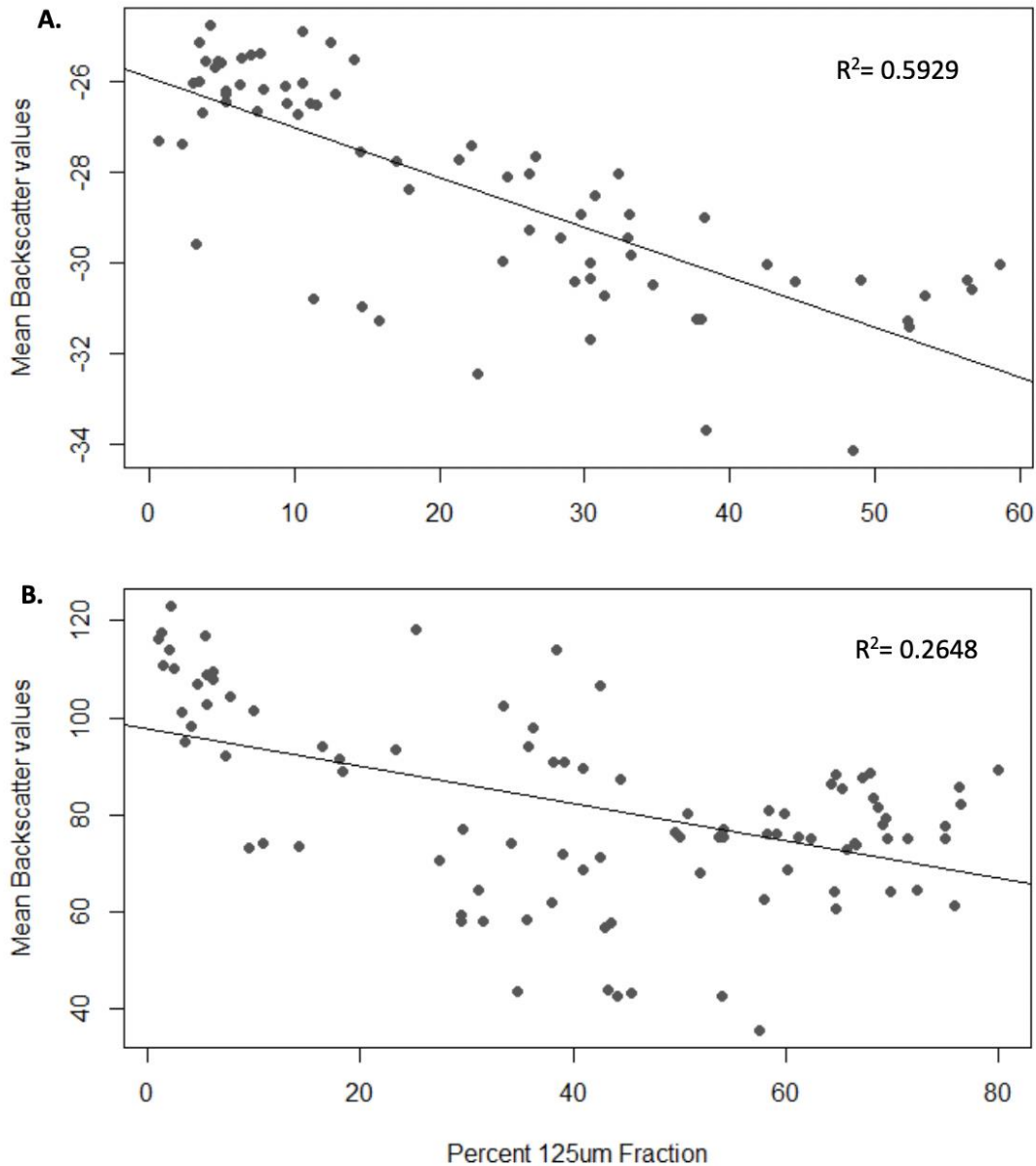
Figure 19-6. The relationship between mean backscatter values and 125 µm fraction in A) offshore from Gladstone ($R^2 = 0.5929$) and, B) Hervey Bay ($R^2 = 0.2648$). There is an inverse correlation between mean backscatter values and the 125 µm fraction in both locations.

19.4.3 *Saucer scallop abundance and sediment grainsize*

Among the relationships between saucer scallop abundance and sediment properties, the strongest correlation occurs between the 125 µm fraction and scallop abundance in Gladstone (Kendall's tau = 0.5473). There were also moderate correlations between scallop abundance and most sediment properties in Gladstone, however, the percentage content of sand (Kendall's Tau = 0.4478) and geometric mean (Kendall's Tau = 0.4184) were the variables with the second and third largest correlation with scallop abundance, respectively (Table 19-3). In general, the correlations between scallop abundance and sediment properties in the Gladstone data were stronger than the relationships in the Hervey Bay data (Table 19-3).

In Hervey Bay the strongest correlation occurs between geometric skewness and scallop abundance (Kendall's tau = 0.2152), however, the second strongest correlation occurs between the 125 µm

fraction and scallop abundance (Kendall's Tau = 0.2040) (Table 19-3). While the third strongest correlation (250 µm fraction and scallop abundance) was of similar strength to the first and second, all remaining correlations in Hervey Bay were trivial (≤ absolute 0.1) (Cohen 1988).

Table 19-3. Correlations between the number of scallops ha^{-1} and sediment properties offshore from Gladstone and in Hervey Bay (correlation coefficient = Kendall's tau).

Sediment property	Gladstone number of scallops ha^{-1}	Hervey Bay number of scallops ha^{-1}
%Gravel	–0.349	0.026
%Sand	0.447	0.034
%Mud	–0.243	–0.0333
16,000 µm fraction	–0.331	–0.004
8000 µm fraction	–0.328	–0.101
4000 µm fraction	–0.327	0.018
2000 µm fraction	–0.218	0.034
1000 µm fraction	–0.213	0.077
500 µm fraction	–0.317	–0.100
250 µm fraction	–0.113	–0.200
125 µm fraction	0.547	0.204
63 µm fraction	0.394	0.089
Geometric mean	–0.418	–0.100
Geometric standard deviation	–0.360	–0.028
Skewness	0.130	0.215

The correlation between the 125 µm fraction and scallop abundance in the Gladstone data indicates a positive relationship when fitted to a linear function (R^2 = 0.5409, p < 0.001) (Figure 19-7a). The variables in the Hervey Bay data reflect a comparably weaker relationship (R^2 = 0.1187, p < 0.01) (Figure 19-7b). However, a notable pattern is present in both locations. The trawls associated with sediment consisting of less than 20% fine sand generally have a lower abundance of saucer scallops. Conversely, trawls in sediment consisting of greater than 20% fine sand reflect comparatively higher scallop abundances. However, trawls with zero scallops also occur in sediment with greater than 20% fine sand in both Gladstone and Hervey Bay.
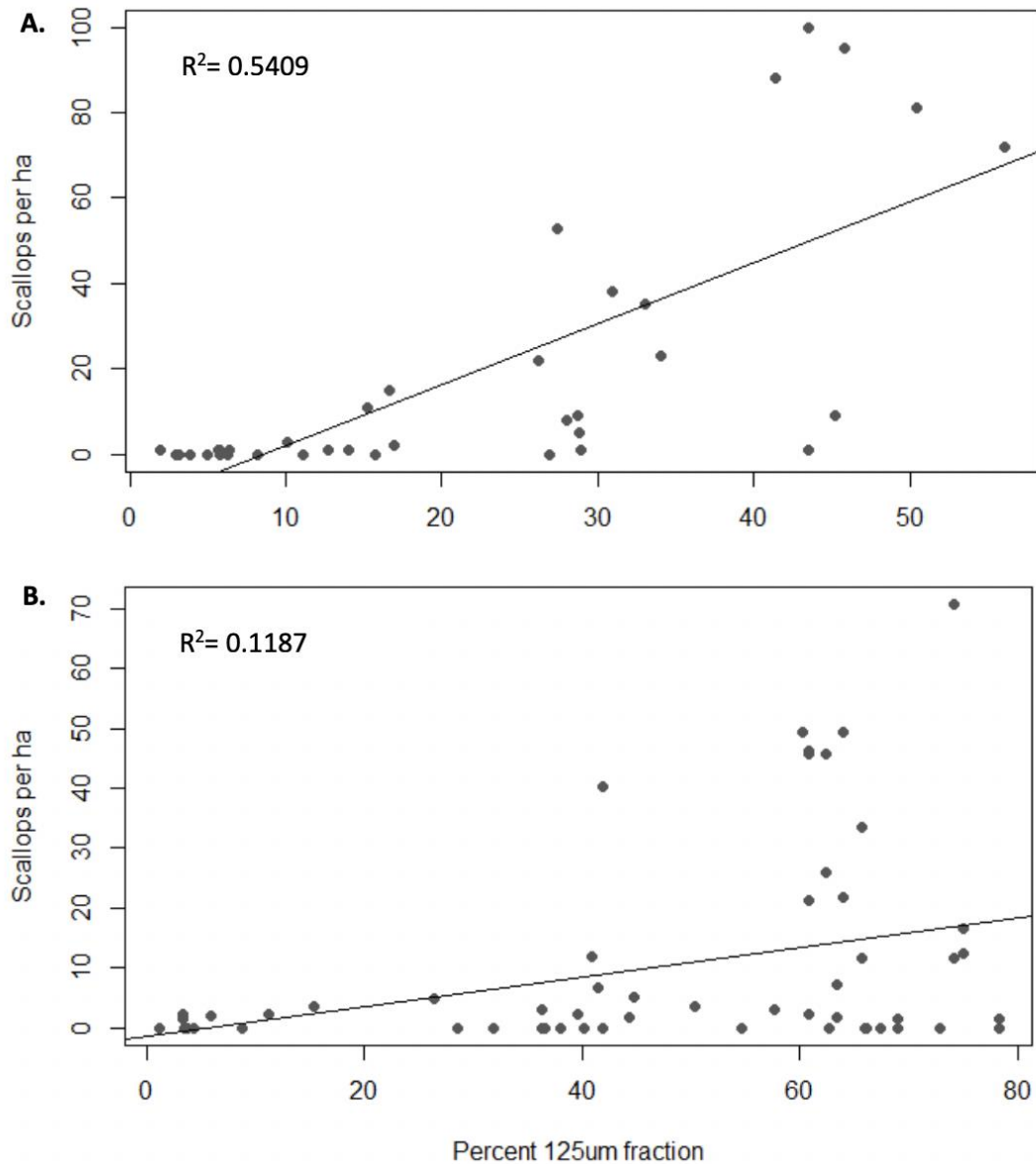
Figure 19-7. The relationship between scallop density and the 125 µm fraction (i.e., fine sand) for A) offshore from Gladstone ($R^2 = 0.5409$) and B) in Hervey Bay ($R^2 = 0.1187$).

This pattern is also reflected in the grainsize-frequency distribution of the sediment samples. On average, the Gladstone trawls had more scallops ha^{-1} than the Hervey Bay trawls. The ten samples linked to the five "best" trawls in Gladstone (highest number of scallops ha^{-1}) generally follow a similar grainsize distribution pattern with peak percentages of fine sand (Figure 19-8). Similarly, the grainsize-frequency distributions of the Hervey Bay sediment ten samples linked to the five "best" trawls (highest number of scallops ha^{-1}) also follow a similar pattern with peak percentages of fine sand (Figure 19-8). However, sediment samples linked to trawls without scallops do not follow a defined grainsize-frequency distribution pattern (Figure 19-8).
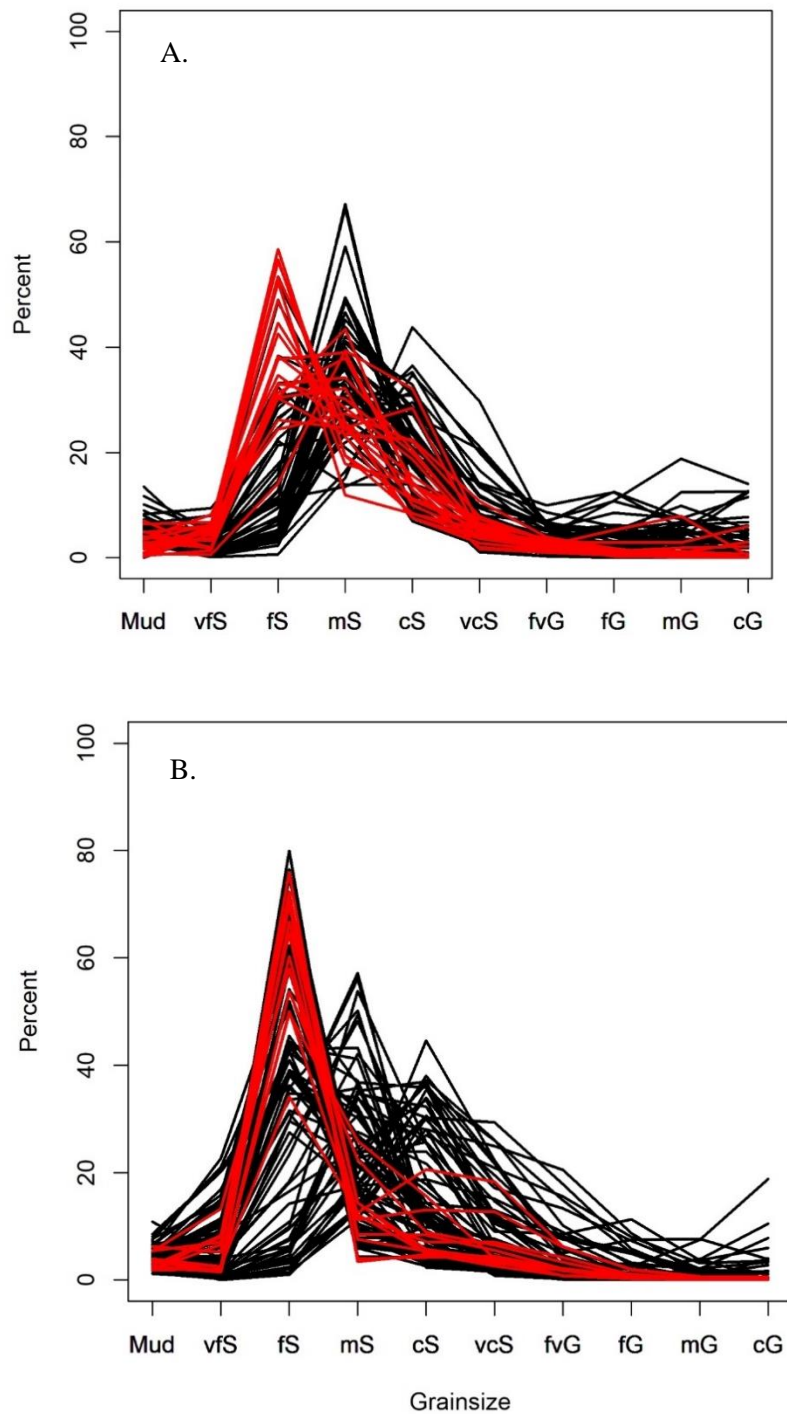
Figure 19-8. Grainsize-frequency distributions of all sediment samples for A) offshore from Gladstone and B) in Hervey Bay. The trawls linked to the five "best" trawls (highest number of scallops ha^{-1}) are pictured in red and generally follow the same sediment grainsize distribution pattern with peak percentages of fine sand.

19.5 DISCUSSION

The presence of significant relationships between saucer scallops, sediment grainsize and acoustic backscatter from two locations within the QECOTF is confirmed in this study. Saucer scallops were correlated with fine sediment and had a high correlation with the 125 µm grainsize fraction. This same

grainsize fraction appears to be the important variable driving sediment/backscatter relationships in the study area.

19.5.1 Backscatter and saucer scallops

Saucer scallops occur within a restricted range of backscatter values which we will define as a "critical range". Scallops from trawls in both Gladstone and Hervey Bay occurred in sediment with lower-than-average backscatter intensity values. However, this range of backscatter values appears to be important for saucer scallop presence, independent of abundance. This pattern indicates an ecological relationship between saucer scallops and the substrate they settle on (Haris *et al.* 2012). The sediment properties controlling this range of lower than average backscatter intensity values may reflect an important functional requirement of the saucer scallop (Haris *et al.* 2012). The presence of this "critical range" relationship between backscatter and scallops has been reported for other benthic species, yet the backscatter intensity values appear to depend on the species (Tully *et al.* 2006; Lanier *et al.* 2007; Smith *et al.* 2017). For example, the Atlantic sea scallop (*P. magellanicus*) has been associated within a range of higher than average backscatter intensity values (Smith *et al.* 2017). The "critical range" of backscatter values associated with benthic species presence can be inferred as suitable habitat (McGonigle and Collier 2014).

By identifying suitable habitat by a "critical range" of backscatter values, it is possible to map habitats by proxy (Brown *et al.* 2012). In this case, areas of lower-than-average backscatter intensity values can be classified as high habitat suitability for saucer scallops. Habitat suitability modelling using acoustic backscatter can reflect species presence, thus is an important tool used in management of marine reserves and commercial fisheries (Degraer *et al.* 2008; Iampietro *et al.* 2008; Galparsoro *et al.* 2009; Monk *et al.* 2010).

It should be noted, there were many trawls without scallops present in locations that had sediment within the "critical range" of backscatter values. It is well known, scallops generally have patchy distributions (Dredge 1985b). The Patagonian Scallop (*Zygochlamys patagonica*) has been described as occurring in discontinuous aggregations (Bogazzi *et al.* 2005). Similarly, the saucer scallop has been reported to occur in distinct aggregations within elongated beds (Dredge 1985b). While the trawls in this study were generally separated by between 1 and 4 km, the patchy nature of scallop distributions may have implications for sampling and may account for the trawls with zero scallops. Studies suggest certain drivers other than sediment alone may contribute to the patchy nature of scallop distribution. For example, aggregations of the Patagonian Scallop have been associated with regional upwelling events (Bogazzi *et al.* 2005) and Queensland saucer scallop commercial catch rates have been shown to be highly correlated with certain oceanographic variables, including Chlorophyll A and properties of the Capricorn Eddy (Courtney *et al.* 2015). Therefore, while lower backscatter values may represent a type of seabed that is suitable for saucer scallop settlement, oceanographic variables may make a suitable seabed uninhabitable.

It is possible these factors may have a greater influence on saucer scallop distribution than sediment properties, thus may explain the areas of suitable substrate lacking the presence of saucer scallops. In other words, identifying areas of suitable habitat by this "critical range" of backscatter values does not guarantee the presence of saucer scallops. It is also possible the low scallop catch in suitable substrate may reflect the depleted state of the stock (Yang *et al.* 2016). Despite the possible influence of other variables, the "critical range" association described through this study indicates it is possible to map saucer scallop habitats with acoustics. However, to extract any relevant ecological information, it is important to identify the likely substrate characteristics controlling the backscatter response through ground-truthing.

19.5.2 Sediment properties and backscatter

The particularly high modelling accuracy in both offshore Gladstone and Hervey Bay (~97% of the variance explained) from this study indicates that sediment grainsize properties can be adequate predictors of acoustic backscatter intensity (Huang *et al.* 2018). The results of this study also indicate

that providing sediment grainsize at a 1 Phi resolution results in improved predictions of backscatter intensity. Historically, the sediment grainsize properties differentiated through backscatter have generally been mud, sand and gravel (Ferrini and Flood 2006; Smith *et al.* 2017; Huang *et al.* 2018). However, using primarily the 125 μm grainsize fraction it is possible to largely explain the acoustic-sediment relationship in both Gladstone offshore and Hervey Bay. This higher resolution interpretation of backscatter intensity may have important implications for habitat mapping as it may allow the detection of specific sediment niches.

The percentage of fine sand (125 μm fraction) in the sediment was found to be the most important sediment property in both models and has a significant negative correlation with backscatter intensity. This correlation corroborates previous research; finer sediments generally have low backscatter response while sediments with high percentages of gravel have a high backscatter response due to their relative densities (Ryan and Flood 1996; Collier and Brown 2005; Anderson *et al.* 2008; Huang *et al.* 2018). This pattern is present in both study locations, however the correlation found in Gladstone was stronger. The strong negative correlation between backscatter and percentage of fine sand reflects the importance of results from the Gladstone Random Forest model. Thus, the percentage of fine sand is clearly the primary driver of backscatter response in Gladstone. Results from Hervey Bay indicate the backscatter values may be controlled by a combination of factors. The percentage of fine sand remained the most important explanatory variable in the model, however, the importance value was only slightly greater than the second most important variable, mean grainsize. Variations in the relative importance of sediment grainsize properties for predicting backscatter intensity between survey sites have been reported in previous studies (Ferrini and Flood 2006).

The variations seen in the results between Gladstone and Hervey Bay may also reflect the different sonar systems used and relative frequencies between survey locations (Ryan and Flood 1996). Different sonar systems and frequency used have certain trade-offs. Higher frequency signals allow for higher resolution of the benthic surface (Anderson *et al.* 2008). Lower frequency signals, on the other hand, allow greater penetration into the seabed, resulting in additional information pertaining to the make-up of the subsurface seabed (Anderson *et al.* 2008). However, the data acquired from lower frequency signals are of a lower resolution (Anderson *et al.* 2008). The choice of frequency can be particularly important for layered sediment, like coarse dredged material under fine mud (Brown *et al.* 2019). However, a comparative survey over the same patch of seabed would be needed to understand the relationships between different sonar frequencies.

It is important to note, other seabed characteristics can also influence backscatter intensity. Seabed roughness (seabed substrate, microtopography, landforms etc.) has been reported to change the backscatter signal regardless of the sediment type (Borgeld *et al.* 1999; Lamarche and Lurton 2018). It is clear from the results of this study; sediment grainsize properties are important explanatory variables for backscatter intensity in the survey locations. However, the addition of relative seabed roughness and other physical and biological variables (i.e., vegetation) into predictive models may further improve backscatter predictions. This data can be acquired from underwater video and photo analysis (Smith *et al.* 2007; Huang *et al.* 2018).

19.5.3 *Saucer scallop abundance and sediment grainsize*

The correlation between the abundance of saucer scallops and the percentage of fine sand in the sediment in both study locations indicates the saucer scallop, much like other commercial scallop species has a preferred sediment niche (Smith *et al.* 2017). This sediment niche confirms and improves upon the previously held understanding that saucer scallops prefer sand (Welch *et al.* 2014). To the best of our knowledge, the saucer scallop preference for fine sand (phi-scale) was previously unknown (Brand 2006; Welch *et al.* 2014; Courtney *et al.* 2015). This preference for fine-sand may be related to the saucer scallop's need to bury itself within sediment, unlike other species such as the Atlantic sea scallop (*P. magellanicus*) which live on, rather than in, the seabed (Brand 2006).

Interestingly, high proportions of fine sand are found in sediment throughout the areas sampled offshore from Gladstone and Hervey Bay, and possibly throughout large proportions of the entire fishery. Historic sediment grainsize-frequency distribution data from the surrounding areas corroborate this finding (Grimes 1991) (Figure 19-9). A study investigating sediments from Fraser Island found grainsize-frequency distributions similar to sediment samples from this study (i.e., strong peaks in fine sand and medium sand) (Grimes 1991). Fraser Island is 169 nautical miles south of Gladstone, adjacent to the southern tip of Hervey Bay and is one of the world's largest sand islands (Figure 19-1) (Boyd *et al.* 2004). This island is located at the convergence of tropical and subtropical zones and is thus subject to high energy sediment transport. Fraser Island and surrounding sandy areas (including offshore Gladstone and Hervey Bay) are likely to be deposits from the interaction of the East Australian Current, prevailing south-easterly winds, waves and longshore currents (Boyd *et al.* 2004). Therefore, the sediments contributing to the preferred saucer scallop habitats found in this study are of a similar sedimentary environment to, and may be of the same origin as, the sediments found on Fraser Island. However, additional research is needed to explore this possibility.
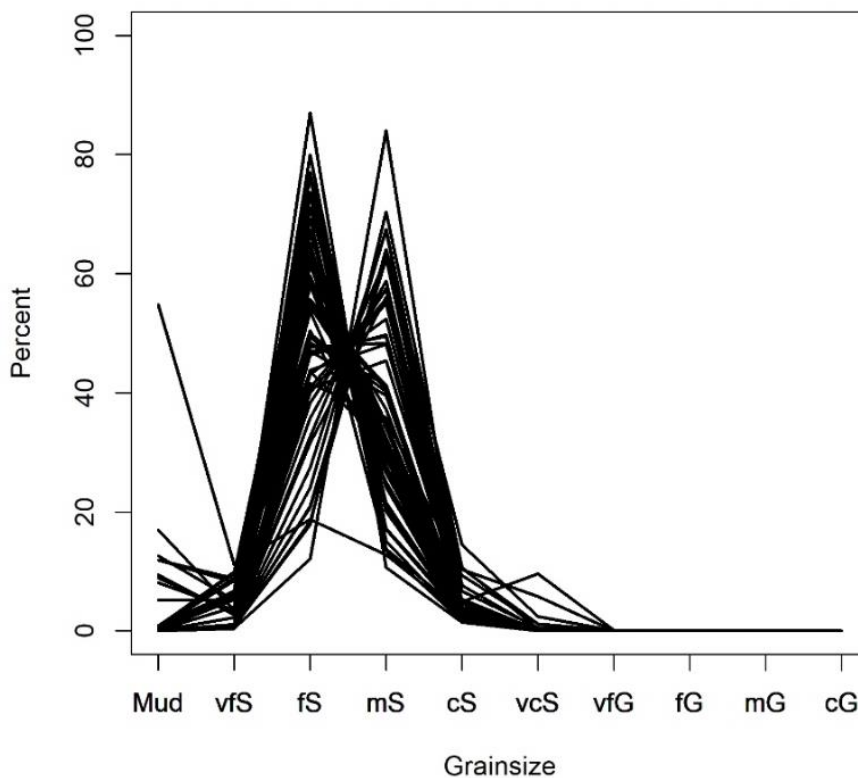
Figure 19-9. Grainsize-frequency distribution from sediment samples from a study on Fraser Island (Grimes, 1992). All samples follow a similar grainsize frequency distribution with peak percentages of fine and muddy sand.

19.5.4 Implications for the fishery and future work

The results of this study provide an important foundation for habitat suitability mapping which can assist in monitoring and assessing the scallop stock. Saucer scallops are more likely to occur in sediment with a higher percentage of fine sand, which may be their preferred habitat. Multibeam surveys with ground-truthed backscatter are likely to provide good indications of favourable scallop habitat due to the strong correlation between fine sand and backscatter. However, multibeam mapping of the entire fishery is unlikely due to the high cost and vast spatial extent of the stock. To scale these results up to determine saucer scallop habitat distribution across the entire fishery, a combination of regional sediment distribution modelling, multibeam mapping and predictive modelling with additional variables are necessary. Sediment distribution modelling involves interpolating point samples to create a continuous dataset over regional spatial scales (Li *et al.* 2011c) (also see section 20, page 157). Multibeam mapping would also provide information on how geomorphic features (bedforms, plains, furrow, swales, channels, etc.) influence scallop distribution. The addition of these covariates, bathymetric derivatives and oceanographic data into predictive models would likely supplement the relationships observed herein and aid development of scallop habitat maps (Brown *et al.* 2012; Smith *et al.* 2017).

An understanding of habitat preferences is useful for predicting scallop distributions in survey areas (Smith *et al.* 2006; Brown *et al.* 2012; Smith *et al.* 2017). Maps of the varying grades of scallop habitat could be overlaid with the trawl fishing effort, and therefore used to improve the estimation of fishing mortality (F), which is important for stock assessment and management (Smith *et al.* 2017).

19.5.5 Conclusions

This study showed that acoustic backscatter and sediment composition can be helpful for understanding the distribution of saucer scallops in southeast Queensland. Specifically, the study confirmed the presence of significant relationships between backscatter, sediment grainsize and saucer scallop abundance. The strength and nature of these relationships are integral for mapping saucer scallop habitat suitability. Habitat suitability maps may help explain the distribution of fishing effort, improve indices scallop abundance and fishing mortality, and improve management advice for the fishery. We conclude that:
1. Saucer scallops primarily occurred on sediment with a relatively narrow range of backscatter intensity values (i.e., critical range), which was lower than the average backscatter of the sampled areas.
2. Backscatter values can be accurately estimated using sediment grainsize properties. The percentage of fine sand (i.e., 125 µm fraction) had the highest correlation with backscatter.
3. In both the Gladstone and Hervey areas, the percentage of fine sand (125 µm fraction) had the highest correlation with scallop abundance, although the distribution of scallops was patchy.
4. Sediment data of 1 Phi resolution improved the correlation between backscatter intensity and scallop abundance. Sediment data of this resolution should be incorporated into future studies.
5. Detailed multibeam mapping of the region, with co-located scallop sampling, would likely provide further understanding of scallop habitat preferences and distribution.

20 Appendix 8. Modelling the distribution of marine sediments in southeast Queensland

This section of the report addresses Objective 2) *Undertake exploratory analyses on the relationship between saucer scallop abundance and bottom substrate*

20.1 ABSTRACT

Several commercially fished scallop species have well defined preferences for certain seabed substrates. However, sediment sample data are generally scarce, unevenly scattered and patchy. Therefore, prior to investigating relationships between saucer scallops and sediments, there is a need to develop comprehensive maps of the distribution of marine sediment types in southeast Queensland. Inverse Distance Weighted (IDW), three variants of Random Forest (RF), three variants of Generalised Boosting Method (GBM), and four variants of hybrid methods were used to predict the distribution of six seabed sediment properties (mud, sand, gravel, calcium carbonate, mean grainsize and fine sand) in southeast Queensland. Predictions using a simple IDW method were used as a baseline to be compared against RF, GBM, and their hybrid methods. RF, GBM and their hybrid methods used up to 11 covariates to aid predictions of sediment distribution. The predictive models demonstrated that: 1) models that excluded latitude and longitude as covariates performed poorly, 2) models that used only sediment data that had co-located high-resolution bathymetry measures commonly outperformed models that used the entire sediment dataset which included interpolated bathymetry data, and 3) a hybrid model between IDW and GBM that only used samples that were co-located with high-resolution bathymetry data was the most accurate model on average. Predictions for mud and calcium carbonate, using the highest ranking model (i.e., RFb), were the most accurate with a Variance Explained by cross validation (VEcv) of 76.1 and 82.3, respectively. Predictions for gravel, using the highest ranking model (i.e., IDW) were the least accurate with a VEcv of 33.0. The resulting sediment property maps can be used to explain the distribution of saucer scallops and improve the indices of scallop abundance used for stock assessment and management.

20.2 INTRODUCTION

For most regions around the Australian coastline, sediment sample data are only available as scarce and unevenly scattered point samples (Li *et al.* 2011a). To gain a better understanding of the regional distribution of sediment compositions and their associated benthic habitats, the sediment properties at unsampled locations need to be predicted. Using the data from sampled locations, spatial interpolation methods can be used to predict the environmental properties at an unsampled location. The development of spatially continuous data can then be used to further an understanding of spatial relationships between sediments and habitats, as well as be used in many important areas of environment management and conservation, such as decision making and risk management (Torgersen *et al.* 2006; Li and Heap 2008; Li *et al.* 2011a).

Spatial interpolation methods currently used in the marine environment to predict environmental variables are classified into five categories; 1) non-geostatistical spatial interpolation methods, 2) deterministic or non-geostatistical methods, 3) stochastic or geostatistical methods, 4) machine learning methods, and 5) combinations of these methods (Li *et al.* 2011a; Li *et al.* 2011c). Previous studies have considered a wide range of interpolation methods to predict sediment distributions in the marine environment (Li and Heap 2008; Li *et al.* 2011a; Li *et al.* 2011c). Li *et al.* (2011a), in a review of interpolation methods applied to sediment sample data, concluded that machine learning methods generally outperform other spatial interpolation. Li *et al.* (2011c) also concluded that machine learning methods may also introduce artefacts into the interpolated datasets, and as a result, visual inspection of the resulting datasets is required to ensure they are fit for purpose. Machine learning methods can be used to produce generalized maps of environmental variables and combined with either deterministic or geostatistical methods to interpolate sample residuals. More recently, these combined interpolation methods have been shown to be as effective as, or more effective than,

machine learning alone (Li *et al.* 2011a; Sanabria *et al.* 2013; Appelhans *et al.* 2015; Tadić *et al.* 2015; Li *et al.* 2017).

Many commercial scallop species have well defined sediment niches (Brand 2006). The link between sediment composition (dominantly gravel) and distribution improved the analysis of survey data and modelling for the Atlantic sea scallop (*P. magellanicus*) stock (Miller *et al.* 2019). This has led to improved management of the fishery through successful rotation of closure areas, limiting fishing in optimal habitats, and reducing fishing effort overall (Kostylev *et al.* 2003; Smith and Rago 2004; Brown *et al.* 2012; Smith *et al.* 2017). Knowledge of the similar relationships between saucer scallops and seabed substrate could lead to improved modelling of the stock and management outcomes in Queensland. At present however, there is scant information on saucer scallop habitat types.

Welch *et al.* (2010) indicated that *Y. balloti* shows a preference for substrates that are both soft (to enable the scallops to burrow) and have a high sand content. The previous section of this report (section 19.4.3, page 149) concluded that trawls with the highest scallop densities were associated with sediments that were composed of at least 30% fine sand (125–250 μm). Regionally, the saucer scallop fishery is split into a number of strata that have been used for monitoring scallop abundance (Jebreen *et al.* 2008). Within the strata, SRAs have been associated with relatively high scallop densities and have been closed to fishing since September 2016 (Figure 20-1). Differentiating the seabed structure and composition of the SRAs from other strata may provide insights into the habitat preferences of scallops at a regional scale.

An extensive sediment sample dataset exists for the Great Barrier Reef region (Mathews *et al.* 2007). Improvements to sediment datasets and predictions could be achieved through the addition of new and previously unavailable historical data and refinement of interpolation methods. A series of optimally interpolated marine sediment datasets is expected to be important for understanding the distributions of saucer scallops more broadly within the fishery. These data may also be important for understanding the distribution of other commercially important species in southeast Queensland such as Moreton Bay bugs (*Thenus australiensis, Thenus parindicus*) and spanner crabs (*Ranina ranina*).

This section of the report aims to:
1) Compile an extensive set of sediment sample analyses for southeast Queensland that extends the previous work of Mathews *et al.* (2007).
2) Identify an optimum method for interpolation of sediment properties across southeast Queensland.
3) Assess the importance of covariates latitude and longitude in model performance.
4) Given the 'patchy' distribution of high-resolution bathymetry data in the study area, compare models that use only those sediment data that are co-located with high-resolution bathymetry measures against those that use the entire sediment dataset which includes interpolated bathymetry.
5) Develop a series of optimally interpolated maps of mud, sand, gravel, calcium carbonate, mean grainsize and fine sand for southeast Queensland.
6) Compare sediment composition of the SRAs against other survey strata and areas.

20.3 METHODS

20.3.1 *Study area*

The study spatial domain in southeast Queensland extends from the Swain Reefs to the southern tip of Fraser Island (21° S – 27° S), bounded by the mainland to the west and the Tasman Sea to the east (149°30' – 153°20' E) (Figure 20-1). The study area covers 320,000 m^2 of the sea floor and depths varying from 0 to 4000 m. Within the study area lies the Queensland saucer scallop trawl fishery, extending from Fraser Island to Yeppoon (Courtney *et al.* 2015) bounded by the mainland to the west and the Capricorn-Bunker reefs to the east.

Previous studies concluded the continental shelf of southeast Queensland to be dominated by sandy sediments with a minor amount of gravel (Maxwell and Maiklem 1964; Marshall 1977, 1980; Mathews *et al.* 2007). Mud is commonly found in concentrations of 5% or less on the shelf except where samples have been taken near large river systems. Mud content also increased considerably off the shelf where it can reach greater than 90% in the Tasman Sea and Capricorn Channel. The southeast Queensland shelf contains large river systems (i.e., the Fitzroy River) that transport terrigenous sediments to the coastal zone and major coral reef ecosystems (i.e., the Capricorn-Bunker Group). As a result, the distribution and concentration of calcium carbonate in sediment is highly variable.
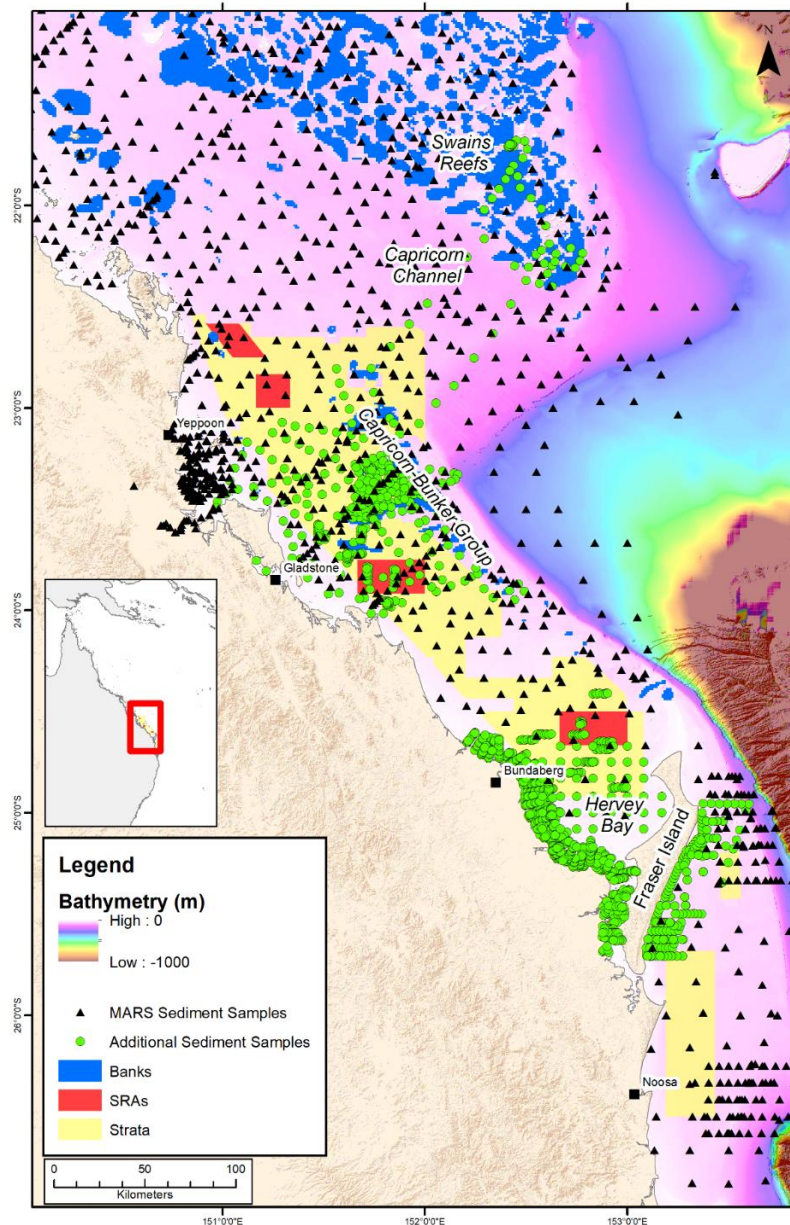
Figure 20-1. Map of study area showing regional bathymetry, key geographic areas, mapped coral reefs (banks), saucer scallop fishery survey strata and scallop replenishment areas (SRAs). Also shown are the locations of previously acquired sediment samples and the newly acquired samples.

20.3.2 Sediment samples

The study area has been surveyed sporadically since 1964. Sediment samples were sourced from Geoscience Australia's MARine Sediment (MARS) database. Additional sediment samples were sourced from recent surveys conducted in 2018 and 2019 as part of the current project (see section 18, page 119), and previous studies by Maxwell and Maiklem (1964), Marshall (1977), Stephens *et al.* (1988), Tarabbia (1990) and Ribbe (2014).

Sediment grainsize is commonly calculated via sieving but can also be achieved by laser diffraction and a range of other methods (Syvitski 1991). Sediment samples are commonly reported as the relative proportions of their gravel, sand and mud. Gravel is considered to be sediment with a grainsize greater than 2000 μm, sand from 63 to 2000 μm and mud < 63 μm (Wentworth 1922). Fine sand (125–250 μm) was included specifically as it was considered an important predictor of scallops (see section 19.4.3, page 149). Sediment mean grainsize (MGS) is measured using the Folk (1954) graphic mean method and measured in Phi (logarithmic) units. On this scale, the Phi diameter of a particle is calculated by the negative logarithm to the base 2 of the particle diameter, in millimetres (Donoghue 2016). Calcium carbonate ($CaCO_3$) is reported as the total percentage relative to other mineral grains and is commonly measured through acid dissolution (Siesser and Rogers 1971).

In total an additional 1177 gravel/sand/mud, 475 calcium carbonate, 1386 mean grainsize, and 302 fine sand sediment samples were added to the existing MARS database (Table 20-1). The spatial density of sediment samples was highest around Yeppoon, Gladstone, Hervey Bay, Fraser Island and in areas of the Capricorn-Bunker reefs (Figure 20-2). Sample density was rarely greater than 1 or 2 per 10 km^2 elsewhere on the continental shelf and very low in depths greater than 500 m. Modelling the distribution of sediments in southeast Queensland was based upon using the six abovementioned sediment properties as response variables.

Table 20-1. Number of sediment samples collected by each survey for mud (M), sand (S) and gravel (G), CaCO3, and mean grainsize and fine sand (FS), and the data source for each survey. The Geoscience Australia MARine Sediment database (MARS) can be publicly accessed from http://dbforms.ga.gov.au/pls/www/npm.mars.search. * is the year of publication and may not represent the year the data were obtained or processed.

Survey	M/S/G samples	CaCO$_3$ samples	MGS samples	FS samples	Source	Year
Fitzroy Keppel	176	60	86	86	MARS Database	2003–2004
Fitzroy Vibracoring Programme	20	14	10	10	MARS Database	2003
GBR Seabed Biodiversity Project Lady Basten Cruise 1	170	170	170	170	MARS Database	2003
Great Barrier Reef Seabed Biodiversity Project Lady Basten Cruise 3+4	255	255	256	256	MARS Database	2004–2006
Queensland Northern Fisheries 1994–1999	124	0	0	0	MARS Database	1994–1999
Reef Rescue Marine Monitoring Program	29	0	0	0	MARS Database	2011–2012
Sonne_SO15	190	52	186	0		1980
Southern Barrier Reef and Northern Tasman Sea	195	195	0	0	MARS Database	1970
Southern Queensland Margin	102	207	8	4	MARS Database	1991
Tasman Sea and Bass Strait	2	2	0	0	MARS Database	1972
TOTAL – MARS samples	1263	955	716	526		
FRDC Project 2017-048	166	165	166	166	Current FRDC 2017-048 project	2018–2019
Hervey Bay Coast	721	0	742	0	Stephens *et al.* (1988)	1988*
Hervey Bay and its estuaries	47	0	47	47	Ribbe (2014)	2014*
Capricorn Channel	0	0	184	0	Marshall (1977)	1997*
Southern Great Barrier Reef	158	310	158	0	Maxwell and Maiklem (1964)	1964*
Great Sandy Strait	85	0	89	89	Tarabbia (1990)	1990*
TOTAL – Additional samples	1177	475	1386	302		
TOTAL – All samples	2440	1430	2102	828		

20.3.3 *Predictive variables*

To improve the performance of spatial interpolation methods, covariates were included in the predictive models. An important covariate in the spatial interpolation of seabed sediments is bathymetry (Verfaillie *et al.* 2006; Li *et al.* 2011a). Bathymetry data were sourced from Beaman (2010) at 100 m resolution. The bathymetry dataset is a compilation of multiple individual datasets, acquired from ship-based multibeam and single beam echosounder surveys, airborne LiDAR bathymetry surveys and satellite data (Beaman 2010). The high-resolution bathymetry dataset has been interpolated to fill in missing data points to provide 100% coverage over the study area. An additional eight derivatives of the bathymetry were calculated as important predictive variables in the prediction of sediment distributions (Table 20-2).

'Coast' represented the distance from a given location to the nearest point along the Australian coast, and was derived from a vector coastline file of Wessel and Smith (1996). The distance from coast calculation was undertaken using ArcGIS ArcMap 10.6.1 (ESRI 2018). The resulting file was then converted to a raster dataset and combined with the bathymetry derivatives.

'Banks' represented the presence and absence of geomorphic bank features on the seabed. Geomorphic bank features are features raised more than 15 m above the surrounding seabed with at least one steep slope greater than approximately 2 degrees. Banks was derived from the 100 m resolution bathymetry data produced by Beaman (2010) using the method described by Harris et al. (2013).
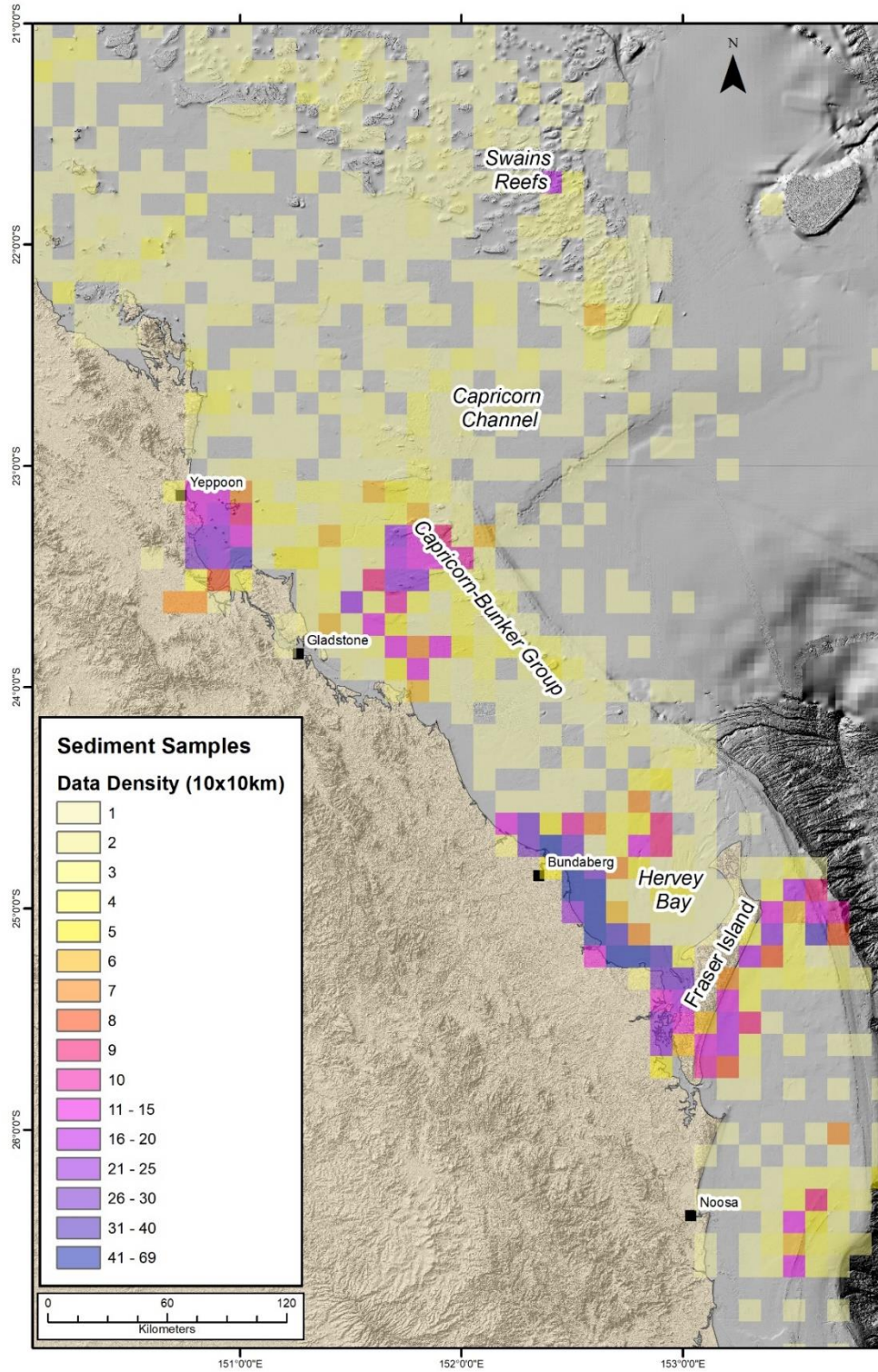
Figure 20-2. Density of sediment samples in southeast Queensland.

Table 20-2. Predictive variables and a description of what they measure.

Number	Predictive variable	Variable name	Details/description
1	Banks	banks	Identifies the location of deep reef habitats
2	Bathymetry	bathy	Depth to the seabed
3	Northing	north	Aspect of raster cell (X component)
4	Easting	east	Aspect of raster cell (Y component)
5	Latitude	y	'Y' coordinates of a given point
6	Longitude	x	'X' coordinates of a given point
7	TPI	tpi	Topographic Position Index (measures concavity/flatness/convexity)
8	Slope	slope	Slope gradient of the seabed (measured in degrees)
9	StdDev 1	stdddev_1	Standard deviation of bathymetry (measured at a distance of one pixel)
10	StdDev 5	stddev_5	Standard deviation of bathymetry (measured at a distance of five pixels)
11	Coast	coast	Distance from the coastline (km)

20.3.4 Predictive models

Twelve predictive models were compared to determine the optimal model to map the distribution of the six sediment composition properties. Deterministic interpolation methods (i.e., Inverse Distance Weighted, IDW) were compared to machine learning methods and their hybrid methods. The different machine learning methods compared were the commonly used Random Forest (RF) and Boosted Regression Tree (GBM) algorithms. The models tested: 1) the degree to which excluding the latitude and longitude variables impacted predictions, 2) whether using only those sediment sample data that had co-located high-resolution bathymetry measures improved model accuracy compared to using all sediment data which included interpolated bathymetry data, and 3) if hybrid interpolation methods (RFIDW and GBMIDW) improved predictions compared to basic RF and GBM (Table 20-3). Although the various sediment datasets were obtained over several decades (Table 20-1) no temporal variation in sediment properties was considered in the models. IDW does not require any statistical assumptions to be met (Chen and Liu 2012). Similarly, machine learning methods are robust against outliers and do not require statistical assumptions to be met (Cutler *et al.* 2009). The predictive models were carried out in R using the 'spm' package (Li 2019c). This package has functions to run each of the methods of interest as well as their hybrids, to assess model accuracy, test variable importance and produce spatial predictions.

Table 20-3. Full name and description for the abbreviations of all predictive models.

Method	Test
IDWd	IDW with default values
IDW	IDW with optimized values
RF	Random Forrest with all variables
RFxy	Random Forrest without Lat/Lon variables
RFb	Random Forrest with all variables, only using samples that were co-located with high res bathy
RFIDW	Random Forrest/IDW with all variables
RFIDWb	Random Forrest/IDW with all variables, only using samples that were co-located with high res bathy
GBM	GBM with all variables
GBMxy	GBM without Lat/Lon variables
GBMb	GBM with all variables, only using samples that were co-located with high res bathy
GBMIDW	GBM/IDW with all variables
GBMIDWb	GBM/IDW with all variables, only using samples that were co-located with high res bathy

20.3.5 *Inverse Distance Weighted Interpolation*

The IDW method is a deterministic or non-geostatistical spatial interpolation method (Li *et al.* 2011a) which relies on the assumption that an unsampled point within a given neighbourhood has an attribute value equal to the weighted average of known sampled values within the neighbourhood. The distances between the unsampled point and each sampled point within the neighbourhood is inversely related to the weights for each of the sampled points. This assumes that the values of sampled points close to the unsampled point are more alike than points further away (Lu and Weng 2007).

There were two parameters which could be adjusted in the IDW method, the number of points used in the prediction (nmax) and the distance power weighting parameter (idp). As the distance from prediction and the value of the power parameter increases, the weight of each sampled point decreases, giving samples near the prediction a higher weight and a greater influence on the final estimation. In this study two IDW methods were considered; a default IDW method (IDWd) and an optimised IDW method (IDW). IDWd used the default parameters determined by Li *et al.*, (2019), where idp = 2 and nmax = 12. The cross-validation function in spm (i.e., idwcv) was used to determine the optimal parameters for IDW, comparing the weights ranging from 1.4 to 3.0 at increments of 0.1 for idp and the number of samples ranging from 4 to 16 at increments of 1 for nmax.

20.3.6 *Random Forest*

Random Forest (RF) is a machine learning method based on an ensemble of decision trees (Breiman 2001; Kingsford and Salzberg 2008). Decision trees are formed from a set of sampled points with known attribute values which are analysed and classified based on a set of variables to generate a predicted attribute value for an unsampled point. At each node a decision tree will split the samples into groups that are the most different, or form subgroups with samples that are the least different (Kingsford and Salzberg 2008). RF can produce accurate predictions by taking the predicted attribute values from the ensemble of trees and assigning the average of the attribute values to the unsampled point. The values used by each decision tree in a RF model are sampled independently from a training set of known sample values and all trees within the ensemble have the same distribution. Advantages of RF are the improvement in classification accuracy through the growth of multiple trees and the insensitivity to 'noisy' or strongly correlated predictor variables (Breiman 2001).

There were two parameters which could be adjusted in the RF method, the number of trees used in the prediction (ntree) and the number of variables tried at each node (mtry). The number of trees has an influence on the predictive accuracy of the model, while the number of variables tried at each node also influences the predictive accuracy but at the cost of diminishing diversity in individual trees. The cross-validation function in spm (i.e., rfcv) was used to determine the optimal parameters for all RF models, comparing the number of trees ranging from 500 to 5000 at increments of 500 for ntree and the number of variables ranging from 3 to 9 at increments of 1 for mtry.

20.3.7 *Generalised Boosting Method*

Boosted Regression Tree or Generalised Boosting Method (GBM) is another machine learning method based on an ensemble of decision trees (Kingsford and Salzberg 2008). GBM improves the accuracy of predictions through the fitting of multiple decision trees repetitively. Utilising the boosting method, a random subset of sampled points is chosen to build a tree. Each tree built produces a suggestion to improve the accuracy of the model which is used to weight the selected sampled points to build a new decision tree. Sampled points which have been poorly modelled are more likely to be chosen in a consecutive tree, improving the accuracy of the final predictions (Elith *et al.* 2008; Benton 2015). Advantages of GBM are the increase in predictive ability, capability to be flexible and understanding of complex environmental relationships (Hjort and Marmion 2008). GBM is similar to RF in many respects, however, GBM models improve tree performance over time and present a weighted average result. In comparison, RF simply produce a predetermined number of

trees and present an average of the final result. GBMs are expected to theoretically give superior results to RF but are also more complex and time consuming to train.

There were two parameters which could be adjusted in the GBM; the number of trees used in the prediction (ntree) and the learning rate (lrate). The number of trees has an influence on the predictive accuracy of the model, while the learning rate ensures that no individual tree will lead the model to focus too strongly on certain characteristics of the data or to produce final estimates reflecting sampled points. The cross-validation function in spm (i.e., gbmcv) was used to determine the optimal parameters for all GBM models, comparing the number of trees ranging from 1000 to 10,000 at increments of 1000 for ntree and the fraction each tree contributes to the developing model with values of 0.1, 0.01, 0.001, 0.0001 and 0.00001 for lrate.

20.3.8 Hybrid methods

Two hybrid methods were considered: the combination of RF with IDW (RFIDW) and GBM with IDW (GBMIDW). In each model RF or GBM was applied first, followed by the application of IDW to the residuals of these models. Final sediment predictions for each of these hybrid methods were produced by combining the predicted values of each model with the corresponding interpolated residual values (Li *et al.* 2011a). The cross-validation functions in spm (i.e., rfidwcv and gbmidwcv) were used to determine the optimal parameters for all hybrid models, comparing the ranges for ntree, mtry, lrate, idp and nmax as defined above for the corresponding interpolation method.

20.3.9 Variable importance

The importance of a predictor variable gives an indication of how much the variable contributes to the predictive accuracy of the model. The importance of predictor variables for RF was based on average variable importance (AVI). A function in spm, avi was used and iterated 100 times to stabilise the variable importance generated by the RF algorithm. The values for mtry and ntree were set to the default values (a function of the number of remaining predictor variables to use as the mtry parameter and a value of 500 was used for the ntree parameter (Li 2019c). The importance of predictor variables for GBM was based on relative variable influence (RVI). Importance of predictor variables was determined by a function in spm, rvi. The values for lrate and ntree were set to the optimum parameter values for the corresponding model.

20.3.10 Model validation

The performance of the IDW, RF and GBM models developed was assessed through ten-fold cross validation. In ten-fold cross validation the sediment sample dataset is randomly divided into ten approximately equally sized data subsets. One of these subsets is retained to validate the predictions produced by the model given a dataset containing the remaining nine subsets. The process was replicated for each of the ten subsets until each subset has been used as a validation dataset, producing ten prediction datasets (Kohavi 1995). Based on the findings of previous studies, the ten-fold cross validation process was repeated for 100 iterations (Li 2013b; Li *et al.* 2014; 2019). The error produced by these predictions was defined as the Variance Explained by cross validation (VEcv) and was used to select the optimum model. The VEcv values for each model were compared in Mann-Whitney tests to determine the differences in the predictive accuracy between the various models developed for the prediction of seabed sediment distributions.

20.3.11 Assessment of predictive models

The best performing method for each of the sediment parameters was achieved by ranking each model based on VEcv from 1–12. The highest rank, modal rank, and average rank for each method was then calculated to determine the overall best performing method for predicting each sediment distribution in southeast Queensland. Plots of sediment composition for the southeast Queensland, scallop survey strata and the SRAs were calculated to provide insights into sediment distributions. The final sediment distribution maps were then inspected for artefacts.

All modelling was carried out using R 3.6.2 (R Core Team 2019). The gstat for geostatistical modelling (Pebesma 2004; Gräler *et al.* 2016), randomForest for RF (Liaw and Wiener 2002), and gbm for GBM (Greenwell *et al.* 2019) packages form part of the base of the spm package. To produce the final map of predicted sediment distribution in southeast Queensland for each of the sediment properties the most accurate predictive model was used. All maps were produced using ArcGIS ArcMap 10.6.1 (ESRI 2018).

20.4 RESULTS

20.4.1 Comparison of mud content models

A summary of the accuracy of the IDW, RF, GBM, RFIDW and GBMIDW models for predicting mud content is illustrated in Figure 20-3. A summary of the outputs produced by each optimal predictive model is displayed in Table 20-4. A statistical comparison of the predictive models using Mann-Whitney tests is provided in Table 20-5.

The top three models for predicting mud content were RFb, RFIDW and GBMIDWb. These models explained the most variation by the cross validation with a VEcv of 76.1, 75.6 and 75.6, respectively. Overall, the RFb model was the most accurate. The most important covariates used by the top models for predicting the mud content were x, y, bathy and coast. Among the top three models, RFb was significantly more accurate than RFIDW and GBMIDWb in terms of VEcv (%) based on the Mann-Whitney tests (with p-values < 0.002). There was no significant difference in predictive accuracy between the RFIDW and GBMIDWb models in terms of the Mann-Whitney tests (with p-value = 0.937).

The predictive accuracy of the RF, GBM, and GBMIDW models increased by only using those sediment samples that had co-located high-resolution bathymetry measures, compared to using all sediment data with interpolated bathymetry. The RFb, GBMb and GBMIDWb models (with VEcv values of 76.1, 72.2 and 75.6, respectively) were significantly more accurate than the RF, GBM and GBMIDW models (with VEcv values of 71.2, 62.6 and 70.1, respectively) based on the Mann-Whitney tests (with p-values < 0.0001). However, RFIDWb was less accurate than the RFIDW model, since the VEcv of RFIDW (75.6) was lowered through the exclusion of sediment samples that do not intersect high-resolution bathymetry in comparison with RFIDWb (with a VEcv of 75.0).

It was evident that the exclusion of latitude and longitude as covariates in the machine learning methods (models developed for RF and GBM) decreased the accuracy of the predictions for mud content. The difference in VEcv for RFxy and GBMxy (52.6 and 47.4, respectively) significantly increased by 10% between these models and the next best ranked model, GBM with a VEcv of 62.6 (with p-values < 0.0001).
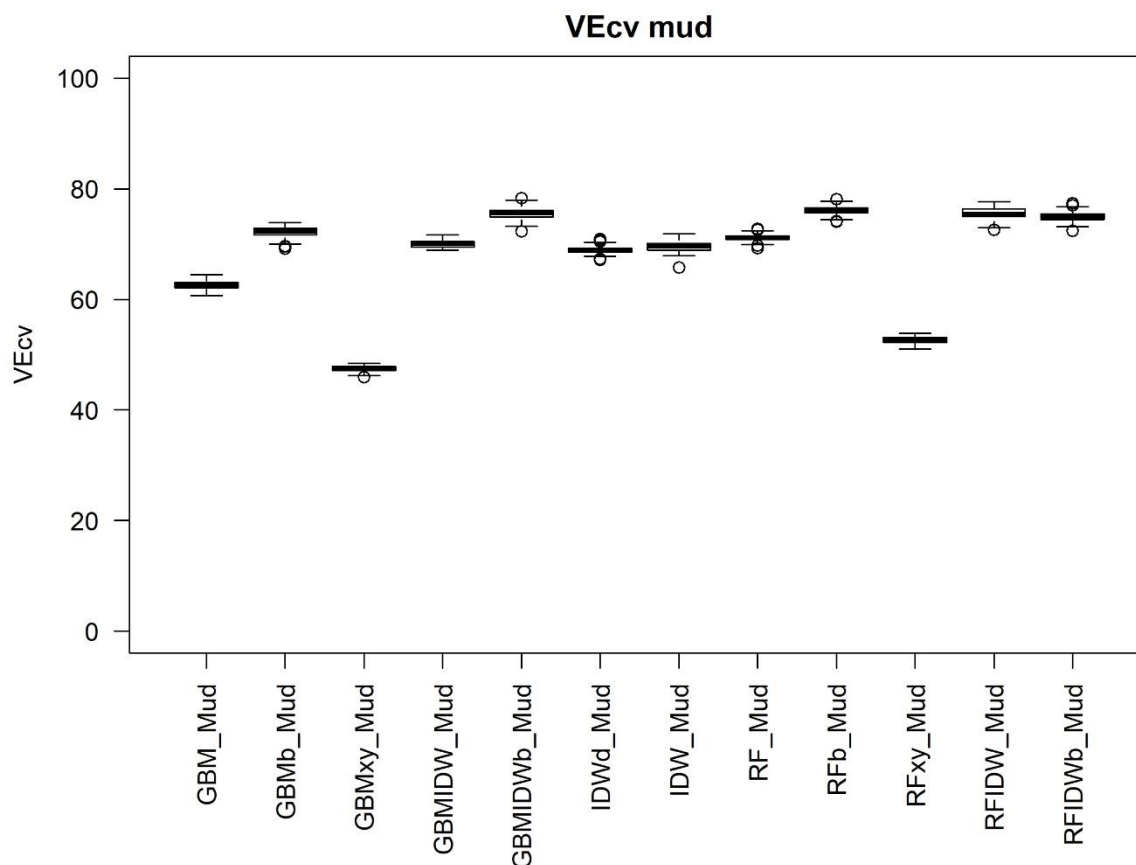
Figure 20-3. The VEcv (%) of the GBM, GBMIDW, IDW, RF, and RFIDW models for predicting seabed mud content.

Table 20-4. Comparison of the predictive models developed for mud content. Number of sediment samples used by each model, the optimal training variables used within each method, the top four covariates used within each model, the mean VEcv (%) produced by each model and the rank of each model based on the mean VEcv (%).

Model	Number of samples	Optimal Training Variables	Top 4 important covariates	Mean VEcv (%)	Rank
IDWd	2382	**Min Error:** 69.3 **idp:** 2 **nmax:** 12	-	68.9	9
IDW	2382	**Min Error:** 71.1 **idp:** 1.7 **nmax:** 6	-	69.6	8
RF	2382	**Min Error:** 71.6 **mtry:** 8 **ntree:** 1000	x y bathy coast	71.2	6
RFxy	2382	**Min Error:** 45.2 **mtry:** 9 **ntree:** 500	bathy coast stddev1 slope	52.6	11
RFb	1233	**Min Error:** 77.2	x	76.1	1

Model	Number of samples	Optimal Training Variables	Top 4 important covariates	Mean VEcv (%)	Rank
		mtry: 8 **ntree:** 3500	y bathy coast		
RFIDW	2382	**Min Error:** 78.5 **mtry:** 5 **ntree:** 3000 **idp:** 3 **nmax:** 8	x y bathy coast	75.6	2
RFIDWb	1233	**Min Error:** 78.3 **mtry:** 5 **ntree:** 7000 **idp:** 1.8 **nmax:** 12	x y bathy coast	75.0	4
GBM	2382	**Min Error:** 64.8 **ntree:** 10000 **lrate:** 0.1	bathy coast x y	62.6	10
GBMxy	2382	**Min Error:** 48.6 **ntree:** 2000 **lrate:** 0.01	bathy coast stddev5 east	47.4	12
GBMb	1233	**Min Error:** 73.2 **ntree:** 8000 **lrate:** 0.01	bathy x coast y	72.2	5
GBMIDW	2382	**Min Error:** 72.7 **lrate:** 0.001 **ntree:** 4000 **idp:** 1.8 **nmax:** 12	x y bathy coast	70.1	7
GBMIDWb	1233	**Min Error:** 78.4 **lrate:** 1.00E–04 **ntree:** 6000 **idp:** 2.2 **nmax:** 8	x y bathy coast	75.6	3

Table 20-5. Comparisons of VEcv (%) of the spatial predictive models developed for mud content. The difference between models is based on the Mann-Whitney test.

Model	p-value										
	GBM _Mud	GBMb _Mud	GBMxy _Mud	GBMIDW _Mud	GBMIDWb _Mud	IDWd _Mud	IDW _Mud	RF _Mud	RFb _Mud	RFxy _Mud	RFIDW _Mud
GBM_Mud											
GBMb_Mud	0										
GBMxy_Mud	0	0									
GBMIDW_Mud	0	0	0								
GBMIDWb_Mud	0	0	0	0							
IDWd_Mud	0	0	0	0	0						
IDW_Mud	0	0	0	0.001	0	0					
RF_Mud	0	0	0	0	0	0	0				
RFb_Mud	0	0	0	0	0.002	0	0	0			
RFxy_Mud	0	0	0	0	0	0	0	0	0		
RFIDW_Mud	0	0	0	0	0.937	0	0	0	0.002	0	
RFIDWb_Mud	0	0	0	0	0.002	0	0	0	0	0	0.001

20.4.2   Comparison of sand content models

A summary of the accuracy of the predictive models developed for IDW, RF, GBM, RFIDW and GBMIDW on predicting sand content is illustrated in Figure 20-4. A summary of the optimal outputs produced by each predictive model is displayed in Table 20-6. A comparison of the predictive models is provided in Table 20-7.

The top three models for predicting sand content were RF, GBMIDWb and RFb. These models explained the most variance by the cross validation with a VEcv of 53.0, 52.6 and 52.2, respectively. Overall, the RF model was the most accurate. The most important covariates used by the top models for predicting sand content were x, y, bathy and coast. Among the top three models, RF was significantly more accurate than GBMIDWb and RFb in terms of VEcv (%) based on the Mann-Whitney tests (with p-values < 0.013). There was no significant difference in predictive accuracy between the GBMIDWb and RFb models in terms of the Mann-Whitney tests (with p-value = 0.109).

The accuracy of the RFIDW and GBMIDW models increased by only using those sediment samples that had co-located high-resolution bathymetry measures, compared to using all sediment data with interpolated bathymetry. The GBMIDWb (with VEcv of 52.6) model was significantly more accurate than the GBMIDW model (with VEcv of 51.1) which included all sediment samples, based on the Mann-Whitney tests (with a p-value < 0.0001). There was no significant difference in accuracy in terms of VEcv (%) between the RFIDW and RFIDWb models (51.7 and 51.9, respectively) based on the Mann-Whitney test (with a p-value = 0.171). However, RFb and GBMb were less accurate than the RF and GBM models, since the VEcv of RF (53.0) and GBM (45.8) were lower through the exclusion of sediment samples that do not intersect high-resolution bathymetry in comparison with RFb (with a VEcv of 52.2) and GBMb (with a VEcv of 39.3).

It was evident that the exclusion of latitude and longitude as covariates in the machine learning methods (models developed for RF and GBM) decreased the accuracy of the predictions for sand content. The difference in VEcv for RFxy and GBMxy (34.8 and 30.3, respectively) significantly increased by 5% between these models and the next best ranked model, GBMb with a VEcv of 39.3 (with p-values < 0.0001).
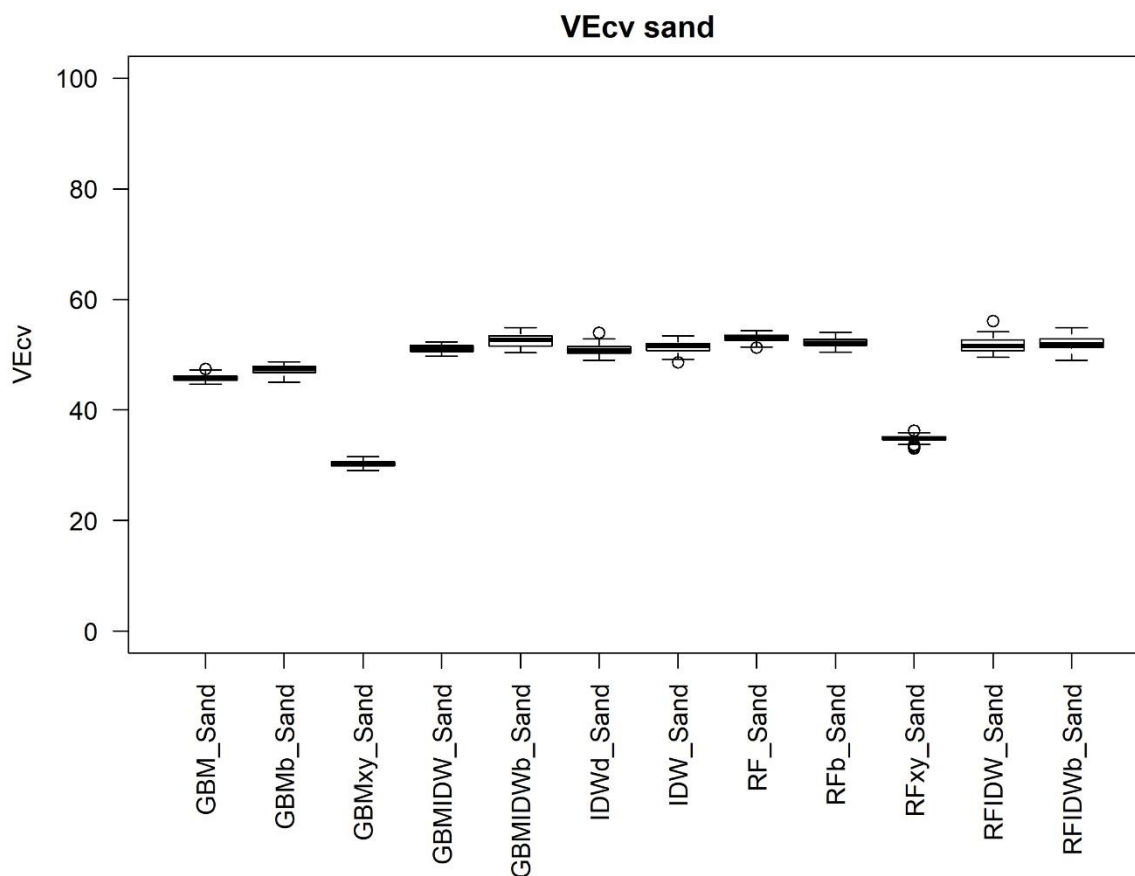
Figure 20-4. The VEcv (%) of the GBM, GBMIDW, IDW, RF, and RFIDW models for predicting seabed sand content.

Table 20-6. Comparison of the predictive models developed for sand content. Number of sediment samples used by each model, the optimal training variables used within each method, the top four covariates used within each model, the mean VEcv (%) produced by each model and the rank of each model based on the mean VEcv (%).

Model	Number of samples	Optimal Training Variables	Top 4 important covariates	Mean VEcv (%)	Rank
IDWd	1677	**Min Error:** 49.9 **idp:** 2 **nmax:** 12	-	50.9	8
IDW	1677	**Min Error:** 53.1 **idp:** 1.7 **nmax:** 14	-	51.4	6
RF	1677	**Min Error:** 53.0 **mtry:** 6 **ntree:** 1000	x y bathy coast	53.0	1
RFxy	1677	**Min Error:** 29. 9 **mtry:** 3 **ntree:** 2500	bathy coast stddev5 slope	34.8	11
RFb	1006	**Min Error:** 52.6 **mtry:** 8	x bathy	52.2	3

Model	Number of samples	Optimal Training Variables	Top 4 important covariates	Mean VEcv (%)	Rank
		ntree: 3000	y		
			coast		
RFIDW	1677	**Min Error:** 55.2	x	51.7	5
		mtry: 9	bathy		
		ntree: 1000	y		
		idp: 3	coast		
		nmax: 10			
RFIDWb	1006	**Min Error:** 55.4	x	51.9	4
		mtry: 9	bathy		
		ntree: 7000	y		
		idp: 3	coast		
		nmax: 10			
GBM	1677	**Min Error:** 46.9	bathy	45.8	10
		ntree: 3000	x		
		lrate: 0.01	y		
			coast		
GBMxy	1677	**Min Error:** 30.9	bathy	30.3	12
		ntree: 3000	coast		
		lrate: 0.01	stddev5		
			east		
GBMb	1006	**Min Error:** 48.4	bathy	47.3	9
		ntree: 8000	y		
		lrate: 0.01	x		
			coast		
GBMIDW	1677	**Min Error:** 53.9	x	51.1	7
		lrate: 0.001	y		
		ntree: 8000	bathy		
		idp: 1.4	coast		
		nmax: 10			
GBMIDWb	1006	**Min Error:** 56.7	x	52.6	2
		lrate: 1.00E–05	bathy		
		ntree: 8000	y		
		idp: 1.8	coast		
		nmax: 8			

Table 20-7. Comparisons of VEcv (%) of the spatial predictive models developed for sand content. The difference between models is based on the Mann-Whitney test.

Model	p-value										
	GBM_Sand	GBMb_Sand	GBMxy_Sand	GBMIDW_Sand	GBMIDWb_Sand	IDWd_Sand	IDW_Sand	RF_Sand	RFb_Sand	RFxy_Sand	RFIDW_Sand
GBM_Sand											
GBMb_Sand	0										
GBMxy_Sand	0	0									
GBMIDW_Sand	0	0	0								
GBMIDWb_Sand	0	0	0	0							
IDWd_Sand	0	0	0	0.166	0						
IDW_Sand	0	0	0	0.008	0	0					
RF_Sand	0	0	0	0	0.013	0	0				
RFb_Sand	0	0	0	0	0.109	0	0	0			
RFxy_Sand	0	0	0	0	0	0	0	0	0		
RFIDW_Sand	0	0	0	0.038	0.001	0.001	0.654	0	0.001	0	
RFIDWb_Sand	0	0	0	0	0.025	0	0.011	0	0.16	0	0.171

20.4.3   Comparison of seabed gravel content models

A summary of the accuracy of the IDW, RF, GBM, RFIDW and GBMIDW models for predicting gravel content is illustrated in Figure 20-5. A summary of the optimal outputs produced by each predictive model is displayed in Table 20-8. A comparison of the predictive models is provided in Table 20-9.

The top three models for predicting gravel content were IDW, RF and GBMIDWb. These models explained the most variation in terms of their VEcv (33.0, 32.9 and 32.5, respectively). Overall, the IDW model was the most accurate. The most important covariates used by the top machine learning method model for predicting the gravel content were y, x, coast and bathy. Among the top three models, IDW was not significantly more accurate than RF (with a p-value = 0.444) but was significantly more accurate than GBMIDWb in terms of VEcv (%) based on the Mann-Whitney tests (with p-value < 0.05). There was no significant difference in predictive accuracy between the RF and GBMIDWb models in terms of the Mann-Whitney tests (with p-value = 0.09).

The accuracy of the RFIDW and GBMIDW models did not significantly increase by only using those sediment samples that had co-located high-resolution bathymetry measures, compared to using all sediment data with interpolated bathymetry, based on the Mann-Whitney tests (with p-values = 0.493 and 1, respectively), although the RFIDWb and GBMIDWb models (with VEcv values of 32.1 and 32.5, respectively) ranked higher than models that included all sediment samples. However, RFb and GBMb models with a VEcv of 29.0 and 22.2, respectively, were less accurate than the RF and GBM models, with a VEcv of 32.9 and 25.0, respectively.

It was evident that the exclusion of latitude and longitude as covariates in the machine learning methods (models developed for RF and GBM) decreased the accuracy on the predictions for gravel content. The difference in VEcv for RFxy and GBMxy (11.4 and 9.7, respectively) significantly increased by 14% between these models and the next best ranked model, GBM with a VEcv of 25.0 (with p-values < 0.0001).
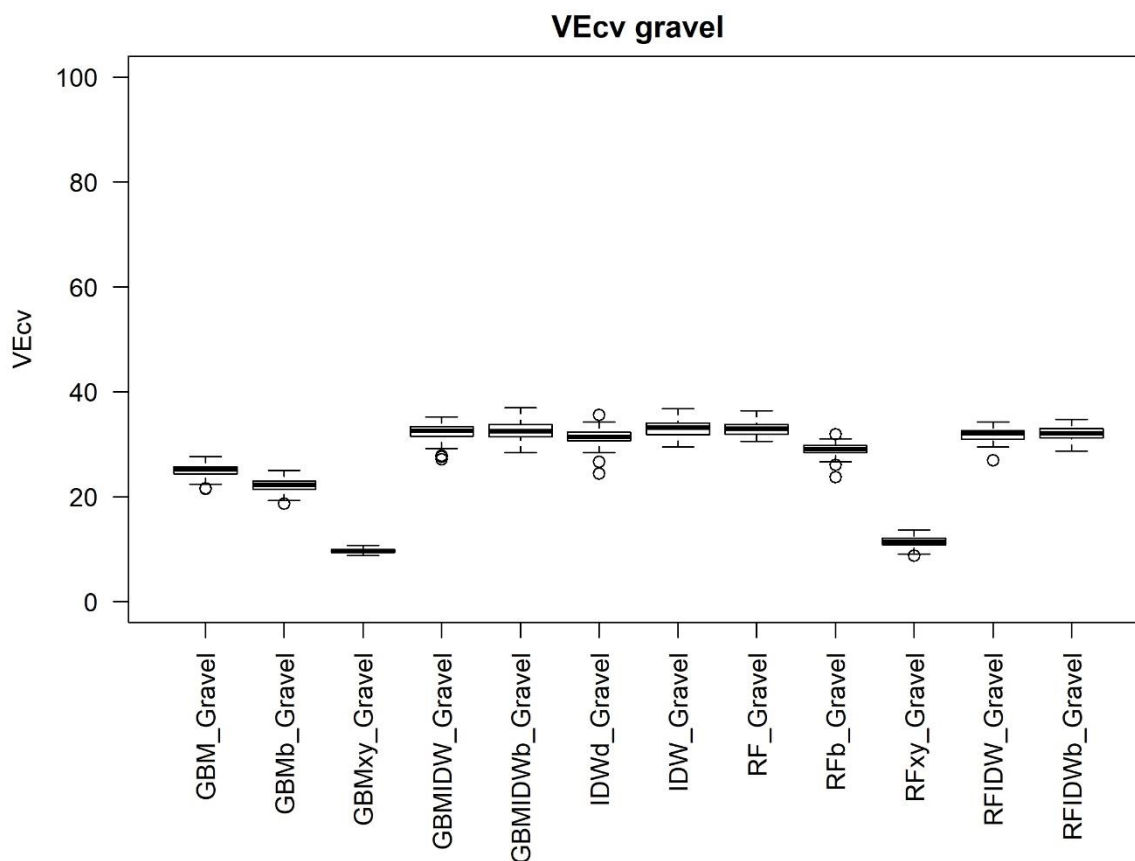
Figure 20-5. The VEcv (%) of the GBM, GBMIDW, IDW, RF, and RFIDW models for predicting seabed gravel content.

Table 20-8. Comparison of the predictive models developed for gravel content. Number of sediment samples used by each model, the optimal training variables used within each method, the top four covariates used within each model, the mean VEcv (%) produced by each model and the rank of each model based on the mean VEcv (%).

Model	Number of Samples	Optimal Training Variables	Top 4 important covariates	Mean VEcv (%)	Rank
IDWd	1669	**Min Error:** 30.1 **idp:** 2 **nmax:** 12	-	31.4	7
IDW	1669	**Min Error:** 35.5 **idp:** 1.4 **nmax:** 16	-	33.0	1
RF	1669	**Min Error:** 34.0 **mtry:** 5 **ntree:** 1000	y x coast bathy	32.9	2
RFxy	1669	**Min Error:** 9.3 **mtry:** 6 **ntree:** 500	stddev1 slope coast bathy	11.4	11
RFb	1004	**Min Error:** 30.5	y	29.0	8

Model	Number of Samples	Optimal Training Variables	Top 4 important covariates	Mean VEcv (%)	Rank
		mtry: 7 **ntree:** 1000	x coast bathy		
RFIDW	1669	**Min Error:** 36.0 **mtry:** 7 **ntree:** 1000 **idp:** 3 **nmax:** 10	y x coast bathy	31.9	6
RFIDWb	1004	**Min Error:** 36.5 **mtry:** 5 **ntree:** 5000 **idp:** 3 **nmax:** 12	y x coast bathy	32.1	5
GBM	1669	**Min Error:** 27.3 **ntree:** 5000 **lrate:** 0.01	y x coast stddev5	25.0	9
GBMxy	1669	**Min Error:** 10.3 **ntree:** 9000 **lrate:** 0.001	coast stddev5 tpi bathy	9.7	12
GBMb	1004	**Min Error:** 24.5 **ntree:** 6000 **lrate:** 0.01	y x coast tpi	22.2	10
GBMIDW	1669	**Min Error:** 35.7 **lrate:** 1.00E–05 **ntree:** 8000 **idp:** 1.6 **nmax:** 12	y x coast bathy	32.3	4
GBMIDWb	1004	**Min Error:** 36.3 **lrate:** 0.001 **ntree:** 2000 **idp:** 1.6 **nmax:** 10	y x coast bathy	32.5	3

Table 20-9. Comparisons of VEcv (%) of the spatial predictive models developed for gravel content. The difference between models is based on the Mann-Whitney test.

Model	p-value										
	GBM _Gravel	GBMb _Gravel	GBMxy _Gravel	GBMIDW _Gravel	GBMIDWb _Gravel	IDWd _Gravel	IDW _Gravel	RF _Gravel	RFb _Gravel	RFxy _Gravel	RFIDW _Gravel
GBM_Gravel											
GBMb_Gravel	0										
GBMxy_Gravel	0	0									
GBMIDW_Gravel	0	0	0								
GBMIDWb_Gravel	0	0	0	1							
IDWd_Gravel	0	0	0	0	0						
IDW_Gravel	0	0	0	0.025	0.041	0					
RF_Gravel	0	0	0	0.088	0.09	0	0.444				
RFb_Gravel	0	0	0	0	0	0	0	0			
RFxy_Gravel	0	0	0	0	0	0	0	0	0		
RFIDW_Gravel	0	0	0	0.061	0.056	0.034	0	0	0	0	
RFIDWb_Gravel	0	0	0	0.226	0.269	0.006	0.001	0.001	0	0	0.493

20.4.4   *Comparison of seabed calcium carbonate content models*

A summary of the accuracy of the IDW, RF, GBM, RFIDW and GBMIDW models for predicting calcium carbonate content is illustrated in Figure 20-6. A summary of the optimal outputs produced by each predictive model is displayed in Table 20-10. A comparison of the predictive models is provided in Table 20-11.

The top three models for predicting seabed calcium carbonate content were RFb, GBMIDWb and RFIDWb. These models explained the most variation in terms of VEcv (82.3, 82.0 and 80.9, respectively). Overall, the RFb model was the most accurate. The most important covariates used by the top models for predicting the calcium carbonate content were x, coast, y and bathy. Among the top three models, RFb was significantly more accurate than GBMIDWb and RFIDWb in terms of VEcv (%) based on the Mann-Whitney tests (with p-values < 0.0001). The GBMIDWb also had significantly higher predictive accuracy than the RFIDWb model in terms of the Mann-Whitney tests (with p-value < 0.0001).

The accuracy of the RF, RFIDW, GBM, and GBMIDW models increased by only using those sediment samples that had co-located high-resolution bathymetry measures, compared to using all sediment data with interpolated bathymetry. The RFb, RFIDWb, GBMb and GBMIDWb models, with VEcv values of 82.3, 80.9, 78.4 and 82.0, respectively, were significantly more accurate than the RF, RFIDW, GBM and GBMIDW models (with VEcv values of 80.4, 78.5, 75.5 and 79.4, respectively) which included all sediment samples, based on the Mann-Whitney tests (with p-values < 0.0001).

It was evident that the exclusion of latitude and longitude as covariates in the machine learning methods (models developed for RF and GBM) decreased the accuracy of the calcium carbonate predictions. The difference in VEcv for RFxy and GBMxy (53.8 and 49.0, respectively) significantly increased by 21% between these models and the next best model, GBM with a VEcv of 75.5 (with p-values < 0.0001).

VEcv CaCO3
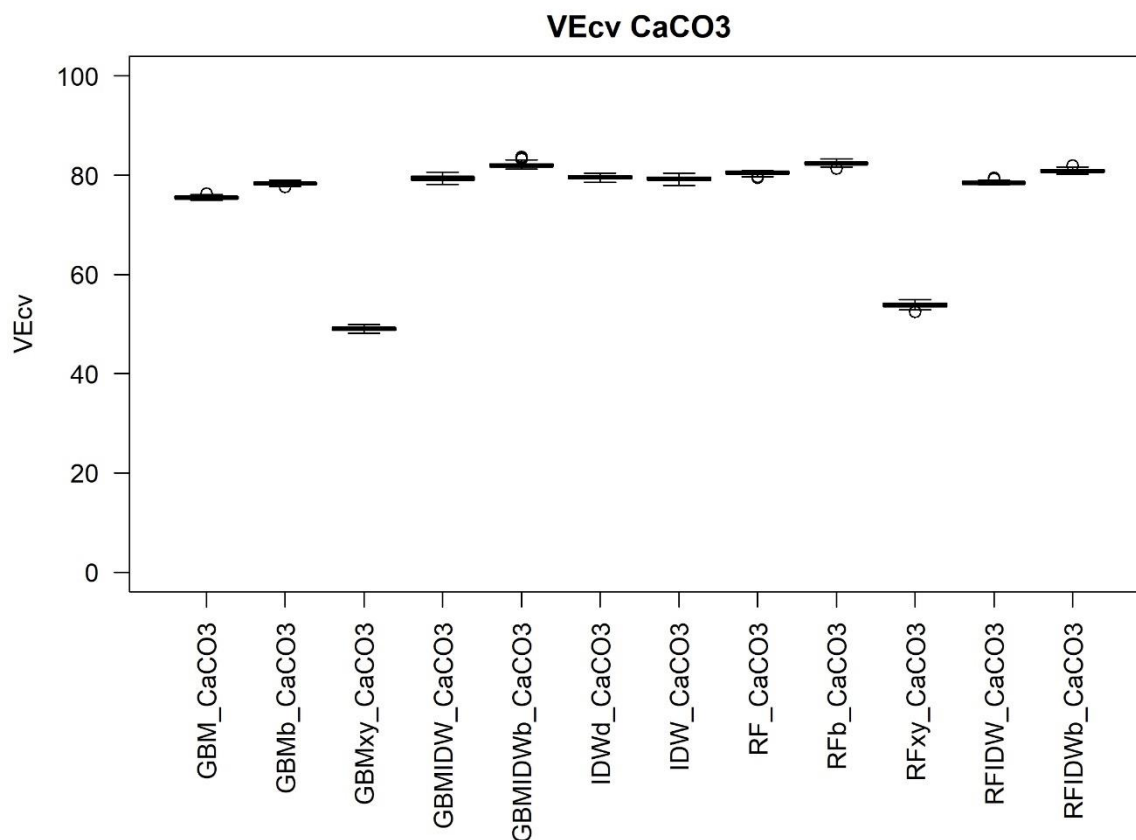
Figure 20-6. The VEcv (%) of the GBM, GBMIDW, IDW, RF, and RFIDW models for predicting seabed calcium carbonate content.

Table 20-10. Comparison of the predictive models developed for calcium carbonate content. Number of sediment samples used by each model, the optimal training variables used within each method, the top four covariates used within each model, the mean VEcv (%) produced by each model and the rank of each model based on the mean VEcv (%).

Model	Number of samples	Optimal Training Variables	Top 4 important covariates	Mean VEcv (%)	Rank
IDWd	1399	**Min Error:** 79.3 **idp:** 2 **nmax:** 12	-	79.5	5
IDW	1399	**Min Error:** 80.4 **idp:** 2.3 **nmax:** 10	-	79.2	7
RF	1399	**Min Error:** 79.2 **mtry:** 8 **ntree:** 4500	x coast y bathy	80.4	4
RFxy	1399	**Min Error:** 45.2 **mtry:** 8 **ntree:** 4500	coast bathy stddev5 banks	53.8	11

Model	Number of samples	Optimal Training Variables	Top 4 important covariates	Mean VEcv (%)	Rank
RFb	919	**Min Error:** 82.2 **mtry:** 7 **ntree:** 1500	x coast y bathy	82.3	1
RFIDW	1399	**Min Error:** 79.7 **mtry:** 5 **ntree:** 7000 **idp:** 2.8 **nmax:** 6	x coast y bathy	78.5	8
RFIDWb	919	**Min Error:** 82.3 **mtry:** 5 **ntree:** 3000 **idp:** 2 **nmax:** 12	x coast y bathy	80.9	3
GBM	1399	**Min Error:** 75.9 **ntree:** 9000 **lrate:** 0.01	x coast y bathy	75.5	10
GBMxy	1399	**Min Error:** 49.6 **ntree:** 10000 **lrate:** 0.01	coast bathy stddev5 north	49.0	12
GBMb	919	**Min Error:** 79.3 **ntree:** 4000 **lrate:** 0.01	x coast y stddev5	78.4	9
GBMIDW	1399	**Min Error:** 80.7 **lrate:** 1.00E–05 **ntree:** 2000 **idp:** 1.8 **nmax:** 8	x coast y bathy	79.4	6
GBMIDWb	919	**Min Error:** 83.9 **lrate:** 1.00E–05 **ntree:** 6000 **idp:** 1.8 **nmax:** 10	x coast y bathy	82.0	2

Table 20-11. Comparisons of VEcv (%) of the spatial predictive models developed for calcium carbonate content. The difference between models is based on the Mann-Whitney test.

Model	p-value										
	GBM $\_CaCO_3$	GBMb $\_CaCO_3$	GBMxy $\_CaCO_3$	GBMIDW $\_CaCO_3$	GBMIDWb $\_CaCO_3$	IDWd $\_CaCO_3$	IDW $\_CaCO_3$	RF $\_CaCO_3$	RFb $\_CaCO_3$	RFxy $\_CaCO_3$	RFIDW $\_CaCO_3$
GBM_CaCO$_3$											
GBMb_CaCO$_3$	0										
GBMxy_CaCO$_3$	0	0									
GBMIDW_CaCO$_3$	0	0	0								
GBMIDWb_CaCO$_3$	0	0	0	0							
IDWd_CaCO$_3$	0	0	0	0.161	0						
IDW_CaCO$_3$	0	0	0	0.053	0	0					
RF_CaCO$_3$	0	0	0	0	0	0	0				
RFb_CaCO$_3$	0	0	0	0	0	0	0	0			
RFxy_CaCO$_3$	0	0	0	0	0	0	0	0	0		
RFIDW_CaCO$_3$	0	0.009	0	0	0	0	0	0	0	0	
RFIDWb_CaCO$_3$	0	0	0	0	0	0	0	0	0	0	0

20.4.5   Comparison of seabed mean grainsize models

A summary of the accuracy of the IDW, RF, GBM, RFIDW and GBMIDW models for predicting mean grainsize is illustrated in Figure 20-7. A summary of the optimal outputs produced by each predictive model is displayed in Table 20-12. A comparison of the predictive models is provided in Table 20-13.

The top three models for predicting mean grainsize were RFIDW, RFIDWb and RFb. These models explained the most variation in terms of VEcv (62.7, 62.7 and 62.6, respectively). Overall, the RFIDW was the most accurate. The most important covariates used by the top models for predicting mean grainsize were x, bathy, y and coast. Among the top three models, RFIDW was not significantly more accurate than RFIDWb or RFb in terms of VEcv (%) based on the Mann-Whitney tests (with p-values of 0.519 and 0.925, respectively). There was also no significant difference in predictive accuracy between the RFIDWb and RFb models in terms of the Mann-Whitney tests (with p-value = 0.515).

The accuracy of the RF, GBM and GBMIDW models increased by using only those sediment samples that had co-located high-resolution bathymetry measures, compared to using all sediment samples which included interpolated bathymetry. The RFb, GBMb and GBMIDWb models (with VEcv values of 62.6, 56.1 and 62.4, respectively) were significantly more accurate than the RF, GBM and GBMIDW models (with VEcv values of 59.5, 48.8 and 59.0, respectively) which include all sediment samples, based on the Mann-Whitney tests (with p-values < 0.0001). There was, however, no significant difference between the RFIDW and RFIDWb models, both of which had VEcv of 62.7.

It was evident that the exclusion of latitude and longitude as covariates in the machine learning methods (models developed for RF and GBM) decreased the accuracy of the mean grain size predictions. The difference in VEcv for RFxy and GBMxy (42.7 and 35.0, respectively) significantly increased by 6% between these models and the next best ranked model, GBM with a VEcv of 48.8 (with p-values < 0.0001).
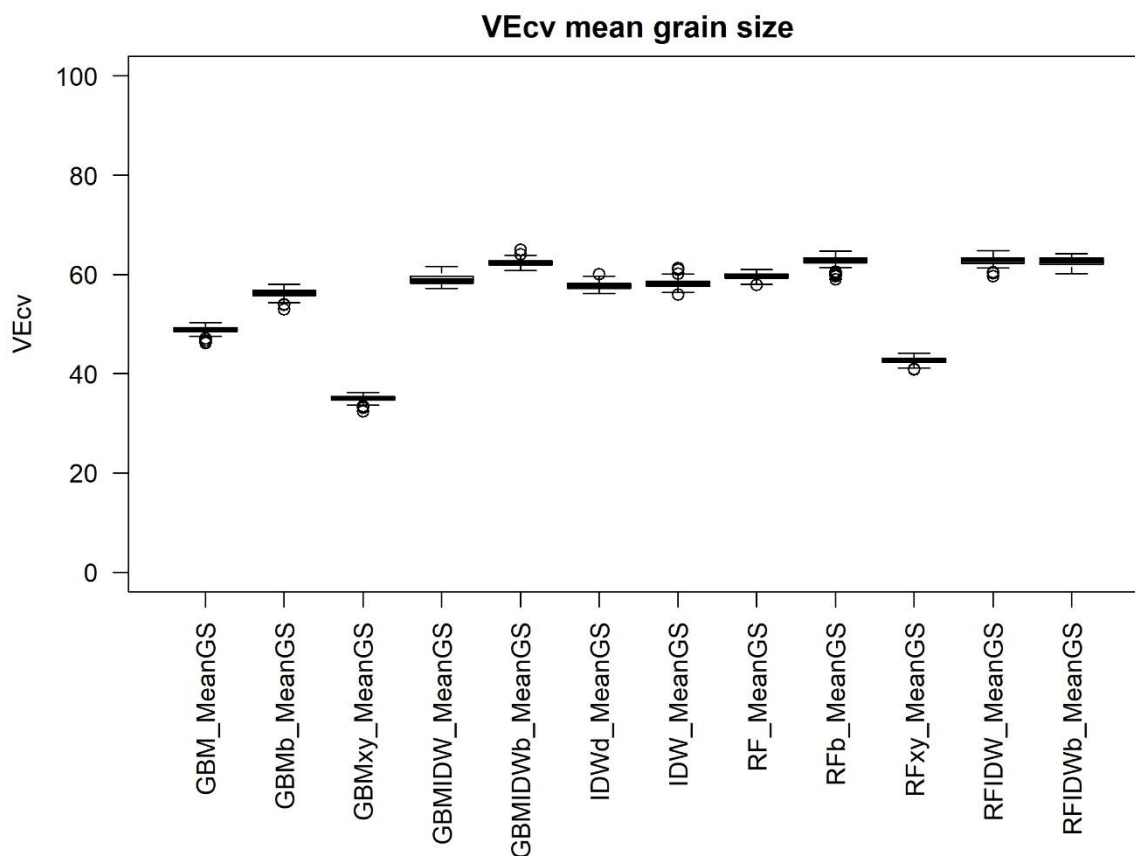
Figure 20-7. The VEcv (%) of the GBM, GBMIDW, IDW, RF, and RFIDW models for predicting seabed mean grainsize.

Table 20-12. Comparison of the predictive models developed for mean grainsize. Number of sediment samples used by each model, the optimal training variables used within each method, the top four covariates used within each model, the mean VEcv (%) produced by each model and the rank of each model based on the mean VEcv (%).

Model	Number of samples	Optimal Training Variables	Top 4 important covariates	Mean VEcv (%)	Rank
IDWd	2094	**Min Error:** 59.6 **idp:** 2 **nmax:** 12	-	57.8	8
IDW	2094	**Min Error:** 60.2 **idp:** 1.5 **nmax:** 8	-	58.1	7
RF	2094	**Min Error:** 59.9 **mtry: 9** **ntree:** 3500	x y bathy coast	59.5	5
RFxy	2094	**Min Error:** 39.8 **mtry:** 6 **ntree:** 1500	bathy coast stddev5 slope	42.7	11
RFb	1097	**Min Error:** 63.4	x	62.6	3

Model	Number of samples	Optimal Training Variables	Top 4 important covariates	Mean VEcv (%)	Rank
		mtry: 8 **ntree:** 2000	bathy y coast		
RFIDW	2094	**Min Error:** 65.4 **mtry:** 7 **ntree:** 3000 **idp:** 2.2 **nmax:** 10	x bathy y coast	62.7	1
RFIDWb	1097	**Min Error:** 65.2 **mtry:** 3 **ntree:** 7000 **idp:** 2.2 **nmax:** 10	x bathy y coast	62.7	2
GBM	2094	**Min Error:** 49.4 **ntree:** 7000 **lrate:** 0.01	bathy y x coast	48.8	10
GBMxy	2094	**Min Error:** 36.5 **ntree:** 7000 **lrate:** 0.01	bathy coast stddev5 tpi	35.0	12
GBMb	1097	**Min Error:** 57.3 **ntree:** 6000 **lrate:** 0.01	bathy y x stddev5	56.1	9
GBMIDW	2094	**Min Error:** 61.9 **lrate:** 1.00E–04 **ntree:** 8000 **idp:** 2 **nmax:** 8	x y bathy coast	59.0	6
GBMIDWb	1097	**Min Error:** 66.3 **lrate:** 1.00E–04 **ntree:** 2000 **idp:** 2.2 **nmax:** 12	x bathy y coast	62.4	4

Table 20-13. Comparisons of VEcv (%) of the spatial predictive models developed for mean grainsize. The difference between models is based on the Mann-Whitney test.

Model	p-value										
	GBM _MeanGS	GBMb _MeanGS	GBMxy _MeanGS	GBMIDW _MeanGS	GBMIDWb _MeanGS	IDWd _MeanGS	IDW _MeanGS	RF _MeanGS	RFb _MeanGS	RFxy _MeanGS	RFIDW _MeanGS
GBM_MeanGS											
GBMb_MeanGS	0										
GBMxy_MeanGS	0	0									
GBMIDW_MeanGS	0	0	0								
GBMIDWb_MeanGS	0	0	0	0							
IDWd_MeanGS	0	0	0	0	0						
IDW_MeanGS	0	0	0	0	0	0.002					
RF_MeanGS	0	0	0	0	0	0	0				
RFb_MeanGS	0	0	0	0	0.004	0	0	0			
RFxy_MeanGS	0	0	0	0	0	0	0	0	0		
RFIDW_MeanGS	0	0	0	0	0.025	0	0	0	0.925	0	
RFIDWb_MeanGS	0	0	0	0	0.059	0	0	0	0.515	0	0.519

20.4.6 Comparison of seabed fine sand (125 µm) content models

A summary of the accuracy of the IDW, RF, GBM, RFIDW and GBMIDW models for predicting fine sand content is illustrated in Figure 20-8. A summary of the optimal outputs produced by each predictive model is displayed in Table 20-14. A comparison of the predictive models is provided in Table 20-15.

The top three models for predicting fine sand content were GBMIDWb, RFIDWb and RFb. These models explained the most variation in terms of the VEcv (61.5, 60.9 and 58.3, respectively). Overall, the GBMIDWb model provided the most accurate predictions. The most important covariates used by the top models for predicting fine sand content were y, x, coast and bathy. Among the top three models, GBMIDWb was significantly more accurate than RFIDWb and RFb in terms of VEcv (%) based on the Mann-Whitney tests (with p-values < 0.002). The RFIDWb also had significantly higher accuracy than the RFb model in terms of the Mann-Whitney tests (with p-value < 0.0001).

The accuracy of the RF, RFIDW, GBM and GBMIDW models increased by using only those sediment samples that had co-located high-resolution bathymetry measures, compared to using all sediment samples which included interpolated bathymetry. The RFb, RFIDWb, GBMb and GBMIDWb models (with VEcv values of 58.3, 60.9, 50.4 and 61.5, respectively) were significantly more accurate than the RF, RFIDW, GBM and GBMIDW models (with VEcv values of 52.3, 52.9, 44.5 and 54.9, respectively) which include all sediment samples, based on the Mann-Whitney tests (with p-values < 0.0001).

It was evident that the exclusion of latitude and longitude as covariates in the machine learning methods (models developed for RF and GBM) decreased the accuracy of the fine sand content predictions. The difference in VEcv for RFxy and GBMxy (23.7 and 22.7, respectively) significantly increased by 20% between these models and the next best ranked model, GBM with a VEcv of 44.5 (with p-values < 0.0001).
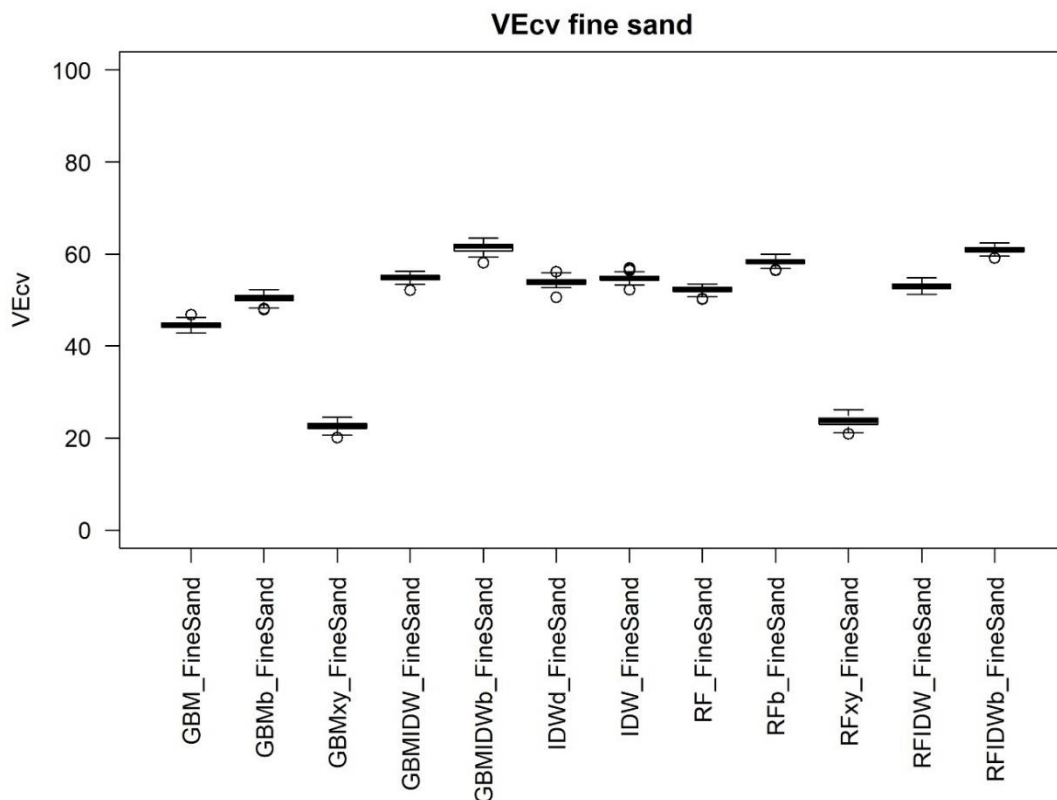
Figure 20-8. The VEcv (%) of the GBM, GBMIDW, IDW, RF, and RFIDW models for predicting seabed fine sand content.

Table 20-14. Comparison of the predictive models developed for fine sand content. Number of sediment samples used by each model, the optimal training variables used within each method, the top four covariates used within each model, the mean VEcv (%) produced by each model and the rank of each model based on the mean VEcv (%).

Fine Sand	Number of samples	Optimal Training Variables	Top 4 important covariates	Mean VEcv (%)	Rank
IDWd	828	**Min Error:** 53.9 **idp:** 2 **nmax:** 12	-	54.0	6
IDW	828	**Min Error:** 56.6 **idp:** 1.7 **nmax:** 11	-	54.8	5
RF	828	**Min Error:** 52.7 **mtry:** 6 **ntree:** 500	**var** y x bathy coast	52.3	8
RFxy	828	**Min Error:** 20.9 **mtry:** 9 **ntree:** 500	**var** bathy coast stddev5 slope	23.7	11

Fine Sand	Number of samples	Optimal Training Variables	Top 4 important covariates	Mean VEcv (%)	Rank
RFb	646	**Min Error:** 58.3 **mtry:** 7 **ntree:** 5000	**var** y x coast bathy	58.3	3
RFIDW	828	**Min Error:** 55.5 **mtry:** 7 **ntree:** 3000 **idp:** 3 **nmax:** 12	**var** y x bathy coast	52.9	7
RFIDWb	646	**Min Error:** 63.2 **mtry:** 3 **ntree:** 7000 **idp:** 1.8 **nmax:** 8	**var** y x coast bathy	60.9	2
GBM	828	**Min Error:** 44.9 **ntree:** 4000 **lrate:** 0.01	**var** y x coast bathy	44.5	10
GBMxy	828	**Min Error:** 24.7 **ntree:** 2000 **lrate:** 0.1	**var** bathy coast east stddev5	22.7	12
GBMb	646	**Min Error:** 51.5 **ntree:** 10000 **lrate:** 0.01	**var** y x coast bathy	50.4	9
GBMIDW	828	**Min Error:** 56.7 **lrate:** 1.00E–05 **ntree:** 2000 **idp:** 1.4 **nmax:** 10	**var** y x bathy coast	54.9	4
GBMIDWb	646	**Min Error:** 64.4 **lrate:** 0.001 **ntree:** 2000 **idp:** 2.6 **nmax:** 10	**var** y x coast bathy	61.5	1

Table 20-15. Comparisons of VEcv (%) of the spatial predictive models developed for fine sand. The difference between models is based on the Mann-Whitney test.

Model	p-value										
	GBM_FineSand	GBMb_FineSand	GBMxy_FineSand	GBMIDW_FineSand	GBMIDWb_FineSand	IDWd_FineSand	IDW_FineSand	RF_FineSand	RFb_FineSand	RFxy_FineSand	RFIDW_FineSand
GBM_FineSand											
GBMb_FineSand	0										
GBMxy_FineSand	0	0									
GBMIDW_FineSand	0	0	0								
GBMIDWb_FineSand	0	0	0	0							
IDWd_FineSand	0	0	0	0	0						
IDW_FineSand	0	0	0	0.617	0	0					
RF_FineSand	0	0	0	0	0	0	0				
RFb_FineSand	0	0	0	0	0	0	0	0			
RFxy_FineSand	0	0	0	0	0	0	0	0	0		
RFIDW_FineSand	0	0	0	0	0	0	0	0	0	0	
RFIDWb_FineSand	0	0	0	0	0.002	0	0	0	0	0	0

20.4.7 Comparison of models

A comparison of models for all six sediment properties is provided in Table 20-16. Across the six sediment properties IDW, RF, RFb, RFIDW and GBMIDWb achieved the highest ranking of 1 while RFIDWb achieved the highest ranking of 2. This result indicates that many of the methods tested had the potential to rank highly when predicting sediment composition. The overall lowest median and average rank (2.5 and 2.5, respectively) was achieved by GBMIDWb model and was considered to be the best performing method on average. RF, RFb and RFIDWb (with median ranks of 4.5, 3 and 3.5, respectively, and average ranks of 4.3, 3.2 and 3.3, respectively) were also highly ranked overall. For each of the sediment properties the highest ranking model was RFb for mud, RF for sand, IDW for gravel, RFb for calcium carbonate, RFIDW for mean grainsize and GBMIDWb for fine sand. Maps for the distribution of each of the six sediment properties were generated using the highest ranking model (Figures 20-10 to 20-15).

Table 20-16. Overall comparison of the models based on VEcv (%). Best rank, median rank and average rank were based on their accuracy to predict each of the six sediment properties.

Method	Best rank	Median rank	Average rank
IDWd	5	7.5	7.2
IDW	1	6.5	5.7
RF	1	4.5	4.3
RFxy	11	11	11.0
RFb	1	3	3.2
RFIDW	1	5.5	4.8
RFIDWb	2	3.5	3.3
GBM	9	10	9.8
GBMxy	12	12	12.0
GBMb	5	9	8.5
GBMIDW	4	6	5.7
GBMIDWb	1	2.5	2.5

Overall, the hybrid methods did not always provide a significant improvement over basic machine learning methods. The models developed for GBMIDW and GBMIDWb consistently outperformed GBM and GBMb, respectively, over the six sediment properties. However, the models developed for RFIDW and RFIDWb did not consistently outperform RF and RFb, respectively, over the six sediment properties.

On average across the six sediment properties, the RF, RFIDW, GBM, and GBMIDW models that used only sediment data that had co-located high-resolution bathymetry data outperformed models that used the entire sediment dataset which included extrapolated bathymetry data. The RFb, RFIDWb, GBMb, and GBMIDWb models excluded between 22 and 48% of the total sediment samples available (Table 20-17).

Table 20-17. Summary of total number of sediment samples lost by excluding samples which do not intersect high-resolution bathymetry data.

Sediment property	Total samples available	Samples intersecting bathymetry data	Total samples excluded	Percentage excluded
Mud	2382	1233	1149	48%
Sand	1677	1006	671	40%
Gravel	1669	1004	665	40%
Calcium carbonate	1399	919	480	34%
Mean grainsize	2094	1097	997	48%
Fine sand	828	646	182	22%

The models developed for RF and GBM excluding the covariates latitude and longitude (i.e., RFxy and GBMxy) were the worst performing models across all six sediment properties, with the lowest scores for best, median and average ranks. By comparison, the basic RF model, which included latitude and longitude, but was otherwise the same as RFxy, was consistently one of the best performing models.

Figure 20-9 shows a summary of the VEcv for the modelled sediment parameters and methods tested. Overall, there was considerable variation both between methods and between sediment parameters. Predictions for calcium carbonate were the most accurate overall with VEcv greater than 80% for most methods. Predictions for mud, mean grainsize and fine sand had a VEcv greater than 60% for their best performing methods. The top methods for predicting sand had a VEcv greater than 50%. Predictions for gravel were the weakest overall with the best models achieving a VEcv of less than 35%.
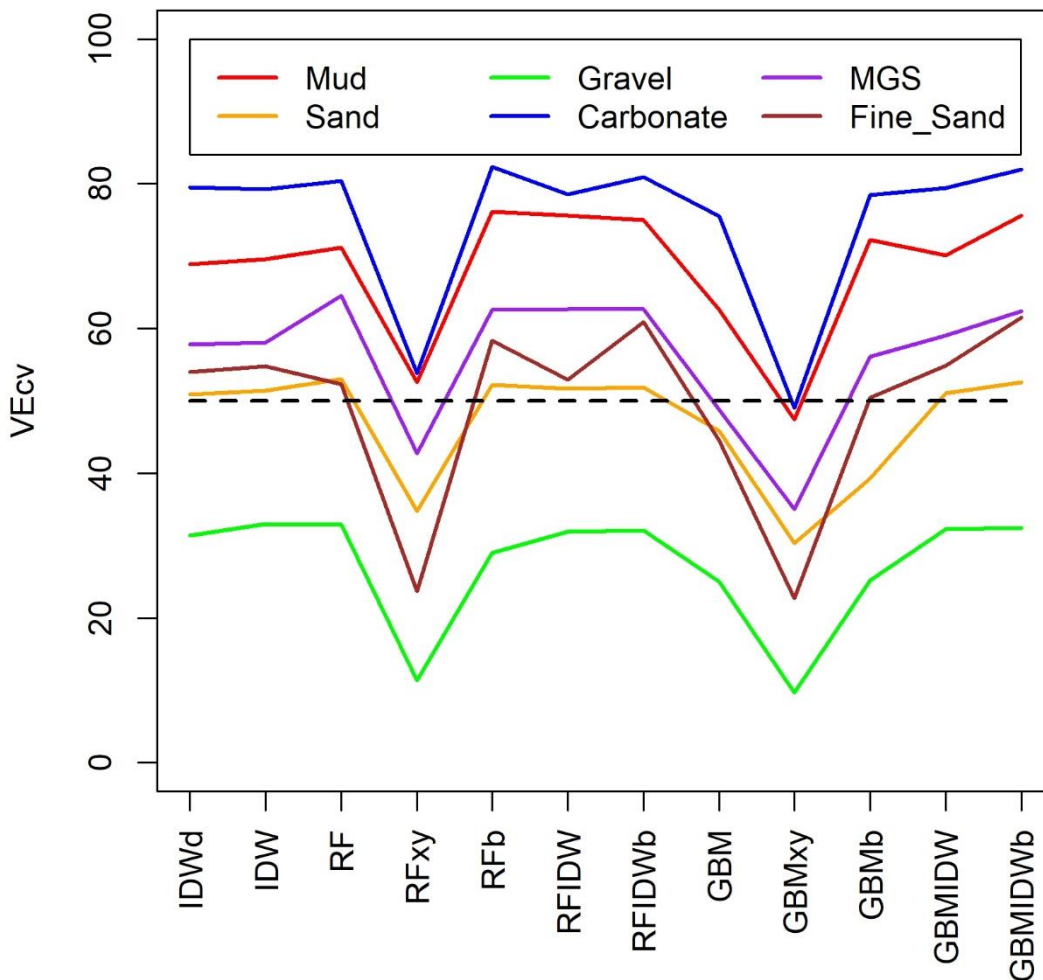
Figure 20-9. Summary of VEcv (%) of the IDW, RF, RFIDW, GBM and GBMIDW models for all sediment properties. A reference VEcv of 50% (dashed line) is shown.

20.4.8 Observations from optimum sediment predictions

Predicted mud content along the shelf and surrounding the Swain Reefs was low (Figure 21-10). Mud content was comparatively high within the Tasman Sea and peaked in the Capricorn Channel where it commonly exceeded 80%. Overall, mud content tended to be low within the study area. Within the scallop survey strata mud content was very low with approximately 50% of the region predicted to have less than 2% mud. Within the SRA's the predicted mud content was higher at 4–5%. Linear

artefacts in the predictions for mud occurred south of the Capricorn Channel, but were considered to be weak.

Predicted sand content was low in the Capricorn Channel (generally less than 20%) and offshore (less than 50%), and high (generally greater than 70%) on the inner shelf and reefal areas (i.e., the Capricorn-Bunker Group and the Swain Reefs) (Figure 20-11). Sand content was highly variable across the study area. Both the scallop survey strata, including the SRAs, generally showed high sand content that was greater than 80%. Linear artefacts in the sand prediction were considered weak to negligible.

The model indicated that gravel content was very low in the study area and restricted to isolated patches on the edge of the shelf off Fraser Island, the northern region of the Swain Reefs, the Capricorn-Bunker Group and in the far north west and north east of the study area (Figure 20-12). Overall gravel content in the study area was generally less than 20%. Gravel content within the scallop strata and SRA was commonly 5–8%. However, samples with no gravel were rare in these areas. Strong 'bulls-eye' linear artefacts occurred in the gravel predictions, mostly surrounding patches of high gravel content in deep water where there were comparatively few samples.

Predicted calcium carbonate content was low along the inner shelf of the study area and in a small 'patch' within the Capricorn Channel (Figure 20-13). Calcium carbonate content was relatively high around the Capricorn-Bunker Group, Swain Reefs, offshore from Fraser Island and on the continental slope, at depths greater than 100 m. Overall calcium carbonate content was highly variable across the study area and generally low in the scallop survey strata at approximately 5–40%. In the SRAs calcium carbonate varied from approximately 10–60%. Linear artefacts occurred in the calcium carbonate predictions, mostly in deep water where there were comparatively few samples. A strong north/south orientated artefact was apparent on the east side of the study area and a strong east/west orientated artefact was present to the south of the Capricorn Channel and to the south of the Bunker-Bunker Group.

Predicted mean grainsize (Figure 20-14) was large (i.e., low Phi values) around the Swain Reefs, Capricorn-Bunker Group, and offshore banks and small (i.e., high Phi values) on the continental slope at depths greater than 100 m. Mean grainsizes were lowest in the Capricorn Channel. Overall the mean grainsize ranged from approximately 1–5 Phi, or from coarse sand to coarse silt (Wentworth 1922). Mean grainsizes in the scallop survey strata and SRAs commonly ranged from 1–3 Phi, i.e., coarse sand to fine sand. Linear artefacts in the mean grainsize predictions were considered to be weak to negligible. Weak linear artefacts occurred in the predicted mean grainsize dataset, mainly in deep water where there were comparatively few samples.

Predictions for fine sand content were moderately high throughout the inner shelf, but were particularly high in the Yeppoon area, throughout Hervey Bay and extending to the shelf surrounding Fraser Island (Figure 20-15). The predicted fine sand content was low in surrounding reefal environments and on the continental slope, at depths greater than 100 m. Overall, there were higher concentrations of fine sand in the SRAs than the adjacent scallop survey strata. A strong north/south orientated artefact occurred on the east side of the study area intersecting Hervey Bay and the Capricorn-Bunker Group.
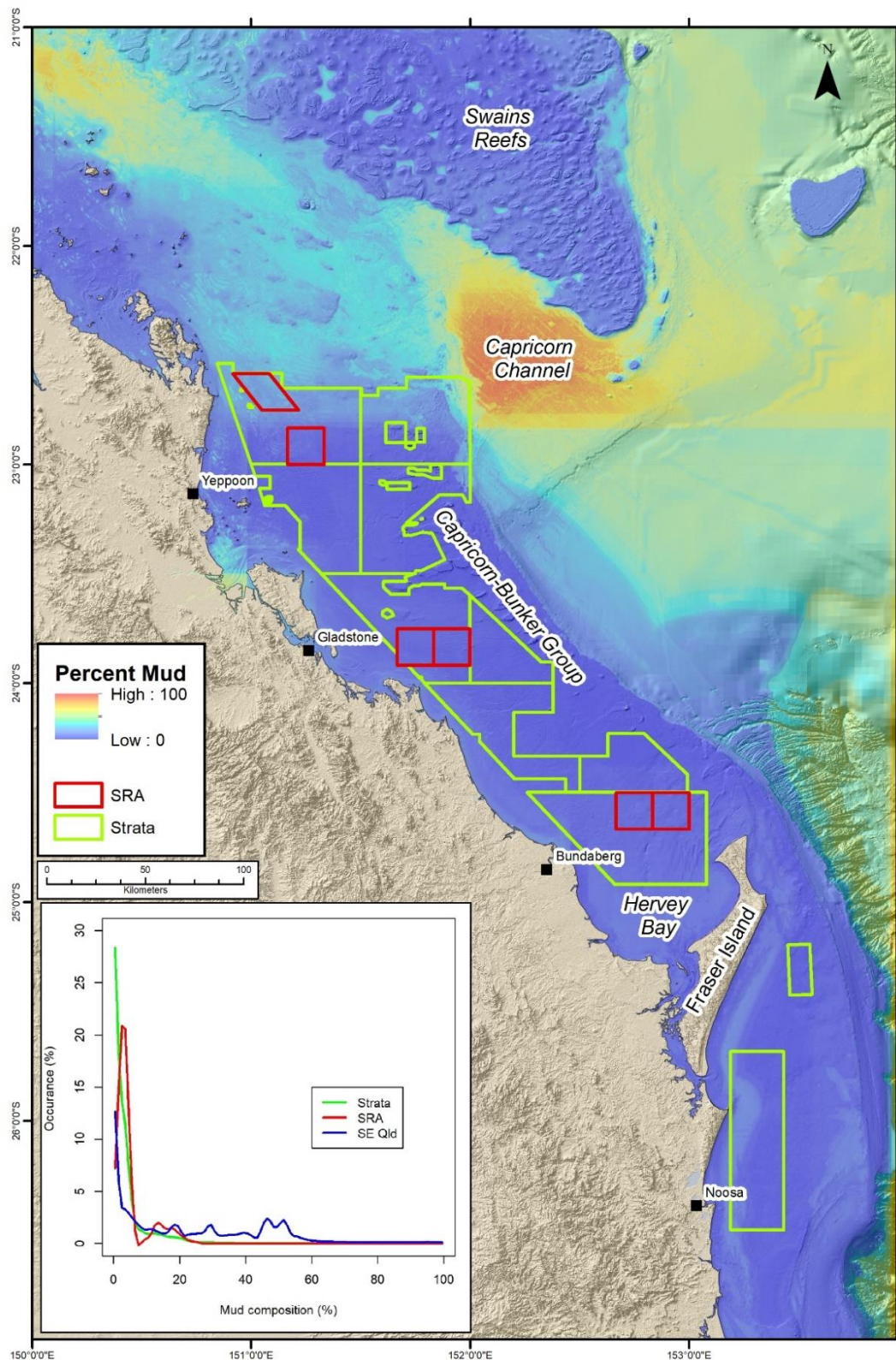
Figure 20-10. Predicted spatial distribution of seabed mud content in southeast Queensland using the RFb model overlaid on bathymetry. Also shown are key geographic areas, saucer scallop fishery survey strata and the scallop replenishment areas (SRAs). Distribution curves of interpolated pixel values indicate the percentage of mud predicted within the survey strata, SRAs and southeast Queensland.
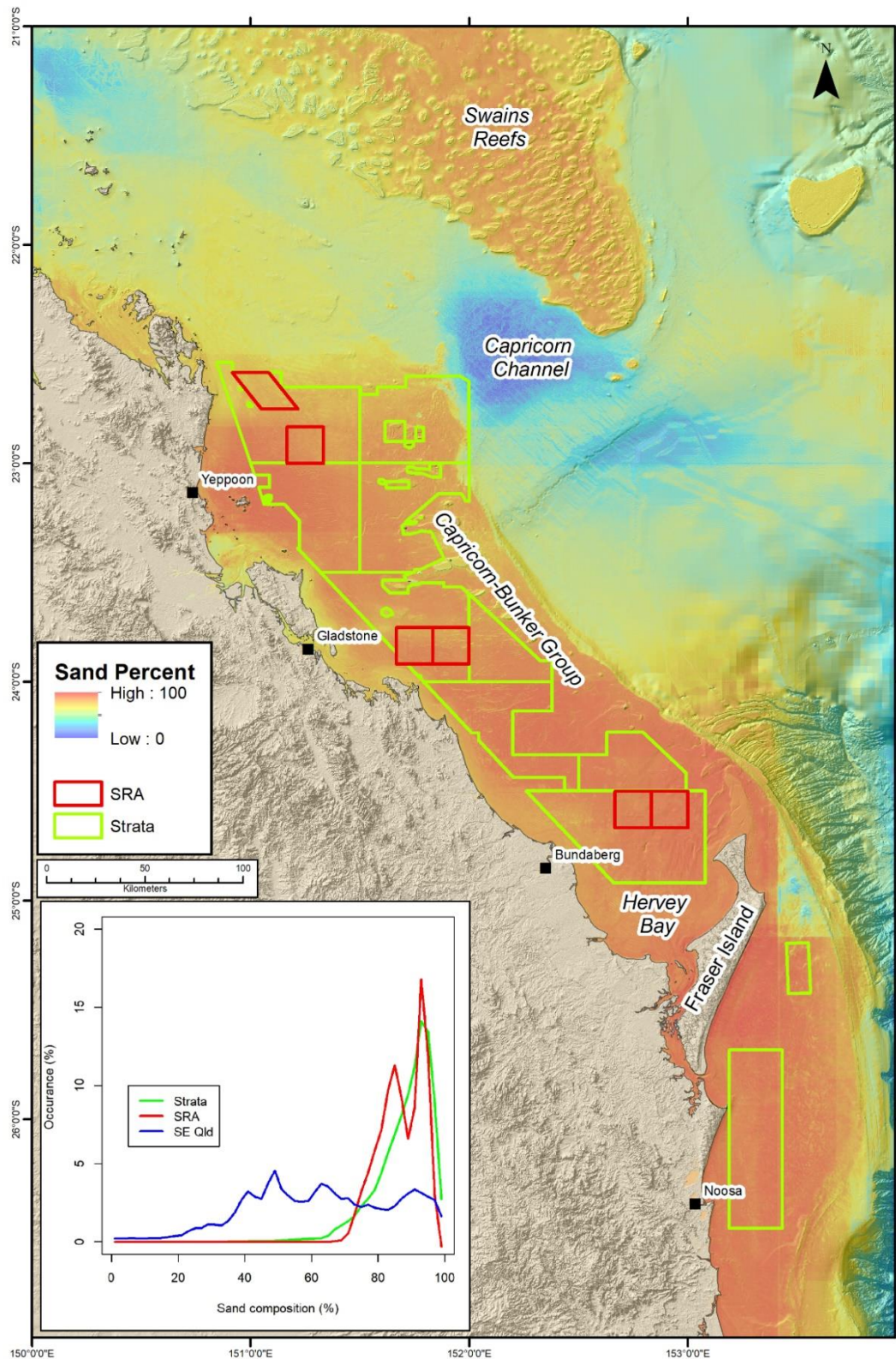
Figure 20-11. Predicted spatial distribution of seabed sand content in southeast Queensland using the RF model overlaid on bathymetry. Also shown are key geographic areas, saucer scallop fishery survey strata and the scallop replenishment areas (SRAs). Distribution curves of interpolated pixel values indicate the percentage of sand predicted within the survey strata, SRAs and southeast Queensland.
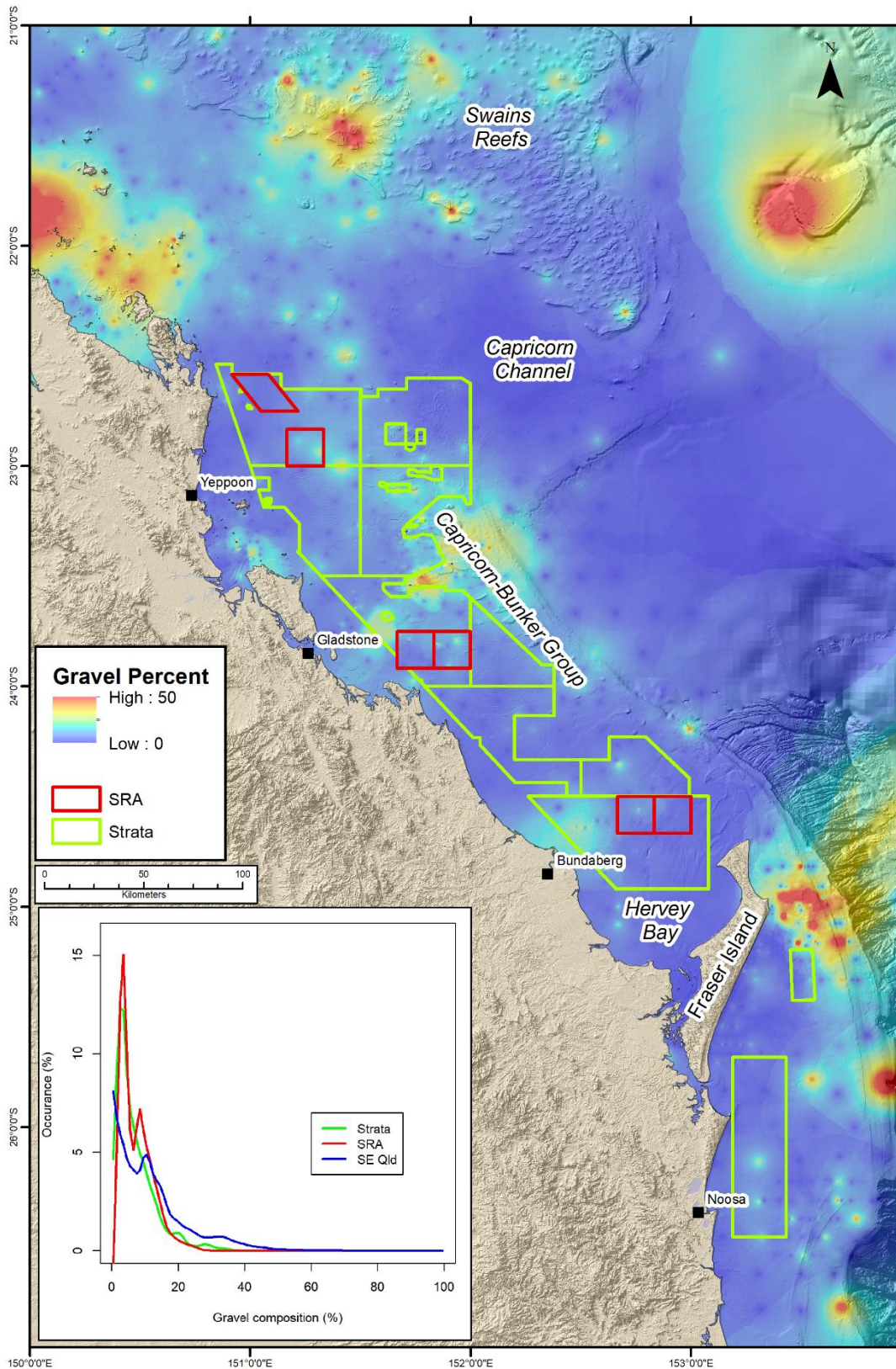
Figure 20-12. Predicted spatial distribution of seabed gravel content in southeast Queensland using the IDW model overlaid on bathymetry. Also shown are key geographic areas, saucer scallop fishery survey strata and the scallop replenishment areas (SRAs). Distribution curves of interpolated pixel values indicate the percentage of gravel predicted within the survey strata, SRAs and southeast Queensland.
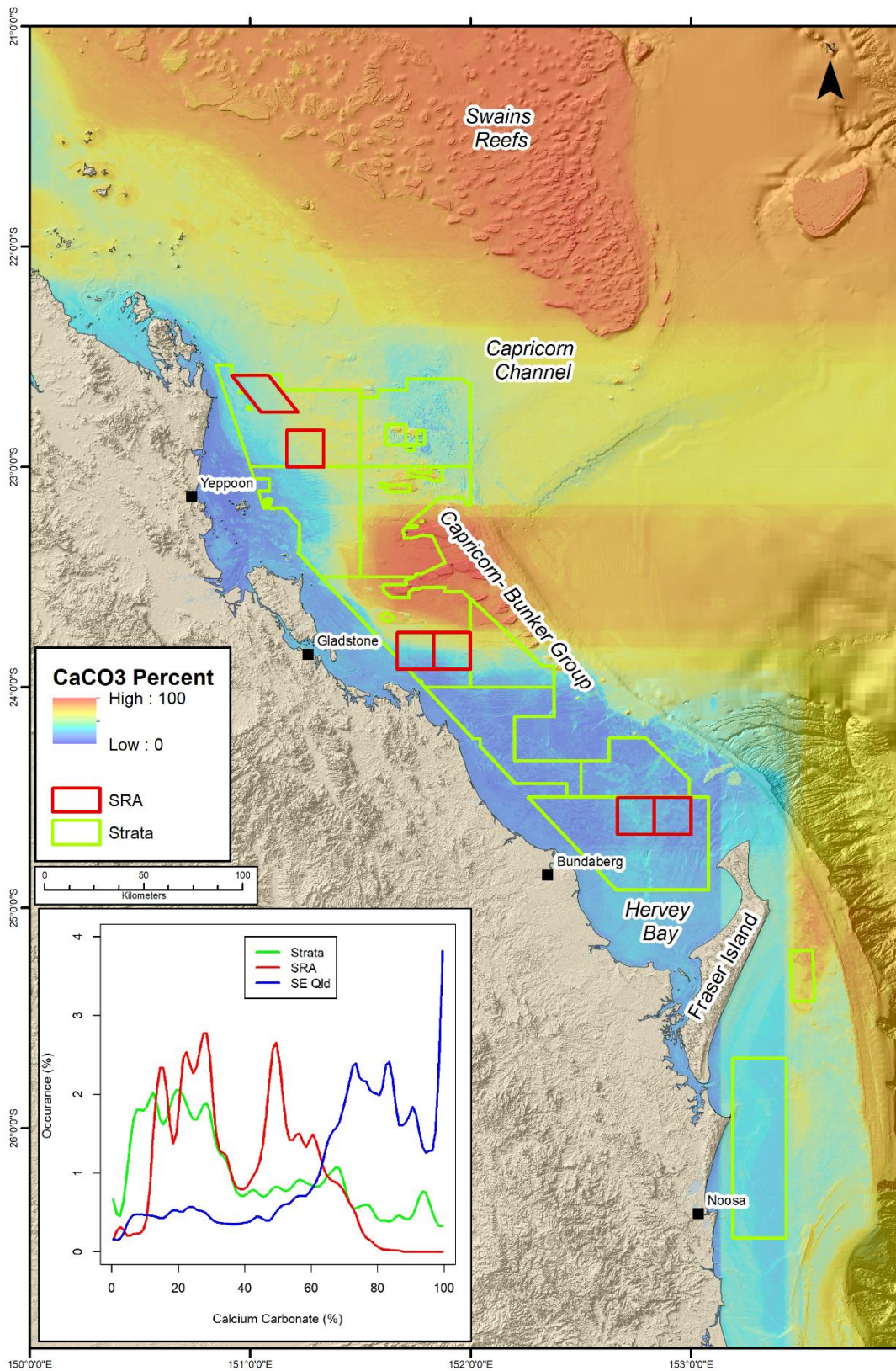
Figure 20-13. Predicted spatial distribution of seabed calcium carbonate content in southeast Queensland using the RFb model overlaid on bathymetry. Also shown are key geographic areas, saucer scallop fishery survey strata and the scallop replenishment areas (SRAs). Distribution curves of interpolated pixel values indicate the percentage of calcium carbonate predicted within the survey strata, SRAs and southeast Queensland.

196
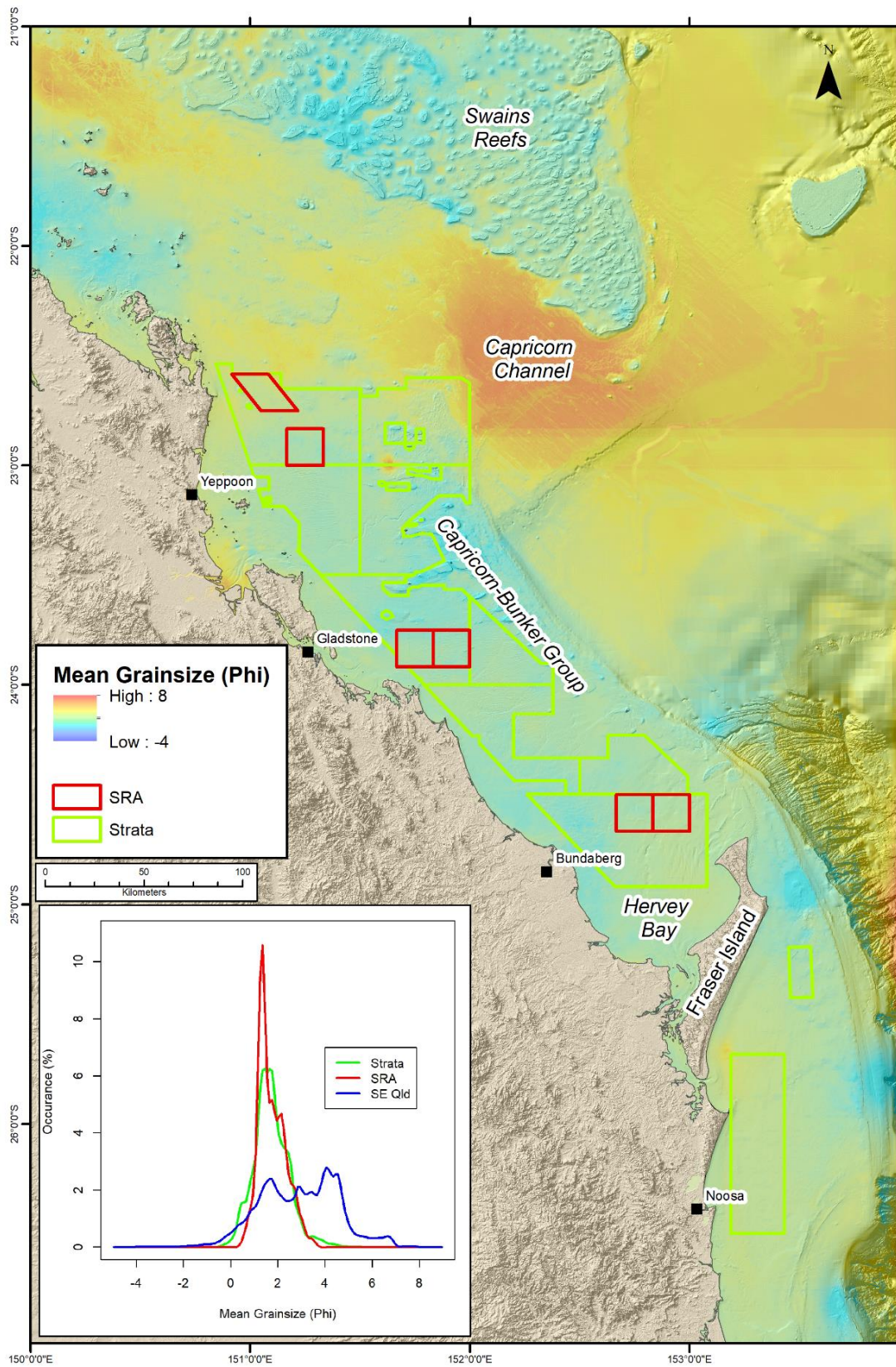
Figure 20-14. Predicted spatial distribution of seabed mean grainsize in southeast Queensland using the RFIDW model overlaid on bathymetry. Also shown are key geographic areas, saucer scallop fishery survey strata and the scallop replenishment areas (SRAs). Distribution curves of interpolated pixel values indicate the mean grainsize predicted within the survey strata, SRAs and southeast Queensland.
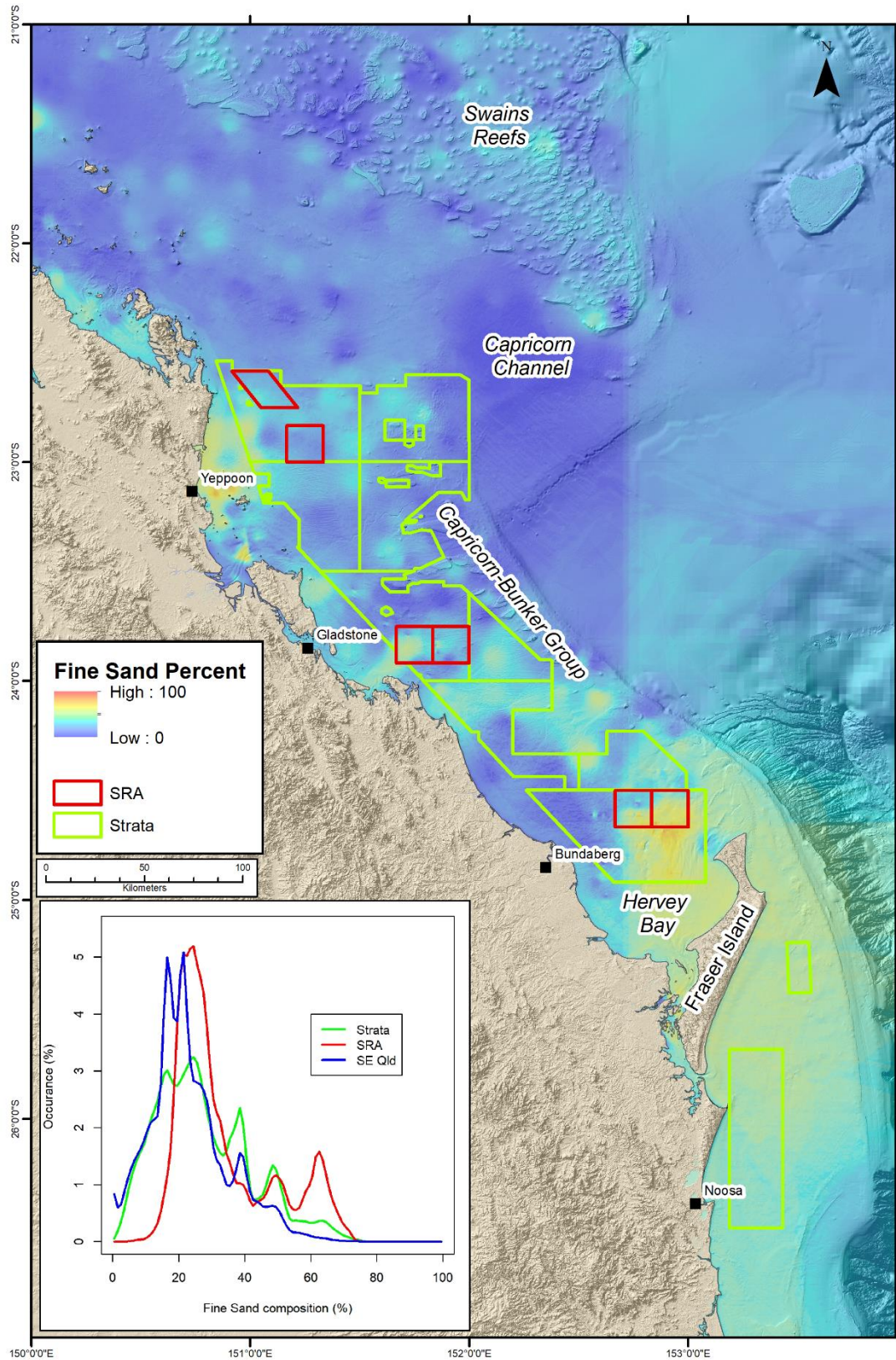
Figure 20-15. Predicted spatial distribution of seabed fine sand content in southeast Queensland using the GBMIDWb model overlaid on bathymetry. Also shown are key geographic areas, saucer scallop fishery survey strata and the scallop replenishment areas (SRAs). Distribution curves of interpolated pixel values indicate the percentage of fine sand predicted within the survey strata, SRAs and southeast Queensland.

20.5 DISCUSSION

20.5.1 Compilation of sediment samples

The MARS database was a significant source of data for this study, however, significant additional sources of data were digitised from the current FRDC project sampling, reports (Marshall 1977; Stephens *et al.* 1988; Ribbe 2014), scientific papers (Maxwell and Maiklem 1964), and theses (Maiklem 1966; Tarabbia 1990). These additional sources provided information for areas that were previously data poor, such as Hervey Bay. Regardless of the amount of data that were added, data density on the continental shelf was generally low with most 10 km^2 patches of seabed generally having ≤ 1 sample (Figure 20-2). On the continental slope and in the Tasman Sea data density dropped significantly and likely reduced the accuracy of the predictions in these areas. Data are limited due to the expense and objective of the surveys. Furthermore, most surveys have targeted a specific region, such as Hervey Bay (Stephens *et al.* 1988; Ribbe 2014) and were not systematic such as the survey carried out by Marshall (1977). The final predictions of sediment properties, however, are expected to be an improvement on past mapping that either did not have access to the volume of data for this research (Marshall 1977) or did not extend as far south as Fraser Island (Mathews *et al.* 2007).

20.5.2 Predictive accuracy of models

Hybrid statistical models, such as RFIDW and GBMIDW, have been shown to be effective tools for predicting sediment distributions and other environmental variables (Li *et al.* 2011c; 2013a; Sanabria *et al.* 2013; Li *et al.* 2017; 2019). In our study GBMIDW and GBMIDWb significantly outperformed the GBM and GBMb models, however, the RFIDW and RFIDWb models did not improve upon the RF and RFb models (Table 20-16). This was consistent with Li (2013a) and indicates that it cannot be assumed that hybrid methods will outperform other methods in all situations.

The bathymetry model used for generating covariates in the predictive model was a combination of higher resolution datasets and spatial interpolation (Beaman 2010). Given that the study area was comparatively rich in sediment samples (i.e., greater than 2000) it was decided to test if the machine learning models would be more accurate if they were trained on locations that intersected these higher-resolution datasets rather than interpolated data. This comparison was novel as it has not been attempted in the literature before and would determine if the models could produce better results with less training data under the assumption that the training data would provide superior correlations between sediments and seabed texture. Overall, models that used only sediment data that had co-located high-resolution bathymetry data (i.e., RFb, RFIDWb, GBMb, GBMIDWb) outperformed models that used the entire sediment dataset which included interpolated bathymetry data (i.e., RF, RFIDW, GBM, GBMIDW).

All models greatly outperformed the RF and GBM models which excluded latitude and longitude as covariates, indicating the importance of these variables for the machine learning predictions. Including latitude and longitude as predictor variables has been examined by Li *et al.* (2010; 2011a) and found to be associated with the creation of linear artefacts. While linear artefacts were apparent in all predictions produced by RF and GBM models, they were considered negligible in most. 'Bulls-eye' type artefacts were also common in the IDW models due to the weighting of equal data points surrounding known sampled points (Li *et al.* 2011a).

Li (2016) classified model predictions using VEcv into five categories (Table 20-18). Using these categories, the final prediction of calcium carbonate ranked as 'excellent'. Predictions for mud, sand, mean grainsize, and fine sand were 'good'. The prediction for gravel was on the poor side of 'average' and could be considered unreliable as a result. The overall poor prediction of gravel is not well understood. It is assumed that measurements of gravel did not share the same degree of spatial autocorrelation as other parameters. It is also possible that the most accurate sediment predictions, which were for mud and calcium carbonate, were partitioned into broadly homogenous provinces (i.e., mud was low on the shelf and high in the deep sea; or calcium carbonate was high near reef and low elsewhere on the shelf). The same observation cannot be made for gravel which would appear to have

a more 'patchy distribution'. The prediction accuracy for mud (VEcv of 75.6%) and calcium carbonate (VEcv of 82%) were higher than those reported by Li (2016) and Li *et al.* (2012; 2017; 2019).

Table 20-18. Classification of the accuracy of predictive models in terms of VEcv.

VEcv range	Model accuracy
VEcv ≤ 10%	Very poor
10% < VEcv ≤ 30%	Poor
30% < VEcv ≤ 50%	Average
50% < VEcv ≤ 80%	Good
80% < VEcv	Excellent

20.5.3 *Important variables for sediment property predictions*

In this study all variables were considered in the modelling of each sediment property and overwhelmingly, for all final predictions, the four most important factors were latitude (y), longitude (x), depth (bathy) and distance from coast (coast). The dominance of latitude and longitude was an indication of strong spatial autocorrelation, where samples that were close to each other were more likely to be similar than samples that were further away. This is reflected in the Tobler (1970) first law of geography which states that "everything is related to everything else, but near things are more related than distant things". Distance to coast has been identified as an important variable for predicting seabed sediments in Australia by Li (2013a) and Li *et al.* (2011a; 2011c; 2012; 2019), as it has some influence on the transportation and deposition of mud from onshore to locations with low seabed gradients. Bathymetry has also been shown to influence sediment distribution (Verfaillie *et al.* 2006; Li *et al.* 2010; 2011c).

The predictions for sediment distributions were visually consistent with previous maps of the region by Marshall (1977, 1980) which delineated key geomorphic provinces within the study area. Reefal areas such as the Capricorn-Bunker Group and the Swain Reefs were characterised by coarse sediments that were high in calcium carbonate, sand, and comparatively high in gravel, consistent with reef environments. The deeper parts of the study area such as the Capricorn Channel and the continental slope/Tasman sea were characterised by comparatively fine sediment that was high in mud content but with highly variable concentrations of calcium carbonate. The highest concentrations of mud were located in the Capricorn Channel with parts of the continental slope containing significant amounts of sand. The inner and mid continental shelf was characterised by low mud (less than 5%), high sand, and variable amounts of gravel and calcium carbonate. The predicted distribution of mean grainsizes across the study area corresponds to the content predictions for mud, sand, gravel and calcium carbonate.

Predictions for fine sand content were very low across the study area (less than 30%), except in sediments adjacent to Fraser Island. Predicted fine sand content was very low in the deep water and on the continental slope, moderately low on the continental shelf and surrounding reefs, and moderately high surrounding Fraser Island and a small area off the coast in the north of the study area. Reports of Phi-resolution sediment parameters are not commonly reported in the literature and thus not incorporated into other broader studies of sediment distributions (Marshall 1977; Mathews *et al.* 2007; Li *et al.* 2010). Despite being reported less often and rarely accounting for more than 30% of any sample, the predictions for fine sand were comparatively accurate (with VEcv greater than 60%) compared to gravel (with VEcv of approximately 33%).

Overall, the SRAs tended to display higher concentrations of mud and fine sand, and a broader range of calcium carbonate content, than the other scallop survey strata but maintained similar levels of sand and gravel, and a consistent range of mean grainsizes. The elevated amount of fine sand in the SRAs is noteworthy given the high correlation between scallop abundance and fine sand, demonstrated in the

previous section 19.4.3 (page 149). Further fishery-wide co-located sampling is required to provide further insight into this relationship.

20.5.4 Limitations and improvements

The sediment predictions generally improved by the application of machine learning methods, as found by Li *et al.* (2010; 2011c; 2014; 2017; 2019). It is likely that further improvement could be achieved through the application of variable selection (Li *et al*, 2019) and the inclusion of oceanographic covariates. Including oceanographic outputs from the GBR-scale eReefs hydrodynamic model (Steven *et al.* 2019) may also provide additional covariates to explain the sediment distributions. Sediments on the Great Barrier Reef are a result of both modern and ancient processes, as well as hydrodynamic biological processes (Wolanski 1994; Hopley 2011). Tidal currents, or a derivative thereof, may provide an indicator of sediment mobility, transport and deposition in southeast Queensland and further improve the predictions.

Random Forest and Boosted Regression Tree methods are commonly assumed to be 'less susceptible' to noisy and highly correlated predictors (Breiman 2001; Díaz-Uriarte and De Andres 2006; Elith and Leathwick 2011). However, noisy and irrelevant covariates can limit the accuracy of RF and GBM methods and commonly 'feature selection' is undertaken to identify the most instructive covariates to use in any prediction. Implementing variable selection techniques within R by using VSURF (Genuer *et al.* 2019) or Boruta (Kursa and Rudnicki 2010) may further improve predictions (Li *et al.* 2017).

20.6 CONCLUSION

This study was the first to use machine learning techniques to predict the distribution of six sediment properties at a high spatial resolution in southeast Queensland. Predictions of seabed sediment distributions have been derived from a regional bathymetry compilation and its derivatives, sediment data sourced from an online database and scientific literature, and from additional sediment samples recently acquired as part of the current project. Key results from this study were:

1. Predictions were significantly improved by using hybrid models that combine machine learning methods and geostatistics, compared to machine learning models alone. The overall and best performing model for predicting seabed sediment distributions in southeast Queensland was GBMIDWb.
2. Predictive accuracy increased significantly when latitude and longitude were included.
3. Models that used only sediment data that had co-located high-resolution bathymetry measures commonly outperformed models that used the entire sediment dataset which included extrapolated bathymetry data.
4. The most important variables contributing to model accuracy were latitude (y), longitude (x), depth (bathy) and distance from coast (coast).
5. Further investigation should explore the inclusion of oceanographic covariates, including proximity to influential river systems, and variable selection to improve model accuracy.
6. The regional maps developed for each of the six sediment properties provide insight into the geomorphic and oceanographic processes affecting the seafloor. Knowledge of sedimentary distributions can be used to identify seabed habitats and improve management of the regional marine environment and associated fisheries.

21   Appendix 9. Historic saucer scallop distributions in Southeast Queensland – a comparison of spatial prediction methods

This section of the report addresses Objective 2) *Undertake exploratory analyses on the relationship between saucer scallop abundance and bottom substrate*

21.1 ABSTRACT

The relationship between seabed composition and the density of Queensland saucer scallops (*Y. balloti*) is poorly understood. However, studies of the Atlantic sea scallop (*P. magellanicus*) fishery indicate that the inclusion of seabed composition data can improve the analysis of scallop catch rates and stock assessment. Inverse Distance Weighted (IDW), Ordinary Kriging (OK), and four variants of Random Forest (RF) were used to predict the distribution of saucer scallops in the fishing grounds from 1997–2000 and 2017–2019. Two of the RF models contained regional sediment data layers to assess the degree to which sediment distribution data improve predictions of scallop densities. The inclusion of sediment data improved predictions in some scallop survey years but was generally outperformed by OK and a simple RF model using latitude, longitude and bathymetric derivatives only. The OK model reproduced localised peaks and troughs in the sample datasets while the RF model produced a more generalised result. Averaging predictions of scallops over multiple years clearly identified broad lobes of prospective saucer scallop habitats between the coast and Capricorn-Bunker reefs, and offshore of Fraser Island. Within these lobes there are regional 'highs' in saucer scallop density overlapping with the SRAs within the fishery. Pearson's correlation coefficients showed that very coarse sand, coarse sand, mean grainsize, skewness, medium sand2 (i.e., mean sand and finer sediment), and mud variables had low to moderate correlations with scallops in most years but commonly did not contribute greatly to improved model accuracy. Improved model accuracy could be obtained by applying hybrid interpolation techniques and optimal feature selection methods. Additional modelling of these datasets based on these recommendations is suggested as future research.

21.2 INTRODUCTION

Worldwide, scallop fisheries are notorious for their large fluctuations in abundance and subsequent variability in catch. Queensland saucer scallops (*Y. balloti*) are no exception with commercial catches varying dramatically over time (Welch *et al.* 2010). Regional-scale hydrodynamic modelling and satellite-based remote sensing datasets have provided numerous insights into drivers of inter-annual variability in scallops catch rates, however, they lack the resolution needed to understand the spatial distribution of scallops on the seabed (Courtney *et al.* 2015). Reported difficulties in modelling the abundance and recruitment of scallops has indicated that it is highly likely that factors occurring at very small spatial scales (e.g., < 1 km^2) play a significant role in determining the abundance of Queensland saucer scallops. Such factors could include bottom composition, bottom aspect, or exposure to tidal currents (Welch *et al.* 2010).

Research on the Atlantic sea scallop fishery (*P. magellanicus*) found that scallop density estimates can be improved by including seafloor properties in the analyses (Kostylev *et al.* 2003; Brown *et al.* 2012; Smith *et al.* 2017; Miller *et al.* 2019). The benefits from these improvements include more accurate stock assessment, knowledge of potential scallop reseeding areas and marine protected areas, and potentially less impact on the seabed. Currently, a significant gap in Queensland saucer scallop research is a detailed understanding of the relationship between sediment texture and scallop distribution. Anecdotal evidence indicates that Queensland saucer scallops have a preference for substrates that are both soft (to enable the scallops to burrow) and have a high sand content (Welch *et al.* 2010). More recently, correlations between saucer scallop abundance and sediment samples from the Gladstone and Hervey Bay regions indicate that saucer scallops prefer areas where the proportion of fine sand (sediment grainsize of 125–250 μm) exceeds 30% (see section 19.4.3, page 149). Thus, it is hypothesised that spatial modelling of scallop distributions that included seabed composition data

would likely explain the patchy distribution of this species and lead to improved assessment and management of the fishery.

Annual fishery-independent scallop survey data were acquired for the years 1997–2000 (Dichmont *et al.* 2000; Jebreen *et al.* 2008) and 2017–2019 (see section 16, page 43). Spatially continuous maps of scallop distributions within the fishery could have an important role in planning, risk assessment and decision making. These layers, however, are usually not readily available and need to be interpolated from trawl datasets. Spatial interpolation techniques are essential for predicting the spatially continuous data of environmental properties for the unsampled locations using data from limited point observations within a region. Spatial interpolation and prediction methods can be largely classified into four groups (Li and Heap 2008): 1) deterministic or non-geostatistical methods (e.g., Inverse Distance Weighted, IDW), 2) geostatistical methods (e.g., ordinary kriging, OK), 3) combined methods (e.g., regression kriging and co-kriging), and 4) machine learning (ML) methods (e.g., Random Forest, Support Vector Machine, Boosted Regression Trees, etc.).

ML methods use predictor variables (or co-variates) to provide improved spatial predictions and these methods are commonly applied to predictions of seabed substrate (Li *et al.* (2011a; 2011c; 2019), Li (2019c)), soil properties (Li *et al.* 2018; Kurina *et al.* 2019), climate (Reinhardt and Samimi 2018; Franco *et al.* 2020), species distribution (Guisan and Zimmermann 2000; Shan *et al.* 2006; Cutler *et al.* 2007; Marmion *et al.* 2009) and ecological modelling (Li *et al.* 2017; 2018; Willcock *et al.* 2018), and have been demonstrated to be superior to IDW and OK in most comparative studies. IDW and OK are 'exact' interpolators, and as a result, it is expected that these methods will generate an estimate that is the same as any sampled location. By contrast, Random Forest (RF) is considered an inexact interpolator and will generate a predicted value that is different from an observed location. Inexact interpolators commonly produce a smoother and more generalized surface than an exact interpolator (Burrough and McDonnell 1998). Li *et al.* (2011c) concluded that a visual assessment of spatial predictions is recommended to assess whether model outputs are 'fit for purpose'. For example, Li *et al.* (2011c) concluded that the inclusion of x and y coordinates as predictor variables commonly improved the accuracy of predictions and resulted in superior models but these models also included linear artefacts, and similarly, IDW methods commonly display 'bulls-eyes' artefacts.

The key objective of this section of the report was to create optimal regional saucer scallop distribution maps for the years 1997–2000 and 2017–2019 using the LTMP saucer scallop data. The maps can be used to better understand the spatial and temporal variability in scallop distribution and to accurately delineate highly productive regions. The study also assessed the relationships between scallops and seabed substrate at the fishery-scale. This was achieved by:
1. Comparing IDW and OK predictions of scallop distributions with ML methods (specifically RF).
2. Assessing the degree to which adding x and y coordinates as covariates improve RF model performance.
3. Assessing the degree to which adding sediment composition as covariates improve RF model performance and compare relationships between regional sediment and scallop datasets.
4. Providing optimum spatial models of saucer scallop distributions for the years 1997–2000 and 2017–2019, and an overall estimate of mean scallop distributions.
5. Providing a series of recommendations for the prediction of saucer scallops.

21.3 METHODS

21.3.1 *Study region*

The saucer scallop is one of the main target species caught by the QECOTF (O'Neill and Leigh 2007). The scallop fishery extends from Fraser Island to Yeppoon (between 22°S and 27°S) (Courtney *et al.* 2015) and is bounded by the mainland to the west and the Capricorn-Bunker reefs to the east. The outline of the study area is shown in Figure 21-1. Management of the fishery has included the rotational opening and closing of highly productive Scallop Replenishment Areas (SRAs) as a means

of controlling catch and effort. The location and number of SRAs have changed over time (Jebreen *et al.* 2008) although they have remained largely fixed since 1997 (Figure 21-1) and permanently closed to fishing since September 2016. Within the fishery, saucer scallops are commonly targeted in depths between 20 and 60 m.
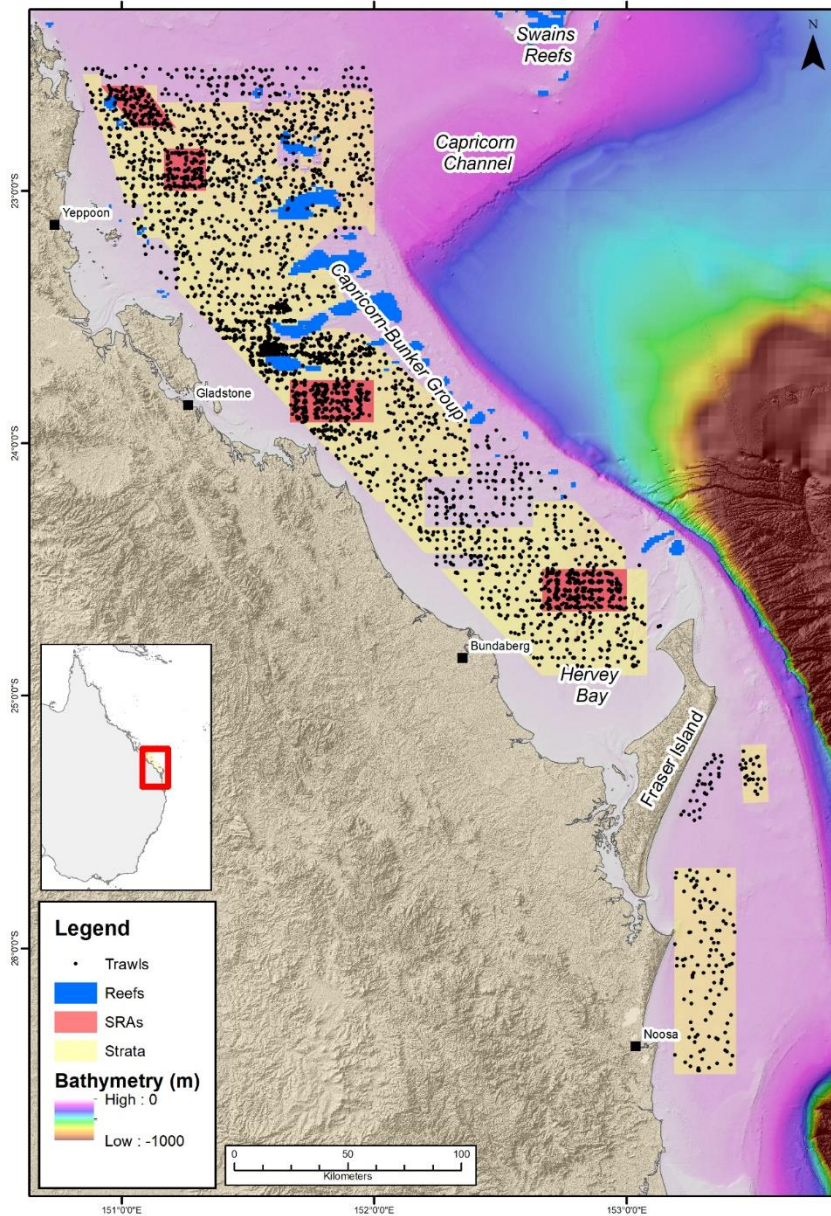
Figure 21-1. Regional map of the southeast Queensland coast showing key geographic areas, locations of the scallop survey strata, LTMP trawl survey sites, and mapped coral reefs.

21.3.2 Annual fishery-independent scallop survey data

Annual fishery-independent trawl surveys have been conducted periodically within the scallop fishery between 1997 and 2019 (Figure 21-1) (detailed description of the survey design and catch rate analyses are provided in section 16, page 43). The survey was carried out comprehensively from 1997–2000, but significantly downscaled from 2001–2006 due to funding cuts, terminating in 2006. Following concern over the poor stock status in 2016 (Yang *et al.* 2016), the Queensland Government reintroduced the full survey design in 2017, repeating the survey in 2018 and 2019. The same

stratified random design was implemented from 2017–2019, enabling the abundance indices to be compared with the earlier 1997–2000 surveys. A key difference between the 1997–2000 and the 2017–2019 surveys was that the later included two additional strata in the southern extent of the fishery east of Fraser Island, and thus covered a broader spatial area. Predictions of scallops for this research were based on the abundance measures (i.e., number of scallops per hectare) for the 1+ scallop age class and based upon the midpoint of each survey trawl.

21.3.3 Predictive variables

A 100 m resolution bathymetry raster dataset was sourced from Beaman (2010). The grid is a compilation of bathymetry data sourced from ship-based multibeam and single beam echosounder surveys, airborne LiDAR bathymetry survey and satellite data. Bathymetric data coverage is not 100% within the 100 m raster and interpolation has been used to fill these gaps. Nine derivatives of the bathymetry were calculated to act as potential covariates for scallop density (Table 21-1). Seventeen sediment raster layers were also generated as possible covariates for scallop density. These layers were interpolated from regional sediment sample analysis using the method described in section 20, page 157. The sediment sample data were separated into two categories; basic statistics (percentages of mud, sand and gravel, carbonate and mean Phi grainsize); and high-resolution (using grainsize measured at 1 Phi interval and their derived statistics) (Table 21-1). The higher resolution Phi interval sediment statistics were based on the findings from section 19, page 139. The Phi scale is a logarithmic scale used to express sediment grainsize. Further details of the scale can be found in Wentworth (1922) and section 18.3.6, page 123.

Table 21-1. Predictive variables used in analysis.

Variable	Abbreviation	Source/Method
Banks	banks	Identifies the location of deep reef habitats
Bathymetry	bathy	Depth to the Seabed (Beaman 2010)
Coast_dist	coast	Distance from the coast (km)
Easting	east	Aspect of raster cell (x component)
Northing	north	Aspect of raster cell (y component)
x	x	'y' coordinate (latitude) of raster cell
y	y	'x' coordinate (longitude) of raster cell
Slope	slope	Slope gradient of the seabed (degrees from horizontal)
StdDev_1	stddev1	Standard deviation of bathymetry measured within a distance of 1 raster cell
StdDev_5	stddev5	Standard deviation of bathymetry measured within a distance of 5 raster cells
TPI	tpi	Topographic Position Index (measures of local concavity/flatness/convexity)
Gravel	gravel	Percent gravel from interpolated sediment data
Sand	sand	Percent sand from interpolated sediment data
Mud	mud	Percent mud from interpolated sediment data
MGS	mgs	Interpolated mean grainsize measured in Phi
Carbonate	carb	Interpolated Percent calcium carbonate
Very fine sand	vfs	Interpolated very fine sand (63–125 μm)
Fine sand	fs	Interpolated fine sand (125–250 μm)
Medium sand	ms	Interpolated medium sand (250–500 μm)
Coarse sand	cs	Interpolated coarse sand (500–1000 μm)
Very coarse sand	vcs	Interpolated very coarse sand and finer (1000–2000 μm)
Very fine sand2	vfs2	Interpolated very fine sand and finer (< 125 μm)
Fine sand2	fs2	Interpolated fine sand and finer (< 250 μm)
Medium sand2	ms2	Interpolated medium sand and finer (< 500 μm)
Coarse sand2	cs2	Interpolated coarse sand and finer (< 1000 μm)
Very coarse sand2	vcs2	Interpolated very coarse sand and finer (< 2000 μm)
Standard deviation	sd	Interpolated grainsize standard deviation measured in Phi
Skewness	skew	Interpolated grainsize skewness measured in Phi

21.3.4 Correlations between scallop trawl density and predictor variables

To assess the correlation between scallop densities and the predictor variables the midpoint of each scallop trawl for each year was intersected with each of the 28 predictor variables. Pearson's correlation coefficient was used to estimate the strength of the linear relationships between scallops and predictor variables. Correlation between 0.3 and 0.4 were considered weak, greater than 0.4 were considered moderate, and correlations less than 0.3 were considered to indicate the absence of a linear correlation.

21.3.5 Predictive models

Predictions of scallop density were undertaken for each year that the Queensland Government has undertaken a scallop trawl survey (i.e., 1997–2000 and 2017–2019. Note the survey was also undertaken from 2001–2006, but at a much- reduced scale and as a result, data from these years have been omitted for these analyses). The R package 'spm' was used for the spatial predictive modelling (Li 2019a). The package implements IDW, geostatistical (OK) and machine learning (Random Forest, RF) methods as well as their hybrid methods for spatial predictions. IDW (default and optimised), Ordinary Kriging (optimised) and four variants of RF were used for the prediction of scallop distributions for each year with a comprehensive scallop survey. The four variants of RF were designed to assess the impact of adding x and y parameters, adding basic sediment grainsize parameters, and adding high-resolution sediment grainsize parameters (Table 21-2). Adding or removing the x and y parameters would provide insights into how the exclusion of these parameters limit linear artefacts in the final rasters and the extent to which model accuracy is reduced. Adding or removing sediment grainsize parameters would provide insights into what degree sediment grainsize can improve prediction of scallops and what parameters are the most important for predicting scallops.

Table 21-2. Predictive models used in analysis for each comprehensive survey year.

Method	Test
IDWd	Default IDW interpolation
IDW	Optimised IDW interpolation
OK	Ordinary Kriging Interpolation
RF	Random Forest – excluding x/y
RF_en	Random Forest – including x/y
RF_en_sed	Random Forest – including x/y and basic sediment grainsize statistics
RF_en_sed_phi	Random Forest – including x/y and all sediment grainsize statistics

21.3.6 Inverse Distance Weighted Interpolation

The Inverse Distance Weighted (IDW) method estimates the values of an attribute at unsampled points using a linear combination of values at sampled points weighted by an inverse function of the distance from the point of interest to the sampled points (Li and Heap 2008; Li *et al.* 2011b). The assumption is that sampled points closer to the unsampled point are more similar to it than those further away in their values. The method has two tunable parameters, the number of points used in the prediction and the power (weighting) parameter. The influence of each sample diminishes with both the distance from the prediction location and the value of the power parameter. As a result, samples closer to the prediction location have a stronger influence on the estimation. Two IDW models were used: 1) a default IDW method (samples = 12 and power = 2, Li *et al.* (2019)), and 2) an optimized IDW method that compared all possible combinations of:
- power (ranging from 1.4 to 3.0 in increments of 0.2), and
- number of samples (ranging from 4 to 16 in increments of 1).

21.3.7 Ordinary Kriging

Kriging utilises the spatial correlation between samples to make predictions at unsampled locations. Kriging is undertaken as a two-step process where, 1) a variogram is fitted to the spatial covariance

structure of the sample data, and 2) weights derived from the covariance structure are used to make predictions at unsampled locations (Li and Heap 2008; Li *et al.* 2011b). Kriging will generally outperform simple interpolation methods such as IDW if moderate spatial autocorrelation exists in the sample dataset. An optimised Ordinary Kriging model was produced by comparing all possible combinations of:

- sample data transforms ('none', 'square root', 'arcsine' and 'log' transforms),
- number of samples (ranging from 4 to 16 in increments of 2), and
- variogram model ('Exponential', 'Spherical', and 'Gaussian').

21.3.8 Random Forest

Random Forest is a robust ensemble learning method that makes predictions from multitudes of regression trees (Breiman 2001; Cutler *et al.* 2007). RF achieves predictions by averaging responses over the large number of trees used and are considered to be comparatively insensitive to highly correlated predictor variables and 'noisy' predictor variables. An optimised RF model was produced by comparing all possible combinations of:

- number of Trees (ranging from 500, 750, 1000, 1500, 2000–6000 in increments of 1000)
- number of variables tried at each node (increasing from 3 in increments of 1 up to the maximum number of variables within the model)

21.3.9 Selection of optimum model parameters

Ten-fold cross validation was used to assess optimum model parameters for the IDW, OK, and RF models. In 10-fold cross validation the input data are resampled evenly into 10 data subsets. Of these subsets, one is retained for validation while the remaining nine are used for model training. The cross validation is then repeated 10 times using each of the data subsets for validation each time. The predictive models were run using each combination of model parameters. The optimum model was selected on the basis of the maximum Variance Explained by the Cross Validation (VEcv) metric, reported as a percentage (Li 2017).

21.3.10 Accuracy and comparison of predictive models

After determining optimal model parameters, the models were each run 60 times to assess the variance in the final model in response to variations in the testing and training datasets. The median VEcv of each model was used to identify the 'best' model. Mann-Whitney tests were then used to compare the accuracy of each model within each yearly survey. The Mann-Whitney test was used to identify which of the models generated were significantly different from others using a 0.95 confidence interval (Li 2019b). Within each RF model the average variable importance (AVI) was also calculated to determine which variables had comparatively high importance and consequently a significant impact on the model result. AVI data for each model and year was compiled to assess which variables consistently influenced the outcomes of the RF models.

21.3.11 Model ranking, post processing and visual inspection

The best performing method over the 7 years of scallop surveys was identified by ranking each model within each year from 1 to 7 based on its highest rank, modal rank, and average rank. For all methods, the average scallop densities were calculated using the predictions for all years in the study. Additional average scallop densities were calculated for the period 2017–2019 as these years had trawl data from offshore of Fraser Island which was lacking in the earlier surveys. Visual inspection of the best methods was then undertaken to make comparisons between methods and identify artefacts.

21.4 RESULTS

21.4.1 Correlations

Of the 28 covariates, only six had a moderate (± 0.4–0.7) correlation with 1+ age class scallops in at least four of the seven years and were considered to potentially have some influence on scallop distribution (Table 21-3). No covariates displayed strong (± 0.7–1.0) correlations. Seven covariates were occasionally correlated with scallops and 11 covariates had no correlation with the 1+ scallops. The covariates that had at least four weak (± 0.3–0.4) or moderate correlations were very coarse sand, coarse sand, mean grainsize, skewness, medium sand2 (i.e., mean sand and finer sediment), and mud. Coarse sand was the only covariate that was significant in 6 of the 7 years of scallop surveys. These correlations suggest:

1. The positive correlation of scallops with very coarse sand and coarse sand indicates scallops prefer a seabed with a comparatively high component of these grainsizes.
2. A negative correlation of skewness and mean grainsize (based on a Phi grainsize scale) with scallops similarly indicates a habitat preference for comparatively coarse sediments.
3. A negative correlation with mud indicates the scallops prefer sediments with a minimal amount of sediment less than 64 μm.
4. Correlations between scallops and fine sand were inconclusive at a regional scale.
5. Despite correlations with very coarse sand and coarse sand, correlations with gravel were poor.

Table 21-3. Correlation between the 1+ age class of scallops and raster-based covariates using Pearson's correlation coefficient. Weak correlations (± 0.3–0.4) are highlighted in light grey, moderate correlations (± 0.4) are highlighted in darker grey. Asterix (*) indicates covariates with a correlation greater than ± 0.3 in four or more years of scallop surveys.

| Covariate | Pearson's correlation coefficient | | | | | | | |
	1997	1998	1999	2000	2017	2018	2019	Weak/Mod
banks	−0.026	−0.106	−0.01	0.028	−0.08		−0.066	0/0
bathy	0.086	0.301	0.531	0.104	0.219	0.51	0.204	1/2
north	0.075	0.13	0.102	−0.002	−0.043	0.126	−0.048	0/0
east	−0.022	−0.14	−0.102	0.037	−0.006	−0.072	−0.097	0/0
x	0.013	−0.157	−0.337	0.026	−0.261	0.063	−0.289	1/0
y	−0.141	−0.064	−0.001	−0.175	0.168	−0.179	0.193	0/0
tpi	0.033	0.078	−0.009	0.054	−0.03	−0.03	−0.105	0/0
slope	0.102	−0.031	−0.096	0.053	−0.165	−0.061	−0.094	0/0
stddev1	0.141	−0.033	−0.073	0.076	−0.172	−0.054	−0.099	0/0
stddev5	0.017	−0.052	−0.112	−0.005	−0.178	−0.118	−0.111	0/0
coast	−0.09	−0.331	−0.528	−0.258	−0.283	−0.229	−0.309	2/1
carb	0.363	0.319	0.173	0.371	−0.069	−0.012	0.027	3/0
gravel	0.315	0.174	0.164	0.274	−0.111	0.124	−0.045	1/0
mgs*	−0.356	−0.457	−0.536	−0.301	−0.126	−0.295	−0.266	2/2
mud*	−0.293	−0.409	−0.515	−0.268	−0.307	−0.322	−0.37	4/1
sand	0.103	0.3	0.49	0.167	0.345	0.254	0.347	2/1
cs*	0.402	0.494	0.393	0.291	−0.088	0.308	0.025	2/2
cs2	−0.285	−0.394	−0.322	−0.278	−0.099	−0.4	−0.242	2/1
fs	−0.142	−0.195	0.076	0.043	0.364	0.044	0.252	1/0
fs2	−0.262	−0.398	−0.327	−0.11	0.133	−0.179	−0.012	2/0
ms	−0.051	−0.06	0.052	−0.215	−0.185	−0.183	−0.146	0/0
ms2*	−0.372	−0.473	−0.392	−0.309	0.004	−0.389	−0.149	4/1
sd	−0.068	−0.271	−0.4	−0.071	−0.291	−0.166	−0.288	1/0
skew*	−0.254	−0.429	−0.539	−0.243	−0.418	−0.512	−0.465	0/5
vcs*	0.362	0.46	0.439	0.364	0.205	0.485	0.374	3/3
vcs2	−0.18	−0.247	−0.14	−0.151	−0.006	−0.253	−0.15	0/0
vfs	−0.105	−0.203	−0.237	0.098	0.023	−0.202	−0.058	0/0
vfs2	−0.234	−0.396	−0.52	−0.193	−0.214	−0.357	−0.262	2/1

21.4.2 Scallop predictions for the 1997 survey

A summary of the accuracy of the predictive models developed for the 1997 1+ age class data is shown in Figure 21-2. A summary of the outputs produced by each optimal predictive model is displayed in Table 21-4 and a statistical comparison of the predictive models using Mann-Whitney tests is provided in Table 21-5.

Figure 21-2 and Table 21-4 indicate that the RF_1997_en, RF_1997_en_sed, and RF_1997_en_sed_phi were the best performing models with VEcv of 70.8, 66.0, and 63.9, respectively. The most important covariates for the RF_1997_en model were y, x, coast and bathymetry (Table 21-4). The Mann-Whitney test indicated that OK_1997, IDW_1997 and IDWd_1997 were not significantly different, and that RF_1997_en_sed_phi was not significantly different from OK_1997 and IDW_1997 but was different to IDWd_1997 (Table 21-5). The worst performing model was RF, which had a significantly reduced VEcv of 28.2, due to excluding the x and y covariates compared to the second worst performing model, IDWd_1997 with a VEcv of 63.5. The inclusion of sediment sample data increased the predictive power when comparing RF_1997 and RF_1997_sed (28.2 VEcv compared to 66.5). However, the addition of the high-resolution sediment data decreased the VEcv to 63.9, a weaker result than only using the basic sediment sample metrics.
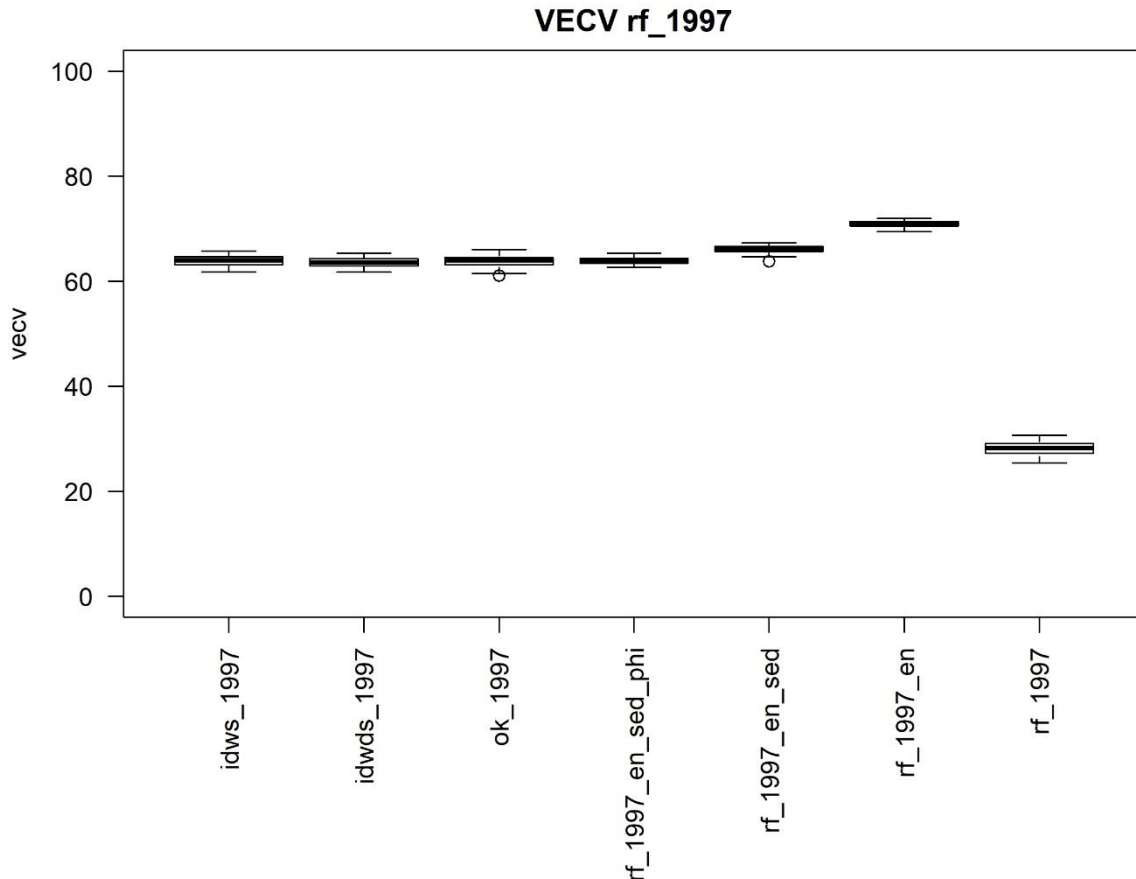
Figure 21-2. Box plot of Variance Explained by cross validation for six predictive models of saucer scallop distributions using 1997 fishery-independent survey data.

Table 21-4. Summary statistics of saucer scallop predictions using the 1997 fishery-independent survey data.

Method	VEcv_M	Rank	Best 6 Covariates	Model parameters
idw_1997	63.8	4		Pow = 2.3, Samples = 7
idwd_1997	63.5	4		Pow = 2, Samples = 12
ok_ 1997	63.8	4		Trans = none, Samples = 12, Var = Sph
rf_ 1997_en_sed_phi	63.9	3	cs, x, y, vcs, ms2, mud	Mtry = 12, Trees = 1000
rf_ 1997_en_sed	66.0	2	x, y, carb, mud, coast, sand	Mtry = 13, Trees = 4000
rf_1997_en	70.8	1	x, y, coast, bathy, stddev1, slope	Mtry = 7, Trees = 1000
rf_1997	28.2	7	bathy, coast, stddev1, slope, stddev5, tpi	Mtry = 9, Trees = 6000

Table 21-5. Mann-Whitney comparisons of VEcv using 1997 fishery-independent survey data. Using a 95% confidence interval identifies model comparisons with p-values of less than 0.05 as being significantly different.

	idws_1997	idwds_1997	ok_1997	rf_1997_en_sed_phi	rf_1997_en_sed	rf_1997_en	rf_1997
idws_1997	1	0.05	0.795	0.811	0	0	0
idwds_1997	0.05	1	0.085	0.019	0	0	0
ok_1997	0.795	0.085	1	0.939	0	0	0
rf_1997_en_sed_phi	0.811	0.019	0.939	1	0	0	0
rf_1997_en_sed	0	0	0	0	1	0	0
rf_1997_en	0	0	0	0	0	1	0
rf_1997	0	0	0	0	0	0	1

21.4.3 Scallop predictions for the 1998 survey

A summary of the accuracy of the predictive models developed for the 1998 1+ age class data is shown in Figure 21-3. A summary of the outputs produced by each optimal predictive model is displayed in Table 21-6 and a statistical comparison of the predictive models using Mann-Whitney tests is provided in Table 21-7.

Figure 21-3 and Table 21-7 indicate that the RF_1998_en and RF_1998_en_sed_phi were the best performing models with VEcv of 66.7 and 66.0, respectively. The best covariates for the best performing model (RF_1998_en) were x, coast, y and bathymetry (Table 21-6). The Mann-Whitney test indicated that the IDW_1998 and IDWd_1998 models were not statistically different to each other. OK_1998 and RF_1998_en_sed were also not statistically different (Table 21-7). The worst performing model was RF_1998, which had a significant reduced VEcv of 40.7, due to excluding the x and y covariates, and was considerably less accurate than the next model IDWd_1998 with a VEcv of 63.3. The inclusion of sediment sample data increased predictive power when RF_1998 was compared against RF_1998_en_sed (40.7 VEcv compared to 64.8). Adding high-resolution sediment data increased the accuracy of the RF_1998_en_sed_phi model, which had a VEcv of 66.0. However, overall, the comparatively simple RF_1998_en model was superior despite lacking sediment sample data.
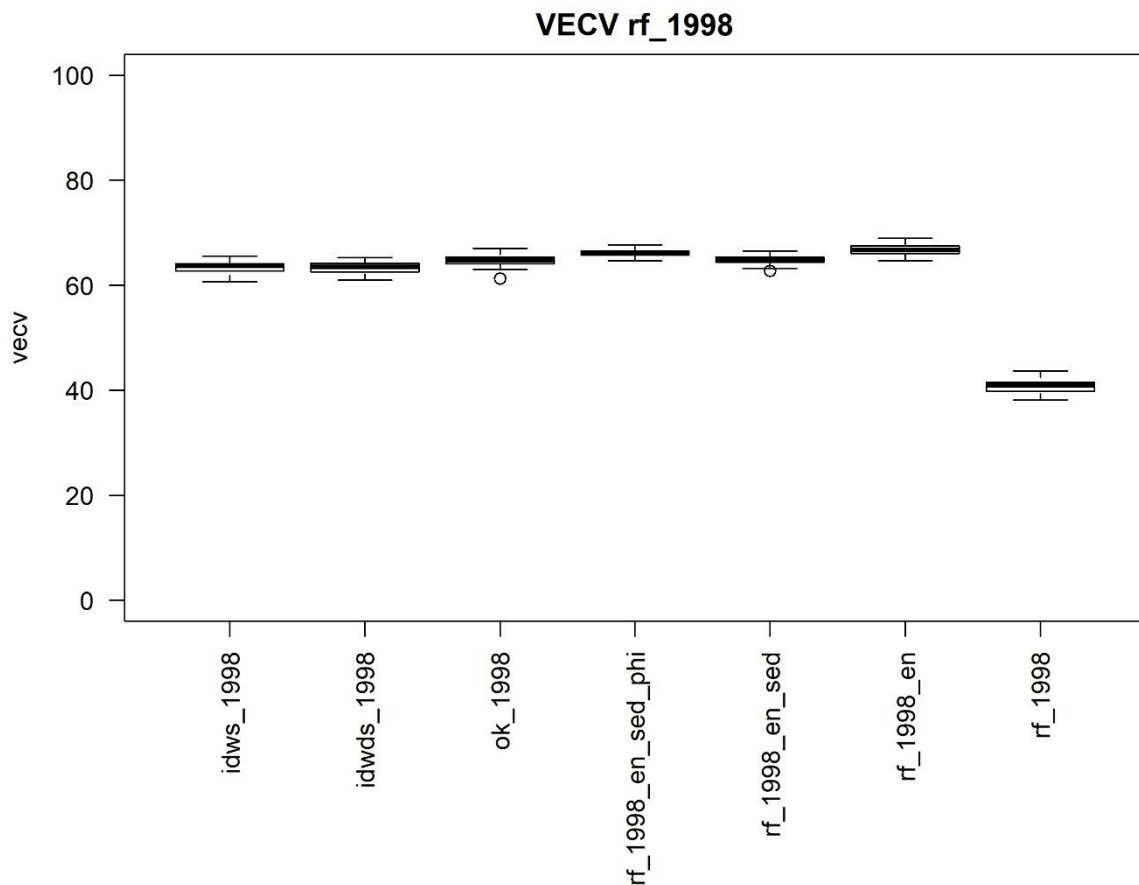
Figure 21-3. Box plot of Variance Explained by cross validation for six predictive models of saucer scallop distributions using the 1998 fishery-independent survey data.

Table 21-6. Summary statistics of saucer scallop predictions using 1998 fishery-independent survey data.

Method	VEcv_M	Rank	Best 6 Covariates	Model Parameter
idw_1998	63.4	5		Pow = 2.6, Samples = 16
idwd_1998	63.3	5		Pow = 2, Samples = 12
ok_1998	64.7	3		Trans = log, Samples = 10, Var = Gau
rf_1998_en_sed_phi	66.0	2	x, cs, mud, sd, coast, y	Mtry = 500, Trees = 18
rf_1998_en_sed	64.8	3	x, mud, coast, y, carb, sand	Mtry = 11, Trees = 1500
rf_1998_en	66.7	1	x, coast, y, bathy, slope, stddev5	Mtry = 11, Trees =6000
rf_1998	40.7	7	bathy, coast, slope, stddev1, stddev5, north	Mtry = 9, Trees = 2000

Table 21-7. Mann-Whitney comparisons of VEcv using the 1998 fishery-independent survey data. Using a 95% confidence interval identifies model comparisons with p-values of less than 0.05 as being significantly different.

	idws_1998	idwds_1998	ok_1998	rf_1998_en_sed_phi	rf_1998_en_sed	rf_1998_en	rf_1998
idws_1998	1	0.598	0	0	0	0	0
idwds_1998	0.598	1	0	0	0	0	0
ok_1998	0	0	1	0	0.305	0	0
rf_1998_en_sed_phi	0	0	0	1	0	0	0
rf_1998_en_sed	0	0	0.305	0	1	0	0
rf_1998_en	0	0	0	0	0	1	0
rf_1998	0	0	0	0	0	0	1

21.4.4 Scallop predictions for the 1999 survey

A summary of the accuracy of the predictive models developed for the 1999 1+ age class data is shown in Figure 21-4. A summary of the outputs produced by each optimal predictive model is displayed in Table 21-8 and a statistical comparison of the predictive models using Mann-Whitney tests is provided in Table 21-9.

Figure 21-4 and Table 21-8 indicate that the RF_1999_en_sed, RF_1999_en and RF_1999_en_sed_phi were the best performing models with VEcv of 72.6, 68.6, and 68.0, respectively. Overall RF_1999_en_sed was the best performing model and the important covariates were coast, x, mud, sand, bathymetry and y (Table 21-8). Despite the inclusion of sediment data into the RF_1999_en_sed model, the most important sediment covariates (mud and sand) ranked 3rd and 4th behind coast and x. The worst performing model was RF_1999, with a significantly reduced VEcv of 50.5, due to excluding the x and y covariates compared to the second least accurate model, IDWd_1999 with a VEcv of 66.2. The Mann-Whitney test indicated that the IDWd_1999 model was not significantly different from the IDW_1999 model (Table 21-9). The inclusion of sediment sample data increased the predictive power of RF_1999 compared to RF_1999_sed (50.5 VEcv compared to 72.6). However, the addition of high-resolution sediment data lead to a slight decrease in the accuracy of the model (RF_1999_en_sed_phi with a VEcv of 68.0).
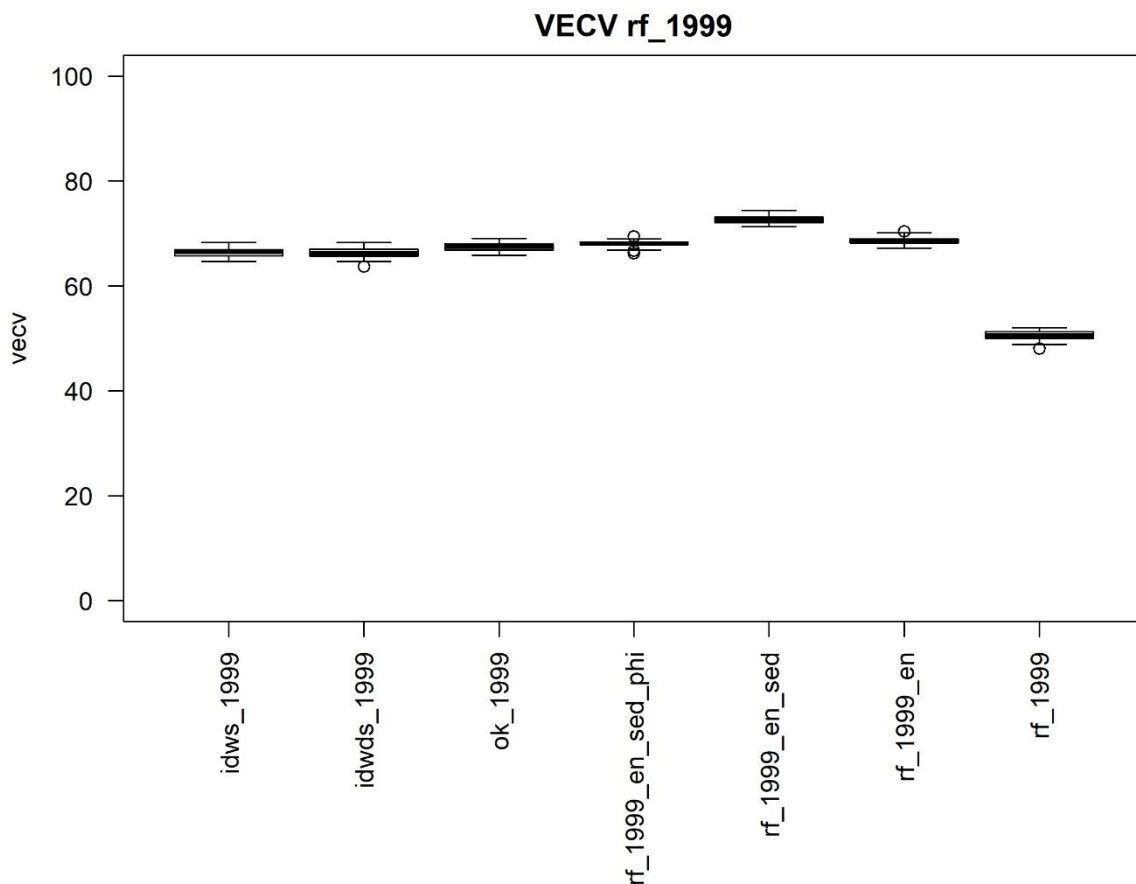
Figure 21-4. Box plot of Variance Explained by cross validation for six predictive models of saucer scallop distributions using the 1999 fishery-independent survey data.

Table 21-8. Summary statistics of saucer scallop predictions using the 1999 fishery-independent survey data.

Method	VEcv_M	Rank	Best 6 Covariates	Model Parameters
idw_1999	66.4	5		Pow = 2.4, Samples = 9
idwd_1999	66.2	5		Pow = 2, Samples = 12
ok_1999	67.4	4		Trans = none, Samples = 4, Var = Sph
rf_1999_en_sed_phi	68.0	3	coast, sand, bathy, x, mud, vfs2	Mtry = 12, Trees = 500
rf_1999_en_sed	72.6	1	coast, x, mud, sand, bathy, y	Mtry = 9, Trees = 500
rf_1999_en	68.6	2	coast, x, bathy, y, stddev5, stddev1	Mtry = 7, Trees = 2000
rf_1999	50.5	7	coast, bathy, stddev5, stddev1, slope, tpi	Mtry = 9, Trees = 1000

Table 21-9. Mann-Whitney comparisons of VEcv using 1999 LTMP data. Using a 95% confidence interval identifies model comparisons with p-values of less than 0.05 as being significantly different.

	idws_1999	idwds_1999	ok_1999	rf_1999_en_sed_phi	rf_1999_en_sed	rf_1999_en	rf_1999
idws_1999	1	0.33	0	0	0	0	0
idwds_1999	0.33	1	0	0	0	0	0
ok_1999	0	0	1	0	0	0	0
rf_1999_en_sed_phi	0	0	0	1	0	0	0
rf_1999_en_sed	0	0	0	0	1	0	0
rf_1999_en	0	0	0	0	0	1	0
rf_1999	0	0	0	0	0	0	1

21.4.5 Scallop predictions for the 2000 survey

A summary of the accuracy of the predictive models developed for the 2000 1+ age class data is shown in Figure 21-5. A summary of the outputs produced by each optimal predictive model is displayed in Table 21-10 and a statistical comparison of the predictive models using Mann-Whitney tests is provided in Table 21-11.

Figure 21-5 and Table 21-10 indicate that OK_2000 was the best performing model with a VEcv of 68.6. RF_2000_en, IDW_2000, and IDWd_2000 were the next best performing models and were not significantly different based on the Mann-Whitney test (Table 21-11). The worst performing model was RF_2000 which had a significantly reduced VEcv (32.5) due to excluding the x and y covariates when compared to the second worst model (RF_2000_en_sed_phi with VEcv of 67.0).
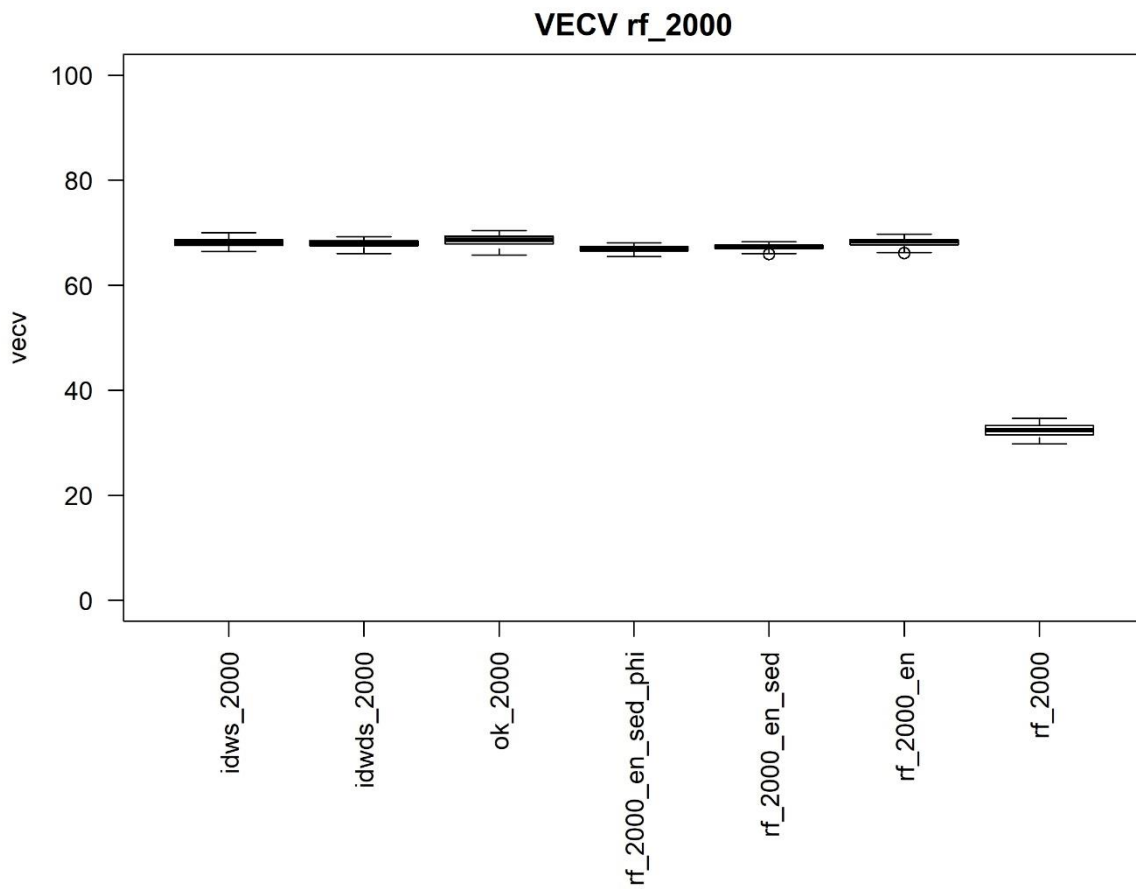
Figure 21-5. Box plot of Variance Explained by cross validation for six predictive models of saucer scallop distributions using the 2000 fishery-independent survey data.

215

Table 21-10. Summary statistics of saucer scallop predictions using the 2000 fishery-independent survey data.

Method	VEcv_M	Rank	Best 6 Covariates	Model Parameters
idw_2000	68.1	2		Pow = 3, Samples = 12
idwd_2000	68.0	2		Pow = 2, Samples = 12
ok_2000	68.6	1		Trans = log, Samples = 8, Var = Sph
rf_2000_en_sed_phi	67.0	6	x, carb, mud, vcs, sand, cs	Mtry = 15, Trees = 6000
rf_2000_en_sed	67.3	5	x, carb, mud, sand, y, coast	Mtry = 7, Trees = 4000
rf_2000_en	68.2	2	x, y, coast, bathy, stddev1, stddev5	Mtry = 9, Trees = 750
rf_2000	32.5	7	coast, bathy, stddev1, slope, stddev5, east	Mtry = 7, Trees = 500

Table 21-11. Mann-Whitney comparisons of VEcv using the 2000 fishery-independent survey data. Using a 95% confidence interval identifies model comparisons with p-values of less than 0.05 as being significantly different.

	idws_2000	idwds_2000	ok_2000	rf_2000_en_sed_phi	rf_2000_en_sed	rf_2000_en	rf_2000
idws_2000	1	0.216	0.014	0	0	0.613	0
idwds_2000	0.216	1	0	0	0	0.116	0
ok_2000	0.014	0	1	0	0	0.024	0
rf_2000_en_sed_phi	0	0	0	1	0.004	0	0
rf_2000_en_sed	0	0	0	0.004	1	0	0
rf_2000_en	0.613	0.116	0.024	0	0	1	0
rf_2000	0	0	0	0	0	0	1

21.4.6 Scallop predictions for the 2017 survey

A summary of the accuracy of the predictive models developed for the 2017 1+ age class data is shown
in Figure 21-6. A summary of the outputs produced by each optimal predictive model is displayed in
Table 21-12 and a statistical comparison of the predictive models using Mann-Whitney tests is
provided in Table 21-13.

Figure 21-6 and Table 21-12 indicate that the OK_2017, IDW_2017, and RF_2017_en were the best
performing models with VEcv of 61.8, 58.4, and 57.1, respectively. Mann-Whitney tests indicated that
all models were statistically different (Table 21-13). The worst performing model was RF_2017 with a
VEcv of 25.9, which was substantially lower than the second worst performing model
RF_2017_en_sed with the VEcv of 55.3. The inclusion of sediment sample data increased the
predictive power when comparing RF_2017 with RF_2017_en_sed and RF_2017_en_sed_phi (25.9
VEcv compared to 55.3 and 56.0, respectively). However, the RF_2017_en model outperformed
RF_2017_en_sed and RF_2017_en_sed_phi in the absence of sediment data.
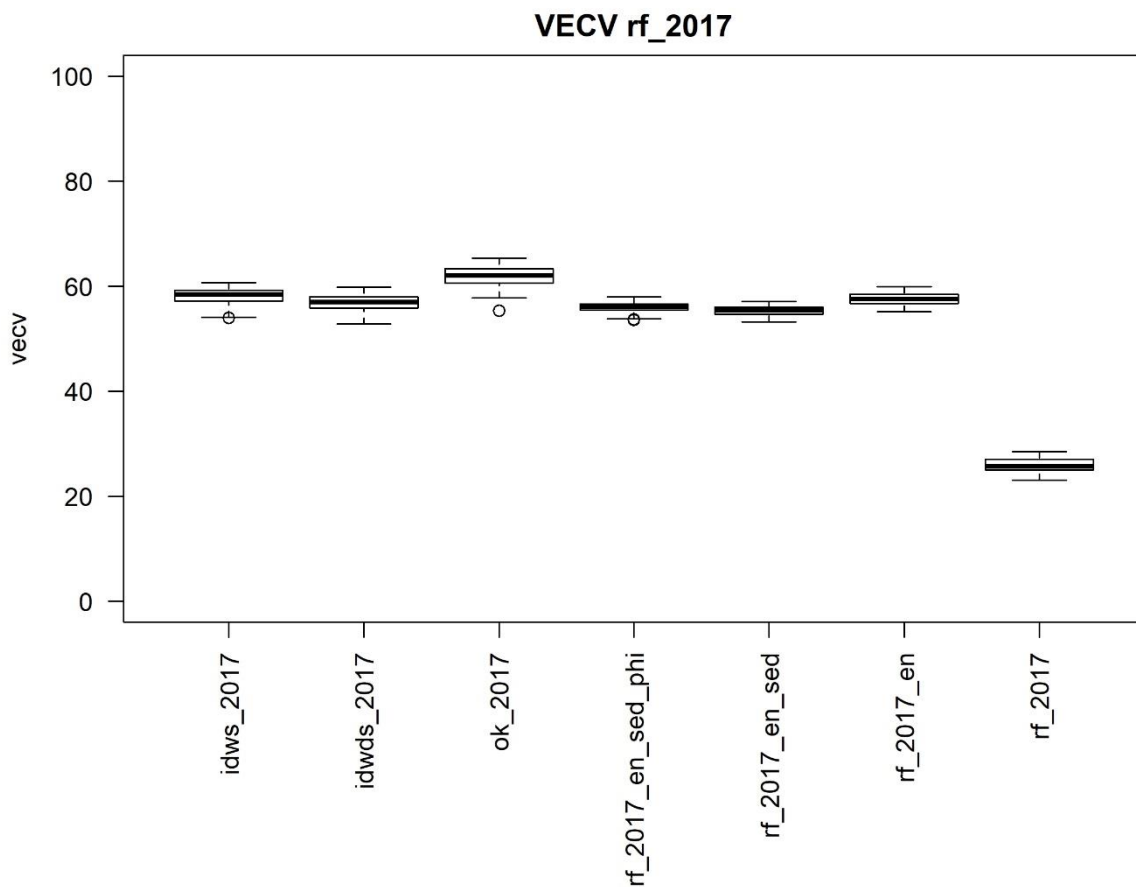
Figure 21-6. Box plot of Variance Explained by cross validation for six predictive models of saucer scallop
distributions using the 2017 fishery-independent survey data.

Table 21-12. Summary statistics of saucer scallop predictions using the 2017 fishery-independent survey data.

Method	VEcv_M	Rank	Best 6 Covariates	Model Parameters
idw_2017	58.1	2		Pow = 1.7, Samples = 7
idwd_2017	56.8	4		Pow = 2, Samples = 12
ok_2017	61.8	1		Trans = none, Samples = 8, Var = sph
rf_2017_en_sed_phi	56.0	5	skew, x, y, mud, vcs, coast	Mtry = 12, Trees = 4000
rf_2017_en_sed	55.3	6	x, mud, coast, y, bathy, sand	Mtry = 13, Trees = 750
rf_2017_en	57.5	3	x, y, coast, bathy, stddev5, slope	Mtry = 11, Trees = 2000
rf_2017	25.9	7	coast, bathy, stddev5, stddev1, slope, east	Mtry = 9, Trees = 6000

Table 21-13. Mann-Whitney comparisons of VEcv using the 2017 fishery-independent survey data. Using a 95% confidence interval identifies model comparisons with p-values of less than 0.05 as being significantly different.

	idws_2017	idwds_2017	ok_2017	rf_2017_en_sed_phi	rf_2017_en_sed	rf_2017_en	rf_2017
idws_2017	1	0	0	0	0	0.004	0
idwds_2017	0	1	0	0	0	0.019	0
ok_2017	0	0	1	0	0	0	0
rf_2017_en_sed_phi	0	0	0	1	0	0	0
rf_2017_en_sed	0	0	0	0	1	0	0
rf_2017_en	0.004	0.019	0	0	0	1	0
rf_2017	0	0	0	0	0	0	1

21.4.7 Scallop predictions for the 2018 survey

A summary of the accuracy of the predictive models developed for the 2018 1+ age class data is shown in Figure 21-7. A summary of the outputs produced by each optimal predictive model is displayed in Table 21-14 and a statistical comparison of the predictive models using Mann-Whitney tests is provided in Table 21-15.

Figure 21-7 and Table 21-14 indicate that the OK_2018 model was the best model with a VEcv of 70.7. However, the Mann-Whitney test indicated that the IDW_2018, IDWd_2018, RF_2018 en_sed, and RF_2018_en_sed_phi models were not significantly different from each other (Table 21-15). These four models have VEcv ranging from 70.2 – 70.3, only marginally less than the OK_2018 model. The worst performing model was RF_2018 with a significantly reduced VEcv of 51.1 due to excluding the x and y covariates. The inclusion of sediment sample data increased the predictive power when RF_2018 was compared against RF_2018_en (VEcv of 51.1 compared to 69.7). The VEcv increased slightly in the two RF models with sediment data compared to the RF models without sediment data.
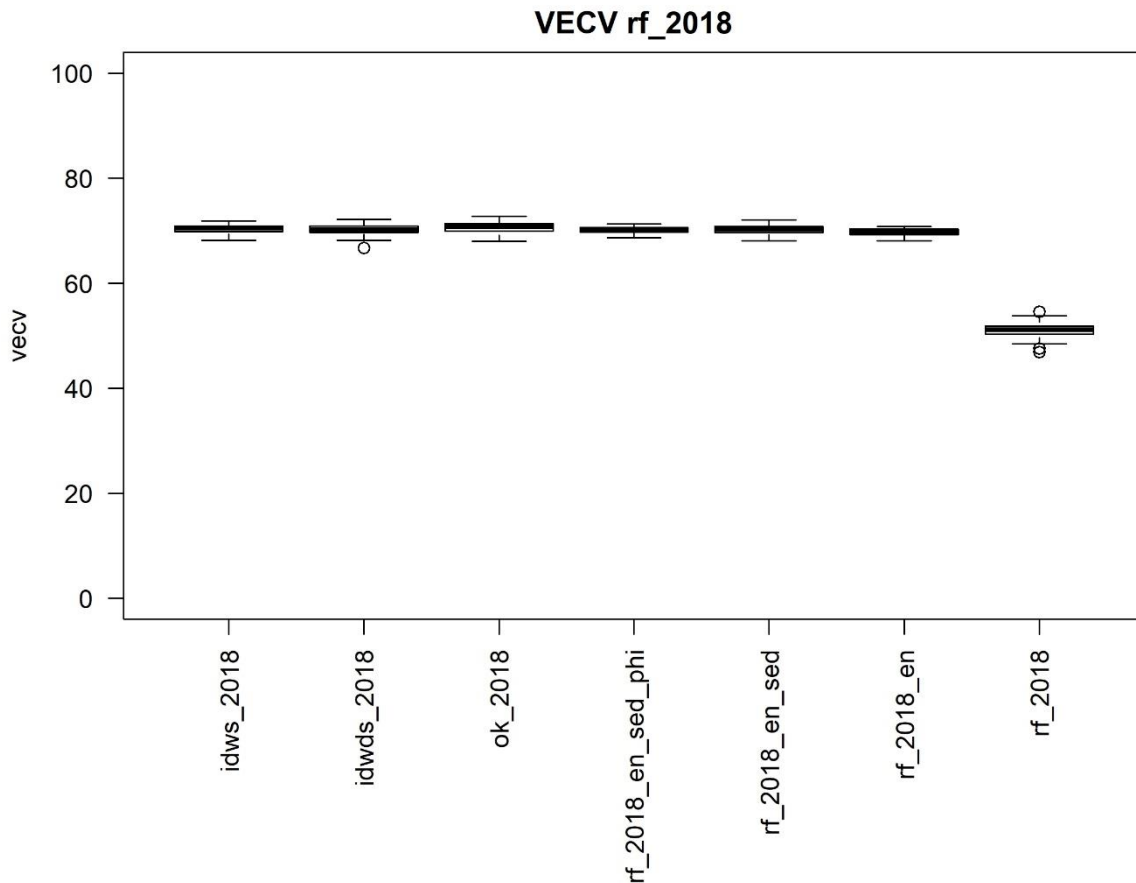
Figure 21-7. Box plot of Variance Explained by cross validation for six predictive models of saucer scallop distributions using the 2018 fishery-independent survey data.

Table 21-14. Summary statistics of saucer scallop predictions using the 2018 fishery-independent survey data.

Method	VEcv_M	Rank	Best 6 Covariates	Model Parameters
idw_2018	70.3	2		Pow = 1.8, Samples = 10
idwd_2018	70.2	2		Pow = 2, Samples = 12
ok_2018	70.7	1		Trans = log, Samples = 12, Var = sph
rf_2018_en_sed_phi	70.2	2	vcs, bathy, y, ms2, skew, cs2	Mtry =15, Trees = 4000
rf_2018_en_sed	70.2	2	x, y, bathy, coast, mud, carb	Mtry = 13, Trees = 1500
rf_2018_en	69.7	6	y, x, coast, bathy, stddev1, slope	Mtry = 7, Trees = 500
rf_2018	51.1	7	bathy, coast, stddev1, slope, stddev5, north	Mtry = 9, Trees = 4000

Table 21-15. Mann-Whitney comparisons of VEcv using the 2018 fishery-independent survey data. Using a 95% confidence interval identifies model comparisons with p-values of less than 0.05 as being significantly different.

	idws_2018	idwds_2018	ok_2018	rf_2018_en_sed_phi	rf_2018_en_sed	rf_2018_en	rf_2018
idws_2018	1	0.42	0.048	0.096	0.455	0	0
idwds_2018	0.42	1	0.011	0.657	0.873	0.001	0
ok_2018	0.048	0.011	1	0.001	0.012	0	0
rf_2018_en_sed_phi	0.096	0.657	0.001	1	0.474	0.001	0
rf_2018_en_sed	0.455	0.873	0.012	0.474	1	0	0
rf_2018_en	0	0.001	0	0.001	0	1	0
rf_2018	0	0	0	0	0	0	1

21.4.8 Scallop predictions for the 2019 survey

A summary of the accuracy of the predictive models developed for the 2019 1+ age class is shown in Figure 21-8. A summary of the outputs produced by each optimal predictive model is displayed in Table 21-16 and a statistical comparison of the predictive models using Mann-Whitney tests is provided in Table 21-17.

Figure 21-8 and Table 21-16 indicate that the OK_2019, IDW_2019, RF_2019_en_sed_phi were the best performing models with VEcv values of 70.4, 67.0, and 67.0, respectively. Mann-Whitney tests indicated that all IDW_2019 and RF_2019_en_sed_phi models were not significantly different (Table 21-17). The worst performing model was RF_2019 had a VEcv of 24.0, due to excluding the x and y covariates compared to the second worst performing model (RF_2019_en_sed with a VEcv of 58.2). The inclusion of sediment sample data increased predictive power when comparing RF_2019 and RF_2019_en to RF_2019_en_sed and RF_2019_en_sed_phi.
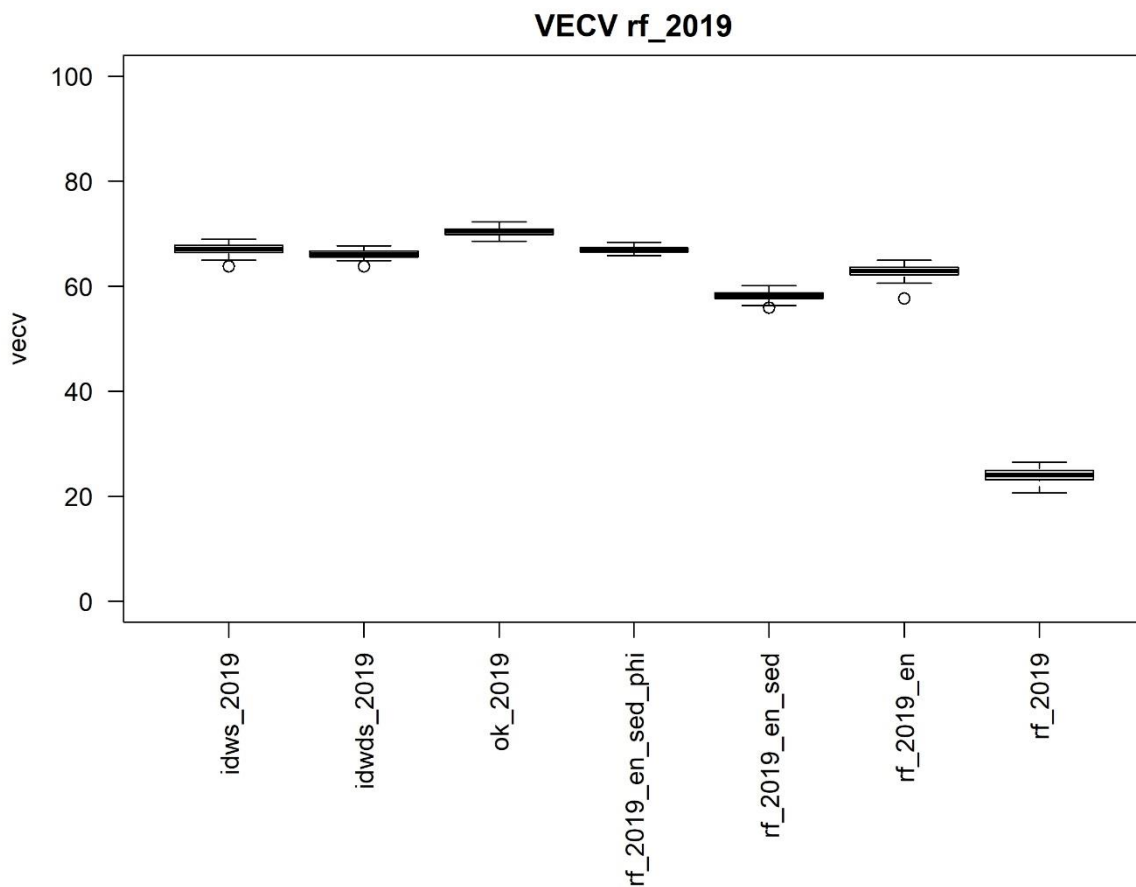
Figure 21-8. Box plot of Variance Explained by cross validation for six predictive models of saucer scallop distributions using the 2019 fishery-independent survey data.

Table 21-16. Summary Statistics of saucer scallop predictions using 2019 fishery-independent survey data.

Method	VEcv_M	Rank	Best 6 Covariates	Model Parameters
idw_2019	67.0	2		Pow = 2.8, Samples = 6
idwd_2019	66.1	4		Pow = 2, Samples = 12
ok_2019	70.4	1		Trans = sqrt, Samples = 10, Var = exp
rf_2019_en_sed_phi	67.0	2	skew, vcs, x, mud, ms, coast	Mtry = 12, Trees = 1000
rf_2019_en_sed	58.2	6	x, mud, y, coast, sand, carb	Mtry = 9, Trees = 500
rf_2019_en	62.8	5	x, y, coast, bathy, slope, stddev1	Mtry = 9, Trees = 4000
rf_2019	24.0	7	coast, bathy, stddev1, slope, east, stddev5	Mtry = 9, Trees = 1500

Table 21-17. Mann-Whitney comparisons of VEcv using 2019 fishery-independent survey data. Using a 95% confidence interval identifies model comparisons with p-values of less than 0.05 as being significantly different.

	idw_2019	idwd_2019	ok_2019	rf_2019_en_sed_phi	rf_2019_en_sed	rf_2019_en	rf_2019
idw_2019	1	0	0	0.497	0	0	0
idwd_2019	0	1	0	0	0	0	0
ok_2019	0	0	1	0	0	0	0
rf_2019_en_sed_phi	0.497	0	0	1	0	0	0
rf_2019_en_sed	0	0	0	0	1	0	0
rf_2019_en	0	0	0	0	0	1	0
rf_2019	0	0	0	0	0	0	1

21.4.9 *Scallop predictions – summary of prediction ranking*

Table 21-18 shows a summary of the ranking of each predictive model over the seven years studied based on their median VEcv. RF_en and OK were identified as the two best performing methods based on the maximum, average, and modal rank. The results of these predictions for the years 1997–2000 and 2017–2019, are shown in Figures 21-9 to 21-15. OK outperforms RF_en on the basis of the average rank with the max and mode being equal for each method, and thus could be considered the best method overall. The results of the Average Variable Importance (AVI) for the RF_en models indicate that x, y, bathy, and coast were consistently the most important covariates (Tables 21-19, 21-20, 21-21). AVI data for the RF and RF_sed models also show that x, y, and coast were strong predictors of scallop distribution. The RF_en_sed_phi models, by comparison, indicated that coarse sand, very coarse sand, and mud were also strong predictors of scallop distributions in addition to x, y and coast (Table 21-22).

The worst performing method was consistently RF, however, the RF algorithm improved significantly with the addition of sediment, and x and y covariates (i.e., the RF_en, RF_en_sed, RF_en_sed_phi models). When compared against the IDW, which was used as a baseline, the other interpolation/prediction algorithms performed comparatively well with an average ranking of 3 and highest ranking of 2. The default IDW method (IDWd) performed acceptably well with an overall ranking of 4. The inclusion of sediment sample data (both basic and high-resolution) did not to have a consistent influence on the modelling. In 1999 the RF_1999_en_sed model was the best performing, while in 2017 RF_2017_en_sed_phi was the second best. However, the two models that contained

sediment sample data had an average rank of 4 and were generally outperformed by RF and OK. All the models, apart from the basic RF, did reach the highest ranking, or second highest ranking, in at least one year and indicating that all of the methods performed to a high standard in some model iterations.

Table 21-18. Overall rankings for predictive models.

Model	1997	1998	1999	2000	2017	2018	2019	Max Rank	Average	Mode
idw	4	5	5	2	2	2	2	2	3	2
idwd	4	5	5	2	4	4	3	2	4	4
ok	4	4	4	1	1	1	1	1	2	1
rf_en_sed_phi	3	2	3	6	5	5	2	2	4	2
rf_en_sed	2	2	1	5	6	3	6	1	4	2
rf_en	1	1	2	2	3	6	5	1	3	1
rf	7	7	7	7	7	7	7	7	7	7

Table 21-19. Overall rankings for covariates based on AVI for RF predictive model (for all years).

	1997	1998	1999	2000	2017	2018	2019	High	Ave	Mode	Count
Bathymetry	1	1	2	2	2	1	2	1	1.6	2	7
Coast_dist	2	2	1	1	1	2	1	1	1.4	1	7
Easting	-	-	-	6	6	-	5	5	5.7	6	3
Northing	-	6	-	-	-	6	-	6	6.0	6	2
Slope	4	3	5	4	5	4	4	3	4.1	4	7
StdDev_1	3	4	4	3	4	3	3	3	3.4	3	7
StdDev_5	5	5	3	5	3	5	6	3	4.6	5	7

Table 21-20. Overall rankings for covariates based on AVI for RF_en predictive model (for all years).

	1997	1998	1999	2000	2017	2018	2019	High	Ave	Mode	Count
Bathymetry	4	4	3	4	4	4	4	3	3.9	4	7
Coast_dist	3	2	1	3	3	3	3	1	2.6	3	7
y	2	3	4	2	2	1	2	1	2.3	2	7
x	1	1	2	1	1	2	1	1	1.3	1	7
Slope	6	5	-	-	6	6	5	5	5.6	6	5
StdDev_1	5	-	6	5	-	5	-	5	5.3	5	4
StdDev_5	-	6	5	6	5	-	6	5	5.6	6	5

Table 21-21. Overall rankings for covariates based on AVI for RF_en_sed predictive model (for all years).

	1997	1998	1999	2000	2017	2018	2019		High	Ave	Mode	Count
Bathymetry	-	-	5	-	5	3	-		3	4.3	5	3
Coast_dist	5	3	1	6	3	4	4		1	3.7	3	7
y	1	4	6	5	4	2	2		1	3.4	4	7
x	2	1	2	1	1	1	1		1	1.3	1	7
Slope	6	-	-	-	-	-	-		6	6.0	-	1
StdDev_5	-	6	-	-	-	-	-		6	6.0	-	1
Sand	-	-	4	4	6	-	5		4	4.8	4	4
Mud	4	2	3	3	2	5	2		2	3.0	2	7
Carbonate	3	5	-	2	-	6	6		2	4.4	6	5

Table 21-22. Overall rankings for covariates based on AVI for RF_en_sed_phi predictive model (for all years).

	1997	1998	1999	2000	2017	2018	2019		High	Ave	Mode	Count
Bathymetry			3			2			2	2.5		2
Coast_dist		5	1		6		6		1	4.5	6	4
y	2	6			3	3			2	3.5	3	4
x	3	1	4	1	2		3		1	2.3	3	6
Sand			2	5					2	3.5		2
Mud	6	3	5	3	4		4		3	4.2	3	6
Carbonate				2					2	2.0		1
Medium sand							5		5	5.0		1
Coarse sand	1	2		6		1			1	2.5	1	4
Very coarse sand	4			4	5		2		2	3.8	4	4
Medium sand2	5					4			4	4.5		2
Coarse sand2						6			6	6.0		1
Very coarse sand2			6						6	6.0		1
Standard deviation		4							4	4.0		1
Skewness						2	5	1		1	2.7		3

21.4.10 Comparison of OK and RF_en models

Final scallop predictions for the OK and RF_en models are shown in Figures 21-9 to 21-15. The averages (all years and 2017–2019 only) for these models are shown in Figure 21-16. A visual comparison the OK and RF_en models for all years (Table 21-23) identified the following results:

1. All final predictions for RF_en and OK contained linear artefacts. The strength of these artefacts varied through all the years. The models for 2019 had considerably fewer artefacts compared to other years. Linear artefacts for the OK models were more prominent at greater distances from sample points. Linear artefacts in the RF_en models were a result of the RF

model trees consistently splitting data based on latitude and/or longitude. Averaged model predictions displayed few to no artefacts in both OK and RF_en models (Figure 21-16).

2. All models commonly mapped the SRAs as high productivity areas. In 2017 both the OK and RF_en model did not map high scallop abundance offshore from Gladstone, however, as this result is consistent across both models it is considered to be a result of the trawl survey data and not the modelling. In 2019 the RF_en model mapped considerably fewer scallops in the Gladstone SRA compared to the OK model. This is likely due to the RF models producing a more generalized result being an inexact interpolator. The OK models, being exact interpolators, typically showed higher scallop abundances in and around the SRAs than the RF_en models and also showed localized peaks in some models that were not observed in RF_en.

3. The average models (Figure 21-16) show high scallop density in around the SRAs in both RF_en and OK. However, the averaged RF_en models also showed lower scallop densities than the OK models. The model averages for the period 2017–2019 provide a clearer delineation of high scallop density areas off the coast of Fraser Island and Noosa due to improved trawl density in those areas over that time.

4. OK predicted high scallop abundance over reefs and in deep water in some years (i.e., 1997). RF_en, due to its use of covariates, commonly predicted low scallop abundance over reefs in shallow water and deep water to produce a more realistic prediction in these environments.

5. The model averages (Figure 21-16) for RF_en showed comparatively high zones of scallop occurrences in a narrow north/south trending band between 20–60 m deep, inshore of the adjacent reefs. The average OK models display the same trend, however, they were not constrained by covariates and produced much higher densities of scallops in coastal zones and on the edge of the continental shelf.

Table 21-23. Visual assessment of scallop predictions for Random Forest (specifically RF_en) and Ordinary Kriging models.

	Random Forest (RF_en)	**Ordinary Kriging (OK)**
1997	Displays strong linear artefacts Reefs are mapped as low scallop abundance SRAs are mapped as high scallop abundance	Displays linear artefact away from sample location Reefs are mapped as low scallop abundance SRAs are mapped as high scallop abundance
1998	Displays strong linear artefacts SRAs are mapped as high scallop abundance	Displays linear artefact away from sample location SRAs are mapped as high scallop abundance
1999	Few linear artefacts SRAs are mapped as high scallop abundance	Displays linear artefact away from sample location SRAs are mapped as high scallop abundance
2000	Displays strong linear artefacts SRAs are mapped as high scallop abundance	Displays linear artefact away from sample location SRAs are mapped as high scallop abundance
2017	Displays strong linear artefacts SRAs are mapped as high scallop abundance except for Gladstone	Displays linear artefact away from sample location SRAs are mapped as high scallop abundance except for Gladstone
2018	Displays few linear artefacts SRAs are mapped as high scallop abundance	Displays linear artefact away from sample location SRAs are mapped as high scallop abundance
2019	Displays few linear artefacts SRAs are mapped as high scallop abundance except for Gladstone	Displays minimal linear artefact away from sample locations SRAs are mapped as high scallop abundance
Average 1997–2000 + 2017–2019	Comparatively few linear artefacts Constrains scallops to expected depth ranges	Comparatively few linear artefacts Predicts scallops in 'deep' and 'shallow' depths
Average 2017–2019	Comparatively few linear artefacts Better definition of scallops around Fraser Island	Comparatively few linear artefacts Better definition of scallops around Fraser Island
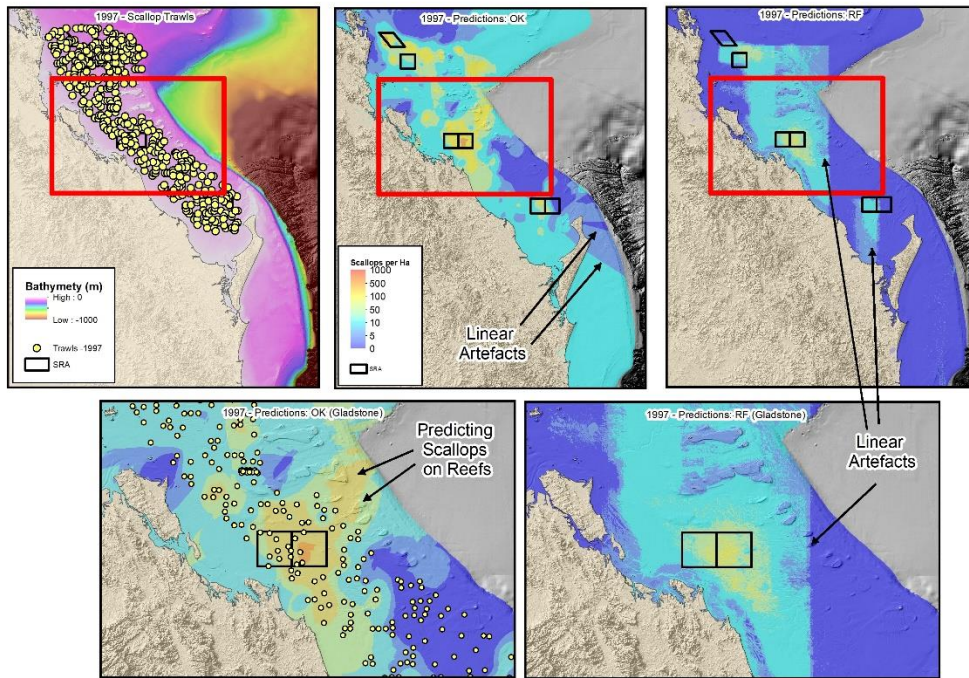
Figure 21-9. Map of scallop predictions for 1997. Maps show distribution of trawls, predictions for OK and RF_en, including details for the Gladstone region.
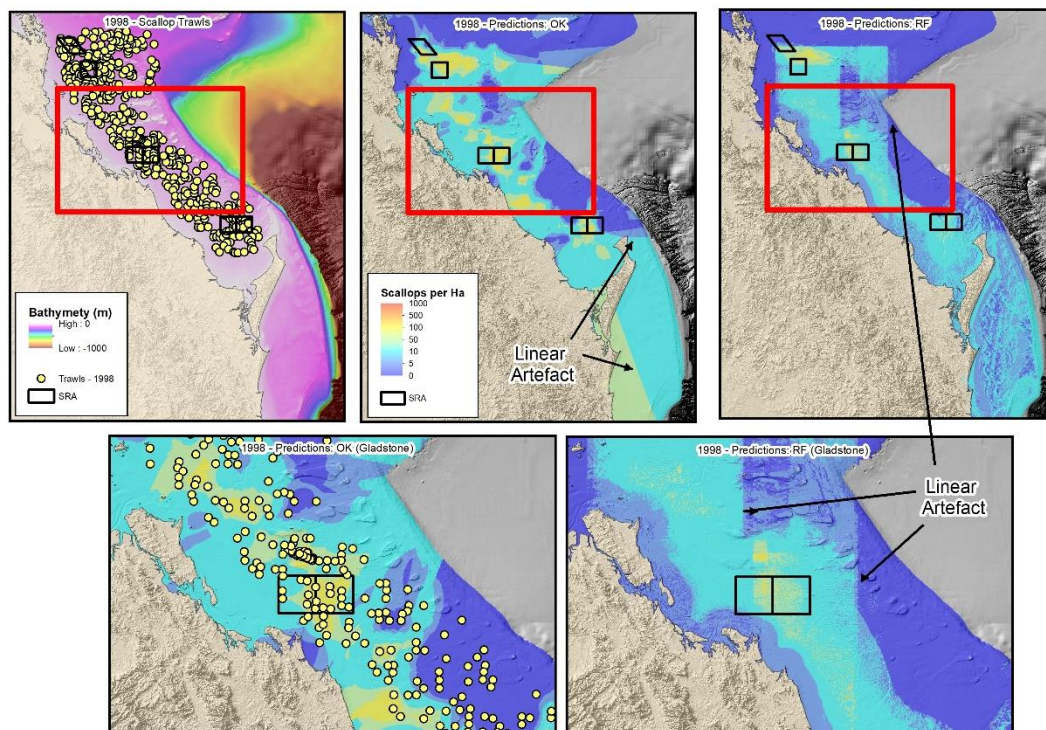
Figure 21-10. Map of scallop predictions for 1998. Maps show distribution of trawls, predictions for OK and RF_en, including details for the Gladstone region.
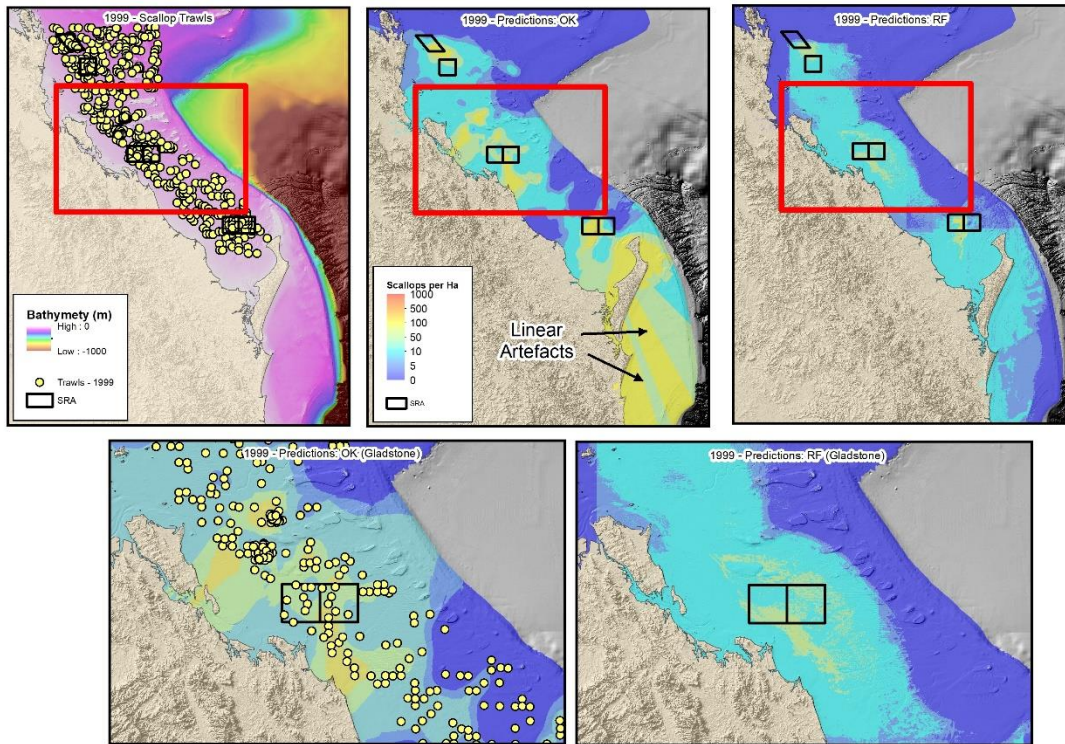
Figure 21-11. Map of scallop predictions for 1999. Maps show distribution of trawls, predictions for OK and RF_en, including details for the Gladstone region.
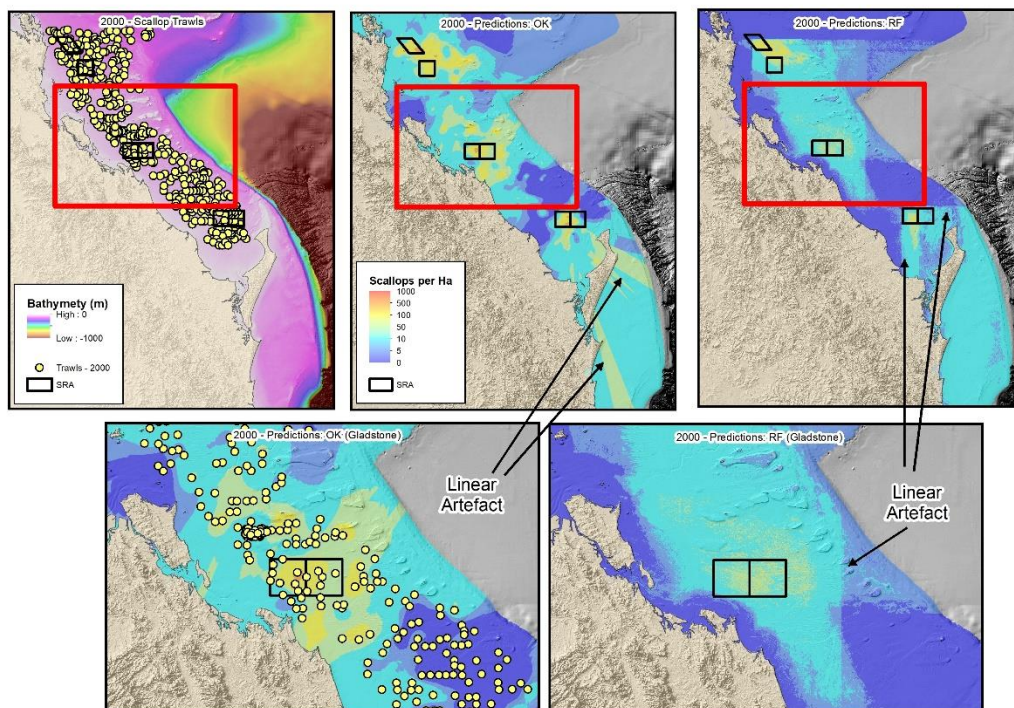
Figure 21-12. Map of scallop predictions for 2000. Maps show distribution of trawls, predictions for OK and RF_en, including details for the Gladstone region.
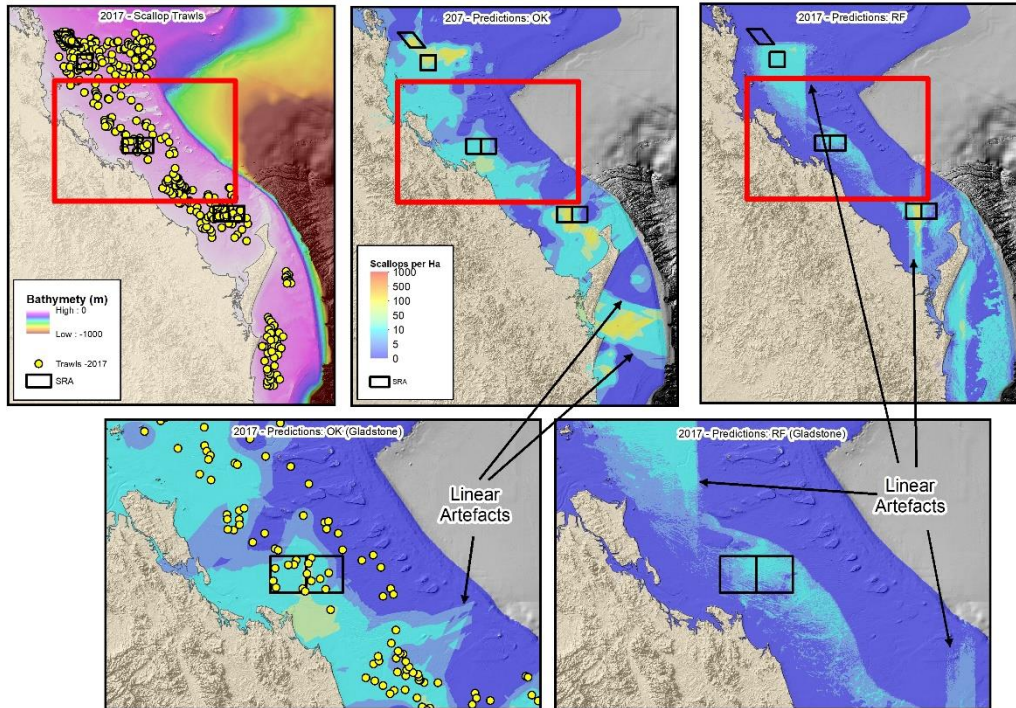
Figure 21-13. Map of scallop predictions for 2017. Maps show distribution of trawls, predictions for OK and RF_en, including details for the Gladstone region.
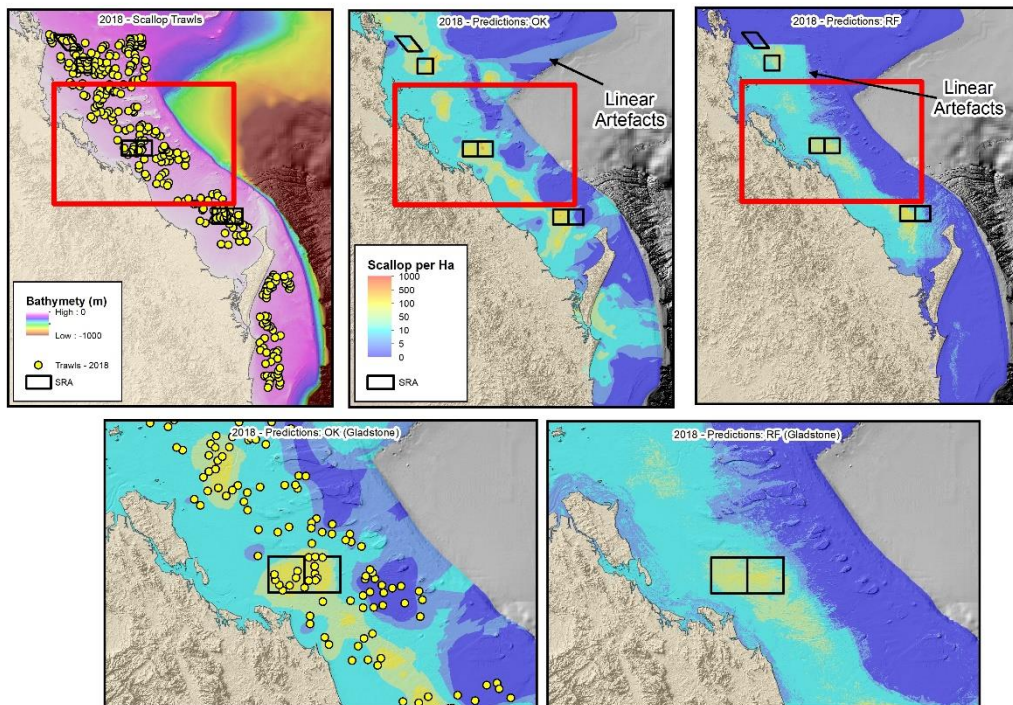
Figure 21-14. Map of scallop predictions for 2018. Maps show distribution of trawls, predictions for OK and RF_en, including details for the Gladstone region.
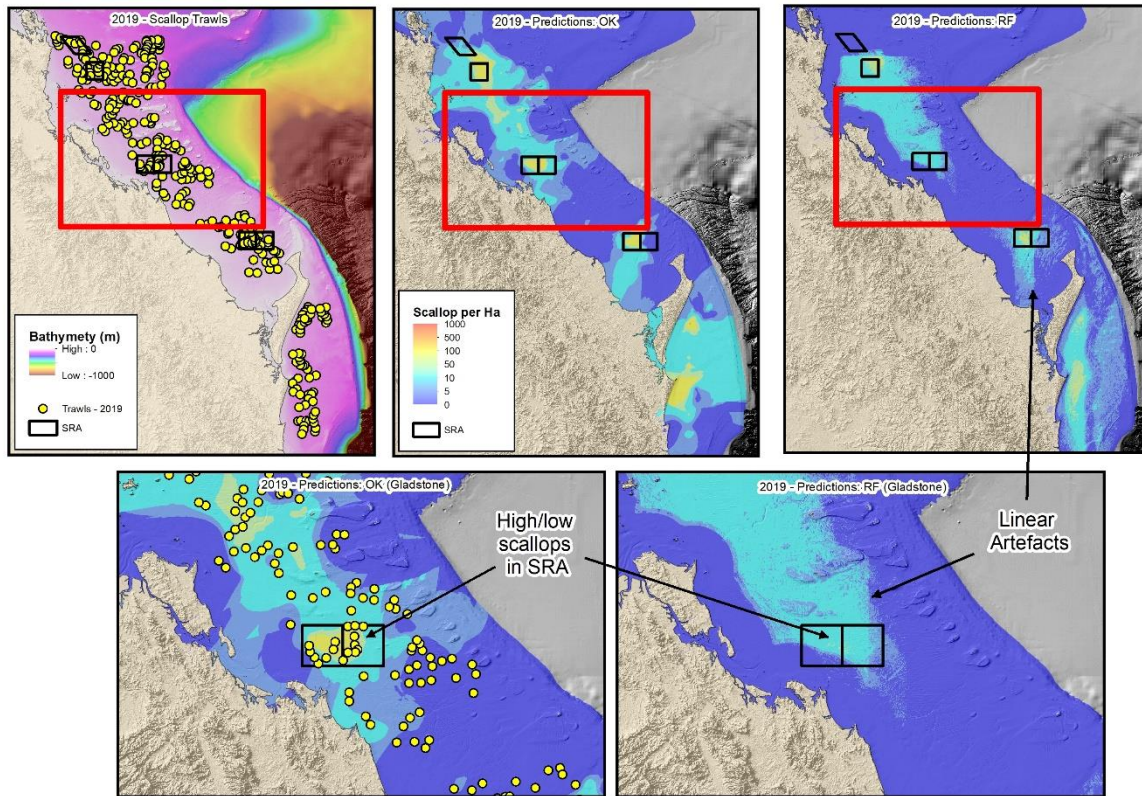
Figure 21-15. Map of scallop predictions for 2019. Maps show distribution of trawls, predictions for OK and RF_en, including details for the Gladstone region.

21.5 DISCUSSION

21.5.1 Comparison of spatial predictors

Through comparisons of scallop predictions from multiple years and using multiple methods it was shown that all of the tested methods except for the basic RF could be the best or second best performing method within a particular survey year. Li *et al.* (2011b), in predicting percentage mud data across the Australian Exclusive Economic Zone, concluded that different methods were superior in different geographical areas and highlighted the difficulty in making any generalizations about what method is 'superior' for a given prediction problem. Likewise, Li *et al.* (2011b) demonstrate that even a simple prediction technique such as IDW could be an effective predictor in some situations, and outperform ML methods in some instances, similar to what was demonstrated here in the prediction of saucer scallops (Table 21-18).

Li *et al.* (2011b) indicated that the inclusion of x and y as predictor variables would lead to artefacts with predictions. Linear artefacts were common in both the OK and RF methods from all years (Figures 21-9 to 21-15). Artefacts in the OK predictions were strongest in predictions far from the trawl locations. By comparison the RF predictions showed strong artefacts wherever the algorithm defines a break in the data. Averaging the predictions across multiple years, however, visibly reduced the appearance of artefacts and could be an effective way to produce a generalized and artefact-free model of scallop predictions. Averaging data from as few as three years (2017-2019) significantly reduced the appearance of artefacts (Figure 21-16).

The basic RF model was consistently the worst performing method in all years and commonly showed a significant loss in accuracy compared to the next second worst performing method. This result highlighted the importance of including x and y as covariates despite the resulting artefacts in these

predictions. Considering that IDW and OK also display artefacts, there should be no reason to exclude x and y when undertaking RF spatial predictions in the future.
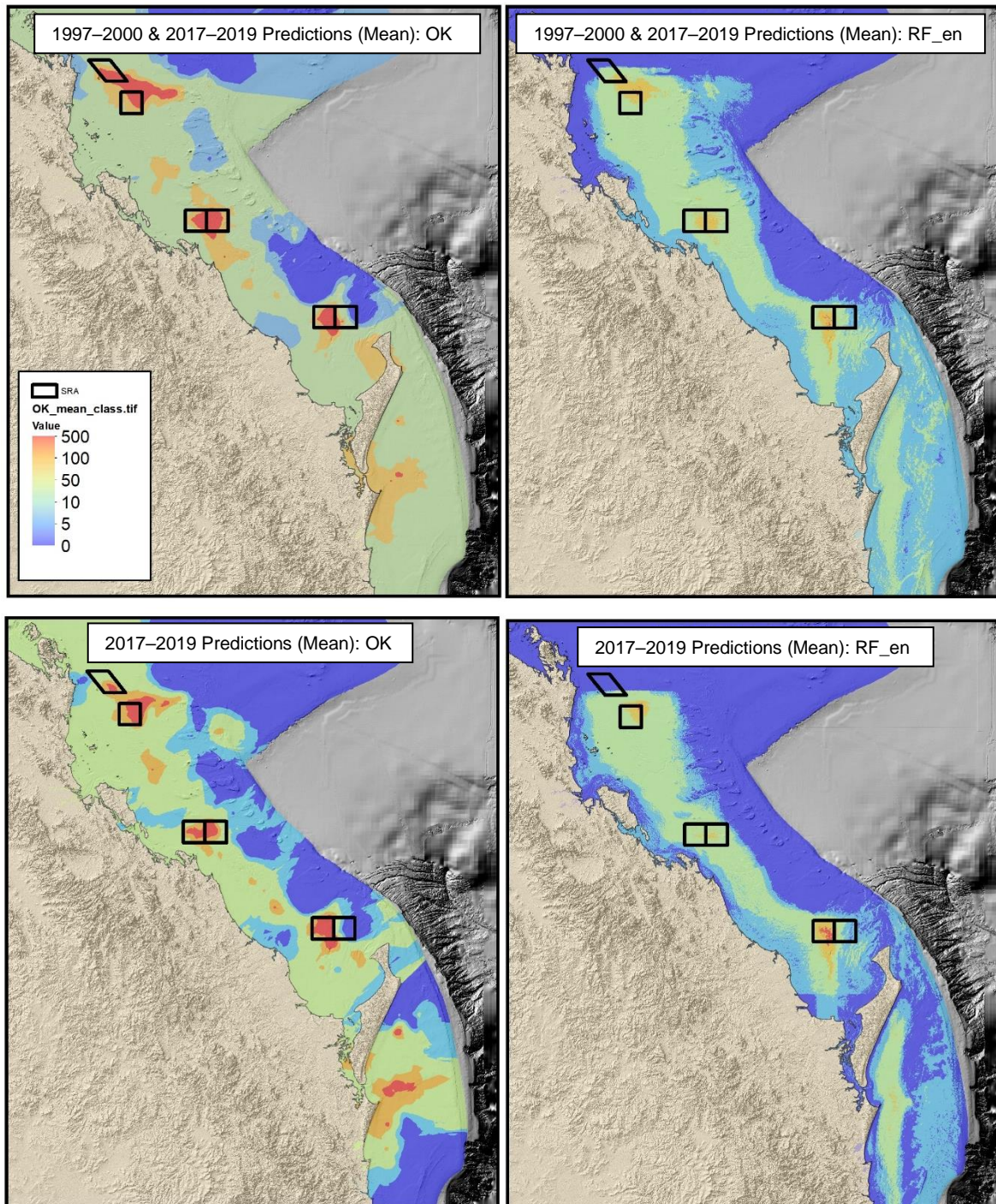
Figure 21-16. Map of mean scallop predictions for OK and RF_en for all years and 2017–2019 only. Note the OK model tends to overestimate the spatial distribution of scallops close to the coast.

21.5.2 Comparison of RF_en and OK

RF_en and OK were assessed to be the two best predictors of scallops. There were two key differences in the RF_en and OK predictions, specifically, 1) being inexact/exact predictors, and 2) the influence of covariates. Predictions of scallops using OK and RF_en from all years identified areas of

high scallop productivity in and around the SRAs and were consistent with previous surveys of the fishery (Jebreen *et al.* 2008). Being an inexact interpolator, the RF predictions provided a more generalized model of scallop density and showed comparatively smooth and lower amplitude peaks in scallop distribution compared to the OK predictions. The application of covariates within the RF_en models results in a more spatially constrained and realistic model of scallop distribution with comparatively few scallops predicted towards the shelf-edge and near the coast. As a result, both the OK and RF_en models have strengths and weaknesses when predicting scallops from yearly surveys.

The model averages (Figure 21-16) for RF_en showed comparatively high zones of scallop occurrences in a narrow north/south trending band in depths between 20 and 60 m, inshore of the adjacent reefs. This zone also overlaps with the SRAs which are known to be areas of comparatively high productivity. Whilst the averaged OK model displayed the same trend, it was not constrained by covariates and produced much higher densities of scallops in coastal zones and on the edge of the continental shelf that are not predicted by RF_en. It is thought that the RF model's use of covariates prevents the overestimation of scallop density, especially in deep and shallow water.

21.5.3 Does the inclusion of sediment data improve scallop predictions?

The RF_en_sed and RF_en_sed_phi models achieved rankings as high as 1 (1997, 1998) and 2 (2019) respectively. As a result, it could be concluded that adding sediment can improve scallop predictions. However, these methods were also outperformed by the RF_en method in four years so it would be erroneous to make a generalization that adding sediment data 'will improve predictions' of scallops within the fishery. The AVI data for the RF models consistently indicate that latitude, longitude and distance to the coast are the most important variables for predicting scallops. These three variables could be interpreted to suggest that the scallops are spatially clustered within the fishery and this is consistent with specific areas that are known scallop aggregations within the fishery, i.e., in and around the SRA's and near Fraser Island (Jebreen *et al.* 2008).

The higher accuracy of the RF_en model over the RF_en_sed model could be attributed to a number of factors:

1. The predictions of sediment properties, despite being statistically robust (see section 20, page 157), possibly did not accurately represent the highly variable nature of the seabed over the study area. Detailed mapping (see section 19, page 139) also provides evidence for a spatially diverse seabed offshore of Gladstone and in Hervey Bay. It is possible that the predicted sediment properties could be considered generalisations only and may not be optimal as covariates for this type of study. More detail acoustic mapping and sediment sampling (with co-located scallop trawls) would provide further detail on the variability of sediments and geomorphology.
2. Oceanographic processes might also play a strong role in the distribution of the saucer scallops and would be consistent with observations from the Atlantic sea scallop (Kostylev *et al.* 2003) and Patagonian scallop (Bogazzi *et al.* 2005) fisheries. Interrogating oceanographic outputs from the Great Barrier Reef eReefs hydrodynamic model (Steven *et al.* 2019) may also lead to additional covariates to explain the distribution of the saucer scallops.
3. The scallop population can be impacted by the temporal and spatial distribution of commercial fishing effort and/or catch. This is evident in the current poor status of the stock, which has been classed as overfished since the 2016 assessment by Yang *et al.* (2016). Future scallop distribution modelling might therefore be improved by incorporating an index of exploitation (i.e., effort, catch or fishing mortality *F*). However, this should be considered carefully because the scallop catch rates used in the models are based on a fishery-independent survey which already considers commercial fishing catch rates in its design.
4. The simple RF_en model appears to perform best using comparatively few 'good' covariates compared to RF models with more covariates. This result is consistent with Li *et al.* (2017; 2019) who concluded the inclusion of 'noisy or irrelevant' covariates may limit the capacity of RF models to select important variables during model training. Noisy predictors may lead to poor model performance despite the widespread acceptance that RF models are less

susceptible to noisy predictors than other ML methods (Díaz-Uriarte and De Andres 2006). Li *et al.* (2019) suggest the implementation of rigorous feature selection methods would improve model performance. For predicting saucer scallops, the exclusion of all noisy or irrelevant covariates should lead to improved model performance and would provide a better indication of how/if the inclusion of sediment data can improve predictions overall.

21.5.4 *Is there a relationship between sediment and scallop predictions?*

Previous studies have identified strong relationships between scallop species and sediment composition (Brand 2006; Dredge 2006; Himmelman *et al.* 2009). Species may prefer hard, consolidated substrates such as the byssally attached *M. varia.* Other species prefer coarse (i.e., gravelly) but unconsolidated substrates, such as the Atlantic sea scallop (*P. magellanicus)* and the Queen scallop (*A. opercular*). The Great or King scallop (*P. maximus*) shows a preference for comparatively fine sediments to enable them to recess into the seabed to avoid predation (Brand 2006; Himmelman *et al.* 2009). Saucer scallops, by comparison, have previously been associated with 'sand' (Welch *et al.* 2010) with recent co-located sampling of scallops and sediment indicating a strong relationship with fine sand. This preference for sand (possibly fine sand specifically) may be related to the scallop's habit of burying and thus may share similar behaviours to *P. maximus.* The co-location of samples that contain both sediment and scallops is very useful for examining the sediment-scallop relationship (see section 19.4.3, page 149). The inclusion of sediment sampling in future scallop annual surveys would be a way to get a regional assessment of the link between scallops and sediments, and evaluate the degree to which regional sediment predictions can be used as habitat proxies.

The regional Pearson's correlation analysis indicated that very coarse sand, coarse sand, mean grainsize, skewness, medium sand2, and mud showed low to medium correlations with saucer scallops over most years (Table 21-3). The results suggested scallops preferred habitats that have comparatively coarse sand compared to the findings in section 19.4.3, page 149, but did not favor areas with high gravel. The overall importance of Phi-scale sediment descriptors (i.e., fine sand, coarse sand, very coarse sand, etc.) indicated that the analysis of sediment in this way could be important for understanding the distribution of scallops and other benthos within the fishery and should be implemented in such studies.

21.5.5 *Conclusions and recommendations for future work*

It was hypothesized that the inclusion of sediment sample data into predictions of saucer scallop distribution should lead to more accurate models. The inclusion of sediment sample data improved predictions in some years, however, the OK and a simple RF model (excluding sediment but including x and y covariates) were the best performing methods overall. This was despite Pearson's correlations indicating that very coarse sand, coarse sand, mean grainsize, skewness, medium sand2, and mud showed low to moderate correlations with the density of the 1+ age class of scallops from fishery-independent surveys in most years. Model averages of scallop predictions identify broad lobes of prospective saucer scallop habitats 1) between the coast and Capricorn-Bunker Group, and 2) offshore from Fraser Island. Within these lobes there are regional 'highs' in saucer scallop density overlapping with known areas of high scallop productivity within the fishery.

Further research that would improve understanding the distribution of saucer scallops within the fishery and confirm linkages between scallops and seabed composition include incorporating:
1. hybrid interpolation/prediction methods, such as RFok and RFidw,
2. feature optimal 'feature selection' into RF-based models,
3. oceanographic variables from the Great Barrier Reef eReefs hydrodynamic model, and
4. sediment sampling into future regional scallop surveys.

22   Appendix 10. Estimating the instantaneous rate of natural mortality (*M*) of saucer scallops (*Ylistrum balloti*) on the Queensland east coast

This section of the report addresses Objective 3) *Derive one or more tagging-based estimates of the saucer scallop's natural mortality rate (M)*

22.1 ABSTRACT

Saucer scallops (*Y. balloti*) were tagged, released and recaptured inside two areas closed to fishing to measure their instantaneous rate of natural mortality (*M*). A total of 13,295 scallops were tagged and 526 recaptured over the 15 month-long experiment (May 2018 to August 2019). Three statistical approaches were applied to the tagging data, based on 1) the Brownie *et al.* (1985) Model 1, 2) a modified version of the Brownie model, and 3) a binomial logistic regression model of recaptures. Estimates of *M* based on the Brownie *et al.* (1985) Model 1 were much higher for tagged scallops that were at liberty over summer months compared to those at liberty over the winter months, indicative of seasonal variation. All three approaches indicated *M* was higher in the Hervey Bay closure (HBA) compared to the Yeppoon closure (YB). The logistic model detected significant effects on the recapture rate of tagged scallops due to closure, scallop size, lunar phase at recapture, recapture trip, the number of days the scallops were at liberty and the interaction between days at liberty and closure. Recapture rates were significantly higher in YB and during the waxing lunar phase. Annual mean estimates of *M* for the whole fishery ranged from a minimum of 1.461 year^{-1} for the logistic model, to 1.501 year^{-1} for the Brownie *et al.* (1985) Model 1, to 1.548 year^{-1} (variable recapture rate) and 1.594 year^{-1} (fixed recapture rate) for the modified Brownie *et al.* method. All three estimates were higher than the previous estimate that was published over 40 years ago and possible reasons for the increase are discussed.

22.2 INTRODUCTION

Saucer scallops (*Y. balloti*) are the basis for commercial trawl fisheries in Western Australia (WA) and Queensland. The species mainly spawns during winter and spring, although there is some geographic variation in spawning seasonality in WA (Dredge 1981; Joll and Caputi 1995b). Laboratory studies indicate a larval phase of 12–25 days prior to post-larvae settling at approximately 200 μm (Rose *et al.* 1988; Cropp 1992; Wang *et al.* 2002). Growth of juveniles to adults is rapid with individuals attaining a shell height (SH) of 90 mm in 6–12 months (Williams and Dredge 1981; Joll 1988). Dredge (1985a) estimated the instantaneous rate of natural mortality (*M*) for saucer scallops (50–110 mm SH) ranged from 0.020–0.025 week^{-1} (1.040–1.300 year^{-1}), which is relatively high and equates to annual mortality rate of about 60%, resulting in few individuals surviving more than three years (Dredge *et al.* 2016).

Queensland saucer scallop catches and catch rates have declined significantly in recent years, causing concern among fishers and prompting further research and quantitative assessments of the stock. Modelling fished populations and the conclusions drawn from stock assessments are heavily influenced by the data and parameters used. The instantaneous rate of natural mortality *M* is one of the most influential parameters used in stock assessments (Hilborn and Walters 1992; Sparre and Venema 1992). Previous assessments of the Queensland saucer scallop by Yang *et al.* (2016) and O'Neill *et al.* (2020) used the midpoint of the range put forward by Dredge (1985a) (i.e., *M* = 0.0225 per week, equivalent to 0.090 per month or 1.170 per year).

To obtain his estimates of *M*, Dredge tagged and released 56 batches of 99 scallops (*n* = 5544) in the fishery and over the following 126 weeks (~2.5 years) the commercial fishing fleet reported a total of 1564 recaptures. It is noteworthy that all the recaptured tagged scallops were caught by the fleet during their normal commercial fishing activities, as this would indicate that the scallop population was declining as a result of both natural mortality *M* and fishing mortality *F* acting simultaneously

over the recapture period. When combined, the mortality rates are referred to as total mortality Z (i.e., $Z = M + F$) and in such studies it is very difficult to quantify the individual components of M and F.

To derive his estimate of M, Dredge plotted the frequency distribution for a total of 393 separate weekly mortality rate estimates from the 56 batches. He acknowledged that the estimates were greater than M, referring to them as $\widehat{M}_{max}$, and then selected minimum values for his range estimate of M, stating "… the lowest estimates of $\widehat{M}_{max}$ therefore tend toward M for the species …".

While the lowest estimates of $\widehat{M}_{max}$ do approach M, it is unclear how close they are. The actual value of $\widehat{M}_{max}$ that Dredge chose to represent M to undertake a yield-per-recruit analysis of the stock was 0.025 week^{-1}, or 1.3 year^{-1}. The values of $\widehat{M}_{max}$ put forward by Dredge are biased upwards because they include an unknown component of fishing mortality F. Taking the minimum value may either under-compensate for that bias, as the minimum value still contains some fishing mortality, or over-compensate by not fully accounting for random variation in the individual estimates. The numbers of tag returns published by Dredge (1985a) vary greatly between the 56 batches: seven batches had no returns at all ($\widehat{M} = \infty$ for those batches), while 11 batches had return rates greater than 50% (lowest $\widehat{M}$ values) and largely determined the final estimate of M. The average return rate was 27.9/99 = 28.2%.

Dredge's estimate may also be affected by non-reporting of recaptured tagged scallops. Although he states, "Loss of tags through non-reporting is thought to have been negligible", no data or evidence are provided to support this. Even in the most well-planned tagging studies which rely on the fleet to report recaptures, it is likely that some recaptures will be unreported, for a range of reasons. If the non-reporting rate is constant over the recapture period, then it may not affect the estimate of M, however, if it varies over time it can have an effect (Hilborn and Walters 1992).

Given these concerns over the Dredge (1985a) estimate and its influence on the saucer scallop stock assessment, there is a strong need to re-examine estimates of M.

Following publication of the Yang *et al.* (2016) report, which concluded the stock to be recruitment overfished, Fisheries Queensland closed the six rotationally-opened SRAs in the fishing grounds indefinitely as a means of reducing fishing pressure and harvest. Closure of the SRAs presented an opportunity to undertake a second tag-recapture experiment to measure M, for three important reasons. Firstly, because the SRAs are associated with relatively high scallop densities, it's likely that a sufficient number of scallops could be caught, tagged, released and recaptured cost effectively inside the areas. Secondly, because the SRAs are closed to fishing, there is no fishing mortality applied to populations inside the closures. As a result, the tagged population would decline solely due to the prevailing natural mortality rate (assuming emigration out of the area is negligible) and the derived estimate of M would be free of the confounding effects of F, unlike the Dredge (1985a) estimate. Thirdly, if the tagged scallops are recaptured inside the closure by a dedicated research vessel sampling program, then any impact on the mortality rate estimates from non-reporting of recaptures by the commercial fleet would be negated (although some underreporting recaptures by researchers is still possible).

This section of the report presents results and analyses of new estimates of M for the Queensland saucer scallop based on a tag-recapture experiment conducted inside two closed SRAs in 2018 and 2019. It is anticipated that the updated estimates will be incorporated in future modelling of the stock and improve the quality of advice from future assessments.

22.3 METHODS

22.3.1 Experimental design

Estimates of the scallop's instantaneous rate of natural mortality M were derived using three statistical approaches for analysing tag-recapture data. The first was based on the Brownie *et al.* (1985) Model 1 for measuring the survival and recovery rate of birds that were banded and recovered annually. This

method, which is further based on the earlier work of Seber (1970) and Robson and Youngs (1971), uses the ratio of recoveries from annual bandings and can be applied to many species including fish. The second approach was a modification of the Brownie *et al.* (1985) Model 1 which avoided using discrete annual ratios and assumed a constant daily rate for *M*. The third approach was a binomial logistic regression model of the probability of recapturing tagged scallops. The model included fixed categorical terms and covariates which enabled estimation of the rate of decline in the tagged population (i.e., the natural mortality rate *M*). Detailed descriptions for each of the three approaches are provided below.

22.3.2 Tagging and recapture procedures

The tag-recapture experiment was located inside two SRAs in the Queensland saucer scallop fishing grounds that have been closed to trawling since September 2016; the Yeppoon B (YB) closure and the Hervey Bay A (HBA) closure (Figure 22-3). All tagging, releases and recapture of tagged scallops were undertaken on board the DAF 14.5 m *RV Tom Marshall* during five field trips (trip 1 May 2018, trip 2 October 2018, trip 3 March 2019, trip 4 May 2019 and trip 5 August 2019) undertaken out of the ports of Bundaberg and Yeppoon.

In trips1–4, scallops were trawl caught in and around the SRAs for tagging and release. When approximately 200 scallops had been tagged, the vessel steamed a short distance (i.e., < 2 nm) to a single fixed release site in the SRA (small green circle in YB and HBA, Figure 22-3) and the tagged scallops were released on the surface. The location of the release site in each SRA was selected based on 1) its proximity within the SRA (e.g., it had to be located at least 2 nm inside the perimeter, well away from any commercial fishing outside the SRA), and 2) its proximity to areas of relatively high commercial catch rates so that adequate numbers of scallops could be caught for tagging, and 3) the release site and surrounding area were suitable for later trawl sampling the tagged scallops. The depth at both release sites site was approximately 35 m.

The vessel deployed a 5 m beam trawl to undertake relatively short trawls of approximately 15 minutes to catch the scallops for tagging (Figure 22-1). Short trawl durations were deployed to minimise trauma and mortality to the scallops, prior to their measurement (shell height, mm), tagging and release. Upon initial capture, scallops were quickly removed from the net codend and placed in an aerated seawater tank on the back deck. Individuals were then removed from the water, measured, tagged and placed back into a second pre-release tank. While the process from initial capture to release took 30–90 minutes, individual scallops were kept out of water for only 2–10 minutes during measuring and tagging.

Trips were undertaken over 8–10 days (~4–5 days per SRA), weather permitting, with the vessel departing from port early each morning, operating all day inside the SRA, and then steaming back to port at night. Trips 1 (May 2018) and 2 (October 2018) were carried out solely to tag and release scallops (i.e., no recaptures). Trips 3 (March 2019) and 4 (May 2019) included both recapturing tagged scallops that had been released during previous trips, and then tagging and releasing additional scallops. Trip 5 (August 2019) was solely for recapturing tagged scallops from the previous four trips, as this was the last trip. Thus, there were four trips (trips1–4) that included tagging and releasing scallops, and three trips (trips 3–5) that included recapturing tagged scallops. Trips were planned to be undertaken over the waxing lunar phase, as scallop catch rates are generally higher during this phase (O'Neill and Leigh 2007), however, poor weather conditions affected the timing of some trips.

It took 1–2 days to complete trawl sampling of the recaptured scallops, followed by another 2–3 days to catch, tag and release additional scallops. Between 1335 and 2059 scallops were tagged and released in each SRA each trip. The shell height (SH) of scallops was measured to the nearest millimetre at the time of tagging and recapture. Hallprint FPN glue-on 8 mm yellow tags, numbered sequentially X000 to X999 (variable alphabetic letter), were glued onto the left valve (i.e., brown valve, Figure 22-1) of each scallop using cyanoacrylate glue.

A trawl sampling recapture grid was designed and centred over the release site in each SRA (Figure 22-3). The grids were 1 nm square, thus representing about 1% of the size of each SRA. Each grid consisted of 17 1-nm transects, with 9 transects in a north-south orientation and 8 transects in an east-west orientation. The central north-south transect passed directly through the release site (small green dot in the centre of the recapture grid, Figure 22-3). All other transects passed at a minimum distance of 0.05, 0.10, 0.25 or 0.50 nm from the release site.

Figure 22-1. The top images show deploying the 5 m beam trawl for catching untagged scallops (left) and emptying the codend (right). Middle images show scallops in holding tank waiting to be measured, tagged and released (left), and measuring and tagging the scallops (right). Bottom images show single and double tagged scallops (left) and releasing tagged scallops (right).

The recapture grid was designed to intensively sample the release site and surrounding area to recapture as many tagged scallops as possible, including those that moved distances up to 0.5 nm (perpendicular) from the release site (or 0.71 nm diagonal distance). Each transect took approximately 22 minutes to trawl sample. Because the same amount of sampling effort was applied during each recapture trip (i.e., the 17 1-nm transects were trawled each recapture trip), variation in the number of recaptured scallops each trip was not affected by varying levels of sampling effort. After trawl sampling each transect and recording the recaptures, the vessel steamed back to the release site in the centre of the grid and any recaptured tagged scallops were then released at the release site. In this way, the occurrence of the tagged scallops was recorded without killing them and the re-released tagged

scallops were left to remain in the tagged population in the centre of the recapture grid, with the potential to provide additional information from latter recapture trips.

22.3.3 Brownie et al. Model 1

The Brownie *et al.* (1985) Model 1 uses data from annual bird bandings and annual recoveries. Recoveries from any given banded cohort are modelled as multinomial variables. The notation and description of the data are provided in Table 22-1, where
N_i is the number of birds banded and released at the start of ith year, $i = 1,...,k$.
R_{ij} is the number bands recovered in year j from birds released in year i, $i = 1,...,k$, $j = 1,...,l$.

Table 22-1. General design of the Brownie *et al.* (1985) Model 1 to measure the recovery and survival rates of banded birds.

Year banded	Number tagged	Year of recovery				
		1	2	3	4	5 = l
1	N_1	R_{11}	R_{12}	R_{13}	R_{14}	R_{15}
2	N_2		R_{22}	R_{23}	R_{24}	R_{25}
3 = k	N_3			R_{33}	R_{34}	R_{35}

The expected number of recoveries for the above design is shown in Table 22-2, where f_i is the probability that a banded bird will be shot and its band reported during the next hunting season and S_i is the probability that a bird will survive one calendar year to the time of the next banding. The expected recoveries are the product of one or more annual survival rates from the year of banding to the year of recovery.

Table 22-2. The expected numbers of band recoveries, based on Brownie *et al.* (1985) Model 1.

Year banded	Number banded	Year of recovery				
		1	2	3	4	5 = l
1	N_1	$N_1 f_1$	$N_1 S_1 f_2$	$N_1 S_1 S_2 f_3$	$N_1 S_1 S_2 S_3 f_4$	$N_1 S_1 S_2 S_3 S_4 f_5$
2	N_2		$N_2 f_2$	$N_2 S_2 f_3$	$N_2 S_2 S_3 f_4$	$N_2 S_2 S_3 S_4 f_5$
3=k	N_3			$N_3 f_3$	$N_3 S_3 f_4$	$N_3 S_3 S_4 f_5$

The maximum likelihood estimator of the recovery rate f_i, denoted by the "hat" (^) over f_i in year i, is

$$\hat{f}_i = \frac{R_i}{N_i}\frac{C_i}{T_i} \qquad , i = 1, ..., k. \tag{1}$$

and the maximum likelihood estimator of the survival rate S_i, (denoted with ^) in year i, is

$$\hat{S}_i = \frac{R_i}{N_i}\left(\frac{T_i - C_i}{T_i}\right)\frac{N_{i+1} + 1}{R_{i+1} + 1}, \qquad i = 1, ..., k - 1. \tag{2}$$

where T_i is formulated with the following equations

$T_1 = R_1$,
$T_i = R_i + T_{i-1} - C_{i-1}$, $i = 2, ..., k$,
and if $l > k$, $T_{k+j} = T_{k+j-1} - C_{k+j-1}$, $j = 1, ..., s$,
$s = l - k$, the number of years beyond the year of the last release when recoveries are recorded, $s \geq 0$,

R_i and C_i represent row and column totals, respectively.

The strength of the Brownie method is that it is not sensitive to variation in catchability over time. Catchability of animals can rise or fall according to, e.g., lunar phase or water temperature, and this does not affect the validity of the results. A trade-off is that the method assumes perfect mixing of animals from different tagging episodes by the time they are recaptured on later trips, and it is sensitive to departures from this assumption.

The experimental design and analysis were applied to examine the survival rate of the saucer scallops and replicated in each scallop replenishment area (HBA and YB), with the following differences:
  1) Scallops were tagged with Hallprint tags rather than bands,
  2) Tagged scallops were recaptured by trawl sampling the 17 1-nm recapture grid transects,
  3) Recaptured tagged scallops were re-released alive back at the release site, whereas recovery of the bird bands was achieved by hunters killing the birds,
  4) Because the lifespan of saucer scallops is shorter than many bird species, the scallop tagging and recapture trips were not annual events, but rather periods between trips varied and were in the order of 3–5 months. As such, survival rate was based on the number of days that tagged scallops were at liberty and then adjusted to an annual rate.

Note that as the above survival rate estimate S_i is not affected by the recapture rate, estimation of f_i is not required in the current application.

22.3.4 Modified Brownie et al. method

The Brownie *et al.* (1985) Model 1 uses ratios of the number of recaptures from multiple annual releases and annual recapture events to derive multiple estimates of the annual survival rate, and hence multiple estimates of *M*.

Because the scallops were tagged and recaptured over shorter and variable periods, the Brownie survival rate estimate can be modified to $S(t_{ij})$ where

$$S(t_{ij}) = \exp(-M * t_{ij}) \tag{3}$$

M is the instantaneous rate of natural mortality per day.
t_{ij} is time at liberty defined as the period (in days) between Tag trip *i* and Recapture trip *j*.
N_i is the number of tagged scallops at Tag trip *i,* and
R_{ij} is the number of recaptured scallops at Recapture trip *j* that were tagged and released at Tag trip *i*.

Because it took more than one day to complete each Tag trip and each Recapture trip, the average time at liberty for recaptures R_{ij} was used.

These modifications to the data notation are reflected in Table 22-3 and Table 22-4.

Table 22-3. The modified Brownie *et al.* (1985) Model 1 design reflects the shorter and more variable periods between tagging trips and recapture trips used in the current saucer scallop study.

Tagging and release trip (release time)	Number released	Number recaptured by trip		
		Recapture trip 3 (March 2019)	Recapture trip 4 (May 2019)	Recapture trip 5 (August 2019)
Tag trip 1 (May 2018)	N_1	R_{13}	R_{14}	R_{15}
Tag trip 2 (October 2018)	N_2	R_{23}	R_{24}	R_{25}
Tag trip 3 (March 2019)	N_3		R_{34}	R_{34}
Tag trip 4 (May 2019)	N_4			R_{45}

Note that the modified method uses a single daily survival rate to estimate the number of expected recaptures and hence a single estimate of *M* (Table 22-4), whereas the Brownie *et al.* (1985) method uses multiple annual survival rate estimates to calculate the expected number of recaptures (Table 22-2).

Because the modified Brownie method assumed that *M* was constant over time, and made the survival fraction a parametric function of *M*, the maximum likelihood estimates could not be calculated explicitly and had to be found by an iterative numerical algorithm. Two model scenarios were considered for the recapture rate *f*; (1) a constant rate applied across the three recapture trips in March, May and August 2019 ($f_1 = f_2 = f_3 = f_i$), and 2) rates were allowed to vary (i.e., f_1, f_2 and f_3 were not necessarily equal). A numerical procedure to estimate recapture rates and *M* was conducted in the R environment 3.6.2 (R Core Team 2019) with package "bbmle" version 1.0.22 (Bolker and R Development Core Team 2019) and is provided in Supplementary material in section 22.6, page 256.

Table 22-4. The expected recaptures from the modified Brownie *et al.* method.

Tagging and release trip (release time)	Number released	Number recaptured by trip		
		Recapture trip 3 (March 2019)	Recapture trip 4 (May 2019)	Recapture trip 5 (August 2019)
Tag trip 1 (May 2018)	N_1	$N_1 S(t_{13})f_3$	$N_1 S(t_{14})f_4$	$N_1 S(t_{15})f_5$
Tag trip 2 (October 2018)	N_2	$N_2 S(t_{23})f_3$	$N_2 S(t_{24})f_4$	$N_2 S(t_{25})f_5$
Tag trip 3 (March 2019)	N_3		$N_3 S(t_{34})f_4$	$N_3 S(t_{35})f_5$
Tag trip 4 (May 2019)	N_4			$N_4 S(t_{45})f_5$

The major assumption in the Brownie models is that batches of tagged animals released at different times will mix. These models do not require any modelling of catchability or reporting rates; only the assumption that these do not depend on when an animal was tagged and released. The logistic regression model requires the major assumption that changes in catchability can be modelled accurately. If that can be done, it is less sensitive to departures from the mixing assumption.

22.3.5 Logistic model

A generalized linear model (GLM) was applied to model the proportion π of scallops that were recaptured from previous tagging trips. The model predicted recapture rates for varying periods at liberty and the estimates of *M* were based on the rate of decline in recapture rates. The model included categorical and continuous explanatory terms.

The binary response variable was based on the number of successes and the number of totals, where successes were the number of recaptured tagged scallops from each tagging trip caught during each recapture trip, and the totals were the number tagged at each tagging trip. The logit link function was used such that π was related to covariates as follows:

$$\ln\left(\frac{\pi}{1-\pi}\right) = \alpha + \boldsymbol{x}^t\boldsymbol{\beta}, \qquad (4)$$

where α is the intercept, $\boldsymbol{x}$ and $\boldsymbol{\beta}$ are the column vectors of covariates and coefficients, respectively. Superscript *t* refers to a matrix or vector transposed hereafter. $\boldsymbol{x}$ includes SRA, scallop size, lunar phase at recapture, days at liberty and the interaction between SRA and days at liberty. The explanatory terms had the following properties:
1. Scallop size is the size at tagging (3 levels: small < 90 mm SH, medium 90–95 mm SH and large > 95 mm SH).
2. SRA (2 levels; HBA and YB).
3. Lunar phase at recapture (2 levels; waxing and waning).
4. Recapture trip (3 levels; trip 3 March 2019, trip 4 May 2019 and trip 5 August 2019).

5   Days at liberty was a continuous variable equal to the number of days between release and recapture. As tagging and recapture trips both exceeded one day, the mean number of days at liberty was used.

The model was developed using GenStat statistical software (GenStat 2016).

22.3.6 Underlying assumptions

The following assumptions were made to make inferences from the tagging data:
1) Recaptured tagged scallops are representative of the scallop population.
2) The survival rate of the scallops was not affected by the tagging process, including being recaptured one or more times.
3) Emigration of scallops from inside to outside of the recapture grid was negligible.
4) Tag loss throughout the experiment was negligible.
5) The decline in the tagged population over time was not affected by fishing.
6) Scallops released during different tagging trips were well mixed by the time they were recaptured.
7) The logistic model accounted for variation in catchability of recaptured tagged scallops.

In regard to assumption 2 above, the cyanoacrylate glue that was used to attach tags to the scallop shell has been used in previous tagging studies on *Y. balloti* (Dredge 1985a; Campbell *et al.* 2010b), however, its possible impacts on scallop behaviour and survival have not been examined. Prior to undertaking the field work, the following laboratory-based pilot study was undertaken to examine these effects.

Scallops were caught by a commercial fisher and transported live from Urangan to the DAF Bribie Island Research Centre in southeast Queensland in May 2017. The effects of the glue on the survival of the scallops were examined from 5/5/2017 to 4/8/2017 (91 days). The glue was applied to one of the scallop's valves (left/brown valve, right/white valve) under four different treatments, including a non-glued control group (Table 22-5). Thirty scallops were subjected to each treatment ($n = 120$ scallops) and individuals from each treatment were equally distributed among three 5000 L fibreglass aquaria for the duration of the experiment (i.e., 10 scallops from each treatment in each tank). Recycled filtered sea water was continuously supplied to the aquaria and the scallops were provided with cultured algae twice daily as a food source. Scallop survival was recorded daily, and dead scallops were removed as soon as they were observed. A logistic binomial regression model of the data was undertaken in Genstat to test for differences in the survival rate between the four treatment groups.

Regarding assumption 4 above, tag loss was examined by double tagging approximately one in 15 scallops (~ 6.5%) in HBA and the loss of any tags was recorded upon their recapture.

22.4 RESULTS

22.4.1 Laboratory pilot study

The logistic binomial regression model of the pilot study data indicated no significant difference among treatments (approx. chi square probability = 0.573) at the end of the experiment. The results suggest that applying the glue had no significant effect on survival compared to the control group.

Table 22-5. Pilot study experiment design and results for examining the effects of the cyanoacrylate glue on the survival rate of scallops. There was no significant effect of the glue on scallop survival rate.

Treatment	Number of scallops	Number alive after 91 days	% survival
Controls (no glue)	30	14	46.7
Single glue droplet applied to Right/White valve	30	18	60.0
Single glue droplet applied to Left/Brown valve	30	19	63.3
Three glue droplets applied to Right/White valve	30	18	60.0

22.4.2 Field tagging

A total of 13,295 scallops were tagged and released in the two SRAs during the four tagging trips (trip 1 May 2018, trip 2 October 2018, trip 3 March 2019 and trip 4 May 2019). The size distribution of tagged scallops in YB ($n = 6260$) ranged from 44 to 107 mm SH with a modal peak of 90 mm SH, while the HBA scallops ($n = 7035$) ranged from 52 to 115 mm SH with a modal peak at 100 mm SH (Figure 22-2).
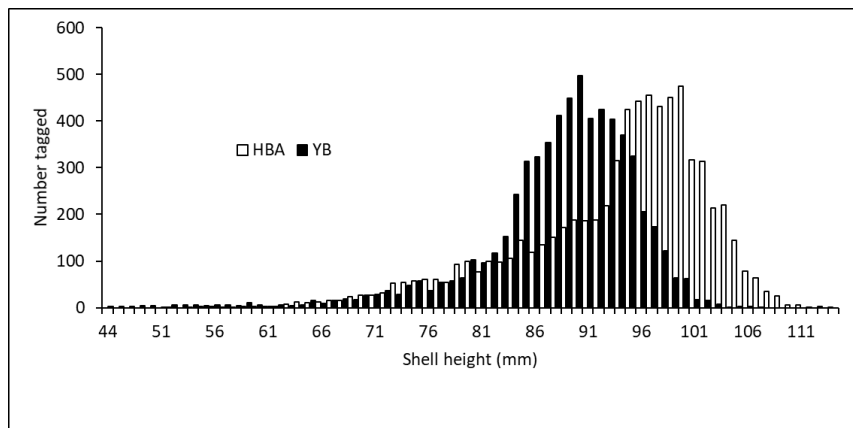
Figure 22-2. Size class distribution of tagged scallops in HBA and YB.

A total of 526 recaptures (4%) were obtained during the three recapture trips (trip 3 March 2019, trip 4 May 2019 and trip 5 August 2019), including 17 recaptures of individuals that were recaptured twice (Table 22-6). Of the 7035 scallops tagged in HBA, 226 were recaptured, including 11 that were recaptured twice. Of the 6260 scallops that were tagged in YB, 300 were recaptured, including 6 that were recaptured twice. Periods at liberty for the 226 recaptured scallops in HBA ranged from 55 to 456 days, with a mean of 171.7 (s.e. 7.4) days. Periods at liberty for the 300 recaptures at YB ranged from 73 to 453 days, with a mean of 205.4 (s.e. 6.0) days.

The precise location that a recaptured tagged scallop entered the net was unknown and limited to the length of the transect (i.e., 1 nm). By weighting the contribution of each transect to the total number of recaptures a density plot of the spatial distribution of recaptures was derived (Figure 22-3). In HBA most recaptured scallops were directly north of the release site, while in YB most recaptures were southeast of the release site.

Table 22-6. The number of scallops that were tagged and released from each tagging trip (i.e., trips 1–4) and the number of recaptures from each Recapture trip (i.e., trips 3–5). The experiment was repeated in two areas that are closed to fishing (i.e., HBA and YB).

HBA	Number tagged	Number recaptured trip 3 (March 2019)	Mean days at liberty when caught trip 3 (March 2019)	Number recaptured trip 4 (May 2019)	Mean days at liberty when caught trip 4 (May 2019)	Number recaptured trip 5 (August 2019)	Mean days at liberty when caught trip 5 (August 2019)	Total recaptures
Tag trip 1 (May 2018)	2006	30	295.1	17	352.9	7	455.3	54
Tag trip 2 (October 2018)	2059	37	157.1	22	215.1	4	317.5	63
Tag trip 3 (March 2019)	1489			71	55.7	20	158.2	91
Tag trip 4 (May 2019)	1481					18	101.3	18
Total	**7035**							**226**
YB								
Tag trip 1 (May 2018)	1411	41	290.5	23	364.0	11	453.0	75
Tag trip 2 (October 2018)	2039	63	170.2	41	243.7	14	332.5	118
Tag trip 3 (March 2019)	1335			34	73.0	28	162.0	62
Tag trip 4 (May 2019)	1475					45	88.8	45
Total	**6260**							**300**

Figure 22-3. The map shows the location of the six SRAs, including YB and HBA, and the 1 nm square recapture grids within YB and HBA (i.e., small dark blue square). The recapture grids comprised about 1% of each SRA. The expanded insets show the recapture grids' details, including the 17 1-nm transects, the release site (green dot) and the derived distribution of recaptures. All tagged scallops were released at the single release site located at the centre of each recapture grid.

22.4.3 *Brownie et al. Model 1 results*

A total of six survival rate estimates $\hat{S}_i$, and hence six instantaneous natural mortality rate estimates M, were derived using the Brownie *et al.* (1985) Model 1 method, three estimates for both HBA and YB (Table 22-7). Estimates of M based on the difference between recapture rates from tagging trip 1 (May 2018) and tagging trip 2 (October 2018) were relatively low at 0.379 year^{-1} and 0.283 year^{-1} for HBA and YB, respectively, indicative of low mortality over this period. We infer that low natural mortality over the winter (June, July and August) and early spring (September) is seasonal and happens every year, but additional field work would be needed to be verify this, as the experiment ran for only 15 months (May 2018–August 2019).

Estimates of M based on recaptures from tagging trip 2 (October 2018) and tagging trip 3 (March 2019) were relatively high at 3.566 year^{-1} and 1.216 year^{-1} for HBA and YB, respectively. Again, we infer that high natural mortality over spring (October, November and December) and summer (January and February) is seasonal, but additional field work would be needed for verification.

Table 22-7. Estimates of the survival rate $\hat{S}_i$ and natural mortality rate M based on Brownie *et al.* (1985) Model 1.

Area	Survival rate ($\widehat{S}_i$)	Difference in days at liberty between trips	M (per year)
[1]HBA	$\hat{S}_{Tag\ trips\ 1,2} = 0.866$	138	0.379
HBA	$\hat{S}_{Tag\ trips\ 2,3} = 0.212$	159	3.566
HBA	$\hat{S}_{Tag\ trips\ 3,4} = 1.048$	57	–0.301
[1]HBA*	$\hat{S}_{Tag\ trips\ 2,4} = 0.224$	216	2.527
[1]YB	$\hat{S}_{Tag\ trips\ 1,2} = 0.911$	120	0.283
[1]YB	$\hat{S}_{Tag\ trips\ 2,3} = 0.566$	171	1.216
[1]YB	$\hat{S}_{Tag\ trips\ 3,4} = 0.523$	74	3.199

* omits all tagging and recapture data from HBA tagging trip 3 (March 2019).
[1] indicates that the survival rate $\hat{S}_i$ was used to derive mean $\hat{M}$ for each SRA (see below).

Tagging trip 3, which was planned for February 2019, was delayed by one month to March, due to Tropical Cyclone Oma, which struck the region in February 2019 (Figure 22-4). As a result of the cyclone, the duration that those scallops that were tagged in HBA in trip 3 and recaptured in trip 4 (May 2019) was relatively short, with a mean of 55.7 days (Table 22-6). The estimate of M for HBA that was based on recaptures from tagging trip 3 (March 2019) and tagging trip 4 (May 2019) was –0.301 year^{-1} (Table 22-7), which is nonsensical and suggested the tagged population was increasing rather than declining. The YB estimate of M based on recaptures from tagging trip 3 (March 2019) and tagging trip 4 (May 2019) was 3.199 year^{-1}, indicating relatively high natural mortality from March (summer) to May (autumn). If data for the HBA tagging trip 3 (March 2019) are omitted, then two estimates of S_i are obtained for HBA and three estimates are obtained for YB (Table 22-7).
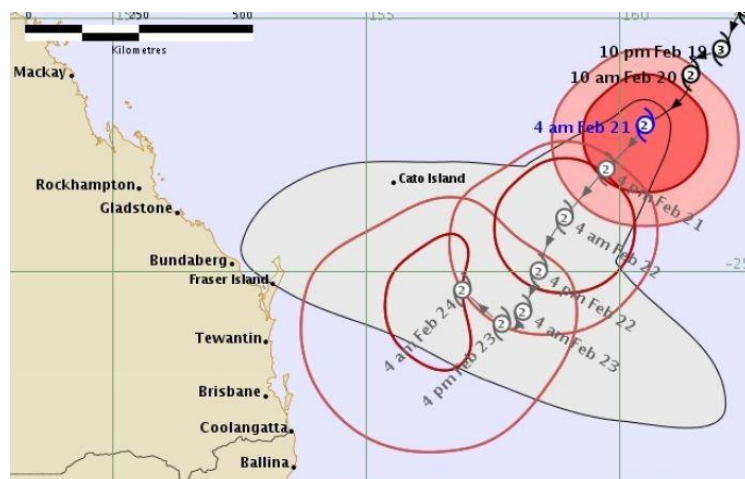
Figure 22-4. Trajectory of tropical cyclone Oma in February 2019 off the southeast Queensland coast. The cyclone delayed tagging trip 3 to March, which shortened the period at liberty for tagged scallops that were recaptured in HBA trip 4 (May 2019). The cyclone may have affected the mixing or catchability of tagged scallops released at HBA (i.e., located between Fraser Island and Bundaberg) in March 2019. Image is from the Australian Bureau of Meterology.

It is noteworthy that more tagged scallops from HBA tagging trip 3 (March 2019) were recaptured during trip 5 (August 2019), than those tagged in tagging trip 4 (May 2019), even though very similar numbers were tagged in both trips. Because the tagged scallops from tagging trip 3 were at liberty longer than those from tagging trip 4, it was expected that fewer of them would have been alive and recaptured during trip 5 (Table 22-6).

Weather again delayed undertaking trip 4 (May 2019) in YB and as a result, those scallops that were tagged and released in YB tagging trip 3 (March 2019) and were recaptured in trip 4 were at liberty longer than their HBA cohort. The mean period at liberty for those scallops that were tagged and released in YB tagging trip 3 (March 2019) and recaptured in trip 4 (May 209) was 73.0 days (Table 22-6). Hence, the relatively short period at liberty did not apply in YB.

The overall recapture rate of scallops that were tagged and released in HBA during tagging trip 3 was 6.1%, which was more than twice that of the other HBA batches of tag recaptures, including those scallops that were tagged during tagging trips 1 and 2, which were subjected to more recapture trips than those of tagging trip 3. Collectively, the recapture data suggest the scallops that were tagged and released in HBA tagging trip 3 had elevated recapture rates. If we omit all tagging and recapture data from HBA trip 3, and recalculate M using the recaptures from tagging trip 2 (October 2018) and tagging trip 4 (May 2019), then we obtain an estimate of $M = 2.527$ year^{-1} over the spring (October and November), summer (December, January, February) and autumn (March and April).

Mean estimates of M (i.e., $\widehat{M}$) for each SRA were derived using the most reliable survival rates ($\hat{S}_i$) (delineated with [1] in Table 22-7) and their respective periods at liberty t_i:

$$\widehat{M} = \frac{-\ln(S_{i1} * S_{i1})}{t_{i1} + t_{i2}} * 365.25 \tag{5}$$

where multiplying by 365.25 converts the estimate to an annual rate. Using this equation, the mean natural mortality rate $\widehat{M}$ for HBA and YB was 1.690 year^{-1} and 1.311 year^{-1}, respectively. The average of the two estimates, 1.501 year^{-1}, can be used to represent the whole fishery.

22.4.4 Modified Brownie et al. method results

Estimates of M from the modified Brownie *et al.* method for HBA were approximately twice that of YB (Table 22-8) and allowing the recapture rate f_i to vary had relatively little effect on the results. Means for the whole scallop fishery, based upon averaging across HBA and YB ranged from 1.548 year^{-1} (variable recapture rate) to 1.594 year^{-1} (fixed recapture rate).

Table 22-8. Summary of M estimates obtained from the modified Brownie *et al.* (1985) method under two recapture rate scenarios.

Recapture rate (*f*) model scenario	M year^{-1} HBA	M year^{-1} YPB	Mean $\widehat{M}$ year^{-1} whole scallop fishery
1) Fixed recapture rate applied to all three recapture trips ($f_1 = f_2 = f_3 = f_i$)	2.133	1.055	1.594
2) No constraints – recapture rates can vary (f_1, f_2 and f_3 were independent)	2.027	1.068	1.548

22.4.5 Logistic model results

The 526 recaptured scallops were allocated across a total of 50 replicates for size class, SRA closure, lunar phase and recapture trip (Table 22-9). No replicates were obtained for the wanning lunar phase during trip 3 or the waxing phase during trip 5. Note that as the number of tagging trips increased, the number of replicates also increased.

Table 22-9. The number of replicates obtained for each treatment combination. Replicates were from the four release tagging trips (i.e., May 2018, October 2018, March 2019 and May 2019).

	Recapture trip 3	Recapture trip 4	Recapture trip 5	Grand total
Large (>95 mm SH)				
Wanning				
HBA	0	0	3	**3**
YB	0	3	3	**6**
Waxing				
HBA	2	3	0	**5**
YB	2	0	0	**2**
Medium (90-95 mm SH)				
Wanning				
HBA	0	0	4	**4**
YB	0	3	4	**7**
Waxing				
HBA	2	2	0	**4**
YB	2	0	0	**2**
Small (less than 90 mm SH)				
Wanning				
HBA	0	0	3	**3**
YB	0	3	4	**7**
Waxing				
HBA	2	3	0	**5**
YB	2	0	0	**2**
Grand total	**12**	**17**	**21**	**50**

The accumulated analysis of deviance for the logistic model indicated that the proportion of tagged scallops that was recaptured was significantly affected by lunar phase at the time of recapture, SRA, recapture trip, scallop size class and the mean days-at-liberty. There was also a significant interaction between days-at-liberty and SRA (Table 22-10).

Table 22-10 Accumulated analysis of deviance for logistic model of tagged scallop recaptures

Change	d.f.	deviance	Mean deviance	Deviance ratio	Approx. chi pr
Lunar phase	1	24.649	24.649	24.65	< 0.001
SRA	1	41.086	41.086	41.09	< 0.001
Recapture trip	2	8.568	4.284	4.28	0.014
Size class	2	10.557	5.279	5.28	0.005
Mean days at liberty	1	85.747	85.747	85.75	< 0.001
Mean days at liberty*SRA	1	6.881	6.881	6.88	0.009
Residual	41	51.041	1.245		
Total	49	228.53	4.664		

The proportion of recaptures was significantly higher during the waxing lunar phase, compared to the waning phase, and significantly higher at YB compared to HBA (Table 22-11). The negative parameter value (–0.0053) indicated that proportion declined significantly with mean days at liberty, as expected. Small (< 90 mm SH) and medium (90–95 mm SH) scallops had a significantly higher proportion recaptured compared to large (> 95 mm SH) scallops. The significant influence among recapture trips (Table 22-10) is attributed to differences between constants, as there were no significant

differences among the parameter values (Table 22-11). The significant interaction between mean days at liberty and SRA indicated that the rate of decline in recaptures differed between the two areas.

Table 22-11. Parameter estimates from the above logistic model. Reference levels were waning for lunar phase, HBA for SRA, and large (> 95 mm SH) for the size class.

Parameter	Estimate	s.e.	t(*)	t pr.	Antilog of Estimate
Constant	−3.763	0.305	−12.34	< 0.001	0.02321
Lunar phase (waxing)	0.556	0.186	2.99	0.003	1.744
SRA (YB)	0.008	0.219	0.03	0.972	1.008
Recapture trip (trip 4 May 2019)	0.125	0.148	0.84	0.398	1.133
Recapture trip (trip 5 August 2019)	−0.103	0.218	−0.47	0.637	0.9023
Size class (Medium 90–95 mm SH)	0.426	0.127	3.35	< 0.001	1.531
Size class (Small < 90 mm SH)	0.447	0.127	3.53	< 0.001	1.563
Mean days at liberty	−0.0053	0.0007	−7.72	< 0.001	0.9947
Mean days at liberty*SRA (YB)	0.00231	0.000885	2.61	0.009	1.002

The above model was used to predict the recapture rate for each SRA and size class for tagged scallops that had been at liberty between 100 and 600 days (Figure 22-5). The predictions reflect the higher recapture rate in YB compared to HBA. An exponential regression was fitted to the predictions to obtain estimates of *M*. For example, the regression for YB can be expressed as $y = 0.0409e^{-0.003x}$, where *y* is the recapture rate (i.e., number caught as a proportion of number tagged), *x* is the mean days at liberty and the exponential value of 0.003 is the daily rate of decline, or *M*. Multiplying the daily rate by 365.25 converts it to an annual rate. Hence *M* for YB was 0.003 day^{-1} or 1.096 year^{-1}. Similarly, the resulting estimate of *M* for HBA was 0.005 day^{-1} or 1.826 year^{-1}. The average for the two areas was 0.004 day^{-1} or 1.461 year^{-1}.

The size class predictions reflect the higher recapture rates for the small and medium size classes (Figure 22-5). There was very little difference between small and medium size classes, but the recapture rate of large scallops was noticeably lower.

An exponential regression was fitted to each of the size class recapture rate predictions. However, while the three regressions differ, they all had the same exponential rate of decline, and hence *M* was 0.004 day^{-1} or 1.461 year^{-1} (i.e., there was no significant interaction between size class and mean days at liberty). Because there was no difference in the exponential rate of decline (i.e., no difference in *M*) among the size classes, the results suggest a difference in catchability, with small and medium size classes having higher catchability than large scallops.

22.5 DISCUSSION

22.5.1 Assumptions

   1) *Recaptured tagged scallops are representative of the scallop population.*

The methods included procedures to reduce the impact of capture, tagging, release and recapture on the behaviour and survival rate of the scallops. To reduce impacts, the duration of trawls used to catch scallops for tagging was limited to 15 minutes, the duration that scallops were held in seawater on the back deck was as short as practically possible, and the duration that scallops were held out of water for measuring and tagging was also minimised. Holding tanks were shaded to reduce the amount of sunlight the scallops were exposed to and tagged scallops were released in relatively small batches, again to reduce the amount of time they were held outside their natural environment. Despite these measures, it's likely that some mortality was imposed on the scallops because of the tagging and

recapturing processes. If this mortality was relatively small and constant throughout the study, then it should have negligible influence on the estimates *M*.
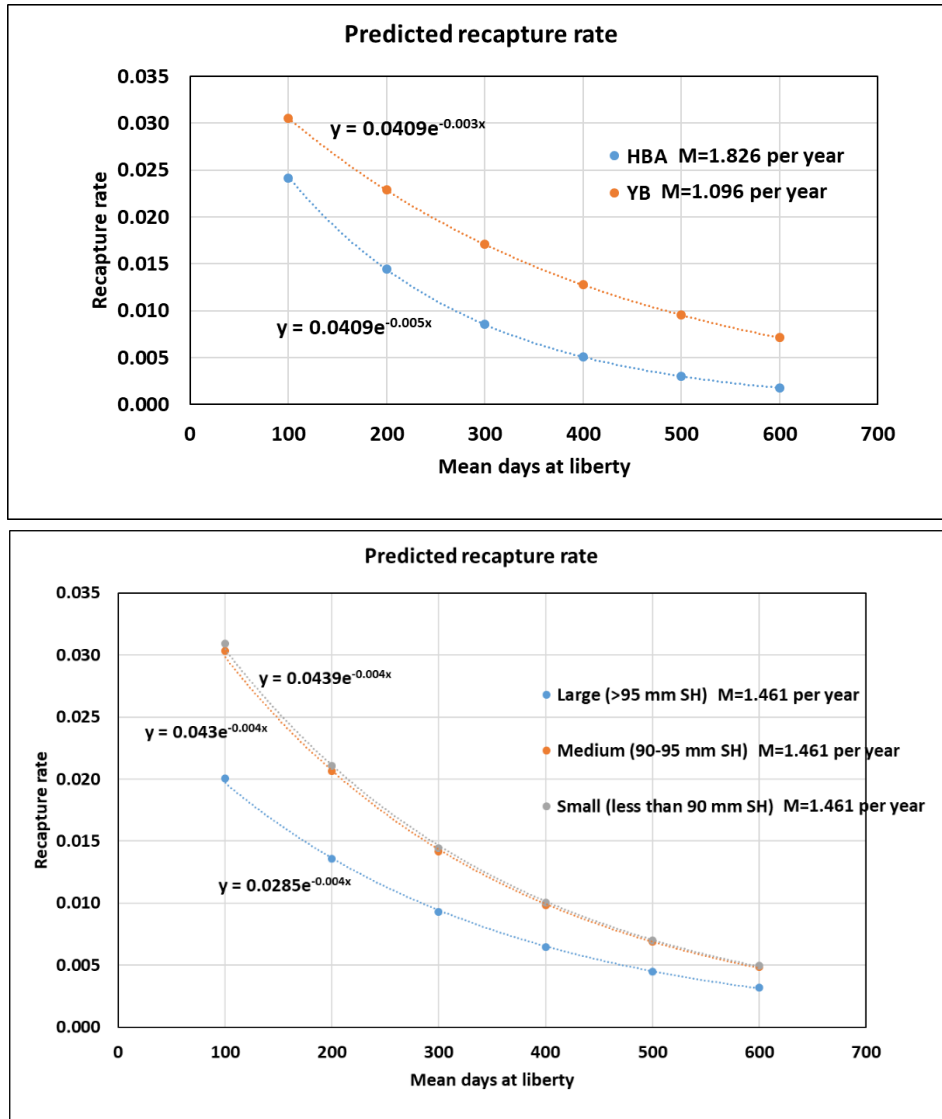
Figure 22-5. The predicted recapture rate of tagged scallops at the two SRAs and for the three size classes. Exponential regressions fitted to the predictions provide estimates of *M*.

The size class frequency distribution of the scallop population is unknown and therefore it is difficult to determine whether the size distribution of the tagged population was representative. The size distribution of the tagged scallops covered a broad range 44–115 mm SH, but it was clearly limited by poor representation of scallops that were < 44 mm SH (Figure 22-2). The poor representation of small size classes is consistent with previous studies that have used trawl gear to sample saucer scallops (Dichmont *et al.* 2000; Courtney *et al.* 2008; Campbell *et al.* 2010b). Collectively, the results from the present tagging study and previous studies indicate that the catchability of small scallops (i.e., < 44 mm SH) by benthic trawl gear is very low. While the size distribution of the tagged population is likely to differ from the untagged population, the resulting estimates of *M* are still highly relevant to the size range considered. In addition, the logistic model included size class as an explanatory term, which is informative for examining size related differences in *M*.

2) *The survival rate of the scallops was not affected by the tagging process, including being recaptured one or more times.*

The pilot study results indicate that the glue used in the tagging process is unlikely to affect survival, however, they do not address all the possible effects of the tagging process on survival. It is unlikely that the 8 mm yellow Hallprint FPN tags, which were glued onto the scallop's left valve, would have altered their catchability or survival rate, because the tags are relatively small and cover approximately 1% of the scallop's valve surface area. Furthermore, as the scallops partially bury, it is unlikely that the tag would have made the scallops more vulnerable to predation.

The impact of recapture on the survival rate was not quantified. Any impact from recapture was reduced by undertaking the recapture trawls along relatively short 1 nm transects, which took about 22 minutes to complete. Recaptured tagged scallops were identified quickly after the codend was emptied, and then placed in aerated seawater on the back deck prior to their details being recorded. The recaptured tagged scallops were then re-released at the release site within minutes of being caught. Although the impact of recapture on survival was not quantified, it is obvious that recapture did not result in 100% mortality because several tagged scallops were recaptured twice.

3) *Emigration of scallops from inside to outside of the recapture grid was negligible.*

A total of 10 tagged scallops (1.9% of the 526 recaptures) were recaptured in the outermost transects of the sampling grids, which passed a minimum distance of 0.5 nm from the release site (Figure 22-3). In HBA, 7 of the 226 (3%) recaptures were caught in the outermost transects after periods at liberty ranging from 158 to 455 days. In YB, 3 of the 300 (1%) recaptured scallops were caught in outermost transects after periods at liberty ranging from 290 to 453 days.

The movement of scallops within each SRA differed, with most recaptures in HBA moving directly north of the release site, while most recaptures moved southeast of the release site in YB. In both areas there were negligible recaptures west of the release site (Figure 22-3).

When results for both HBA and YB are considered, the overall emigration rate (from inside to outside the SRA) was low, as < 2% of recaptures were caught on the outermost transects over the 15-month duration of the study (May 2018 to August 2019). However, it would be unwise to ignore the effect of the emigration rate on the estimates of *M*. The results also suggest that the emigration in HBA was higher than YB, because it had more than twice as many tagged scallops reach the grid perimeter than YB.

Regarding assumption 3 above, the results suggest that while the emigration rate is low, it is unlikely to be negligible and will therefore likely make a small contribution to the estimates of *M*, particularly for HBA.

4) *Tag loss throughout the experiment was negligible.*

A total of 465 scallops were double tagged in HBA to quantify tag loss. Of these, 19 were recaptured (4%), with periods at liberty ranging from 55 to 159 days. All the recaptured scallops had both tags attached, indicating negligible tag loss over this period, thus supporting the assumption 4 above.

5) *The decline in the tagged population over time was not affected by fishing.*

HBA and YB are two of six SRAs that have been closed to trawling for approximately four years. The purpose of the closures is to limit catch and effort applied to the scallop stock, which has been classed as overfished for most of this period. It is possible that the tagged populations inside HBA and YB were subjected to fishing effort, and hence declined due to fishing mortality over the duration of the experiment. However, this is unlikely because fishers are aware of the closures, which are patrolled by the state government Queensland Boating and Fisheries Patrol, and because all trawl vessels in Queensland have been fitted with vessel monitoring systems (VMS) since 2000, which alert the authorities when vessels approach the SRAs. In addition, some commercial fishers also report illegal fishing activity and thus compliance is expected to be high.

The 1-nm recapture grids where the tagging, release and recaptures were undertaken are very small relative to the SRAs. For example, the recapture grids are approximately 3.4 km^2 while HBA and YB SRAs are both approximately 310 km^2 (Figure 22-3). Therefore, the recapture grids make up about 1% of each SRA. Even if some illegal fishing did occur inside the SRAs during the experiment, it is unlikely it would have occurred over the precise location of the recapture grids. For these reasons, it is unlikely that the tagged population was affected by fishing during the study, and therefore the above assumption is upheld.

6) *Scallops released during different tagging trips were well mixed by the time they were recaptured.*

It is difficult to quantify how well the four batches of tagged scallops remained mixed in each SRA after they were released, however, it is important to note that the study intentionally promoted mixing of the batches by releasing all scallops at a single release site (Figure 22-3) e.g., all 7035 tagged scallops in HBA were released at a single release site, and similarly all 6260 tagged scallops in YB were released at a single release site. It is unknown whether mixing increased with time at liberty. In the days and months following release, the scallops generally dispersed in a northerly direction in HBA and towards the southeast in YB. The results indicate that some mixing of the batches occurred, because as the recapture trips progressed, recaptures from the different releases were recorded. For both HBA and YB, Table 22-6 shows that the recaptures in the last recapture trip (i.e., trip 5 August 2019) were composed of scallops that were tagged in each of the previous four tagging trips. The results indicate that some mixing of the batches occurred, and therefore, that this assumption is at least partially upheld.

7) *The logistic model accounted for variation in catchability of recaptured tagged scallops.*

The logistic model accounted for variation in the proportion of recaptures due to SRA, scallop size class, lunar phase, recapture trip and days at liberty, as well as the SRA-days at liberty interaction term. It is often difficult to allocate the variation in catch rates to either abundance or catchability. However, it is reasonable to assume that the strong short-term variation detected in recaptures due to lunar phase was due to variation in catchability. It is unclear if catchability varied with the time at liberty for tagged scallops, since the abundance of tagged scallops declines with time at liberty, due to mortality i.e., the longer the time at liberty, the more scallops die and the fewer that are caught.

It is likely that there are too many influential factors of scallop catchability to include in the model to completely account for variation in catchability. These factors likely include physical oceanographic properties, plankton concentrations (which affect scallop feeding and behaviour) and scallop predator behaviour, and many other influences. Scallop catchability may be affected by SST, and although this was not included in the model, it's influence may have been at least partially captured by including recapture trip as an explanatory term, as this term reflected some monthly and seasonal variation in SST.

The scallop recapture sampling program was designed to limit variation in catchability due to sampling gear by using the same beam trawl and net for recapturing tagged scallops on each recapture trip. In addition, the same amount of sampling effort was applied during each recapture trip, i.e., 17 1-nm transects were sampled at each SRA on each recapture trip. Hence, variation in the number of recaptured tagged scallops was not affected by sampling effort.

Analysis of the Queensland scallop fishery survey data demonstrated that catchability varied significantly with time-of-night scallop (Table 16-6, page 79), however this was also not included in the model. In summary, the logistic model included some factors influencing scallop catchability, which improved the recapture rate predictions and subsequent estimates *M*, compared to using the observed data only, however, it is not possible to include all factors affecting catchability in such a

model. For these reasons, the assumption is partially upheld, but it is important to note that accounting for 100% of the variation in catchability is not practically possible.

22.5.2 Comparing methods

The Brownie *et al.* (1985) Model 1 is designed to calculate the annual survival rate S_i and when applied to comparatively long-lived species (such as birds), the expected number of recaptures is based on the product of multiple annual survival rates. In the current study, estimates of S_i were derived for shorter and variable periods between tagging trips (i.e., months).

Reasons for the unrealistic HBA estimates from tagging trip 3 (March 2019) are unknown, however, they may have been at least partially attributed to Tropical Cyclone Oma, which impacted Hervey Bay more than the Yeppoon region (Figure 22-4). Furthermore, the tagging undertaken in HBA during trip 3 occurred on the 13-14 March 2019, a few days after the cyclone, whereas the tagging undertaken in YB for trip 3 occurred later on 17 March. Although speculative, the water column may still have been in a disturbed state from the cyclone when the scallops were tagged and released in HBA in trip 3. Residual effects of the cyclone may have affected the mixing of scallops that were tagged and released at HBA in trip 3. The Brownie method assumes that animals from different batches are perfectly mixed by the time they are recaptured.

It is also noteworthy that the period at liberty for scallops that were tagged and released in HBA tagging trip 3 (March 2019) and recaptured in trip 4 (May 2019) was the shortest of any batch of recaptures (55.7 days, Table 22-6). The relatively short period at liberty may have affected the catchability of scallops, resulting in their relatively high recapture rate in HBA in trip 4 (May 2019). Even though the period at liberty was short, and therefore the expected number recaptured was high, the proportion of scallops that were tagged in tagging trip 3 (March 2019) and recaptured in trip 4 (May 2019) appears disproportionately high, and was the highest observed for any batch of tagged scallops (i.e., 71 recaptures from 1489 releases, 4.8%, Table 22-6).

We have inferred that the high variation in S_i reflects seasonal variation in survival and hence seasonal variation in the natural mortality rate M; i.e., it happens every year For example, estimates of M that were based on the ratio of recaptures from tagging trip 1 (May 2018) and tagging trip 2 (October 2018) were relatively low at 0.38 year^{-1} and 0.28 year^{-1}, for HBA and YB, respectively, possibly indicating that the scallops experience relatively low natural mortality over winter (June, July, August) and early spring (September). In contrast, the estimate of M for HBA which was based on the ratio of recaptures from tagging trip 2 (October 2018) and tagging trip 4 (May 2019) was relatively high at 2.53 year^{-1}, possibly indicating that the scallops experience relatively high natural mortality over spring (November, December), summer (January, February March) and early autumn (April). Similarly, the YB estimate of M which was based on the ratio of recaptures tagging trip 2 (October 2018) and tagging trip 3 (March 2019) was also comparatively high at 1.22 year^{-1}, possibly indicating relatively high natural mortality over spring (November, December) and summer (January, February). Because our experiment ran for only 15 months (May 2018–August 2019), additional field work would be necessary to be certain of the seasonal variation.

The YB estimate of M that was based on the ratio of recaptures from tagging trip 3 (March 2019) and tagging trip 4 (May 2019) was relatively high at 3.20 year^{-1} and mainly covered two months during autumn (April, May). This high estimate may have been influenced by the relatively short period between tagging trips 3 and 4 (i.e., 74 days), and consequently, the short period at liberty for the 73 scallops from tagging trip 3 that were recaptured during trip 4 (Table 22-7).

The multiple estimates of survival rate S_i from the Brownie *et al.* (1985) Model 1 are therefore useful for examining possible seasonal variation in M. However, because the method generates multiple estimates that are based on the ratio of recaptures from different tagging trips, small anomalies or variations in either of the number of recaptures used for ratio numerator or the denominator can have a marked influence on individual estimates. This was apparent in HBA when the estimate of S_i was

based on recaptures from tagging trip 3 (March 2019) and tagging trip 4 (May 2019). As a result of the high recaptures from tagging trip 3 in trip 4 (71 recaptures) and trip 5 (20 recaptures), and the relatively low recaptures from tagging trip 4 in trip 5 (18 recaptures), the estimate of S_i was larger than 1, indicating the tagged population was increasing rather than declining – a nonsensical result.

In general, the results suggest that estimates of S_i and M obtained via the Brownie *et al.* (1985) Model 1 are more reliable when there is a large time period between tagging trips and the period at liberty is long. This is based on the simple logic that greater contrast in population size occurs when observations are taken over a long period compared to short period. Longer periods between tagging trips and longer periods at liberty allow for a greater proportion of the population to die, which is easier to detect and measure than a small proportion of the population. For these reasons, if the experiment was to be repeated, it would be prudent to increase the minimum periods between tagging trips and the minimum period that scallops are at liberty prior to recapture, to 100 days. These minima are subjective, but nevertheless if applied would likely improve the reliability of the estimates of S_i and M, although the longer periods would also reduce the number tagging trips and recapture trips per year, resulting fewer estimates.

The least reliable estimate of S_i and M, which was based on recaptures from tagging trip 3 (March 2019) and tagging trip 4 (May 2019) in HBA, included recaptures that were at liberty for only 56 days and the period between these tagging trips was only 57 days.

It may also be advisable to avoid tagging scallops during and shortly after the tropical cyclone season, as the residual effects of cyclones may adversely affect the mixing of scallops tagged at that time with those tagged in previous or subsequent episodes. The HBA tagging trip 3 in March 2019 occurred shortly after a cyclone and recovery rates from that batch were substantially higher than other batches, indicating that the HBA trip 3 batch may not have mixed properly with the other batches. The mechanism underlying cyclone impacts is unknown, however it is noteworthy that declines in coral trout (*Plectropomus leopardus*) catch rates following certain types of severe cyclones are believed to stem from reduced catchability rather than reduced abundance (Courtney *et al.* 2015). In brief, the damage caused to reefs from cyclones is thought to predispose prey fish species to greater predation by coral trout, which in turn reduces the trout catchability by fishers. Although scallops are filter feeders, it's possible that cyclones might also affect their behaviour and subsequent catchability.

The modified Brownie *et al.* (1985) model did not utilize recapture ratios and nor was it designed to estimate multiple estimates of S_i or M. Rather, it assumed a constant value for M that was based on numerical optimization, and the number of scallops surviving from a single tagging trip was a function of M and the time of liberty. As such, the modified Brownie *et al.* (1985) method did not result in any spurious estimates of M that may have resulted from unstable ratios of recaptures, but nor did it provide any information on possible seasonal variation in M. It was, however, sensitive to time-varying catchability, including lunar phase.

The logistic model revealed several factors affecting the catch rate of tagged scallops, which is useful for interpreting the data and quantifying M. Lunar phase appeared to have had a strong influence on the number of recaptured tagged scallops during each recapture trip. The antilog of the parameter estimate (1.744, Table 22-11) indicated the recapture rate almost doubled during the waxing phase compared to the waning phase. The tagging trips were planned to be undertaken over the waxing lunar phase, however due to adverse weather conditions, this was not always possible, and some recapture sampling had to be undertaken during the wanning phase, as reflected in the table of treatment replicates (Table 22-9). Including lunar phase as an explanatory term in the logistic model resulted in more accurate recapture rate predictions. Lunar phase affects tidal currents, which appears to affect the catchability of the scallops. Queensland fishers avoid fishing for scallops during the strong spring tidal currents that occur during the full and new moon phases, and fish during the weaker neap tides that occur between the new and full moon, especially the waxing phase. Lunar phase is also taken into account when standardising the scallop commercial catch rate data for stock assessment (O'Neill *et al.*

2003; O'Neill and Leigh 2007; Yang *et al.* 2016), when planning the scallop fishery-independent survey (Dichmont *et al.* 2000) and when modelling the survey catch rates (see section 16.3.8, page 51).

It's likely that the numbers of recaptured scallops that were used in Brownie *et al.* (1985) Model 1 recapture ratios were affected by the lunar phase at recapture, which could explain some of the less reliable ratios and subsequent estimates of *M*. This could be addressed by using the logistic model to derive adjusted recapture rates which standardise for lunar effects. The adjusted numbers could then be used in the ratios.

The proportion recaptured differed significantly between HBA and YB (Table 22-10) and the significant interaction between mean days at liberty and SRA indicated the recapture rate also differed between the two areas. Although the same amount of recapture effort was applied to both recapture grids over the same period (March, May and August 2019), YB (4.8% recaptured) had 50% more recaptures than HBA (3.2% recaptured). The predicted mean proportion recaptured from the model (Table 22-10) was 0.012 (s.e. 0.001) and 0.021 (s.e. 0.002) for HBA and YB, respectively, indicating an even greater disparity between the areas. The results suggest that fewer tagged scallops survived at HBA, resulting in fewer recaptures and a higher estimate of *M* compared to YB. This difference in *M* between the areas was consistent across the three methods (i.e., Brownie *et al.* Model 1, modified Brownie *et al.* and logistic regression).

The influence of size on the proportion recaptured is less clear. Significantly fewer large scallops (> 95 mm SH) were recaptured, which may be because they experienced a higher *M* compared to the smaller size classes. However, since there was no significant interaction between size class and mean days at liberty, there was no significant difference in the rate of decline in recaptures, and hence no significant difference in *M* between size classes (Figure 22-5). If large scallops do experience a higher natural mortality rate, then it may partly explain the spatial difference in *M* observed between the two areas, as the size of scallops in YB was noticeably smaller than HBA (Figure 22-2). It is therefore unclear if the spatial variation in *M* is due to inherent differences between HBA and YB, or due to differences in size-frequency. The disparity in the size class frequency distributions of the tagged scallops between the two areas was expected as it widely known among fishers and researchers that saucer scallops in the Yeppoon region are generally smaller than those elsewhere in the fishery, however the reasons for this remain unknown.

The influence of the cyclone as a potential explanatory term was not considered in the logistic model, however given its trajectory, it is likely that any influence from the cyclone on the recapture data is likely to be higher at HBA than YB (Figure 22-4).

Some of the variation in the estimates obtained from the Brownie *et al.* (1985) Model 1 may be attributed to seasonal variation where *M* peaks in summer (December, January, March) and falls to a minimum in winter (June, July, August). (Note these estimates of *M* from the Brownie *et al.* Model 1 exclude the problematic recaptures from HBA trip 3). Mean estimates of *M* from the two locations, which can be used to represent the whole fishery, were relatively consistent and varied from a minimum of 1.461 year^{-1} for the logistic model, to 1.501 year^{-1} for the Brownie *et al.* (1985) Model 1, to 1.548 year^{-1} (variable recapture rate) and 1.594 year^{-1} (fixed recapture rate) for the modified Brownie *et al.* method. All annual mean estimates of *M* were larger than the range put forward by Dredge (1985a) (i.e., 0.020–0.025 week^{-1} or 1.040–1.300 year^{-1}). The Dredge estimates may be biased upwards because they include fishing mortality. However, they could be biased downwards because they were based on minima over different batches which would, by chance, have had different survival rates.

The estimates of *M* determined here indicate that longevity for *Y. balloti* is shorter than previously thought. For example, if we assume that $M = 1.526$ year^{-1} based on averaging the above annual estimates, there would be 47 scallops surviving after two years (104 weeks) from an initial population of 1000, in the absence of fishing mortality (assuming the size range of scallops was similar to the size range encountered herein). Using the Dredge (1985a) estimate of 1.170 year^{-1}, 96 scallops would be

alive after two years – about twice as many compared to current study average. The natural mortality rate of *P. fumatus*, another more temperate scallop species commercially fished in Australia, was estimated to be 0.52 year^{-1} (Gwyther and McShane 1988), which would result in 354 scallops surviving after two years from an initial population of 1000. A recent assessment of the Atlantic sea scallop (*P. magellanicus*) fishery considered a range in estimates of *M* that were in the order of 0.25 year^{-1} (Northeast Fisheries Science Center 2018). At this rate, 607 of the 1000 scallops would be alive after two years.

Dredge (1985a) derived his estimates of *M* for the period from July 1977 to June 1978, while the current estimates were based on tagging from May 2018 to August 2019. The increase in *M* detected herein over the intervening period (i.e., about 42 years) may be attributed, in part or totally, to a long-term increase in sea surface temperature (SST) in the scallop fishing grounds. In Western Australia recruitment of *Y. balloti* is heavily influenced by SST, and a marine heatwave event in the summer of 2010–11 had a catastrophic impact on the stock (Joll and Caputi 1995a; Lenanton *et al.* 2009; Caputi *et al.* 2014; 2015; 2019). The Queensland commercial fishery logbook catch rates of scallops in November (i.e., traditional commencement of the scallop fishing season) are almost always negatively correlated with bottom and surface water temperatures 5–18 months prior (see Figure 19-6 in Courtney *et al* 2015) and it is noteworthy that winter SST in the Queensland scallop fishing grounds has risen by 0.7–0.8ºC since the 1950s (Figure 22-6). Although the seasonal variation in *M* inferred herein requires confirmation, the Brownie *et al.* Model 1 method indicates that *M* is elevated over late spring and summer, and declines in winter and early spring. It is therefore possible that the increase in *M* may be partly or wholly attributed to increasing SST.
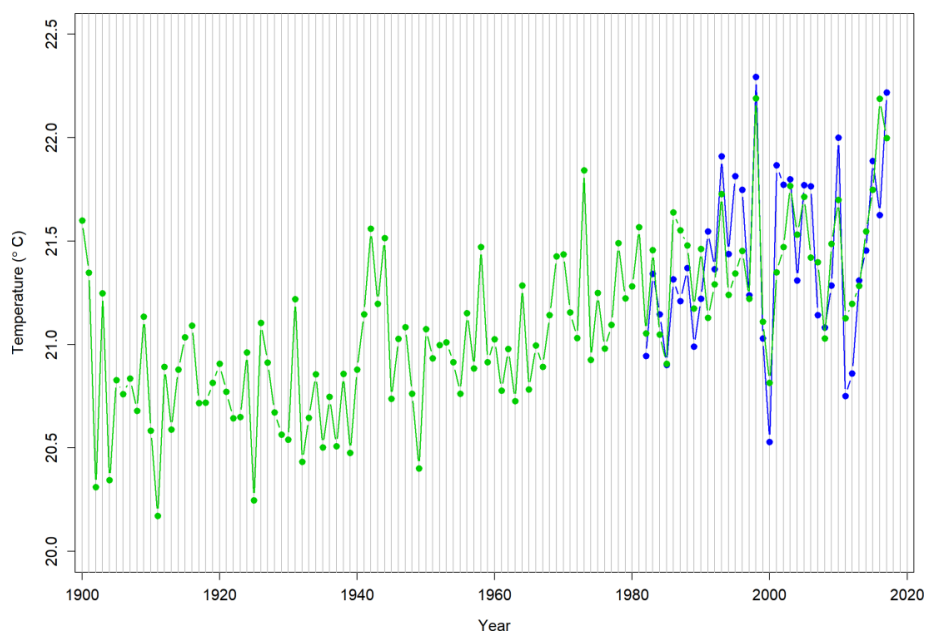
Figure 22-6. The estimated mean winter sea surface temperature (June–August) in the Queensland scallop fishing grounds from the Optimum Interpolation Sea Surface Temperature (OISST) (blue line) and Extended Reconstructed Sea Surface Temperature (ERSST) v5 (green line) NOAA databases, reproduced from O'Neill *et al.* (2020).

The most recent Queensland saucer scallop stock assessment by Wortmann *et al.* (2020) included the logistic model estimate of the natural mortality rate (i.e., *M* = 1.461 year^{-1}), but found it resulted in relatively little overall effect on the assessment outputs compared to using Dredge's (1985a) estimate (*M* = 1.170 year^{-1}). Scallop biomass estimates for 2019 were very low (i.e., < 20% unfished biomass) in model outputs for both estimates of *M*. The assessment did not include environmental influences on the stock, although the authors noted that if *M* increases with SST then it may impact the target

reference points used to manage effort and lower potential yields from the fishery. Future assessments may be improved by incorporating the spatial variation in *M* detected herein, and by incorporating seasonal variation, although further tagging may be required to confirm this.

22.6 **SUPPLEMENTARY MATERIAL. R CODE DEVELOPED FOR APPLYING THE MODIFIED BROWNIE**
***ET AL.* (1985) METHOD FOR ESTIMATING THE NATURAL MORTALITY RATE (*M*) OF SAUCER**
SCALLOPS

```
# Brownie's model:

rm(list = ls())
invisible(gc())
options(scipen=999)

# package
#library(stats4) # MLE: stats4::mle
library(bbmle) # MLE: bbmle::mle2


# directories
fil01 <- "M:/Data/Scallop mortality tagging experiment/MES_Brownie/MES_Brownie/data/"

# DATA
## load data
setwd(fil01)

temp01 <- read.csv("YB_catch.csv")
temp02 <- read.csv("YB_liberty.csv")
temp03 <- read.csv("YB_month.csv")

## model input
noccation <- 4
ntrips <- 3
total_po <- temp01$Number.tagged

recatch <- as.matrix(temp01[,4:6])
liberty <- as.matrix(temp02[,4:6])
cmonth <- as.matrix(temp03[,4:6])

# likelihood function
## Model 1
M1_LL <- function(M, alpha) {

 # occasion 1
 p1 <- rep(0,4)
 p1[1] <- exp(-M*liberty[1,1])*alpha
 p1[2] <- exp(-M*liberty[1,2])*alpha
 p1[3] <- exp(-M*liberty[1,3])*alpha
 p1[4] <- 1-p1[1]-p1[2]-p1[3]
 LL1 <- recatch[1,1]*log(p1[1])+recatch[1,2]*log(p1[2])+recatch[1,3]*log(p1[3])+
       (total_po[1]-recatch[1,1]-recatch[1,2]-recatch[1,3])*log(p1[4])

 # occasion 2
 p2 <- rep(0,4)
 p2[1] <- exp(-M*liberty[2,1])*alpha
 p2[2] <- exp(-M*liberty[2,2])*alpha
 p2[3] <- exp(-M*liberty[2,3])*alpha
 p2[4] <- 1-p2[1]-p2[2]-p2[3]
```

```
LL2 <- recatch[2,1]*log(p2[1])+recatch[2,2]*log(p2[2])+recatch[2,3]*log(p2[3])+
      (total_po[2]-recatch[2,1]-recatch[2,2]-recatch[2,3])*log(p2[4])

# occasion 3
p3 <- rep(0,3)
p3[1] <- exp(-M*liberty[3,2])*alpha
p3[2] <- exp(-M*liberty[3,3])*alpha
p3[3] <- 1-p3[1]-p3[2]
LL3 <- recatch[3,2]*log(p3[1])+recatch[3,3]*log(p3[2])+
      (total_po[3]-recatch[3,2]-recatch[3,3])*log(p3[3])

# occasion 4
p4 <- rep(0,2)
p4[1] <- exp(-M*liberty[4,3])*alpha
p4[2] <- 1-p4[1]
LL4 <- recatch[4,3]*log(p4[1])+
      (total_po[4]-recatch[4,3])*log(p4[2])

-(LL1+LL2+LL3+LL4) # Sum the log likelihoods for all of the data01 points
}


M1 <- mle2(M1_LL,optimizer="nlminb",lower = c(M=0,alpha = 0),upper=c(alpha=1),
   start = list(M =0.0001, alpha = 0.0001))

(est <- summary(M1))

cat("*** Model 1: M = ",(est@coef[1,1]*365)," per year\n",sep="")
flush.console()


## Model 2
M2_LL <- function(M, alpha1,alpha2,alpha3) {

# occasion 1
p1 <- rep(0,4)
p1[1] <- exp(-M*liberty[1,1])*alpha1
p1[2] <- exp(-M*liberty[1,2])*alpha2
p1[3] <- exp(-M*liberty[1,3])*alpha3
p1[4] <- 1-p1[1]-p1[2]-p1[3]
LL1 <- recatch[1,1]*log(p1[1])+recatch[1,2]*log(p1[2])+recatch[1,3]*log(p1[3])+
      (total_po[1]-recatch[1,1]-recatch[1,2]-recatch[1,3])*log(p1[4])

# occasion 2
p2 <- rep(0,4)
p2[1] <- exp(-M*liberty[2,1])*alpha1
p2[2] <- exp(-M*liberty[2,2])*alpha2
p2[3] <- exp(-M*liberty[2,3])*alpha3
p2[4] <- 1-p2[1]-p2[2]-p2[3]
LL2 <- recatch[2,1]*log(p2[1])+recatch[2,2]*log(p2[2])+recatch[2,3]*log(p2[3])+
      (total_po[2]-recatch[2,1]-recatch[2,2]-recatch[2,3])*log(p2[4])

# occasion 3
p3 <- rep(0,3)
p3[1] <- exp(-M*liberty[3,2])*alpha2
```

```
 p3[2] <- exp(-M*liberty[3,3])*alpha3
 p3[3] <- 1-p3[1]-p3[2]
 LL3 <- recatch[3,2]*log(p3[1])+recatch[3,3]*log(p3[2])+
       (total_po[3]-recatch[3,2]-recatch[3,3])*log(p3[3])

 # occasion 4
 p4 <- rep(0,2)
 p4[1] <- exp(-M*liberty[4,3])*alpha3
 p4[2] <- 1-p4[1]
 LL4 <- recatch[4,3]*log(p4[1])+
       (total_po[4]-recatch[4,3])*log(p4[2])

 -(LL1+LL2+LL3+LL4) # Sum the log likelihoods for all of the data01 points
}


M2 <- mle2(M2_LL,optimizer="nlminb",lower = c(M=0,alpha1=0,alpha2=0,alpha3=0),
   upper=c(alpha1=1,alpha2=1,alpha3=1),
   start = list(M =0.0001, alpha1 = 0.0001, alpha2 = 0.0001, alpha3 = 0.0001))

(est <- summary(M2))

cat("*** Model 2: M = ",(est@coef[1,1]*365)," per year\n",sep="")
flush.console()

#############################################################################
## Model 3
M3_LL <- function(M, alpha) {

 # occasion 1
 p1 <- rep(0,4)
 p1[1] <- exp(-M*liberty[1,1])*exp(-alpha*cmonth[1,1])
 p1[2] <- exp(-M*liberty[1,2])*exp(-alpha*cmonth[1,2])
 p1[3] <- exp(-M*liberty[1,3])*exp(-alpha*cmonth[1,3])
 p1[4] <- 1-p1[1]-p1[2]-p1[3]
 LL1 <- recatch[1,1]*log(p1[1])+recatch[1,2]*log(p1[2])+recatch[1,3]*log(p1[3])+
       (total_po[1]-recatch[1,1]-recatch[1,2]-recatch[1,3])*log(p1[4])

 # occasion 2
 p2 <- rep(0,4)
 p2[1] <- exp(-M*liberty[2,1])*exp(-alpha*cmonth[2,1])
 p2[2] <- exp(-M*liberty[2,2])*exp(-alpha*cmonth[2,2])
 p2[3] <- exp(-M*liberty[2,3])*exp(-alpha*cmonth[2,3])
 p2[4] <- 1-p2[1]-p2[2]-p2[3]
 LL2 <- recatch[2,1]*log(p2[1])+recatch[2,2]*log(p2[2])+recatch[2,3]*log(p2[3])+
       (total_po[2]-recatch[2,1]-recatch[2,2]-recatch[2,3])*log(p2[4])

 # occasion 3
 p3 <- rep(0,3)
 p3[1] <- exp(-M*liberty[3,2])*exp(-alpha*cmonth[3,2])
 p3[2] <- exp(-M*liberty[3,3])*exp(-alpha*cmonth[3,3])
 p3[3] <- 1-p3[1]-p3[2]
 LL3 <- recatch[3,2]*log(p3[1])+recatch[3,3]*log(p3[2])+
       (total_po[3]-recatch[3,2]-recatch[3,3])*log(p3[3])
```

```
 # occasion 4
 p4 <- rep(0,2)
 p4[1] <- exp(-M*liberty[4,3])*exp(-alpha*cmonth[4,3])
 p4[2] <- 1-p4[1]
 LL4 <- recatch[4,3]*log(p4[1])+
      (total_po[4]-recatch[4,3])*log(p4[2])

 -(LL1+LL2+LL3+LL4) # Sum the log likelihoods for all of the data01 points
}


M3 <- mle2(M3_LL,optimizer="nlminb",lower = c(M=0,alpha = 0),
   start = list(M =0.01, alpha = 5))

(est <- summary(M3))

cat("*** Model 3: M = ",(est@coef[1,1]*365)," per year\n",sep="")
cat("*** Model 3: Catch rate in March = ",(exp(-est@coef[2,1]*3)),"\n",sep="")
cat("*** Model 3: Catch rate in May = ",(exp(-est@coef[2,1]*5)),"\n",sep="")
cat("*** Model 3: Catch rate in August = ",(exp(-est@coef[2,1]*8)),"\n",sep="")
flush.console()
```